DISSERTATION

CHARACTERIZING AMMONIA CONCENTRATIONS AND DEPOSITION IN THE UNITED

STATES

Submitted by

Yi Li

Department of Atmospheric Science

In partial fulfillment of the requirements

For the Degree of Doctor of Philosophy

Colorado State University

Fort Collins, Colorado

Fall 2015

Doctoral Committee:

      Advisor: Jeffrey L. Collett Jr.

      Sonia M. Kreidenweis
      Emily Fischer
      Jay Ham

ABSTRACT

CHARACTERIZING AMMONIA CONCENTRATIONS AND DEPOSITION IN THE

UNITED STATES

Rapid development of agricultural activities and fossil fuel combustion in the United States led to a great increase of reactive nitrogen (Nr) emissions in the second half of the twentieth century. These emissions have been linked to excess nitrogen (N) deposition in natural ecosystems through dry and wet deposition pathways that can lead to adverse environmental impacts. Furthermore, as precursors of ozone and fine particles, reactive nitrogen species impact regional air quality with resulting effects on human health, visibility, and climate forcing. In this dissertation, ambient concentrations of reactive nitrogen species and their deposition are examined in the Rocky Mountain region and across the country. Particular emphasis is placed on ammonia, a currently unregulated pollutant, despite its important contributions both to nitrogen deposition and fine particle formation.

Continuous measurements of the atmospheric trace gases ammonia (NH_3) and nitric acid (HNO_3) and of fine particle ($PM_{2.5}$) ammonium (NH_4^+), nitrate (NO_3^-) and sulfate (SO_4^{2-}) were conducted using a denuder/filter system from December 2006 to December 2011 at Boulder, Wyoming, a region of active gas production. The average five year concentrations of NH_3, HNO_3, NH_4^+, NO_3^- and SO_4^{2-} were 0.17, 0.19, 0.26, 0.32, and 0.48 $\mu g/m^3$, respectively. Significant seasonal patterns were observed. The concentration of NH_3 was higher in the summer than in other seasons, consistent with increased NH_3 emissions and a shift in the ammonium nitrate (NH_4NO_3)

equilibrium toward the gas phase at higher temperatures. High HNO_3 concentrations were observed both in the summer and the winter. Elevated wintertime HNO_3 production appeared to be due to active local photochemistry in a shallow boundary layer over a reflective, snow-covered surface. $PM_{2.5}$ NH_4^+ and SO_4^{2-} concentrations peaked in summer while NO_3^- concentrations peaked in winter. Cold winter temperatures drove the NH_3-HNO_3-NH_4NO_3 equilibrium toward particulate NH_4NO_3. A lack of NH_3, however, frequently resulted in substantial residual gas phase HNO_3 even under cold winter conditions.

Concentrated agricultural activities and animal feeding operations in the northeastern plains of Colorado represent an important source of atmospheric NH_3 that contributes to regional fine particle formation and to nitrogen deposition to sensitive ecosystems in Rocky Mountain National Park (RMNP) located ~80 km to the west. In order to better understand temporal and spatial differences in NH_3 concentrations in this source region, weekly concentrations of NH_3 were measured at 14 locations during the summers of 2010 to 2014 using Radiello passive NH_3 samplers. Weekly average NH_3 concentrations ranged from 2.8 µg/m^3 to 41.3 µg/m^3 with the highest concentrations near large concentrated animal feeding operations (CAFOs). The annual summertime mean NH_3 concentrations were stable in this region from 2010 to 2014, providing a baseline against which concentration changes associated with future changes in regional NH_3 emissions can be assessed. Vertical profiles of NH_3 were also measured on the 300 m Boulder Atmospheric Observatory (BAO) tower throughout 2012. The highest NH_3 concentration along the vertical profile was always observed at the 10 m height (annual average concentration is 4.63 µg/m^3), decreasing toward the surface (4.35 µg/m^3 at 1 m) and toward higher altitudes (1.93 µg/m^3 at 300 m). Seasonal changes in the steepness of the vertical concentration gradient were observed,

with the sharpest gradients in cooler seasons when thermal inversions restricted vertical mixing of surface-based emissions. The NH_3 spatial distributions measured using the passive samplers are compared with NH_3 columns retrieved by the Infrared Atmospheric Sounding Interferometer (IASI) satellite and concentrations simulated by the Comprehensive Air quality Model with extensions (CAMx), providing insight into the regional performance of each.

U.S. efforts to reduce NO_x emissions since the 1970s have substantially reduced nitrate deposition, as evidenced by strongly decreasing trends in long-term wet deposition data. These decreases in nitrate deposition along with increases in wet ammonium deposition have altered the balance between oxidized and reduced nitrogen deposition. Across most of the U.S., wet deposition has evolved from a nitrate dominated situation in the 1980s to an ammonium dominated situation in recent years. Recent measurements of gaseous NH_3 concentrations across several regions of the U.S., along with longer-established measurements of gas phase nitric acid, fine particle ammonium and nitrate, and wet deposition of ammonium and nitrate, permit new insight into the balance of oxidized and reduced nitrogen in the total (wet + dry) U.S. reactive nitrogen deposition budget. Utilizing observations from 37 monitoring sites across the U.S., we estimate that reduced nitrogen contributes, on average, approximately 65 percent of the total inorganic N deposition budget. Dry NH_3 deposition plays an especially key role in N deposition compared with other N deposition pathways, contributing from 19% to 65% in different regions. With reduced N species now dominating the wet and dry reactive N deposition budgets in much of the country and future estimates suggesting growing ammonia emissions, the U.S. will need to consider ways to actively reduce NH_3 emissions if it is to continue progress toward reducing N deposition to sustainable levels defined by ecosystem critical loads.

ACKNOWLEDGEMENTS

TABLE OF CONTENTS

LIST OF TABLES

LIST OF FIGURES

1. INTRODUCTION

Nitrogen (N) is an essential element for terrestrial and aquatic ecosystems. Since the last century, emissions of anthropogenic reactive nitrogen (N_r) have accelerated dramatically due to fossil fuel combustion and intensive agricultural activities (Erisman et al., 2011; Galloway and Cowling, 2002; Galloway et al., 2008; Liu et al., 2013). Atmospheric reactive nitrogen compounds are deposited to terrestrial and aquatic ecosystems on the earth through dry and wet atmospheric processes. This has raised world-wide concerns due to the adverse environmental impacts of reactive nitrogen, such as decreases in biological diversity, soil acidification and lake eutrophication (Clark and Tilman, 2008; Galloway et al., 2004; Holtgrieve et al., 2011; Janssens et al., 2010; Phoenix et al., 2012). In addition, atmospheric reactive nitrogen (as a primary precursor of ozone and fine particles) has been linked with climate change and human health degradation by many scientific studies (Davidson et al., 2012; Galloway et al., 2004; Gruber and Galloway, 2008).

1.1 Reactive Nitrogen in the Atmosphere

Reactive nitrogen as discussed in this dissertation includes all photochemically reactive and biologically active nitrogen compounds within the Earth's atmosphere in gaseous and particulate form (Wolfe and Patz, 2002). Figure 1.1 summarizes the key sources and processes of reactive nitrogen in the atmosphere. In the gaseous phase, it includes ammonia (NH_3), nitrogen monoxide (NO), nitrogen dioxide (NO_2), nitrous oxide (N_2O), nitrous acid (HNO_2), nitric acid (HNO_3), various forms of organic nitrogen, such as peroxyacetyl nitrate (PAN), amines, acetonitrile, alkyl

nitrates, and peroxynitrates; in the particulate phase, it includes ammonium (NH_4^+), nitrate (NO_3^-) and various forms of organic nitrogen. Reactive nitrogen species exist as inorganic reduced forms of nitrogen (e.g., NH_3, NH_4^+), inorganic oxidized forms (e.g., NO_x, HNO_3, N_2O, NO_3^-), and organic compounds (e.g., urea, amines, proteins, nucleic acids) (Galloway et al., 2004). In this study, we specifically focus on several major inorganic compounds of reduced (NH_3 and NH_4^+) and oxidized (NO_x, HNO_3 and NO_3^-) nitrogen.
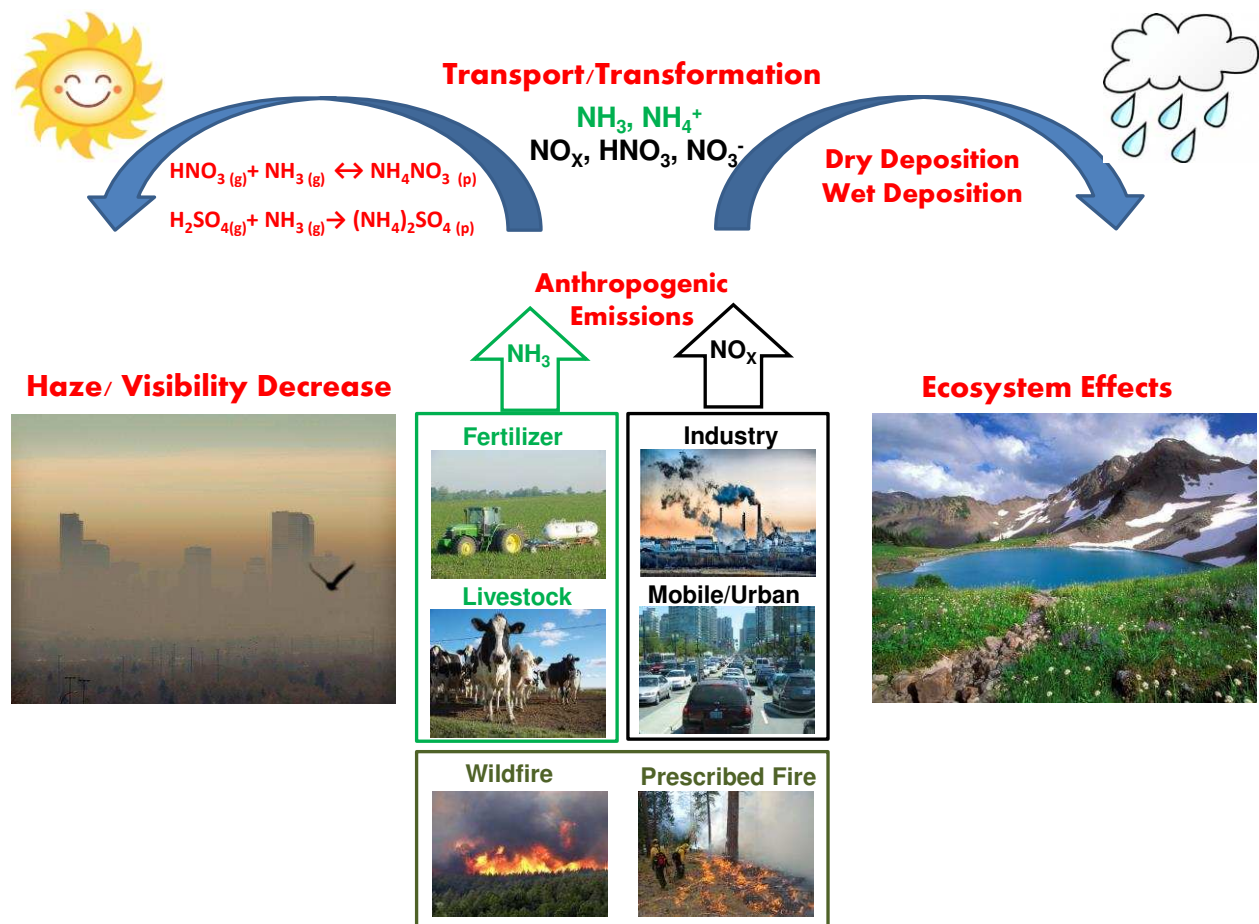
Figure 1.1 Key sources and processes of reactive nitrogen in the atmosphere.

1.1.1 NH$_3$

As the most abundant reactive and basic gas in the atmosphere, ammonia (NH$_3$) can neutralize

ambient acidic species, such as sulfuric acid (H$_2$SO$_4$) and nitric acid (HNO$_3$), which are the most

important acidic species in many (especially polluted) environments. It is widely believed that

agriculture (livestock waste and fertilizer application) represents the largest source of NH$_3$

globally. Clarisse et al. (2009) estimate that atmospheric NH$_3$ is emitted primarily from livestock

waste (39%) and volatilization of NH$_3$-based fertilizers (17%), while the U.S. Environmental

Protection Agency (EPA) attributes over 85% of NH$_3$ emissions in the U.S. to the agricultural

sector   (EPA,   1998).   Hertel   et   al.

(2006) also found that deposition of atmospheric NH$_3$ near an intensive agricultural area would

dominate the overall load of reactive nitrogen from the atmosphere. Agricultural NH$_3$ emissions

have become one of the most significant air pollution problems in recent years and have attracted

growing concern from environmental scientists and government regulators (*Aneja et al.*, 2006).

In recent years, there have been a number of studies on NH$_3$ in urban and rural areas around the

world (Figure 1.2 and Table 1.1). From a global perspective, the lowest NH$_3$ concentrations were

observed at remote areas which were away from anthropogenic activities (agricultural and

industrial). Ammonia concentrations can be similar between urban and rural areas. For example,

the average NH$_3$ concentration near a hog farm (10.5 µg/m^3) in eastern North Carolina, U.S., was

comparable to the concentration in Beijing, China (16.6 µg/m^3), one of the largest megacities in

the world with 19.6 million residents. The NH$_3$ concentration observed mainly depends on the

distance from a major source, such as livestock feedlots, sewage plants or a traffic center. Usually

the NH$_3$ near a coastal area (e.g. Morehead, Thessaloniki, Hong Kong) is lower than the

3

concentration in an inland area (e.g. Lahore, Xinken, Beijing), reflecting the dilution effect of sea and land breezes.

Concentration(μg/m³)

1) Boulder,USA
Dec.2006-Dec.2010

2) Rocky Mountain
National Park,USA
Dec.2008-Dec.2009

3) Clinton,USA
Jan.-Dec.2000

4) Sequoia National Park,
CA. USA
May-Nov.1999

5) Eastern North Carolina,
USA. Sept.-Dec.1997

6) Deurne, Netherlands
Oct.1987-Apr.1990

7) Bilthoven, Netherlands
Oct.1987-Apr.1990

8) Erzgebirge,Germany
Oct.2001-Apr.2003

9) Chunchon, South Korea
Sept.1996-Dec.2000

10) Anmyon-do,South Korea
May 1997-Aug.1998

11) Wolkersdorf,Austria
Nov.1990-Oct.1991

12) Mt. Oyama, Japan
Jan.-Dec.1995

13) Rampur,India
Summer & Winter, 2002

14) Morehead,USA
Jan.-Dec. 2000

15) Kinston,USA
May-Dec. 2000

16) Chicago, IL,USA
April-March 1991

17) Manhattan,USA
July 1999-June 2000

18) Hamilton,Canada
1992-1994

19) Aveiro, Portugal
Aug.1988-May 1989

20) Rome, Italy
Jan.-Dec. 2004

21) Thessaloniki, Greece
April 2002-March 2003

22) Küçük çalticak, Turkey
Aug. 1995-Apr. 1996

23)Sasaguri,Japan
May 2006-
Apr. 2007

24) Nara, Japan
June 1994-May 1995

25) Taichung,Taiwan
Jan.-Dec. 2002

26) Hsinchu, Taiwan
Oct.1994-Apr.1995

27) Seoul, South Korea
Oct.1996-Sept.1997

28) Hong Kong,
China
Autumn, 2000

29) lahore,Pakistan
Dec.2005-Feb.2006

30) Xinken,China
Oct.-Nov. 2004

31) Beijing, China
July-Aug. 2002&2003

Rural Site

Urban Site

NO_3^- NH_4^+ HNO_3 NH_3

5

Figure 1.2 Comparison of selected measurements of the average concentrations of reactive nitrogen species (gaseous NH_3 and HNO_3 and particulate NH_4^+ and NO_3^-). Y-axes are the same for all the plots except the last 3 urban sites. More detailed information on the location and concentration for each site can be found in Table 1.1

Seasonal patterns have been found in long-term NH_3 observations, with lower concentrations in winter than in summer (Bari et al., 2003; Gong et al., 2011; Ianniello et al., 2010; Lee et al., 1999; Lin et al., 2006; Meng et al., 2011; Perrino et al., 2002). This implies that air temperature is one important factor determining NH_3 emissions. However, Vogt et al. (2005) found no such trend in their observations in Münster, Germany. They believed this was due to a great influence of local sources and, therefore, NH_3, HNO_3 and NH_4NO_3 had not reached equilibrium. Elevated NH_3 concentrations were found at rural sites, especially nearby agricultural areas such as a hog farm (McCulloch et al., 1998), indicating the significant impacts of agricultural activities on the NH_3 concentration. Meanwhile, in urban areas, the sources of NH_3 mainly include humans (sweat, breath, smoking), animals, sewage, industrial combustion and road transportation (Sutton et al., 2000). Recently, a number of studies (Carslaw and Rhys-Tyler, 2013; Gong et al., 2011; Huai et al., 2003; Kean et al., 2000; Liu et al., 2014; Loflund et al., 2002; Perrino et al., 2002; Whitehead et al., 2007; Yao et al., 2013) have highlighted the important role that the transportation sector plays in contributing to NH_3 emission, with the widespread application of three-way catalytic converters in motor vehicles since the 1980s producing NH_3 through the reaction between NO and Hydrogen (H_2) as shown in Eqn.1.1 (Kean et al., 2000). However, the emission factor of NH_3 from road traffic remains uncertain.

$$2NO + 5H_2 \rightarrow 2NH_3 + 2H_2O \qquad (Eqn.1.1)$$
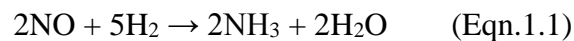
After finding a significant correlation between the ratio of NH_3 to carbon monoxide (CO) (mainly from the traffic sources) and air temperature, Perrino et al. (2002) concluded that ammonia in urban sites depended on three factors: traffic intensity, atmospheric mixing in the boundary layer

and air temperature. Reche et al. (2015) claim that important NH_3 sources in urban environments include vehicular traffic, biological sources (e.g. garbage containers), waste (water and solid) treatment plants and industry.

In the United States (U.S.), a set of Class 1 areas (including National Parks and Wilderness Areas) has been identified for protection from visibility impairment through the Regional Haze Rule. Because oil and gas production regions of the western U.S. are often located near these visibility-protected areas, close attention is paid to their emissions of fine particle precursors. In order to reduce NO_x emissions from natural gas drilling and production activities, for example, selective catalytic reduction (SCR) can be installed on drill rigs. While SCR can yield large reductions of NO_x emissions, there is a risk of increased NH_3 emission to the atmosphere from injected urea or NH_3 that is not completely consumed, especially as the catalyst ages.

Table 1.1 Ambient gaseous NH_3, HNO_3 and particulate NH_4^+, NO_3^- concentrations in µg/m^3 summarized for each site presented in Figure 1.2

Site	Latitude (degrees)	Longitude (degrees)	Period	Reactive Nitrogen Species (unit: µg/m^3)				Reference
				NH_3	HNO_3	NH_4^+	NO_3^-	
Rural	Boulder, USA	42.72	-109.75	12/2006 ~ 12/2011	0.2	0.2	0.3	0.3	(Li et al., 2014)
	Rocky Mountain National Park, USA	40.30	-105.69	11/2008 ~ 11/2009	0.2	0.1	0.2	0.2	(Benedict et al., 2013c)
	Clinton,USA	35.01	-78.32	01/2000 ~ 12/2000	5.3	0.8	1.8	1.7	(Walker et al., 2004)
	Sequoia National Park, USA	36.52	-118.56	05/1999 ~ 11/1999	4.5	2.1	1.3	1.3	(Bytnerowicz et al., 2002)
	Eastern North Carolina,USA	35.59	-77.89	09/1997 ~ 12/1997	10.5	0.2	1.1	0.6	(McCulloch et al., 1998)
	Deurne, Netherlands	51.69	5.80	10/1987 ~ 4/1990	11.6	0.7	3.4	5.7	(Hoek et al., 1996)
	Bilthoven, Netherlands	52.14	5.21	10/1987 ~ 4/1990	3.9	0.3	3.3	5.2	(Hoek et al., 1996)
	Erzgebirge, Germany	50.78	13.70	10/2001 ~ 04/2003	0.5	0.8	1.6	2.2	(Plessow et al., 2005)
	Chunchon, South Korea	37.94	127.75	09/1996 ~ 12/2000	3.1	1.7	2.8	5.7	(Hong et al., 2002)

9

	Anmyon-do, South Korea	36.57	126.34	05/1997 ~ 08/1998	2.0	2.9	N/A	6.1	(Hong et al., 2002)
	Wolkersdorf, Austria	48.39	16.51	11/1990 ~ 10/1991	1.5	1.8	4.5	4.6	(Puxbaum et al., 1993)
	Mt. Oyama, Japan	35.42	139.26	09/1996 ~ 12/2000	0.8	0.8	2.3	1.8	(Igawa et al., 1998)
	Rampur, India	27.17	78.08	Summer & Winter, 2002	6.7	0.7	1.0	1.1	(Gupta et al., 2003)
	Morehead, USA	34.73	-76.73	01/2000 ~ 12/2000	0.6	0.2	0.9	1.1	(Walker et al., 2004)
	Kinston, USA	35.27	-77.58	05/2000 ~ 12/2000	2.5	0.3	1.3	1.4	(Walker et al., 2004)
	Chicago,USA	41.89	-87.63	04/1990 ~ 03/1991	1.6	0.8	2.7	4.2	(Lee et al., 1993)
	Manhattan,USA	40.79	-73.97	07/1999 ~ 06/2000	3.7	1.7	N/A*	N/A*	(Bari et al., 2003)
	Hamilton, Canada	43.25	-79.89	09/1994 ~ 12/1994	4.3	2.0	2.5	1.1	(Brook et al., 1997)
	Aveiro, Portugal	40.76	8.67	08/1988 ~ 05/1989	3.46	0.79	2.2	2.4	(Pio et al., 1991)
	Rome, Italy	41.92	12.49	01/2004 ~ 12/2004	5.6	1.2	1.4	1.2	(Perrino and Catrambone, 2004)
Urban	Thessaloniki, Greece	40.65	22.90	04/2002 ~ 03/2003	2.3	0.8	2.7	2.9	(Anatolaki and Tsitouridou, 2007)
	Küçük Çalticak, Turkey	36.80	30.57	08/1995 ~ 04/1996	1.0	0.4	2.2	2.3	(Soner Erduran and Tuncel, 2001)
	Sasaguri, Japan	33.63	130.53	05/2006 ~ 04/2007	0.8	2.2	3.1	2.0	(Chiwa, 2010)

Location	Lat	Lon	Period					Reference
Nara, Japan	34.69	135.81	06/1994 ~ 05/1995	2.4	1.6	1.7	2.1	(Matsumoto and Okita, 1998)
Taichung, Taiwan	24.14	120.67	01/2002 ~ 12/2002	11.4	2.6	4.6	5.0	(Lin et al., 2006)
Hsinchu,Taiwan	24.82	120.96	06/1994 ~ 05/1995	8	0.7	3	2.8	(Tsai and Perng, 1998)
Seoul, South Korea	37.57	126.98	10/1996 ~ 09/1997	4.3	1.1	4.2	6.0	(Lee et al., 1999)
Hongkong, China	22.44	114.09	Autumn, 2000	2.1	1.3	2.4	1.0	(Yao et al., 2006)
Lahore,Pakistan	31.57	74.34	12/2005 ~ 02/2006	50.1	1.0	16.1	18.9	(Biswas et al., 2008)
Xinken, China	22.65	113.61	10/2004 ~ 11/2004	7.3	6.3	7.2	9.2	(Hu et al., 2008)
Beijing,China	39.99	116.31	06/2002 ~ 08/2002 & 06/2003 ~ 08/2003	16.6	1.9	8.9	14.6	(Wu et al., 2009)

* "N/A" means data were not available in the study

1.1.2 HNO₃

Gaseous nitric acid (HNO$_3$) is one of the most important acidic gases in the atmosphere and a major product of photochemical reactions. During the daytime, the primary source of HNO$_3$ is through atmospheric oxidation of nitrogen oxides (NO$_x$ = NO + NO$_2$), such as the reaction of NO$_2$ with hydroxyl radical (OH) (Eqn. 1.2); during the nighttime, HNO$_3$ can be formed through the heterogeneous hydrolysis of dinitrogen pentoxide (N$_2$O$_5$) and NO$_2$ on the surface of ambient aerosol (Eqn. 1.3 and Eqn 1.4) and reactions of the nitrate radical (NO$_3$) (Eqn. 1.5 and Eqn 1.6) (Bari et al., 2003; Dentener and Crutzen, 1993; Lin et al., 2006). The atmospheric lifetime of HNO$_3$ is only a few days (McElroy, 2002). Because of its water-soluble and sticky characteristics, HNO$_3$ is efficiently removed from the atmosphere through dry and wet deposition processes.

$$NO_2 + OH \rightarrow HNO_3 \qquad \text{(Eqn. 1.2)}$$

$$N_2O_5 + H_2O \rightarrow 2HNO_3 \qquad \text{(Eqn. 1.3)}$$

$$2NO_2 + H_2O \rightarrow HNO_2 + HNO_3 \qquad \text{(Eqn. 1.4)}$$

$$NO_3 + H_2O \rightarrow HNO_3 \qquad \text{(Eqn. 1.5)}$$

$$NO_3 + HONO \rightarrow HNO_3 + NO_2 \qquad \text{(Eqn. 1.6)}$$

Higher HNO$_3$ concentrations are usually observed in urban and suburban areas compared to rural areas (Figure 1.2 and Table 1.1). For example, the average HNO$_3$ concentration in Manhattan, New York was 1.6 µg m^{-3}, two times higher than the concentration measured at a forest site in Germany (0.8 µg m^{-3}) (Plessow et al., 2005). This difference can be explained by increased emissions of NO$_x$ from industrial and traffic sectors in the urban area. The seasonal pattern of

HNO$_3$ concentrations suggest that HNO$_3$ is typically highest in summer and lowest in the winter due to intensive photochemical activity in the summer, which generates higher OH concentrations, as well as increased decomposition of NH$_4$NO$_3$ particles at warmer temperatures (Bari et al., 2003; Lin et al., 2006; Plessow et al., 2005).

1.1.3 Particulate NH$_4^+$, NO$_3^-$ and Gas/Particulate Partitioning

In the particulate phase, NH$_4^+$ and NO$_3^-$ are important inorganic constituents in rural, suburban and urban areas. Due to its alkaline nature, NH$_3$ commonly acts to neutralize acidic compounds such as HNO$_3$ and H$_2$SO$_4$ and form submicron ammonium nitrate (NH$_4$NO$_3$) and ammoniated sulfate (NH$_4$HSO$_4$, (NH$_4$)$_2$SO$_4$, or other forms) particles (Eqn. 1.7 and Eqn 1.8), respectively. Normally, the diameters of these particles are less than a

$$\text{HNO}_3(g) + \text{NH}_3(g) \leftrightarrow \text{NH}_4\text{NO}_3(p) \qquad (\text{Eqn. 1.7})$$

$$\text{H}_2\text{SO}_4(p) + 2\text{NH}_3(g) \rightarrow (\text{NH}_4)_2\text{SO}_4(p) \qquad (\text{Eqn. 1.8})$$
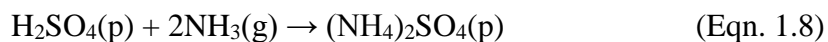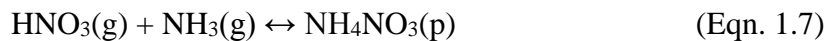
micrometer and measured within PM$_{2.5}$. These submicron particles have longer atmospheric lifetimes than their gas-phase counterparts (on the order of several days), allowing them to be transported to remote areas away from sources before being deposited through dry and wet processes (Aneja et al., 2001; Fowler et al., 1998). PM$_{2.5}$ has been linked to adverse effects on human health, regional visibility, and radiative forcing (Davidson et al., 2005; Ianniello et al., 2010; Langridge et al., 2012; Park et al., 2006; Parry, 2007; Schwartz and Neas, 2000).

In this neutralization process, NH_3 is thermodynamically preferred to react first with H_2SO_4 to form non-volatile ammoniated sulfate aerosol species. Any remaining NH_3 can participate in gas-particle partitioning with HNO_3 (Asman et al., 1998; Bari et al., 2003; Ellis et al., 2011; Sharma et al., 2007). The gas-particle partitioning reaction between NH_3, HNO_3 and NH_4NO_3 is highly dependent on temperature and relative humidity. In an environment with high temperature and low relative humidity, NH_3 and HNO_3 will mostly stay in the gas-phase, but low temperature and high relative humidity enhance NH_4NO_3 formation (Stelson and Seinfeld, 1982). Several studies (Hand et al., 2012; Ianniello et al., 2010; Lee et al., 1999; Lee et al., 2008b; Li et al., 2014; Sharma et al., 2007) have shown high concentrations of NH_3 and HNO_3 in summer and elevated concentrations of NH_4^+ and NO_3^- in winter are partially due to the shift of this reversible equilibrium between particulate and gas phases. For the same reason, formation of NH_4NO_3 is expected to be more favorable during nighttime than daytime as observed in many locations (Du et al., 2010; Ellis et al., 2011; Sharma et al., 2007; Walker et al., 2004; Wen et al., 2015).

Additionally, HNO_3 can react with $CaCO_3$ in soil particles and $NaCl$ in sea salts to form nitrate in coarse particles (particulate matter with aerodynamic diameter in the range from 2.5 to 10 µm) (Eqn. 1.9 and Eqn 1.10) (Lee et al., 2008a; Pakkanen, 1996; Yeatman et al., 2001).

$$HNO_3(g) + NaCl(p) \rightarrow HCl(g) + NaNO_3(p) \qquad \text{(Eqn. 1.9)}$$
$$2HNO_3(g) + CaCO_3(p) \rightarrow Ca(NO_3)_2(p) + H_2O(aq) + CO_2(g) \qquad \text{(Eqn. 1.10)}$$
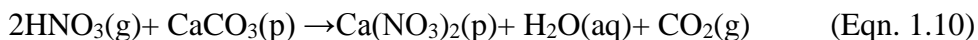
1.2 Nitrogen Deposition

Atmospheric reactive nitrogen sources are dominated by emissions of nitrogen oxides (NO_x =$NO+NO_2$) and ammonia (NH_3) (Galloway et al., 2004). NO_x is produced by fuel combustion from vehicles, electric power generation, and industrial sources and also has natural sources including wildfires, lightning and soil emissions. Emitted NOx can be oxidized to HNO_3 within a short timescale (less than one day) in the atmosphere. For NH_3, Reis et al. (2009) attributed over 80% of NH_3 emissions in the U.S. to the agricultural sector, including emissions from livestock waste and volatilization of N-based fertilizer. Through wet and dry deposition, HNO_3 and NH_3 are rapidly removed from the atmosphere and enter the natural ecosystems in the form of nitrate (NO_3^-) and ammonium (NH_4^+), respectively. HNO_3 and NO_3^- are generally referred to as oxidized nitrogen while NH_3 and NH_4^+ are regarded as reduced N, but both are significant reactive nitrogen inputs in natural ecosystems (Fowler et al., 1998; Galloway et al., 2002).

Both oxidized and reduced nitrogen species are removed from the atmosphere and deposited to aquatic and terrestrial ecosystems, comprising important components of nitrogen deposition. Generally, the removal mechanisms can be divided into dry deposition and wet deposition. Many studies have demonstrated that emissions from human activities increasingly dominate the nitrogen deposition budget at global and most regional scales (Galloway et al., 2004; Liu et al., 2013; Vitousek et al., 1997). National network observations and model simulation studies have shown that within the United States, nitrogen deposition generally exceeds 8 Kg N $ha^{-1} a^{-1}$ in the eastern part and ranges from 1 to 4 Kg N $ha^{-1} a^{-1}$ over most regions in the west, with maxima from 30 to 90 Kg N $ha^{-1} a^{-1}$ downwind of urban and agricultural areas (Fenn et al., 2003; Zhang et al., 2012).

1.2.1 Dry Nitrogen Deposition

Dry deposition is the process by which reactive nitrogen species (gaseous and particulate) are transferred directly from the atmosphere to the surface of the Earth without precipitation. The transport rate between the air and the surface depends, for various species, on atmospheric characteristics as well as the physical and/or chemical properties of the species and the surface. For instance, because of its high solubility, NH_3 can easily be absorbed by the dew or thin water film on leaves and be taken up through the stomata of plants. These are believed to be major pathways for surface uptake of NH_3 (van Pul et al., 2009). Generally speaking, there are many factors that can affect the dry deposition process, including environmental conditions (e.g. relative humidity), characteristics of the deposited surface (e.g. grass or lake) and the characteristics of the species being deposited (e.g. gas or particle), which make the estimation of dry deposition even today a challenging scientific research topic.

Micrometeorological methods for the direct measurement of dry deposition have been developed and applied in many previous studies; these include eddy correlation methods and gradient flux methods (Nicholson, 1988; Pryor et al., 2002; Stocker et al., 1993). The principle disadvantages of the micrometeorological methods lie in the high instrument complexity and cost, which means micrometeorological methods are often impractical for acquiring spatial patterns and trends, especially in national and regional observation networks (van Pul et al., 2009).

As an alternative approach, the inference method can be used to estimate dry deposition (Hicks, 1985; Ruijgrok et al., 1997). In this method, the flux (or rate) of dry deposition (F) is assumed as

a product of the ambient concentration of the species (C) and its deposition velocity (V_d)(Eqn. 1.11).

$$F = C \times V_d \qquad \text{(Eqn. 1.11)}$$

To describe gas dry deposition, the deposition velocity (V_d) is defined as the reciprocal of the sum of three resistance factors (Eqn. 1.12), which are the aerodynamic

$$V_d = (R_a + R_b + R_c)^{-1} \qquad \text{(Eqn. 1.12)}$$

resistance (R_a), quasi-laminar resistance (R_b), and surface or canopy resistance (R_c), respectively (Wesely and Hicks, 2000). To describe particle dry deposition, the surface resistance is often assumed to be zero ($R_c = 0$) because particles are believed to usually adhere to the surface on contact. Additionally, the gravitational settling velocity of particles (V_s) as a function of particle size and density cannot be neglected during the deposition process. Therefore, the particle dry deposition velocity (V_d) can be described as Eqn. 1.13 (Seinfeld and Pandis, 2012) :

$$V_d = (R_a + R_b + R_a R_b V_s)^{-1} + V_s \qquad \text{(Eqn. 1.13)}$$

This inference method has been applied in the Clean Air Status and Trends Network (CASTNET), which is a national observation network operated by the U.S. Environmental Protection Agency. It includes 91 monitoring stations at 88 locations across the country. This network was partially designed to evaluate atmospheric dry deposition by combining the nitrogen species concentrations

(HNO$_3$, NO$_3^-$ and NH$_4^+$) from continuous weekly measurements and modeled deposition velocities (http://epa.gov/castnet/javaweb/docs/annual_report_2012.pdf). Based on the CASTNET report in 2012, the dry nitrogen deposition (not including NH$_3$) values at all sites were less than 2.0 Kg N ha^{-1} a^{-1}, with four eastern sites and two western sites having dry deposition fluxes over 1.8 Kg N ha^{-1} a^{-1}. A recent study (Schwede and Lear, 2014) has shown a significant spatial and temporal distribution of dry deposition in the U.S., with dry deposition constituting more than 50% of the total nitrogen deposition in many regions.

1.2.2 Wet Nitrogen Deposition

Wet nitrogen deposition is the process by which ambient nitrogen species are scavenged by atmospheric hydrometeors (cloud and fog drops, rain, and snow) and subsequently delivered to the surface (Seinfeld and Pandis, 2012). There are different kinds of atmospheric physical processes that contribute to wet deposition; these can be divided into two main groups: below-cloud and in-cloud scavenging.

In-cloud scavenging processes governing wet deposition of aerosols and gases include heterogeneous nucleation of aerosol particles, impaction and interception of aerosol particles by cloud drops, and diffusive scavenging of inactivated particles and soluble gases. Below-cloud scavenging processes include the washout of particles and gases by falling precipitation (rain and snow). Physical mechanisms at play include inertial impaction, interception, and diffusive uptake. Particle scavenging efficiency is greatly affected by the sizes of the hydrometeors and particles (Seinfeld and Pandis, 2012; Twomey, 1977). As secondary air pollutants, most (NH$_4$)$_2$SO$_4$ and

NH_3NO_3 particles are below 1 µm. Therefore, it is generally believed that the contributions of in-cloud scavenging processes of reactive nitrogen are more important than below-cloud scavenging processes (Asman, 1995), especially for particles. However, the contribution of below-cloud scavenging cannot be neglected, especially for soluble gases with local surface-based emission sources. Draaijers et al. (1989) attributed considerable NH_4^+ wet deposition in forest areas to scavenging of NH_3 emissions from agricultural sources in the vicinity. Aneja et al. (2003) found a significant relationship between the NH_4^+ concentration in wet deposition and local NH_3 emission density.

The National Trends Network (NTN) is a national wet deposition observation network in the U.S. operated by the National Atmospheric Deposition Program (NADP) to provide a long-term record of wet deposition. NTN collects weekly samples each Tuesday morning, determines the total precipitation volume, and sends samples to the Illinois State Water Survey's Central Analytical Laboratory (CAL) for chemical ion analysis, which includes nitrogen species (NO_3^- and NH_4^+) (http://nadp.sws.uiuc.edu/lib/data/2013as.pdf).
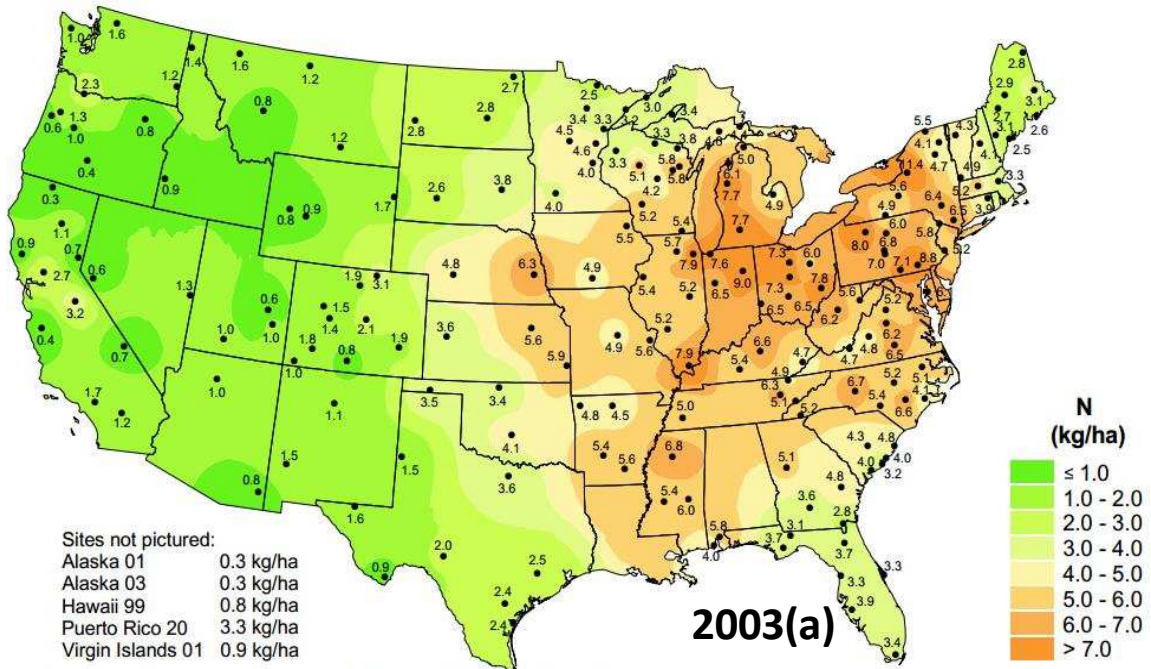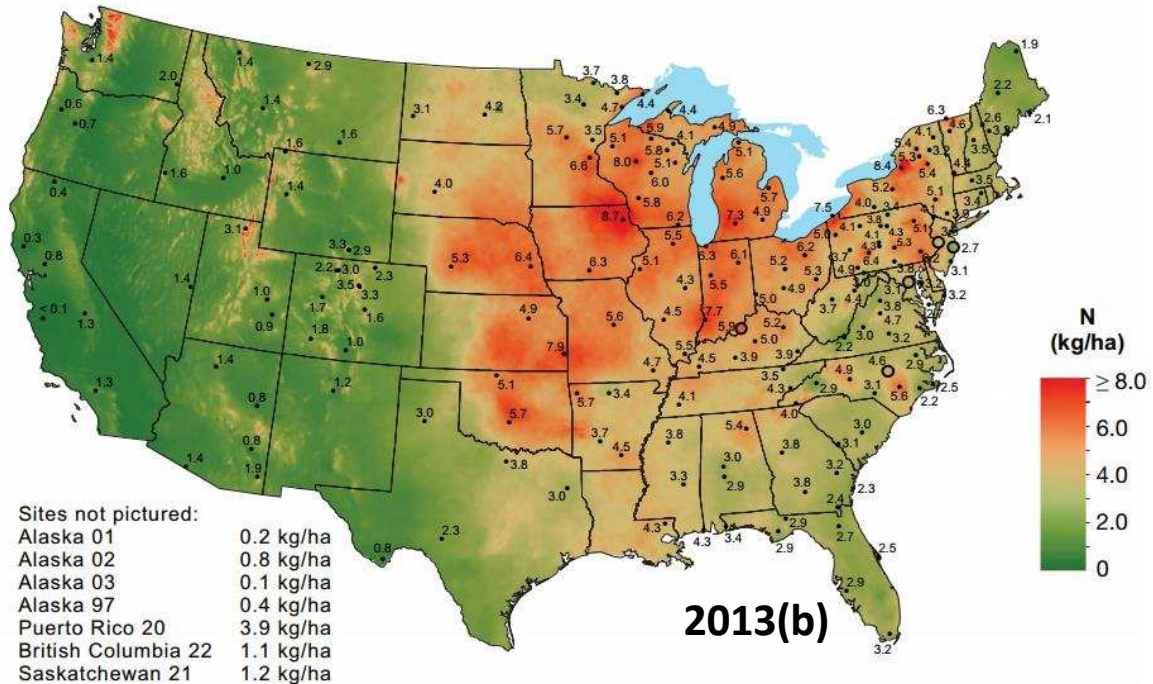
Figure 1.3 Distribution of wet nitrogen deposition (NO_3^-+NH_4^+) in the U.S in 2003 (a) and 2013 (b) (http://nadp.sws.uiuc.edu/lib/dataReports.aspx)

Figure 1.3b illustrates the current status of wet nitrogen (NO_3^-+NH_4^+) deposition across the U.S.

There is significant spatial variability in the wet deposition. Compared with the results from 2003

(Figure 1.3a), wet deposition for many regions of the western U.S. was larger in 2013 than 2003.

This is especially true in the Rocky Mountain region (Fenn et al., 2003; Lehmann et al., 2005), indicating possible influence from increases in urbanization, population, N-fertilizer application and concentrated animal feeding operations.

1.3 Research Objectives

Due to the critical roles of atmospheric nitrogen species in particulate formation and nitrogen deposition, it is imperative to increase understanding of their atmospheric concentrations in the United States. This is especially true for ammonia, which historically has not been regulated and seldom measured, and for locations in the western U.S. where measurements are sparse and contributions of reactive nitrogen species to visibility degradation and nitrogen deposition can be substantial and appear to be growing. Several investigations were undertaken as part of this research to help improve knowledge in these areas.

In order to fully investigate the spatial, seasonal, and inter-annual variations of reactive nitrogen species and their gas-particle partitioning, multi-year observations were conducted in western Wyoming and northeastern Colorado. In addition, nitrogen species data from several regional and national observation networks have been used to investigate reactive nitrogen deposition nationwide. This analysis includes study of regional contributions of various deposition pathways (e.g., dry vs. wet, oxidized vs. reduced N) and their changes over time. In summary, the major research objectives in this dissertation are to:

- Investigate concentrations of NH_3, HNO_3, and fine particles in a rural gas production region, by providing a multi-year observational dataset of seasonal and temporal variations of nitrogen species and the primary factors determining their variabilities. Characterize the major factors controlling the gas/particle partitioning process for NH_4NO_3 in this region.

- Explore spatial and temporal variability of NH_3 concentrations in the important NE Colorado agricultural production region. Compare NH_3 concentrations across the region, considering differences between urban/suburban locations, regions of intense animal production, and natural grasslands. Examine the vertical distribution of NH_3 concentrations and how it varies with season. Document inter-annual variability in NH_3 concentrations in the region. Use this observational dataset to evaluate the ability of chemical transport models and satellite retrievals to accurately represent ambient regional NH_3 concentrations.

- Characterize the spatial and temporal patterns of both dry and wet nitrogen deposition across the U.S. by incorporating observations from several regional and national monitoring networks. Examine multi-decadal trends in oxidized vs. reduced nitrogen wet deposition. Provide, for the first time, a national depiction of the importance of NH_3 dry deposition. Construct a total inorganic reactive nitrogen deposition budget and consider the relative contributions of oxidized and reduced nitrogen species to this budget by region and season.

2. EXPERIMENTAL METHODS

2.1 Sampling Site Locations

2.1.1 Boulder, Wyoming

Western Wyoming is one region of active recent gas development where several air quality concerns have been raised (McMurray et al., 2013). Emissions of NO_x have been of concern both because of possible impacts on regional haze and, especially, due to documented impacts on severe winter O_3 episodes (Schnell et al., 2009). SCR implementation in the region has been active in recent years as one effort to limit winter O_3 episodes. While these winter O_3 episodes are believed to be local in nature, NO_x emission impacts on regional haze may be more widespread. Unfortunately, few measurements exist in the region of NH_3, and haze impact assessments are generally forced to rely on assumed background NH_3 concentrations.

Measurements were made southwest of Boulder, Wyoming (42.719°N, -109.753°W) in the northwestern part of the Pinedale anticline area. Two visibility-protected areas, Bridger Wilderness Area and Fitzpatrick Wilderness Area, are located within 100 km. The Boulder area and nearby natural gas fields are situated on a high plateau between the Wind River Range to the east and the Wyoming Range to the west. Strong surface-based inversions, with inversion pools intersecting topography levels down to 50 m above ground (Schnell et al., 2009), are common in the region, especially during wintertime. The population density in Boulder, Wyoming is sparse with only 8.9 people per square km. The Jonah Gas Field and the Pinedale Anticline Gas Field, together representing one of the largest gas production regions in the U.S., are close to the sampling site with several active gas wells located approximately 3 km west of the sampling site. In 2008, there

were more than 500 permitted wells in the Jonah Gas Field and an additional 3100 wells are expected to be drilled in this field over the next 75 years. Total production in this region in 2011 was nearly 171 billion cubic feet of natural gas and 1.5 million barrels of oil (http://www.encana.com/pdf/communities/usa/JonahField-FactSheet.pdf). NO_x from the gas extraction operations and transportation emissions are the largest contributors to local NO_x emissions (Figure 2.1a). For NH_3 emissions, there are not many large sources in this immediate area. However, the Snake River Valley to the west (200 km) of the measurement site is a large area of intense agricultural activity with elevated NH_3 emissions and concentrations (Clarisse et al., 2009) (Figure 2.1b). Installation of more SCR systems in the Jonah-Pinedale region could elevate local NH_3 concentrations, contributing to more particle formation and visibility degradation.
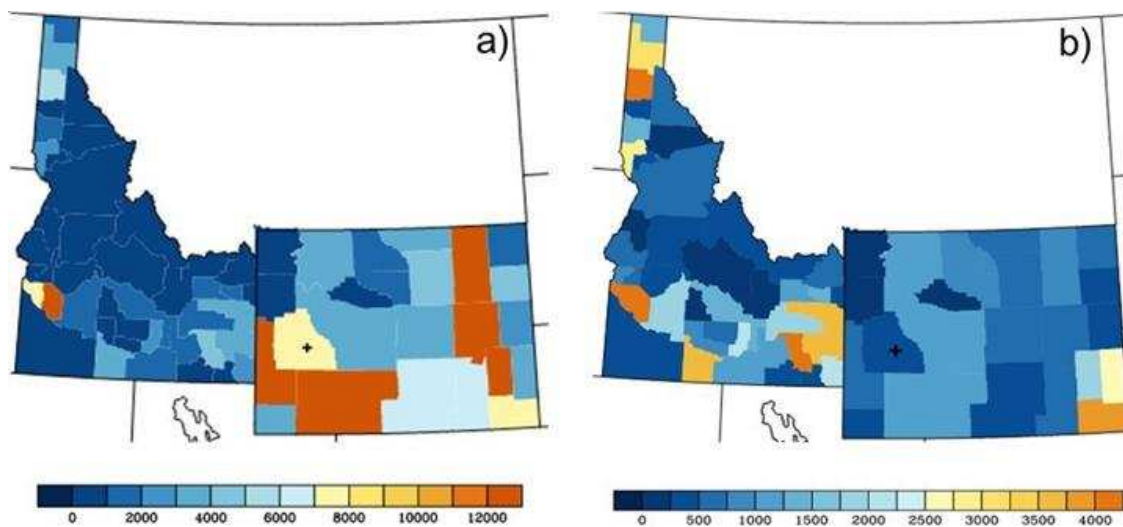
Figure 2.1 Annual emissions (in tons) by county for a) NO_x and b) NH_3 from the 2008 National Emissions Inventory (NEI-2008) (http://www.epa.gov/ttnchie1/net/2008inventory.html). The sampling sites are indicated by a (+) sign.

2.1.2 Northeastern Plains of Colorado

The northeastern plains of Colorado are an intensive agricultural area with many CAFOs, including beef cattle feedlots and dairy operations. The densely populated Front Range urban corridor is also located in this area. In order to gain information about spatial variability of NE Colorado ammonia concentrations, fourteen monitoring sites were selected in the region according to land use categories and distance from known, major NH_3 sources (Table 2.1 and Figure 2.2). Five suburban monitoring sites located in the western part of NE Colorado are representative of areas with little local agricultural influence, especially from animal feeding operations: Louisville (LE), western Fort Collins (FC_W), Loveland (LD), Loveland Golf Course (LGC) and the Boulder Atmospheric Observatory (BAO) tower. Three rural sites (Nunn, NN; Briggsdale, BE; and Ranch, RH), close to the northern boundary of Colorado with Wyoming, are grassland sites with minimal local agricultural influence. Three suburban sites (eastern Fort Collins, FC_E; Severance, SE; and Greeley, GY) as well as three rural sites (Ault, AT; Kersey, KY; and Brush, BH) represent areas close to and likely under strong influence from agricultural activities, including animal feeding operations. For example, the KY site is located approximately 0.4 km from a large beef cattle feedlot (about 100,000 cattle capacity).

Table 2.1 Information on sampling sties

ID	Site Name	Type	Latitude	Longitude	Elevation(m)	Year*	Sampler type
LE	Louisville	Suburban	39.987	-105.151	1698	11	Passive
FC_W	Fort Collins_West	Suburban	40.589	-105.148	1570	10,11,12, 13,14	Passive/URG
LD	Loveland	Suburban	40.438	-105.127	1582	10,11,12, 13,14	Passive
BAO	BAO Tower	Suburban	40.050	-105.004	1584	12	Passive/URG
GC	Golf Course	Golf course	40.426	-105.107	1551	10,11, 12, 13,14	Passive
FC_E	Fort Collins_East	Suburban – agricultural	40.591	-104.928	1562	12, 13	Passive
SE	Severance	Suburban – agricultural	40.572	-104.836	1550	12, 13,14	Passive
GY	Greeley	Suburban – agricultural	40.389	-104.751	1492	10,11, 12, 13,14	Passive
NN	Nunn	Rural	40.821	-104.701	1644	11,12, 13,14	Passive
BE	Briggsdale	Rural	40.635	-104.330	1481	10,11,12,13,14	Passive

RH	Ranch	Rural	40.473	-104.317	1475	10	Passive
AT	Ault	Rural-agricultural	40.612	-104.709	1514	11,12,13,14	Passive
KY	Kersey	Rural-agricultural	40.377	-104.532	1403	10,11, 12, 13,14	Passive
BH	Brush	Rural-agricultural	40.313	-103.602	1286	10,11, 12,13,14	Passive/URG

* Sampling period: 05/20/2010-09/02/2010; 06/02/2011-08/31/2011; 06/21/2012-08/29/2012; 05/30/2013-08/29/2013; 05/29/2014-08/28/2014

Figure 2.2 The locations of 14 observation sites in northeastern Colorado (red, green and yellow colors stand for suburban, agricultural and rural sites, respectively). Sites that did not sample all five years, 2010-2014, have the sampling years indicated.

The BAO tower is a 300 m meteorological tower situated in the southern part of the sampling area (40.050°N, 105.004°W) (Figure 2.2 and Figure 2.3). It has been owned and operated by the National Oceanic and Atmospheric Administration (NOAA) for more than 25 years (http://www.esrl.noaa.gov/psd/technology/bao/). The tower is surrounded by natural grass and wheat fields, and is approximately 400 m west of Interstate 25 and 30 km north of downtown Denver.
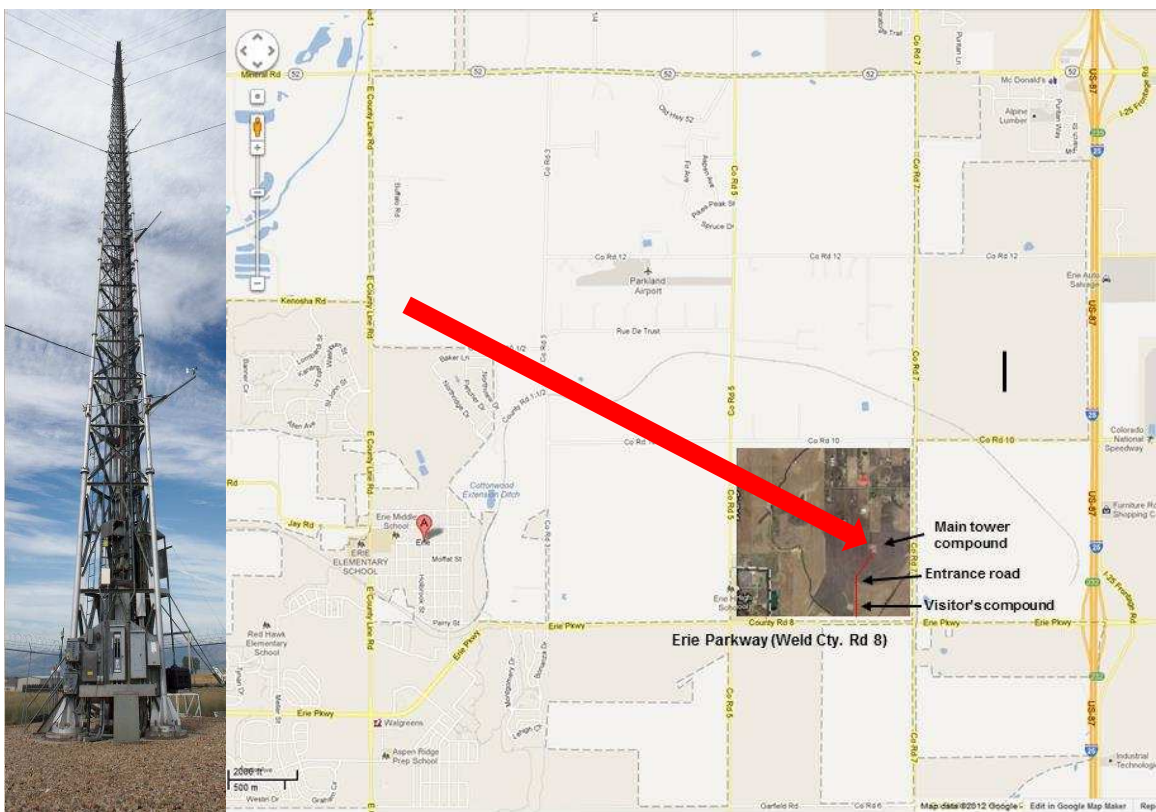
Figure 2.3 Photograph and location of the BAO tower
(http://www.esrl.noaa.gov/psd/technology/bao/)

2.1.3 CASTNET, Pilot IMPROVE NH$_x$, AMoN and NTN Network

Weekly precipitation concentrations of NH_4^+ and NO_3^- were obtained from the NADP National

Trends Network (NTN; http://nadp.isws.illinois.edu/ntn/). Weekly gaseous HNO_3 concentrations

and particulate NH_4^+ and NO_3^- concentrations were obtained from the Clean Air Status and Trends

Network (CASTNET; http://epa.gov/castnet/javaweb/index.html). Bi-weekly concentrations of

gaseous NH_3 were taken from the NADP Ammonia Monitoring Network (AMoN; http://nadp.isws.

illinois.edu/AMoN/). In order to gain greater spatial coverage of NH_3 concentrations, especially in

the western U.S., NH_x ($NH_3+NH_4^+$) measurements with a 1-in-3 day sampling period made in a

pilot Interagency Monitoring of Protected Visual Environments (IMPROVE) NH_x monitoring

29

network (Chen et al., 2014) were also used. More detailed information about these observation networks can be found in Table 2.2.

Wet deposition data were obtained from NTN sites for the periods 1990-1992 and 2010-2012. The number of sites changed due to network development over this period. From 1990-1992 there were 195 sites; 238 sites were available for the 2010-2012 period. Sites were not included if data were unavailable for one or more years in either period examined.

Oxidized and reduced N gas and particle concentrations were obtained for 37 sites (see Table 2.2) where NTN and CASTNET sites were co-located with AMoN and/or IMPROVE NH_x sites. At 30 of these locations two years of measurements (July 2011 to June 2013) were available. The remaining 7 sites had data availability of at least one year.

Table 2.2 Summary of data from U.S. national networks used in the study

Network	Deposition Species	Data Period	Source
AMoN[1]	Dry Deposition: gaseous NH_3	2011-2013	http://nadp.isws.illinois.edu/AMoN
CASTNET[2]	Dry Deposition: gaseous HNO_3, particulate NH_4^+, NO_3	2011-2013	http://epa.gov/castnet/javaweb/index.html
NTN[3]	Wet Deposition: NH_4^+, NO_3^-	1990-2013	http://nadp.isws.illinois.edu/NTN
IMPROVE NHx[4]	Dry Deposition: gaseous NH_3, particulate NH_4^+, NO_3^-	2011-2012	*Chen et al.,* 2014

1   The Ammonia Monitoring Network (AMoN) is operated by the National Atmospheric Deposition Program (NADP), which measures biweekly NH_3 concentrations using passive diffusion (Radiello^{TM}) samplers.

2   The Clean Air Status and Trends Network (CASTNET), funded by the Environmental Protection Agency (EPA) and National Park Service (NPS), which measures weekly HNO_3 and particulate NH_4^+ and NO_3^- concentrations using 3-stage filter pack samplers.

3   The National Trends Network (NTN) is operated by the National Atmospheric Deposition Program (NADP), which measures NH_4^+, NO_3^- concentrations in weekly precipitation samples.

4   The Interagency Monitoring of Protected Visual Environments (IMPROVE) NH_x study, conducted from April 2011 to August 2012, measured the sum of gaseous NH_3 and fine particle NH_4^+ concentrations using a single, acid-coated filters with 1-in-3 day sampling periods. Co-located measurements of NH_4^+, NO_3^- and sulfate (SO_4^{2-}) collected on nylon filters provide two methods to determine the split of measured NH_x between gaseous NH_3 and fine particle NH_4^+; here we assume that fine particle NO_3^- and SO_4^{2-} are fully neutralized by NH_4^+ to estimate the NH_4^+ concentration which was then subtracted from the NH_x concentration to obtain a lower bound estimate of the NH_3 concentration (*Chen et al.,* 2014).

2.2. Sampling Instruments

2.2.1 URG Denuder/Filter System

Denuder/filter pack samplers were used to collect gas and particle phase species at Boulder, WY and at select NE Colorado sites. Concentrations of gaseous NH_3 and HNO_3 and $PM_{2.5}$ inorganic ions (NH_4^+, SO_4^{2-}, NO_3^-, K^+, Mg^{2+} and Ca^{2+}) were sampled using a URG denuder/filter system (Model 3000CA) (

Figure 2.4), which was installed at 1.5 m height, followed by laboratory extraction and analysis by ion chromatography. The URG sampling system has been widely used because of its good performance in sampling gases and particles (Bari et al., 2003; Beem et al., 2010; Edgerton et al., 2007; Lee et al., 2004; Lin et al., 2006). Air was drawn through a Teflon-coated $PM_{2.5}$ cyclone followed by two 242 mm annular denuders connected in series, a 47-mm filter pack containing a nylon filter (Nylasorb, 1μm pore size, Pall Corporation) and another annular denuder (from Dec. 2006 through July 11th 2008, samples were collected used a backup coated filter rather than a 3rd denuder). Air flow was maintained at a constant mass flow rate by means of a mass flow controlled pump (URG Inc.).
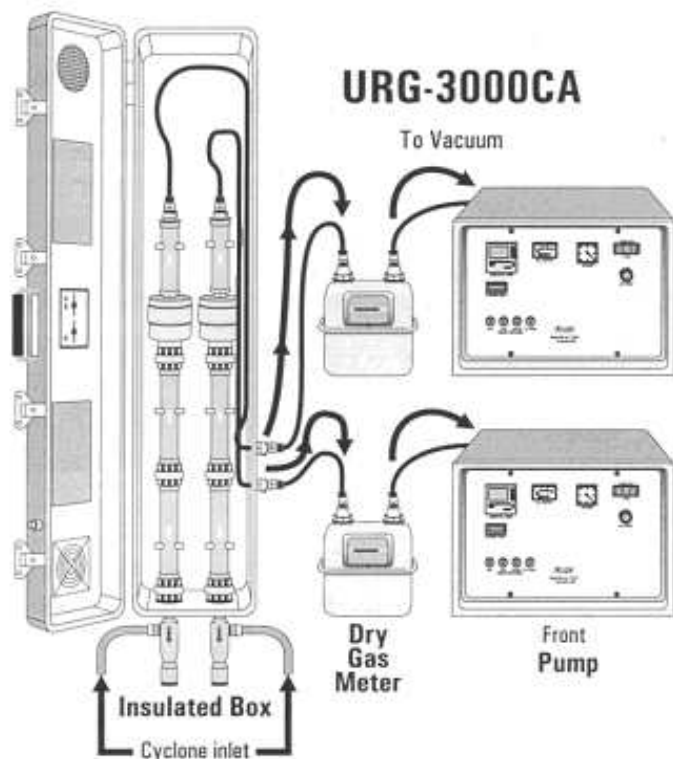
Figure 2.4 Schematic of a dual channel URG annular denuder/filter pack system

For the project in Boulder, Wyoming, The total flow rate through the system was nominally 10 L min^{-1} at ambient conditions. Actual sample volumes were determined using a dry gas meter corrected for sample pressure drop. The first denuder was coated with sodium chloride (NaCl) to collect gaseous HNO_3 and the second was coated with phosphorous acid (H_3PO_3) to collect gaseous NH_3. The last denuder (or coated filter) was phosphorous acid-coated to collect any NH_3 re-volatilized from NH_4^+ salt particles collected on the filter. Nylon filters have been shown to retain volatilized HNO_3, but loss of NH_4^+ can be significant (Yu et al., 2006). The sample trains were prepared in the lab at Colorado State University (CSU), and then shipped weekly and installed by a local site operator. Samples were typically collected twice a week (one 4 day sample and one 3 day sample). After sampling, the sample train was shipped back to the lab at CSU. The denuders

were extracted with 10 ml deionized water, and the extracts refrigerated before analysis. Nylon filters were ultrasonically extracted for 55 min in 6 ml of high purity deionized water. Meteorological data, including temperature, relative humidity and wind speed, were obtained from a co-located weather station (2 m height) operated by Air Resource Specialists, Inc.

For the project in northeastern of Colorado, the URG sampling system was used as a reference method for evaluating the performance of the NH_3 passive samplers. During the same sampling periods as the NH_3 passive samplers, URG denuder/filter-pack sampling systems were also installed at the FC_W, GY and BAO tower sites to measure the concentrations of gaseous NH_3 and HNO_3, as well as fine particulate inorganic ions (NH_4^+, K^+, Na^+, Mg^{2+}, Ca^{2+}, SO_4^{2-}, NO_3^- and Cl^-). Air was drawn first through a Teflon-coated $PM_{2.5}$ cyclone ($D_{50}=2.5$ µm) at the inlet, followed by two annular denuders connected in series. The first denuder was coated with sodium carbonate (Na_2CO_3) solution (10 g of Na_2CO_3 and 10 g of glycerol dissolved in 500 ml of deionized water (18.2 Mohm-cm) and 500 ml methanol) to collect gaseous HNO_3 and sulfur dioxide (SO_2). The second denuder was coated with a phosphorous acid (H_3PO_3) solution (10 g of H_3PO_3 dissolved in 100 ml of deionized water and 900 ml methanol) to collect gaseous NH_3. The air was then drawn through a filter pack containing a 47-mm nylon filter (Nylasorb, pore size 1 µm, Pall Corporation) to collect fine particles, followed by a backup H_3PO_3-coated denuder to capture any NH_3 re-volatilized from NH_4^+ salt particles collected on the nylon filter. The air flow rate was controlled by a URG mass flow-controlled pump; the total flow rate through the system was nominally 3 L/min both at FC_W, GY and BAO.

2.2.2 Passive Sampler

In order to obtain spatial and vertical distributions of NH_3 concentrations, two sampling campaigns were carried out in the northeastern plains of Colorado using Radiello passive NH_3 samplers and URG denuder/filter-pack systems. The Radiello passive NH_3 sampler consists of a cartridge adsorbent (part number: RAD168), a blue microporous cylindrical diffusive body (part number: RAD1201) and a vertical adapter (part number: RAD 122) (Figure 2.5). All Radiello sampler components were obtained from Sigma Aldrich (http://www.sigmaaldrich.com). Measurements of the spatial NH_3 distribution were conducted each summer from 2010 to 2014. During the first summer (2010), measurements were made at nine sites; in 2011, the Ranch (RH) site was removed and the LE and NN sites were added; in 2012, the LE site was removed; two sites, FC_E and SE, were added in 2013. The two site removals were due to property access issues. For the second campaign, measurements of vertical NH_3 concentration profiles were conducted at the BAO tower from December 2011 to January 2013.

Figure 2.5 The Radiello passive NH_3 sampler blue microporous cylindrical diffusive body (left) and cartridge adsorbent (right)

Passive ammonia samplers have been used in several studies because of their reliability, low labor intensity, simplicity and lack of power requirement (Cisneros et al., 2010; Day et al., 2012; Meng et al., 2011; Puchalski et al., 2011; Reche et al., 2015). During sample collection, the sampler was protected from precipitation and direct sunlight by an inverted plastic bucket. Ambient NH_3 diffuses through a microporous diffusive body surface and is captured as ammonium ion by a cartridge impregnated with phosphoric acid (H_3PO_4). A weekly sampling campaign period was implemented in each summer during the study: May 20th to September 2nd 2010, June 2nd to August 31st 2011, June 21st to August 29th 2012, May 30th to August 29th 2013, and May 29th to August 28th 2014. At the BAO tower, NH_3 was sampled at nine heights: 1 m, 10 m, 22 m, 50 m, 100 m,

150 m, 200 m, 250 m and 300 m. Vertical profiles were measured across two week sampling periods from December 13th 2011 to January 9th 2013, except that weekly measurements were conducted during the summer from June 19th to August 30th 2012 when higher concentrations were anticipated. Passive samplers were prepared in an ammonia-free laminar flow hood (Envirco Corporation) and sealed for transport to the field. More detailed information can be obtained at Day et al. (2012).

The ambient NH_3 concentration was calculated based on the characteristics of the passive sampler and the diffusivity of NH_3 in the atmosphere (D_{NH3}), which is a function of local temperature (T) and ambient pressure (P), and can be expressed using Eqn. 2.1:

$$D_{NH3}(T,P) = D_{0,1} \times (\frac{P_0}{P}) \times (\frac{T}{T_0})^{1.81}$$ (Eqn. 2.1)

Where $D_{0,1}$ = 0.1978cm^{2}s^{-1} at T_0 = 273K(0 ^{o}C) and P_0 = 1 atm (*Massman*, 1998). Then, the diffusional flow rate through the NH_3 passive sampler (Q_{NH3}) is given by Eqn. 2.2:

$$Q_{NH3} = D_{NH3}(T,P) \times \frac{A}{\Delta X}$$ (Eqn. 2.2)

where *A* is the passive sampler effective cross-sectional area and ΔX is the passive sampler diffusion distance. For the Radiello NH_3 passive sampler, $A/\Delta X$ represents the geometric constant for radial flow and has been reported to be 14.2 cm, based on actual physical measurements (Day et al., 2012) which differs from the manufacturer's description (http://www.radiello.com/english/nh3_en.htm). Finally, the NH_3 concentration in the air (C_{NH3}) is

calculated from the diffusional flow rate (Q_{NH3}), the duration of sampling time (t) and the mass of NH$_3$ collected on the cartridge (m_{NH3}) as shown below:

$$C_{NH3} = \frac{m_{NH3}}{t \times Q_{NH3}}$$

(Eqn. 2.3)

For the northeastern plains network, hourly temperature data were obtained from nearby CoAGMET weather stations (http://www.coagmet.com/) (Table 2.3). The average meteorological record was fairly consistent from year-to-year. The ambient pressure was calculated based on the elevation of each site. At the BAO tower, temperature and relative humidity were measured by battery-powered sensors (EBI20-TH1, EBRO Inc. Ingolstadt, Germany; http://shop.ebro.com/chemistry/ebi-20-th.html), which were co-located with the NH$_3$ passive samplers at each sampling height (Figure 2.6).

Table 2.3 Meteorological information near the sites during the sampling period in each year.

Station	Wind Direction(degree)					Wind Speed	Temperature	Relative Humidity
	2010	2011	2012	2013	2014	m/s	°C	%
ALT01 (Nearby site: NN, AT)								
BRG01 (Nearby site: BE, BH)								
FTC01 (Nearby site: LD, FC_W, GC)								
FTC03 (Nearby site: SE, FC_E)								
LCN01 (Nearby site: GY, FC_E)								
KSY01 Nearby site: BE, BH)								
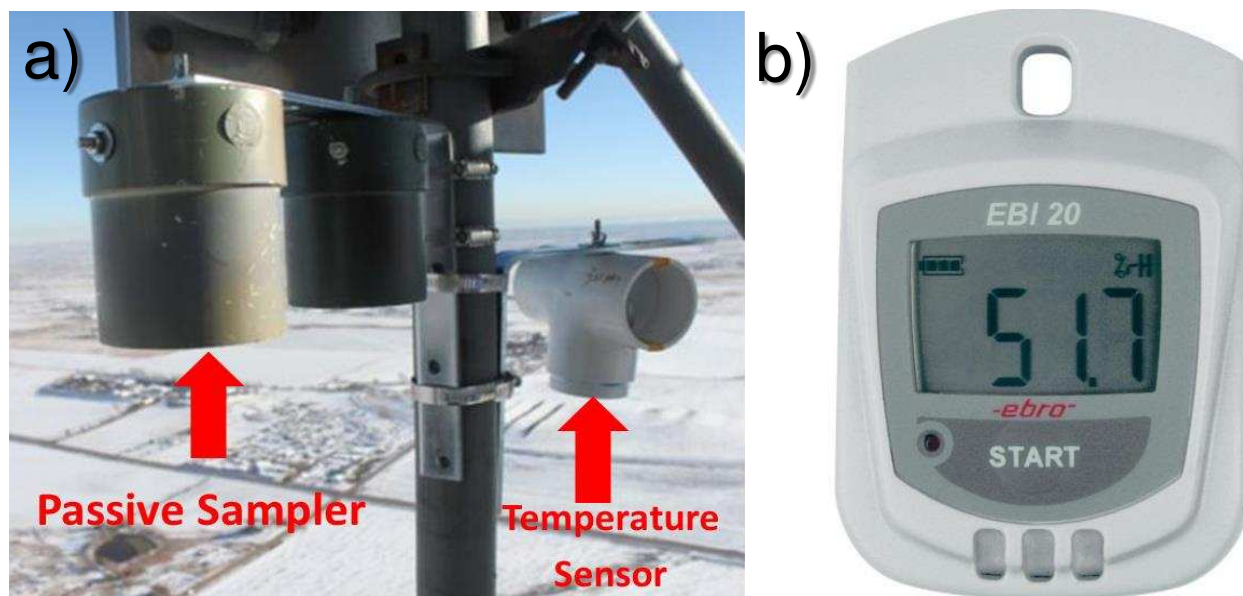
Figure 2.6 Photograph of the installation of the passive sampler (a) and temperature sensor (b) on the BAO tower

2.2.2 Ion Chromatography

Ion chromatography using a Dionex dual channel system was used to analyze the denuder and filter extracts and passive sampler extracts. Cations (Na^+, NH_4^+, K^+, Mg^{2+} and Ca^{2+}) in the samples were separated with a methanesulfonic acid eluent on a Dionex CG12A guard column and CS12A separation column followed by a CSRS ULTRA II suppressor and detected by a Dionex conductivity detector. Anions (Cl^-, NO_3^-, SO_4^{2-}) in the samples were separated with a carbonate/bicarbonate eluent on a Dionex AG14A guard column and AS14A separation column followed by an ASRS ULTRA II suppressor and detected using a Dionex conductivity detector.

2.3 Quality Assurance and Quality Control

For the measurement in Boulder, Wyoming, sample recovery was high, although there were occasional periods where samples could not be collected on the normal schedule (e.g., from bad weather affecting sampler shipment or operator access). Field and laboratory blanks were collected throughout the study and used to determine the method detection limit (MDL) and to blank-correct results. The MDLs for NH_3, HNO_3, NH_4^+, SO_4^{2-}, NO_3^-, K^+, Mg^{2+} and Ca^{2+} were determined as 0.012, 0.012, 0.002, 0.017, 0.001, 0.005, 0.007 and 0.023 μg m^{-3}, respectively. Replicate extract analyses yielded measurement precisions of 5.4%, 3.8%, 3.5%, 0.8%, 2.1%, 4.9%, 7.6%, and 6.2% (relative standard deviation) for NH_3, HNO_3, NH_4^+, SO_4^{2-}, NO_3^-, K^+, Mg^{2+} and Ca^{2+}, respectively.

Replicate Radiello passive samples were collected at FC_W (2011, weekly), BH (2012, 2013 and 2014, weekly), Greeley (2014, weekly), Kersey (2014, weekly) and three different heights (1 m, 100 m and 300 m) of the BAO tower (biweekly; weekly in summer) during the campaign to evaluate the performance of NH_3 passive samplers under different NH_3 concentrations and sampling periods. Comparison of replicate samples yielded good precision (Figure 2.7) with a pooled relative standard deviation of 8.4%. The weekly and
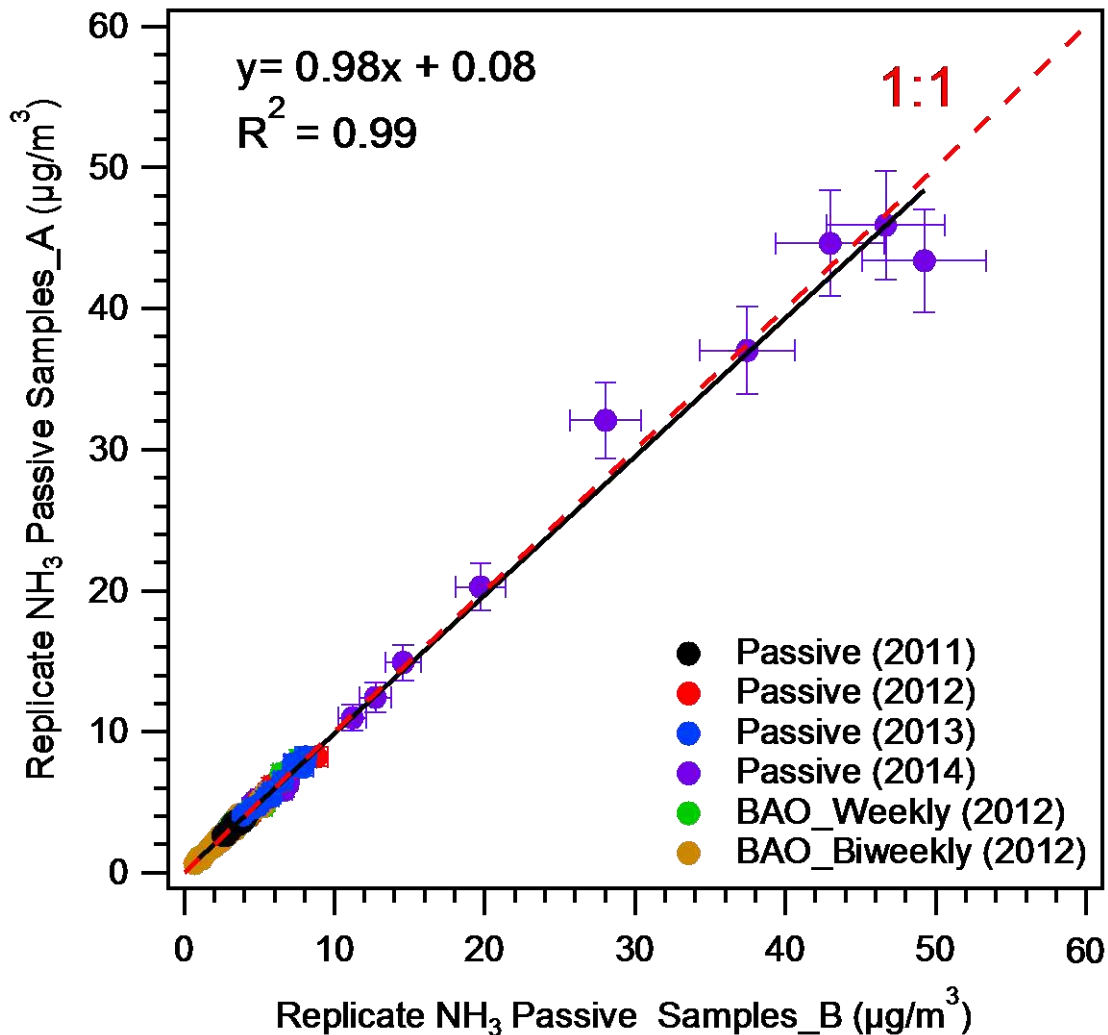
Figure 2.7 Comparison of ammonia concentrations measured by replicate passive samplers. The error bars represent the relative standard deviation of 8.4 % calculated from all 280 pooled replicate samples.

biweekly NH_3 concentrations collected by passive samplers were also in good agreement with measurements by co-located URG denuder samplers for the same sampling durations (a linear least-squares regression fit yielded a squared correlation coefficient (R^2) between the two methods of 0.97 with a slope of 96% and a small positive intercept ($0.18 \, \mu g/m^3$) (Figure 2.8). These findings are consistent with previous studies (Benedict et al., 2013b; Day et al., 2012; Puchalski et al., 2011). Field and laboratory blanks were collected throughout the research campaign and used to

blank correct sample results and determine the minimum detection limits (MDL). From the field

blanks, the MDL was calculated to be 0.27 µg/m^3 for a one-week Radiello passive NH$_3$ sample.
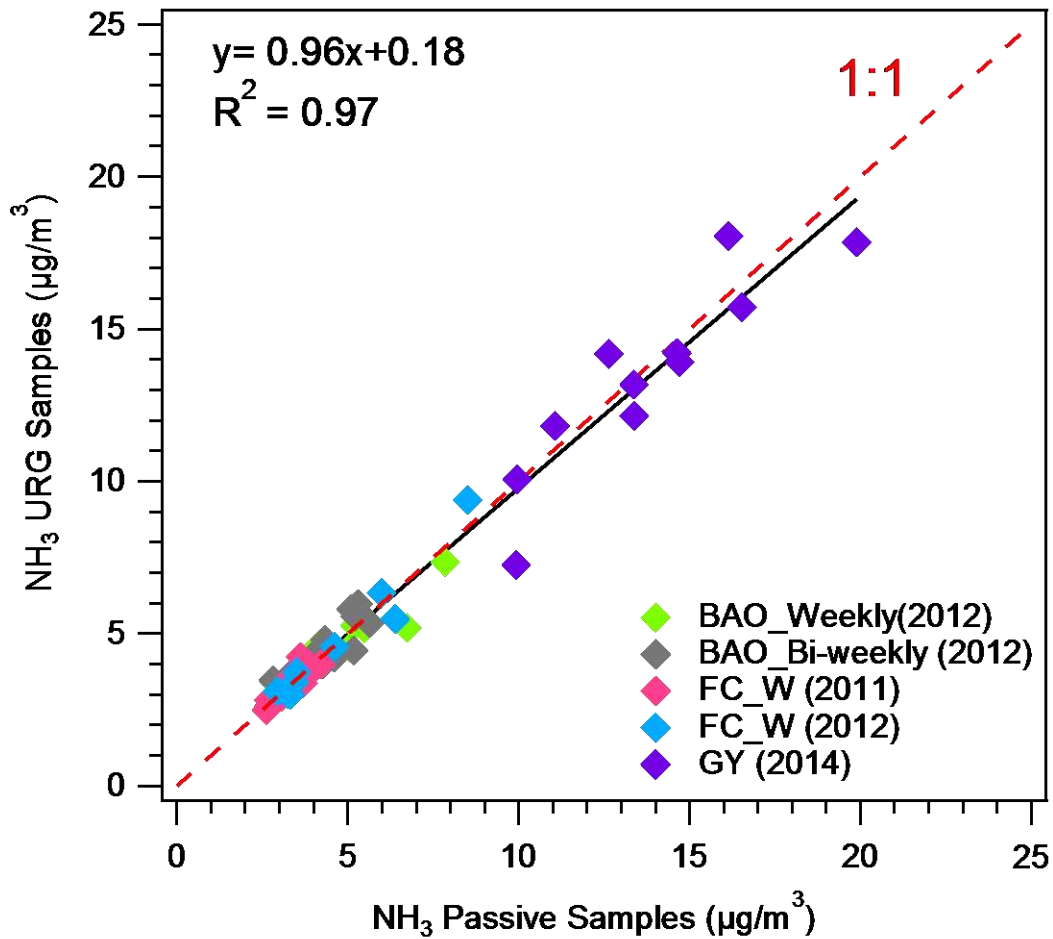
Figure 2.8 Comparison of NH$_3$ concentrations from the Radiello passive samplers and URG samplers

2.4 Nitrogen Deposition Calculation

Wet N deposition was determined from the amount of total precipitation and the aqueous concentrations of NH_4^+ and NO_3^-, as reported by NTN. Dry N deposition was calculated for each species as the product of the N species concentration and a deposition velocity. The deposition velocities of gaseous HNO_3 and particulate NH_4^+ and NO_3^- were provided by CASTNET for each of its measurement sites based upon the MLM (Meyers et al., 1998), with input of on-site meteorology and local site characteristics. Gaps in the meteorological data were addressed by using the CASTNET substitution method (Bowker et al., 2011). The deposition velocity of NH_3 is difficult to determine due to the bi-directional nature of the NH_3 flux which depends strongly on local conditions (Massad et al., 2010) . In order to estimate NH_3 deposition here, its deposition velocity was calculated as 70% of the HNO_3 deposition velocity provided by CASTNET following previous estimates (Beem et al., 2010; Benedict et al., 2013b; Benedict et al., 2013c). To inform the potential uncertainty of this approach, this MLM deposition velocity method was compared to NH_3 fluxes estimated using a two-layer bi-directional flux model (Nemitz et al., 2001). The bi-directional model employs hourly CASTNET meteorology and two-week integrated AMoN NH_3 concentrations to estimate NH_3 exchange with soil and vegetation, as well as net fluxes above the vegetation. Ammonia compensation points and leaf surface resistances were parameterized following the recommendations of (Massad et al., 2010) for natural vegetation. Development of this modeling framework, described in more detail in Appendix A, is ongoing. Thus, the comparison with MLM is constrained to the dominant natural vegetation type at each site for which the Massad et al. (2010) parameterizations are applicable. Due to a lack of data, not all N_r species

are included in the deposition budget. Missing compounds include inorganic (e.g., NO_x and nitrous oxide) and organic N (e.g., peroxyacetyl nitrate and amines) species.

3. MULTI-YEAR OBSERVATIONS OF AMMONIA, NITRIC ACID AND FINE PARTICLES IN A RURAL GAS PRODUCTION REGION[1]

While a number of recent studies have considered the role NH_3 plays in the formation of fine particles across the United States in both urban and rural areas (Bari et al., 2003; Benedict et al., 2013c; Edgerton et al., 2007; Gong et al., 2011; Heald et al., 2012; Nowak et al., 2010; Sharma et al., 2007), knowledge of atmospheric concentrations of NH_3, and their seasonal variability is still rather limited, especially in the interior western United States. Here we present five years of observations of concentrations of gaseous NH_3 and HNO_3 and fine particle concentrations of NH_4^+, SO_4^{2-} and NO_3^- from Boulder, Wyoming, a site in the heart of an active gas production region. These measurements provide the longest term record of NH_3 concentration measurements in this part of the U.S. and provide new insight into typical NH_3 concentrations in the region, their seasonal variability, and the gas-particle partitioning of the NH_3–NH_4^+–HNO_3–NO_3^-–SO_4^{2-} system that is one important contributor to regional haze.

---

[1] *This chapter comprises the results and discussion and summary sections of a paper published in Atmospheric Environment Li, Y., Schwandner, F.M., Sewell, H.J., Zivkovich, A., Tigges, M., Raja, S., Holcomb, S., Molenar, J.V., Sherman, L., Archuleta, C., Lee, T., Collett Jr., J.L., 2014. Observations of ammonia, nitric acid, and fine particles in a rural gas production region. Atmospheric Environment 83, 80-89.. Yi Li is the lead author. Contributing co-authors include Florian M. Schwandner, H. James Sewell, Angela Zivkovich, Mark Tigges, Suresh Raja, Stephen Holcomb, John V. Molenar, Lincoln Sherman, Cassie Archuleta, Taehyoung Lee, Jeffrey L. Collett, Jr.*

From December 2006 through December 2011, 505 samples were collected. The summary of the annual and seasonal mean and standard deviation for all the trace gas concentrations, particulate species concentrations and meteorological parameter values are summarized in Table 3.1. Because of the high latitude of this continental sampling site and the monthly average temperatures, the following months were defined as representing specific seasons, for the purpose of discussing the analytical results below: April and May were defined as spring; June, July and August as summer; September and October as fall; and November through March as winter.

Table 3.1 Seasonal and yearly averages and standard deviations of gases, aerosol species and meteorological parameters.

Season		NH_3	HNO_3	NO_3^-	SO_4^{2-}	NH_4^+	K^+	Mg^{2+}	Ca^{2+}	T	RH	WS
		$\mu g/m^3$	$\mu g/m^3$	$\mu g/m^3$	$\mu g/m^3$	$\mu g/m^3$	$\mu g/m^3$	$\mu g/m^3$	$\mu g/m^3$	°C	%	m/s
Spring	Mean	0.14	0.13	0.18	0.65	0.23	0.01	0.02	0.04	4.80	56.76	5.24
(N=80)	SD	0.12	0.12	0.09	0.33	0.12	0.01	0.03	0.04	4.54	11.10	1.30
Summer	Mean	0.38	0.23	0.11	0.54	0.26	0.03	0.01	0.04	15.67	45.59	4.31
(N=126)	SD	0.23	0.11	0.08	0.23	0.15	0.03	0.01	0.03	3.68	13.10	0.66
Autumn	Mean	0.18	0.18	0.12	0.51	0.22	0.02	0.01	0.05	7.17	54.94	4.12
(N=87)	SD	0.14	0.11	0.07	0.23	0.10	0.01	0.00[a]	0.03	5.37	14.07	1.09
Winter	Mean	0.04	0.19	0.60	0.36	0.28	0.01	0.00[b]	0.02	-7.76	72.54	3.85
(N=212)	SD	0.06	0.18	0.60	0.23	0.17	0.01	0.00[c]	0.03	5.45	8.67	1.76
2007	Mean	0.14	0.22	0.30	0.54	0.29	0.02	0.01	0.03	3.82	57.82	4.17
(N=105)	SD	0.18	0.17	0.28	0.32	0.12	0.03	0.02	0.03	11.43	17.06	1.16
2008	Mean	0.20	0.20	0.36	0.53	0.28	0.01	0.01	0.03	2.33	59.00	4.63

(N=104)	SD	0.27	0.19	0.47	0.31	0.20	0.02	0.02	0.04	10.69	16.91	1.68
2009	Mean	0.23	0.17	0.29	0.47	0.23	0.02	0.00	0.03	3.04	63.27	4.14
(N=101)	SD	0.21	0.10	0.43	0.23	0.12	0.01	0.01	0.04	10.10	13.96	1.22
2010	Mean	0.15	0.17	0.27	0.38	0.22	0.01	0.01	0.03	3.97	59.66	4.25
(N=97)	SD	0.15	0.12	0.41	0.20	0.12	0.01	0.01	0.02	10.58	16.25	1.53
2011	Mean	0.13	0.18	0.37	0.47	0.27	0.02	0.01	0.04	2.46	61.2	4.0
(N=98)	SD	0.15	0.13	0.56	0.26	0.14	0.01	0.01	0.04	10.64	13.81	1.50

[a] The actual value is 0.003.

[b] The actual value is 0.003.

[c] The actual value is 0.004.

[d] N,T, RH and WS represent the number of samples, temperature, relative humidity and wind speed, respectively.

3.1 Concentrations of Ammonia, Nitric Acid and Fine Particle Species and Their seasonal Patterns

Figure 3.1 shows time series of the concentrations of gaseous NH_3 and HNO_3 and $PM_{2.5}$ NH_4^+ and NO_3^- across the five year measurement period. NH_3 concentrations peak in summer while NO_3^- concentrations peak in winter. HNO_3 exhibits a distinct bimodal seasonal concentration pattern with summer and winter maxima. As shown in Figure 3.2, NH_4^+, SO_4^{2-} and NO_3^- were the three most abundant inorganic ions in $PM_{2.5}$ in all seasons. The concentration of NH_4^+ varied least across seasons. During the warm season SO_4^{2-} was the most abundant inorganic anion in $PM_{2.5}$, while during winter the concentration of NO_3^- was highest. More details concerning the trends of each of the trace gas and particulate species will be presented below.
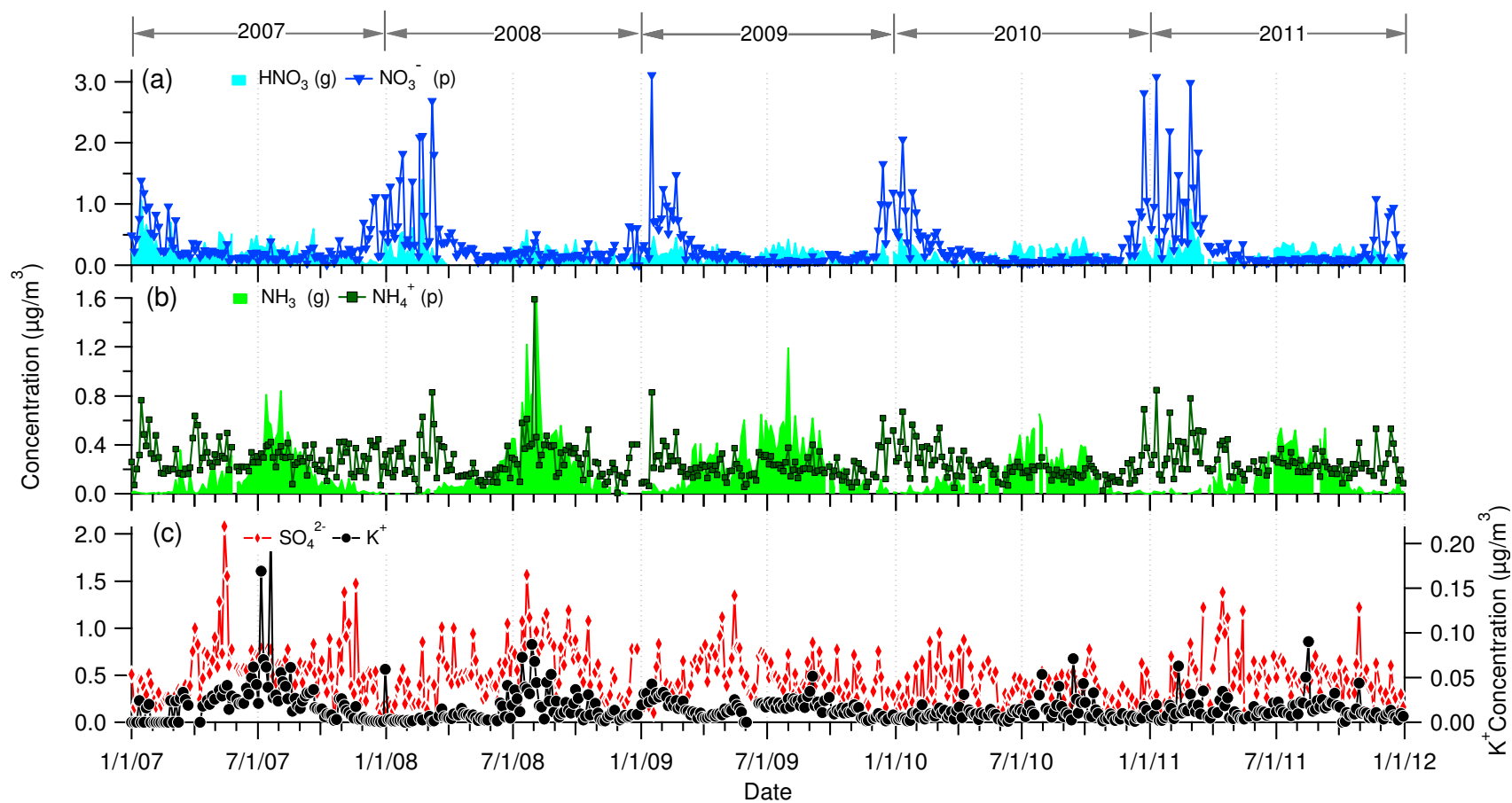
Figure 3.1 Temporal variations of concentrations of (a) HNO_3 and NO_3^-, (b) NH_3 and NH_4^+ and (c) SO_4^{2-} and K^+ from 2007 through 2011 at Boulder, Wyoming.
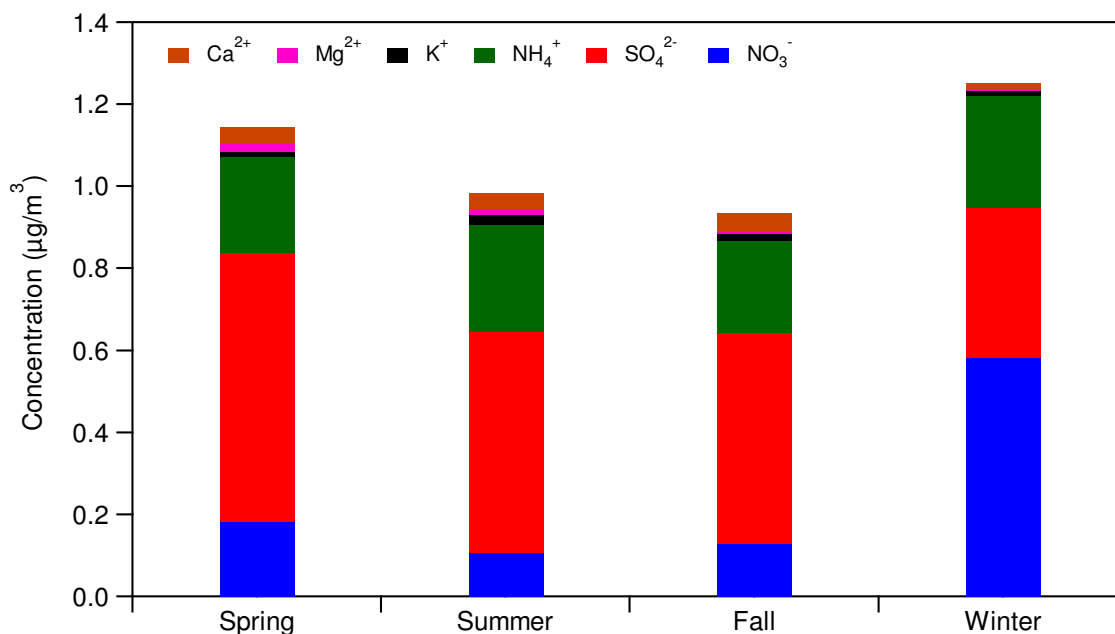
Figure 3.2 Average mass concentrations of the chemical species in PM$_{2.5}$ by season across the 5 year sampling period.

Gaseous NH$_3$ exhibited a clear seasonal concentration pattern, ranging from an average concentration of 0.04 μg m^{-3} in winter to 0.39 μg m^{-3} in summer (Figure 3.3a). The maximum quarterly NH$_3$ average concentration was 0.47 μg m^{-3} in summer 2008, 15 times higher than the winter 2008–2009 average of 0.03 μg m^{-3}. The significantly higher summer concentration reflects a strong influence of temperature. Previous studies have reported similar phenomena (Edgerton et al., 2007; Gupta et al., 2003; Meng et al., 2011; Plessow et al., 2005; Walker et al., 2004). Higher levels of NH$_3$ in the summer are consistent with the positive influence of higher temperatures on NH$_3$ emissions (e.g., from natural soils, agricultural operations, and fires) and the decomposition of particulate NH$_4$NO$_3$ into gaseous NH$_3$ and HNO$_3$.

One potential local source of NH$_3$ is increased use of SCR for high-efficiency NO$_x$ control on drill rigs in the region. While use of SCR increased during the period of observation at Boulder,

however, there is no clear increase in local NH_3 concentrations over the study. The annual mean concentration of NH_3 did not significantly increase during the study period. From 2007 to 2011, the annual NH_3 average concentrations in each year were 0.14, 0.20, 0.23, 0.15 and 0.13 μg m^{-3}, respectively, suggesting that SCR emissions did not noticeably influence local concentrations of ambient NH_3.
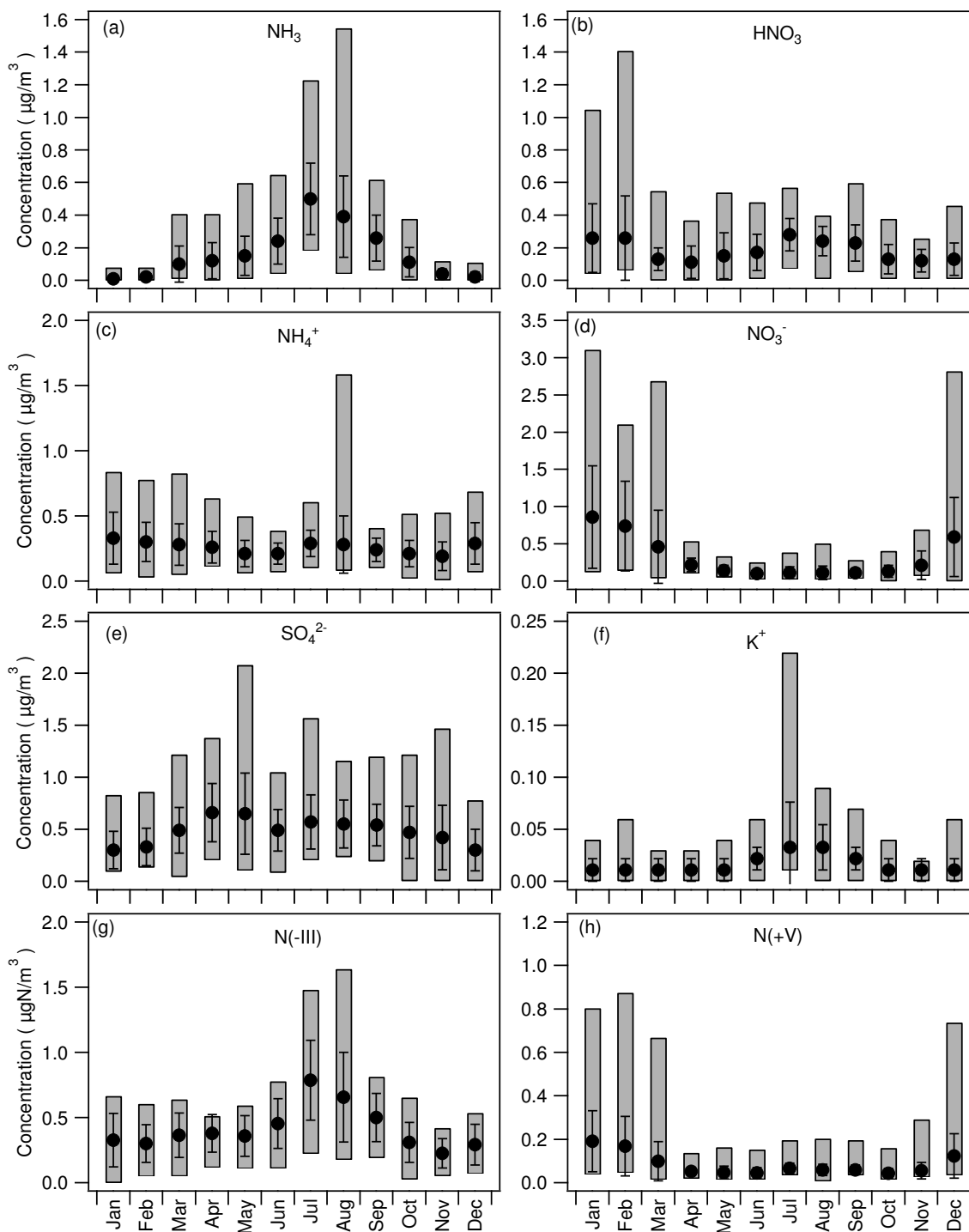
Figure 3.3 The monthly variation of (a) NH_3, (b) HNO_3, (c) NH_4^+, (d) NO_3^-, (e) SO_4^{2-}, (f) K^+, (g) N(-III) and (h) N(+V) concentrations from 2007 to 2011. The grey shading represents minimum and maximum concentrations and the y-error bars represent standard deviations of average concentrations. For panels (a) to (f) the concentrations are expressed in $\mu g/m^3$; in panels (g) and (h) the concentrations are expressed as $\mu g\ N/m^3$.

Table 3.2 shows cross-correlation coefficients for measured trace gases, particle ions and meteorological parameters. Some correlation was found between NH_3 and K^+ ($r^2 = 0.16$). As illustrated by satellite fire-detect images (Figure 3.4), there were more wild fires present around Boulder, Wyoming in 2007 and 2008; the correlation coefficients (r^2) between NH_3 and K^+ in those two years were 0.33 and 0.40. As a marker of biomass burning, the correlation between NH_3 and K^+ may suggest a positive influence of fire emissions on NH_3 concentrations (Anderson et al., 2003; Hegg et al., 1988; McMeeking et al., 2009; Sutton et al., 1995).

Table 3.2 Correlation coefficients (r) between concentrations of trace gases, particulate species and meteorological parameters based on all the data.

Species	NH_3	HNO_3	NO_3^-	SO_4^{2-}	NH_4^+	K^+	Ca^{2+}	RH	WS	T
NH_3	1	0.23	-0.30	0.32	0.06	0.40	0.34	-0.53	0.01	0.72
HNO_3		1	0.43	0.16	0.47	0.29	0.10	-0.19	-0.31	0.12
NO_3^-			1	-0.08	0.63	-0.03	-0.19	0.44	-0.38	-0.54
SO_4^{2-}				1	0.45	0.35	0.46	-0.33	-0.04	0.33
NH_4^+					1	0.28	0.14	0.07	-0.36	-0.11
K^+						1	0.32	-0.46	-0.05	0.41
Ca^{2+}							1	-0.46	0.04	0.41
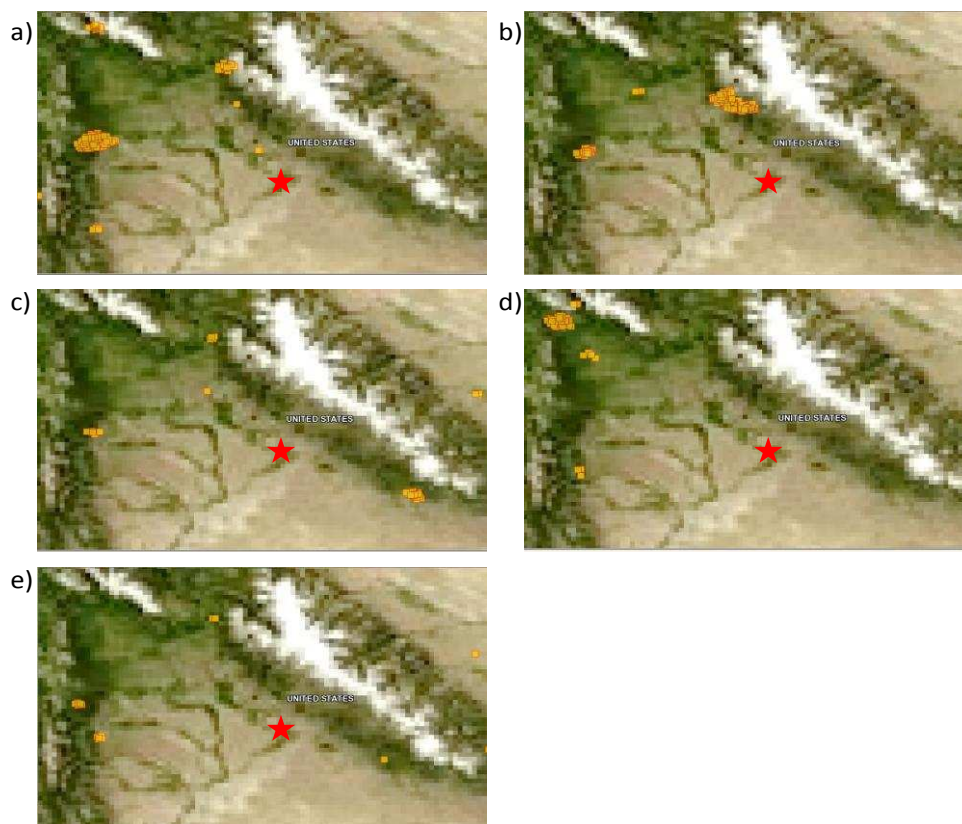
Figure 3.4 Satellite images of wild fires (http://earthdata.nasa.gov/data/nrtdata/firms/active-fire-data) observed in the vicinity of the measurement site (shown as red star) in (a) 2007, (b) 2008, (c) 2009, (d) 2010 and (f) 2011. From 2007 to 2011, the squared correlation coefficients (r^2) between concentrations of NH_3 and K^+ were 0.33, 0.40, 0.02, 0.16 and 0.03.

A background NH_3 mixing ratio of 1 ppbv is often assumed when estimating impacts of NO_x emissions on visibility and regional haze in western regions of the U.S. where ambient NH_3 concentration data are sparse or unavailable. Such estimates might be made, for example, through plume dispersion simulations using CALPUFF or other EPA-preferred models. The 5-year Boulder data records provide a better basis for choosing a representative background NH_3 concentration for the Pinedale region. Figure 3.5 reveals that seasonal mean NH_3 mixing ratios ranged between a maximum of 0.85 ppbv (in summer 2008) and 0.03 ppbv (in winter 2010). The average for the full 5-year study period was 0.30 ppbv, less than one-third of the typically assumed background level. Even if $PM_{2.5}$ NH_4^+ (much of which certainly reacted with sulfuric and nitric

acids upwind of the measurement region) and gaseous NH_3 are combined, the average mixing ratio (0.63 ppbv) remains well below 1 ppbv. Assumption of a 1 ppbv NH_3 background concentration in model simulations, therefore, will lead to an overprediction of visibility impacts associated with local NO_x emissions.
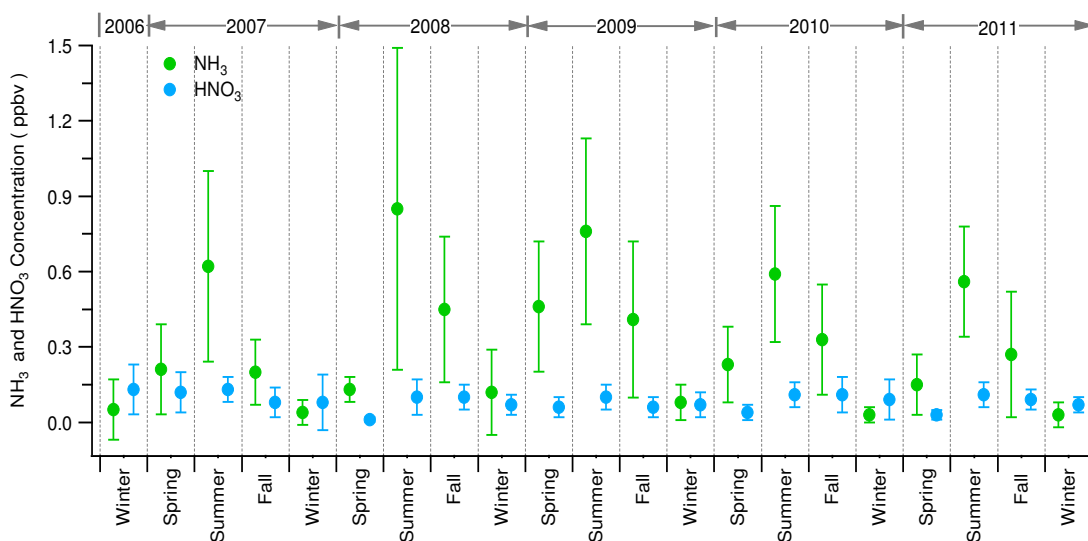
Figure 3.5 The seasonal variations of NH_3 and HNO_3 mixing ratios from 2007 to 2011. The plotted points are the seasonal mean values and the Y-error bars represent standard deviations.

The five year average HNO_3 mixing ratio was observed to be 0.03 ppbv, indicating typically low concentrations of HNO_3 occur in this area. Seasonal mean HNO_3 mixing ratios (Figure 3.5) ranged between 0.13 ppbv (in summer 2007) and 0.01 ppbv (in spring 2008). As illustrated in Figure 3.3b, HNO_3 concentrations display a distinct bimodal seasonal pattern, with higher average concentrations in the summer (0.23 $\mu g\ m^{-3}$) and in mid-winter (January/February average = 0.26 $\mu g\ m^{-3}$) than in other seasons. One also can see in Figure 3.5 that variability in observed HNO_3 concentrations is quite high in January and February. Previous studies have generally shown that HNO_3 peaks in summer with lower concentrations during winter (Adon et al., 2010; Gupta et al.,

2003; Lee et al., 1999; Plessow et al., 2005). Increased concentrations of HNO_3 are expected in the summer because of more intense and longer lasting photochemical activity associated with higher sun angles and longer days. Higher summer temperatures also promote dissociation of NH_4NO_3 back to gaseous NH_3 and HNO_3, as discussed above (Seinfeld and Pandis, 2012). The high winter concentrations observed at Boulder, by contrast, are quite unusual. The peak wintertime HNO_3 concentration climbed as high as 1.40 $\mu g\ m^{-3}$ for a single sample collected from February 22nd–25th in 2008. A closer look at the HNO_3 timeline in Figure 3.1 reveals frequent winter periods of elevated HNO_3 concentrations. Other measurements at Boulder reveal that this area is frequently subject to periods of elevated winter ozone (Schnell et al., 2009) that occur during sunny winter periods when snow covers the ground. Strong nocturnal and morning temperature inversions that set up under these conditions trap local emissions of NO_x and volatile organic compounds, associated largely with local energy production activities, in a shallow mixing layer while daytime photochemical activity is enhanced by strong reflectance from the bright snow surface. The photochemical reactions that generate ozone concentrations well in excess of the U.S. National Ambient Air Quality Standard (NAAQS) can also lead to substantial oxidation of the locally emitted NO_x to HNO_3. While cold winter conditions favor reaction of HNO_3 with NH_3 to form fine particle NH_4NO_3 (as evidenced by the winter NH_4NO_3 spikes in Figure 3.1), the Boulder observations reveal that all gaseous NH_3 has often been consumed during these episodes leaving a substantial fraction of the HNO_3 "trapped" in the gas phase.

Ambient NH_4^+ concentrations at Boulder exhibited little seasonal pattern (Figure 3.3c). The annual mean concentrations for 2007 to 2011 were also similar to each other at 0.29, 0.28, 0.23, 0.22 and 0.27 $\mu g\ m^{-3}$, respectively. Formation of fine particle NH_4^+ is influenced by a variety of factors,

including the availability of gaseous NH_3 and the availability of acidic sulfate aerosol and gaseous HNO_3. Increases in NH_3 and SO_4^{2-} at Boulder during warmer months of the year will tend to increase NH_4^+ concentrations as well. Formation of fine particle NH_4NO_3, however, is favored in winter. As previously discussed, the formation of NH_4NO_3 is thermodynamically favored by high relative humidity and low temperatures. During the winter in Boulder, the average temperature was $-7.8\ °C$ and average relative humidity was 72.5%. These offsetting seasonal patterns appear to result in an overall NH_4^+ concentration pattern that shows little seasonality at Boulder.

The annual average concentrations of $PM_{2.5}\ NO_3^-$ measured at Boulder were 0.30, 0.36, 0.29, 0.27 and 0.37 $\mu g\ m^{-3}$ in 2007 through 2011, respectively. The NO_3^- concentrations exhibited a strong seasonality, with maximum values in winter and minimum values in summer (Figure 3.3d). Because NH_4NO_3 formation is not favored under the warm, dry conditions of summer, the mean summer NO_3^- concentration was only 0.11 $\mu g\ m^{-3}$. In winter, it increased to 0.60 $\mu g\ m^{-3}$, as NH_4NO_3 formation was more strongly favored. As indicated in Figure 3.3d, considerable variability was also observed in winter NO_3^- concentrations, similar to the pattern discussed above for HNO_3, with maximum observed concentrations exceeding 2.0 $\mu g\ m^{-3}$ in December, January, February, and March.

SO_4^{2-} shows a seasonal cycle with maximum values in the warm season (Figure 3.3e). This seasonal pattern is typical of SO_4^{2-}, due to enhanced photochemical activity and higher concentrations of hydroxyl radical, which can oxidize SO_2 to SO_4^{2-} (Behera and Sharma, 2010). In-cloud oxidation of SO_2 to SO_4^{2-} can also be enhanced in summer when hydrogen peroxide

(H_2O_2) concentrations are typically higher (Shen et al., 2012). Annual average concentrations of SO_4^{2-} at Boulder in 2007 through 2011 were 0.54, 0.53, 0.47, 0.38, and 0.47 µg m^{-3}.

In addition to anthropogenic emissions of nitrogen and sulfur species, wild and prescribed fires also contribute significantly to fine particle concentrations in the western U.S. (Jaffe et al., 2008; Malm et al., 2004). Water soluble potassium ion concentrations, one marker of biomass burning (ANDREAE, 1983; Duan et al., 2004), were elevated in summer (Figure 3.3f). The average concentration of K$^+$ in the summer was 0.03 µg m^{-3}, which was nearly three times higher than the value in the winter (Table 3.1). Not surprisingly, summer K$^+$ concentrations varied substantially; inter-annual variability in fire occurrence and the influence of emissions from fires that do occur on air quality at Boulder are expected. Across the sampling period, a number of wild fires occurred upwind of the site in summer.

3.2 Gas-Particle Partitioning

To investigate the seasonal phase changes of NH_3/NH_4^+ and HNO_3/NO_3^-, we define the ammonia gas fraction (F_{NH3} = the NH_3 gas concentration divided by the sum of the NH_3 gas and fine particle NH_4^+ concentrations) and the nitric acid gas fraction (F_{HNO3} = the HNO_3 gas concentration divided by the sum of the HNO_3 gas and fine particle NO_3^- concentrations), where all concentrations are expressed in molar units. The monthly average partitioning for the reduced and oxidized inorganic nitrogen forms is plotted in Figure 3.6. There was a gradual transition from the cooler months, when the particle phase was favored, to the warmer months, when the gas phase was favored, for both species. A maximum monthly average in the gas phase fraction of NH_3 occurred in July

60

(0.64). This was more than 10 times higher than the minimum monthly average of 0.06 which occurred in January. Similarly, the HNO_3 gas fraction ($FHNO_3$) was found to be highest in summer (0.73 in July) and lowest in winter (0.24 in January). The high summer level of F_{NH3} reflects greater NH_3 emissions and the thermodynamic tendency for NH_4NO_3 to dissociate to NH_3 and HNO_3 at high temperature. The higher summer value of F_{HNO3} also reflects the tendency for NH_4NO_3 to dissociate at higher temperatures. The still appreciable winter F_{HNO3} level, which is not typical of previous results (Bari et al., 2003; Gupta et al., 2003; Sharma et al., 2007), reflects the continued photochemical production of HNO_3 at levels which exceed the amount of NH_3 available to participate in NH_4NO_3 formation
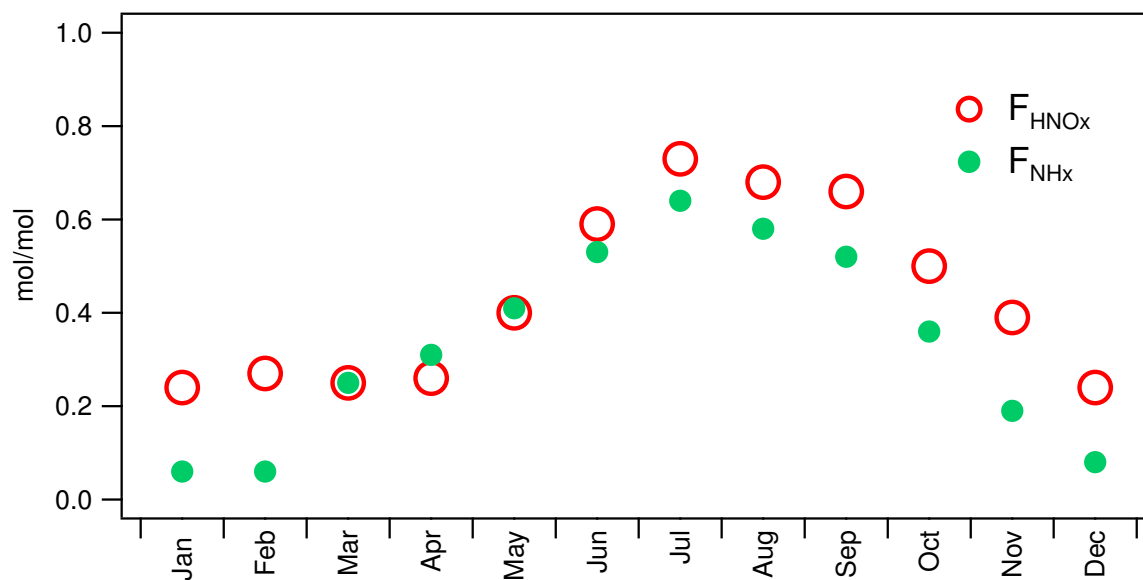
Figure 3.6 Monthly variation of the ammonia conversion ratio (F_{NH3}) and nitric acid conversion ratio (F_{HNO3}).

Shifts in the equilibrium partitioning among gaseous NH_3 and HNO_3 and particulate NH_4NO_3 depend on relative humidity (RH), temperature (T) and the concentrations of NH_3 and HNO_3. Ambient relative humidity at the Boulder measurement site was usually less than the deliquescence relative humidity (DRH) of NH_4NO_3 so that we can simplify matters and consider here formation

of solid NH_4NO_3. Under this condition, this reaction's equilibrium constant (K_p) is the expected

product of the NH_3 and HNO_3 concentrations and is given by the empirical formula (Eqn. 3.1) in

below:

$$\ln K_p = 84.6 - \frac{24200}{T} - 6.1 \times \ln \frac{T}{298} \qquad \text{(Eqn. 3.1)}$$

where K_p is in units of $ppbv^2$ and T is measured ambient temperature in Kelvin (Stelson and

Seinfeld, 1982). The measured, apparent reaction constant (K_m) can be described as Eqn. 3.2:

$$K_m = [NH_3] \times [HNO_3] \qquad \text{(Eqn. 3.2)}$$

where [NH_3] is the gaseous NH_3 mixing ratio (ppbv) and [HNO_3] is the gaseous HNO_3 mixing

ratio (ppbv). NH_4NO_3 formation is favored when K_m exceeds K_p. Figure 3.7 shows the variation

of both the theoretical equilibrium constant (shown as a solid line) and measured constant values

(for each sample) with temperature (1000/T) across all seasons. This presentation of the data

clearly illustrates that NH_4NO_3 formation is only favored during wintertime; even then, it is not

favored during all sample periods. At warmer times of the year, the product of NH_3 and HNO_3

concentrations is insufficient to yield NH_4NO_3 formation at seasonal temperatures.
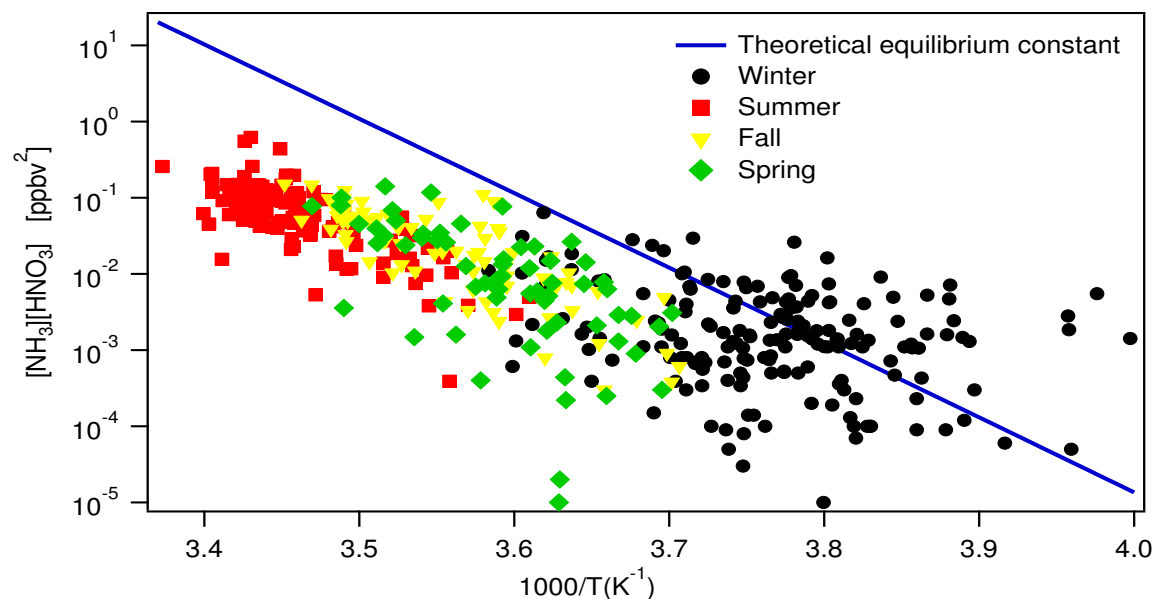
Figure 3.7 Comparison of the measured [NH₃ (gas)][HNO₃(gas)] product with the theoretical equilibrium constant for NH_4NO_3 as a function of temperature across the different seasons.

3.2. Comparison with other measurements

Figure 3.8 presents a comparison of observations from this study with other observations from the Clean Air Status and Trends Network (CASTNET; http://www.epa.gov/castnet/), the Interagency Monitoring of Protected Visual Environments (IMPROVE; http://vista.cira.colostate.edu/improve), the National Atmospheric Deposition Program Ammonia Monitoring Network (AMoN; http://nadp.sws.uiuc.edu/amon/) and seven sets of ambient composition measurements completed by our lab at CSU in the western U.S. (Table 3.3). Concentrations of particle and gas phase species observed at Boulder were, overall, among the lower average concentrations measured across this set of western sites. Comparing mean values of NH_3 and HNO_3 and fine particle NH_4^+, NO_3^-, and SO_4^{2-} at Boulder with the other rural locations, the concentrations measured at Boulder were generally lower than those observed at sites further east such as Santee Sioux, South Dakota, Konza Prairie, Kansas, Cherokee Nation, Oklahoma, and

Palo Duro, Texas. They were also significantly lower than concentrations measured closer to more populated areas, such as those at Sequoia National Park, California, Joshua Tree National Park, California, and Loveland, Colorado. Boulder, Wyoming NH_3 concentrations were substantially lower than NH_3 concentrations measured at sites more strongly impacted by regional agriculture/animal feeding operations, such as Brush, Colorado. Overall concentrations were fairly similar, however, between Boulder and other remote sites in central and western Colorado and in western Wyoming, suggesting some regional representativeness of the concentrations measured in Boulder (aside from the winter ozone episodes). Although the Boulder measurement site is only approximately 65 km from the Snake River Plain Valley, an area of intense agricultural activity with high NH_3 emissions (Clarisse et al., 2009), the low NH_3 concentrations observed at Boulder suggest that the Wyoming (Palisades) Mountain Range blocks at least the most direct transport of these emissions while other local NH_3 emissions are limited in their contributions to ambient NH_3 concentrations.
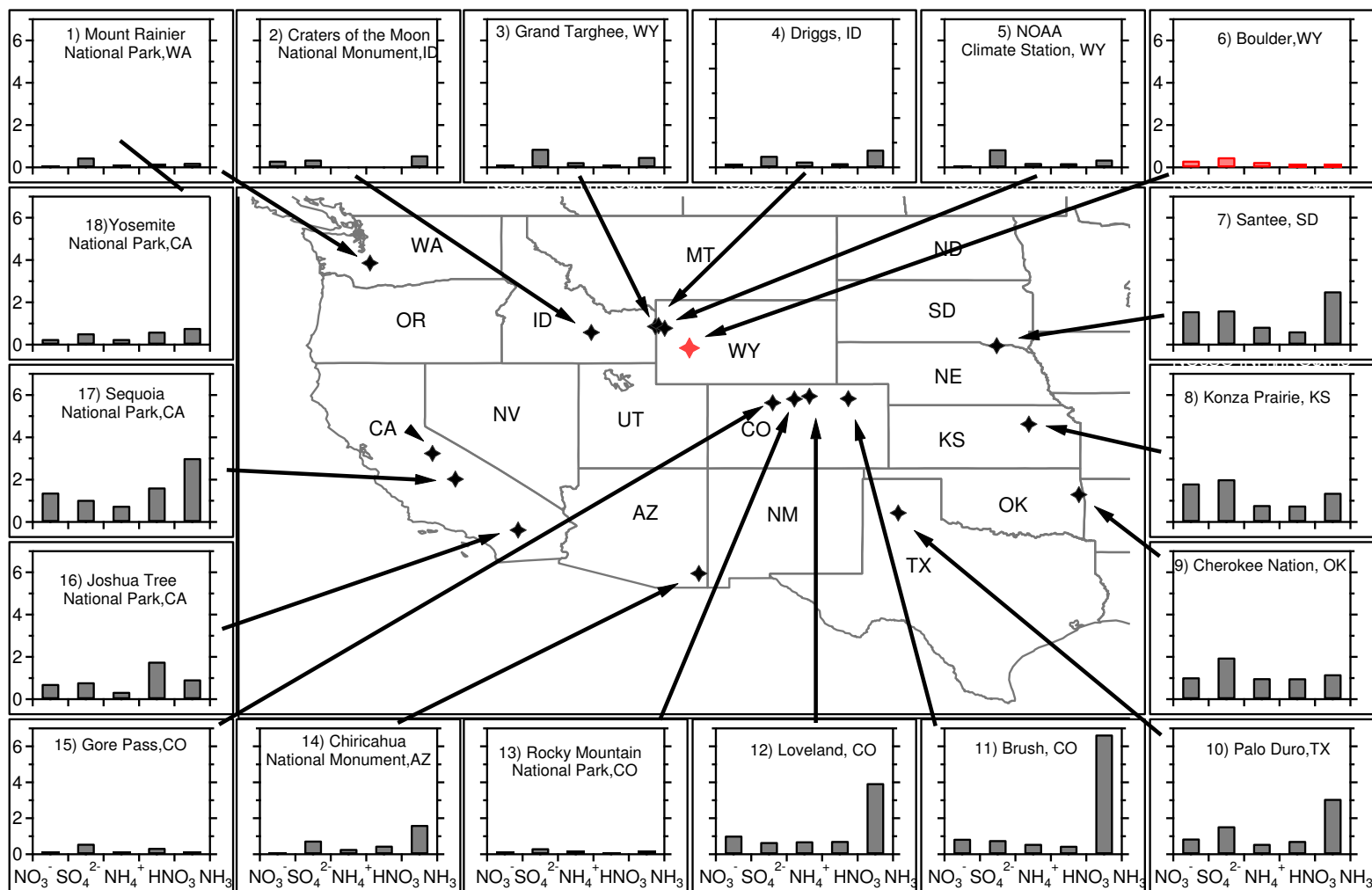
Figure 3.8 Comparison of average levels of gases and aerosol species concentrations for this study and other sampling locations in the western U.S. There was no measurement of NH_4^+ and HNO_3 at Craters of the Moon National Monument, Idaho. Concentrations are in $\mu g/m^3$. More information about the comparison data can be found in Table 3.3.

Table 3.3 Site information, data sources and sampling period for Figure 3.8.

Site	State	HNO_3 NH_4^+		NO_3^- SO_4^{2-}		NH_3	
		Source	Period	Source	Period	Source	Period
Chiricahua NM	AZ	CASTNET[a]	01/02/2007~01/03/2012	IMPROVE[b]	01/03/2007~12/31/2010	AMoN[c]	03/15/2011~01/31/2012
Joshua Tree NP[d]	CA	CASTNET	01/02/2007~01/03/2012	IMPROVE	01/06/2007~12/31/2010	AMoN	03/01/2011~01/31/2012
Sequoia NP	CA	CASTNET	01/02/2007~01/03/2012	IMPROVE	01/03/2007~12/31/2010	AMoN	03/22/2011~01/31/2012
Yosemite NP	CA	CASTNET	01/02/2007~01/03/2012	IMPROVE	01/03/2007~12/31/2010	AMoN	03/15/2011~01/31/2012
Cherokee Nation	KS	CASTNET	01/02/2007~01/03/2012	IMPROVE	01/03/2007~12/31/2010	AMoN	10/30/2007~01/31/2012
Mount Rainier NP	WA	CASTNET	01/02/2007~01/03/2012	IMPROVE	01/03/2007~12/31/2010	AMoN	03/17/2011~01/31/2012
Craters of the Moon NM[e]	ID	N/A	N/A	IMPROVE	01/03/2007~12/31/2010	AMoN	06/07/2010~01/31/2012
Palo Duro	TX	CASTNET	04/24/2007~01/03/2012	CASTNET	04/24/2007~01/03/2012	AMoN	10/30/2007~01/31/2012
Konza Prairie	KS	CASTNET	01/02/2007~01/03/2012	CASTNET	01/02/2007~01/03/2012	AMoN	03/01/2011~01/31/2012
Santee	SD	CASTNET	01/02/2007~01/03/2012	CASTNET	01/02/2007~01/03/2012	AMoN	07/05/2011~02/15/2012
Gore Pass	CO	CSU(Beem et al., 2010)	03/15/2006~04/28/2006 & 07/06/2006~08/11/2006	CSU	03/15/2006~04/28/2006 & 07/06/2006~08/11/2006	CSU	03/15/2006~04/28/2006 & 07/06/2006~08/11/2006
Rock Mountain NP	CO	CSU(Benedict et al., 2013c)	12/01/2008~12/01/2009	CSU	12/01/2008~12/01/2009	CSU	12/01/2008~12/01/2009
Boulder	CO	CSU(Benedict et al., 2013b)	12/01/2006~12/31/2011	CSU	12/01/2006~12/31/2011	CSU	12/01/2006~12/31/2011
Driggs	ID	CSU(Benedict et al., 2013b)	04/06/2011~09/21/2011	CSU	04/06/2011~09/21/2011	CSU	04/06/2011~09/21/2011
Targhee Base	WY	CSU(Benedict et al., 2013b)	04/21/2011~09/21/2011	CSU	04/21/2011~09/21/2011	CSU	04/21/2011~09/21/2011

NOAA Climate Center	WY	CSU(Benedict et al., 2013b)	05/04/2011~09/21/2011	CSU	05/04/2011~09/21/2011	CSU	05/04/2011~09/21/2011
Brush	CO	CSU(Benedict et al., 2013c)	12/11/2008~12/03/2009	CSU	12/11/2008~12/03/2009	CSU	12/11/2008~12/03/2009
Loveland	CO	CSU(Benedict et al., 2013c)	12/11/2008~12/03/2009	CSU	12/11/2008~12/03/2009	CSU	12/11/2008~12/03/2009

[a] CASTNET (The Clean Air Status and Trends Network, http://epa.gov/castnet/).

[b] IMPROVE (Interagency Monitoring of Protected Visual Environments, http://vista.cira.colostate.edu/improve/).

[c] AMoN (The Ammonia Monitoring Network, http://nadp.sws.uiuc.edu/amon/).

[d] NP means National Park.

[e] NM means National Monument.

[f] CSU means Colorado State University.

3.3. Interspecies correlations, the measured ion charge balance, and the importance of organic acids

Figure 3.9 illustrates the correlation between fine particle NH_4^+ and SO_4^{2-} in different seasons. Significant correlations were found in all seasons except in winter. The highest correlation (r^2 = 0.84) was in the fall and the lowest was in the winter (r^2 = 0.15). The weak correlation in winter results from substantial NH_4NO_3 formation during this time period. If one plots the excess NH_4^+ (the amount beyond that needed to fully neutralize fine particle SO_4^{2-}), one finds it to be strongly correlated with fine particle NO_3^- during winter (r^2 = 0.76; slope of 0.81), modestly correlated in fall (r^2 = 0.31; slope of 1.01), and showing almost no correlation in spring and summer (Figure 3.10).
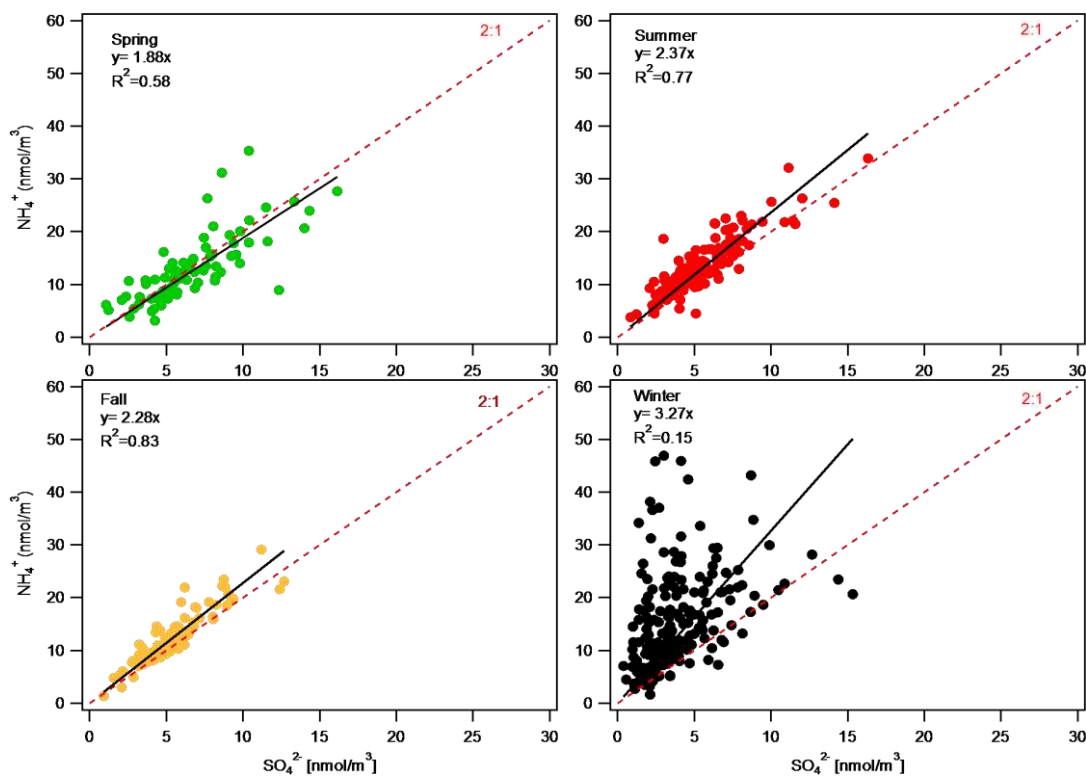
Figure 3.9 Seasonal relationships of NH_4^+ versus SO_4^{2-} concentrations.
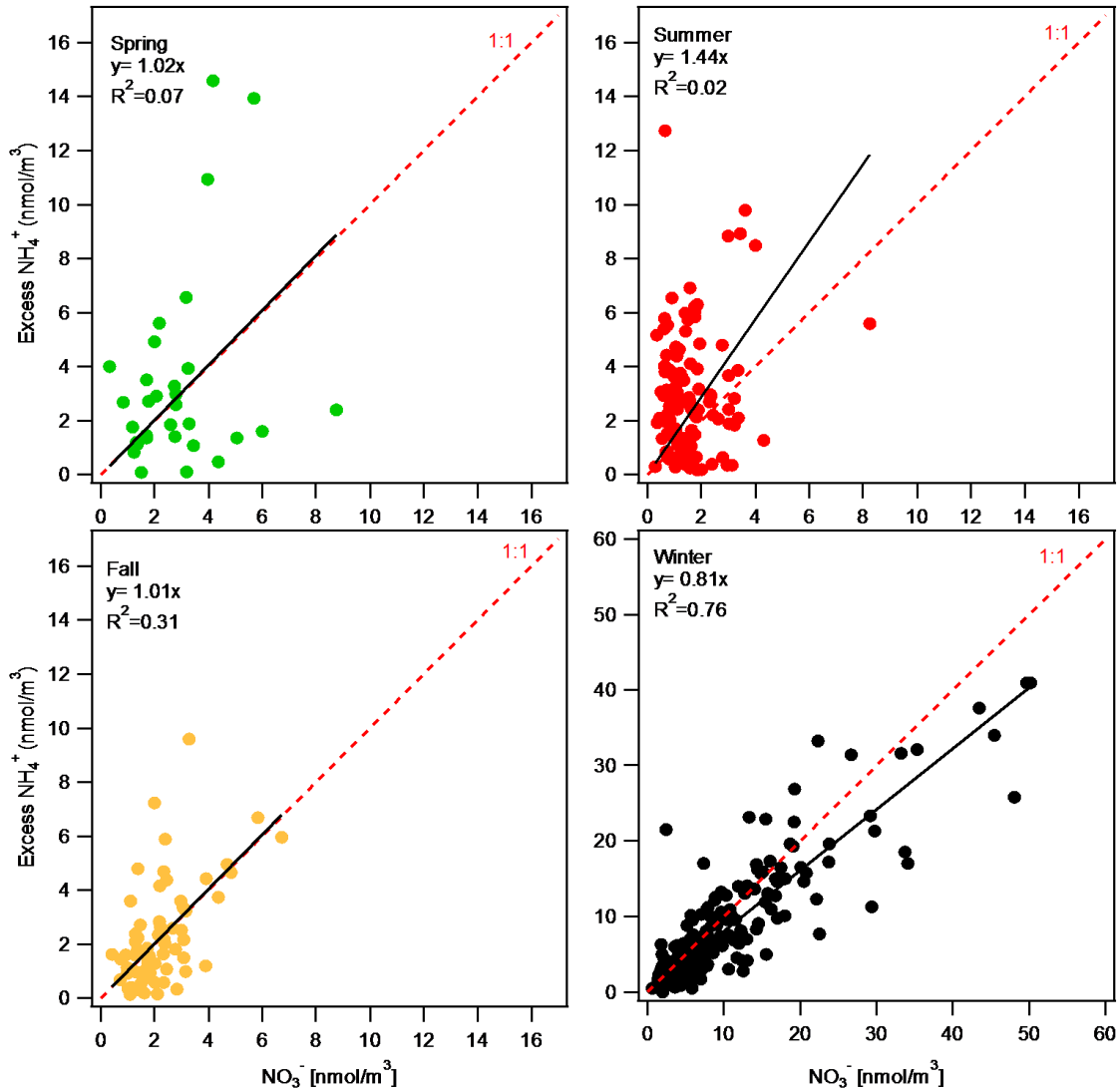
Figure 3.10 Seasonal relationships of excess NH_4^+ versus NO_3^- concentrations.

Overall, on the basis of the seasonal variation of comparisons between NH_4^+ and SO_4^{2-} and excess NH_4^+ and NO_3^-, one can conclude that most fine particle NH_4^+ in summer exists as $(NH_4)_2SO_4$ while both $(NH_4)_2SO_4$ and NH_4NO_3 are found in fine particles in winter. An excess of NH_4^+ in summer when NO_3^- concentrations are low, however, suggests that other unmeasured anionic species might also be important components of the fine particles. This pattern also appears in some fall and spring samples. This issue can be further evaluated by considering the overall ionic charge balance of measured fine particle anion (NO_2^-, NO_3^-, SO_4^{2-}) and cation (NH_4^+, Na^+, K^+, Mg^{2+},

69

Ca^{2+}) concentrations. Figure 3.11 presents the seasonal variation of the ionic charge balance. During spring and winter, the charge balance is very close to 1:1. During fall and, especially, summer, however, the charge balance generally indicates a deficiency of anions. Previous studies (Barsanti et al., 2009; Trebs et al., 2005) have reported that organic acids such as oxalic acid can be important contributors to the charge balance of fine mode aerosols. The warm season anion deficit observed here is consistent with higher organic acid concentrations during summer, coinciding with periods of enhanced photochemical production of secondary organic aerosols and increased biomass burning. Future measurements of summertime Boulder fine particle concentrations will include analysis of oxalate.
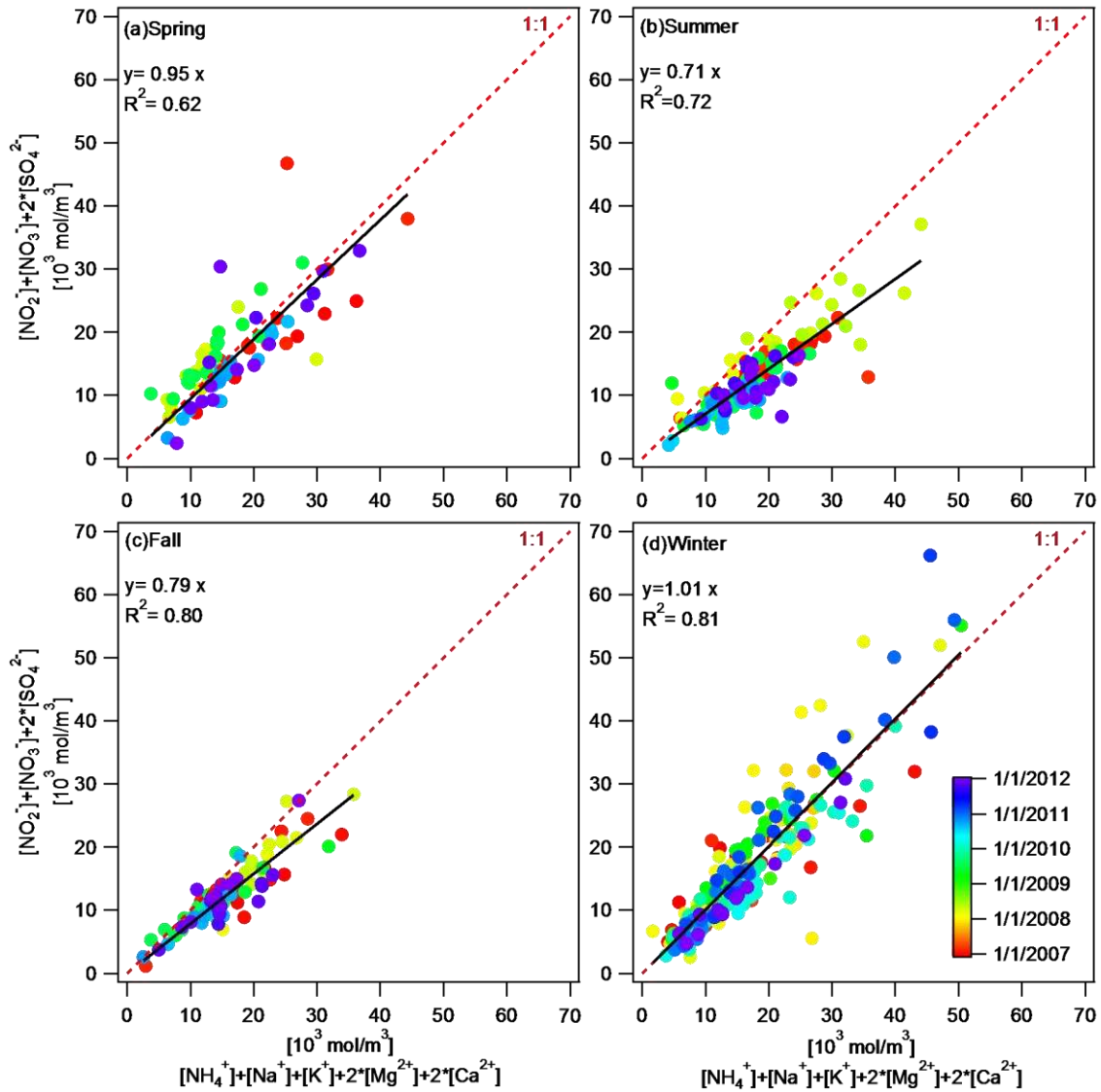
Figure 3.11 Seasonal charge balance, where the different colors represent the various sampling periods.

3.4 Summary

A five-year study of concentrations of gaseous NH_3 and HNO_3 and of fine particle inorganic ions was conducted in an active gas production region in Boulder, Wyoming. The five-year annual mean concentrations of NH_3, HNO_3, NH_4^+, NO_3^- and SO_4^{2-} were 0.17, 0.19, 0.26, 0.32, and 0.48 $\mu g\ m^{-3}$, respectively. NH_3 exhibited a strong seasonal variation, with higher concentrations during the summer and lower concentrations during the winter. The low annual average NH_3 mixing ratio of 0.30 ppb suggests that the default value of 1 ppb often used in regional assessments of visibility impacts from NO_x source emissions is higher than necessary. Observed NH_3 concentrations correlated well with ambient temperature indicating the important influence of temperature on emissions and, likely, the greater long distance transport of those emissions during warmer times of year when mixing layers deepen. By contrast, higher concentrations of particulate NO_3^- were observed in the winter when lower temperatures favor formation of NH_4NO_3. HNO_3 concentrations showed an unusual bimodal seasonal variation with higher levels both in summer (an expected result of active photochemical oxidation and a tendency for NH_4NO_3 to decompose at higher temperatures) and in winter. The unusual winter HNO_3 peak appears to be the result of active photochemical processing of local NO_x emissions in a shallow boundary layer during periods of snow cover and a lack of NH_3 to fully tie up HNO_3 through fine particle NH_4NO_3 formation. Examination of the equilibrium thermodynamics of NH_4NO_3 formation, seasonal local temperatures, and available concentrations of gaseous NH_3 and HNO_3, indicates that NH_4NO_3 should be expected primarily in winter, as observed.

4. SPATIAL AND VERTICAL VARIABILITY OF AMMONIA IN NORTHEASTERN COLORADO[2]

4.1 Spatial distributions of NH_3

Large spatial differences in NH_3 concentrations were found in the northeastern plains of Colorado with mean NH_3 concentrations ranging from 2.83 µg/m^3 to 41.33 µg/m^3 as illustrated in Figure 4.1. Also included in Figure 4.1 are estimated NH_3 emissions from major feedlots in northeastern Colorado. The feedlots were classified into categories based on the type of animals raised (data were provided by the Colorado Department of Public Health and Environment) and NH_3 emissions were calculated following Eqn. 4.1:

$$NH_3 \text{ Emission} = \sum (\text{Population} \times \text{Emission Factor}) \quad \text{(Eqn. 4.1)}$$

where the NH_3 emissions are the total NH_3 emitted from each feedlot in tons per year (converted from kg to tons for Figure 4.1). Population is the animal population in each feedlot and the emission factor was specified for each kind of animal: 44.3, 38.1, 3.37, 0.27, 6.50 and 12.2 kg NH_3/head/year, for beef cattle, dairy cows, sheep, poultry, swine and horses, respectively (Todd

---

[2] *This chapter is an expanded draft of material for the results and discussion and summary sections of a planned journal manuscript submission. Yi Li will be the lead author. Contributing co-authors include Xi Chen, Martin Van Damme, Tammy M. Thompson, Derek Day, Alexandra Boris, Amy P. Sullivan, Bonne Ford, Jay Ham and Jeffrey L. Collett, Jr.*

et al., 2013; USEPA, 2004). 73% of the total regional feedlot emissions are contributed by beef feedlots. Many large sources are located within several 10s of km to the south, east, and north of Greeley. Other large sources are located further east along the South Platte River with some smaller sources (mostly dairies) located further west in the sampling region, closer to the urban corridor.
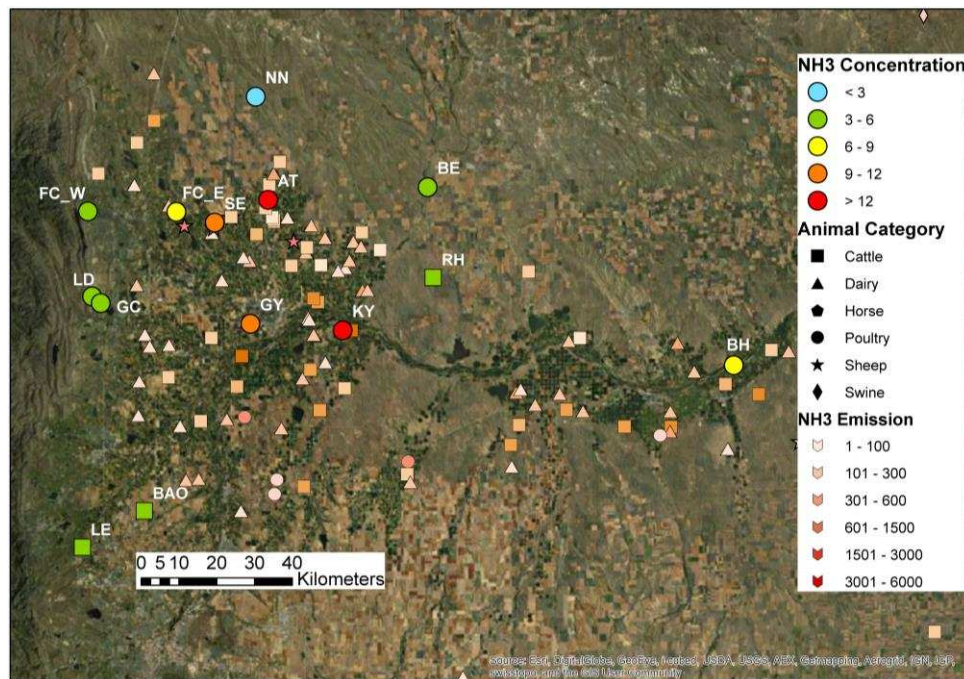
Figure 4.1 NH$_3$ concentrations and feedlot distribution in northeast Colorado. All sites indicated by circles include at least 3 years measurement in summer. NH$_3$ concentrations at the RH, LE and BAO sites (squares) were only measured in the summers of 2010, 2011 and 2012, respectively. The color of each measurement site indicator (circle or square) represents the NH$_3$ average concentration (unit: µg/m^3) at each site determined by the passive samplers. The color of each diamond represents the predicted annual NH$_3$ emissions (unit: ton/year) based on the equation above.

The lowest average ambient NH$_3$ concentrations in the sampling network were found at remote grassland sites such as NN and BE: 2.82 µg/m^3 and 3.14 µg/m^3, respectively. Concentrations of NH$_3$ at suburban sites were somewhat higher than at these remote, rural sites, indicating possible impacts of human activities, such as emissions from vehicles equipped with three-way catalytic converters, local waste treatment, and fertilization of yards and parks, on local NH$_3$ concentrations.

74

The measured weekly average NH_3 concentration at the Loveland golf course (GC) site was 5.12 $\mu g/m^3$ with a range of 1.81 $\mu g/m^3$ to 7.87 $\mu g/m^3$, showing only slightly elevated values compared to NH_3 concentrations at other nearby suburban sites (FC_W and LD), suggesting that golf course fertilization at this location is probably not a major, regional NH_3 source. The highest ambient NH_3 concentrations were consistently observed at sites near extensive animal feeding operations. Compared to the remote sites (NN and BE), an approximately 2-5 fold increase in NH_3 concentrations was observed at BH and AT (6.29 and 13.9 $\mu g/m^3$), rural sites under the influence of nearby animal feeding operation emissions. A 13-fold increase in NH_3 concentrations was observed from the grassland NN and BE sites (2.82 and 3.14 $\mu g/m^3$) to KY (41.33 $\mu g/m^3$), 0.4 km from a feedlot with almost 100,000 cattle.

The average summertime NH_3 concentrations sampled at each site spanning several years did not exhibit any statistically significant ($p<0.1$) inter-annual trends (Figure 4.2), except for BH which exhibits a decreasing trend. Trend analysis was conducted using Theil regression (Theil, 1992) and the Mann-Kendall test (Gilbert, 1987; Marchetto et al., 2013). We define an increasing trend as the slope of Theil regression greater than zero and a decreasing trend as a negative slope, while the statistical significance of a trend was determined by the Mann-Kendall test (p-value). A 90th percentile significance level ($p<0.10$) was assumed as in a previous study (Hand et al., 2012). The power of these analyses are limited by the relatively small number of measurement years to date; additional power for assessing interannual trends will become available as more years of measurements are completed. Data from the Colorado Agricultural Statistics Report (2014, http://www.nass.usda.gov/Statistics_by_State/Colorado/Publications/Annual_Statistical_Bulletin /Bulletin2014.pdf) indicate that Weld, Larimer, and Morgan counties (three major counties

located in the northeastern plains of Colorado) did not show significant growth in livestock numbers between 2009 and 2013. The total annual numbers of beef cows, milk cows, cattle and calves in these counties were 985, 974, 996, 1039 and 991 thousand head, respectively, in the four years from 2009 to 2013. A number of best management practices (BMPs) are under evaluation to help agricultural producers in the region reduce NH_3 emissions as part of efforts to reduce reactive nitrogen deposition in Rocky Mountain National Park. The baseline regional concentration information gathered here will be critical in helping to evaluate the success of future efforts to reduce NH_3 emissions.
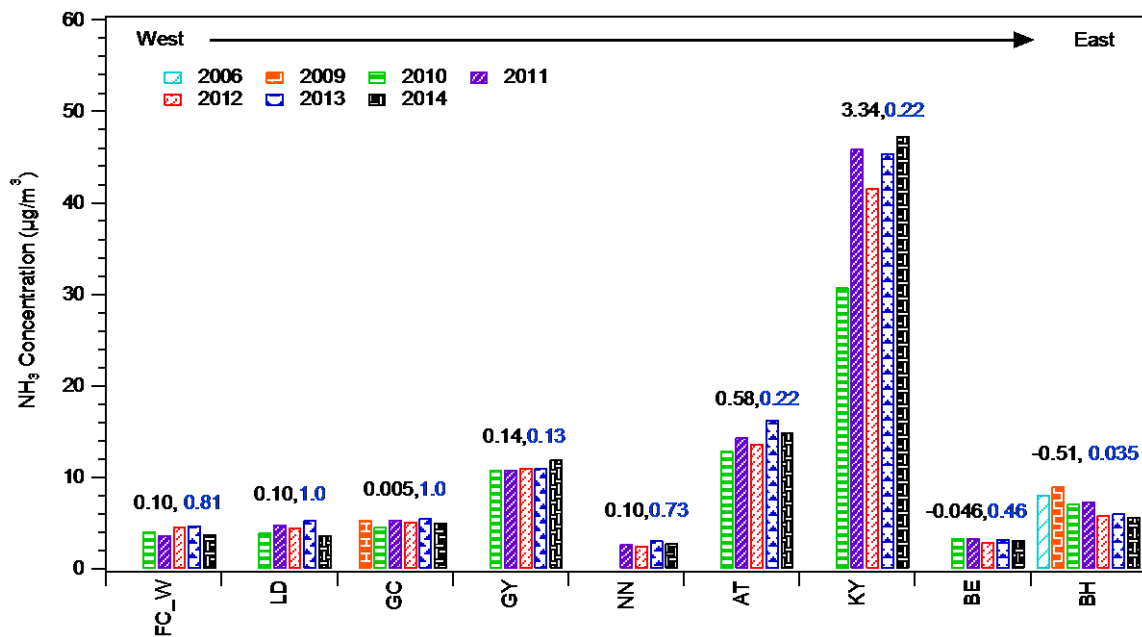
Figure 4.2. Average concentrations of NH_3 in each summer (approximately June through August) across the nine sites. In 2006 (07/06-08/10), ambient NH_3 concentrations were sampled by a URG system (daily) at the BH site; in 2009 (06/11-08/27) ambient NH_3 concentrations were sampled by a URG system (weekly) at the GC and BH sites; in 2010 (06/17-09/02), 2011 (06/16-08/31), 2012 (06/21-08/29), 2013 (06/20-08/29) and 2014(06/19-08/28), ambient NH_3 concentrations were all sampled by Radiello ammonia passive samplers across all the sites. The slope of the Theil regression and "p-value" for each site are labeled in black and blue, respectively

Weekly average atmospheric NH_3 concentrations at each observation site are plotted for summers 2010-2014 in Figure 4.3. These observations again show the general similarity, at a given location, of summertime concentrations across several years. Some variation from week to week is expected due to differences in meteorology. Emissions, for example, are influenced by temperature, dispersion is influenced by turbulence and mixing layer depths, and removal is influenced by precipitation and turbulence. One clear outlier period is the elevated NH_3 concentrations observed at FC_W at the beginning of summer 2012 (*Figure 4.3*c). The maximum weekly average NH_3 concentration at this site ($8.55\ \mu g/m^3$) was measured during June 21-28, 2012. This was more than double the average NH_3 concentration in 2010 ($4.13\ \mu g/m^3$) and 2011 ($3.76\ \mu g/m^3$) (see *Table 4.1*). During this elevated concentration period, the High Park Fire, one of the largest fires recorded in Colorado history at $353\ km^2$ burned, was burning in the mountains west of Fort Collins and the city was frequently impacted by smoke. The fire was first spotted on June 9, 2012 and declared 100% contained on June 30, 2012 (http://en.wikipedia.org/wiki/High_Park_fire). During the wildfire period, on-line instruments (Picarro NH_3 analyzer and Teledyne CO analyzer) were also set up to measure CO and NH_3 concentrations near the FC_W site. A significant correlation between CO and NH_3 was found during the wildfire (Prenni et al., 2012). Elevated NH_3 concentrations in the High Park Fire plume are evidence of the importance of wild and prescribed burning as a source of atmospheric NH_3, reinforcing similar findings from previous studies (Coheur et al., 2009; Prenni et al., 2014; Sutton et al., 2000).

Table 4.1 Summary of summer NH_3 concentrations (units: µg/m^3) measured from 2010 to 2014

Site	All years			2010 05/20-09/02			2011 06/2-08/31			2012 06/21-08/29			2013 05/30-08/29			2014 05/29-08/28		
	Ave	Max	Min	Ave	Max	Min	Ave	Max	Min	Ave	Max	Min	Ave	Max	Min	Ave	Max	Min
LE	3.33	5.23	2.27	--	--	--	3.33	5.23	2.27	--	--	--	--	--	--	--	--	--
FC_W	4.12	8.55	1.95	4.13	5.88	3.02	3.76	4.72	2.79	4.63	8.55	2.92	4.45	6.13	1.95	3.78	4.98	2.39
LD	4.45	10.37	2.29	4.17	6.29	2.67	4.81	6.94	3.61	4.57	10.37	2.55	5.08	7.16	2.29	3.68	5.82	2.83
BAO	5.09	7.84	2.85	--	--	--	--	--	--	5.09	7.84	2.85	--	--	--	--	--	--
GC	5.12	7.87	1.81	4.85	7.68	3.01	5.30	7.87	3.87	5.22	7.27	3.74	5.34	7.11	1.81	4.92	6.18	4.07
FC_E	8.56	11.38	5.52	--	--	--	--	--	--	8.36	10.84	5.52	8.30	11.25	5.80	8.99	11.38	6.92
SE	9.19	13.79	4.52	--	--	--	--	--	--	9.34	13.14	6.24	8.52	12.67	4.52	9.70	13.79	7.10
GY	11.30	19.02	5.19	10.39	13.11	7.94	12.90	19.02	8.40	11.07	14.51	6.68	10.52	12.54	5.19	11.72	14.95	9.35
NN	2.82	4.01	1.43	--	--	--	2.78	3.88	1.51	2.59	3.54	1.68	3.01	3.95	1.69	2.84	4.01	1.43
BE	3.14	5.40	1.42	3.18	4.48	1.90	3.33	4.90	2.55	2.99	4.58	2.12	3.00	3.62	1.42	3.15	5.40	2.24
RH	3.27	5.01	1.90	3.27	5.01	1.90	--	--	--	--	--	--	--	--	--	--	--	--
AT	13.94	20.47	6.56	12.55	16.16	9.13	13.78	18.61	8.82	13.70	19.27	9.25	15.13	20.47	6.56	14.49	19.03	10.44
KY	41.33	73.78	23.30	31.05	42.82	23.30	45.96	73.78	30.32	41.65	53.55	25.93	42.67	68.61	25.20	46.57	68.82	29.22
BH	6.29	10.83	3.59	6.54	9.67	3.67	7.26	10.83	5.09	5.45	8.52	3.80	5.99	7.80	3.59	5.62	6.79	4.47
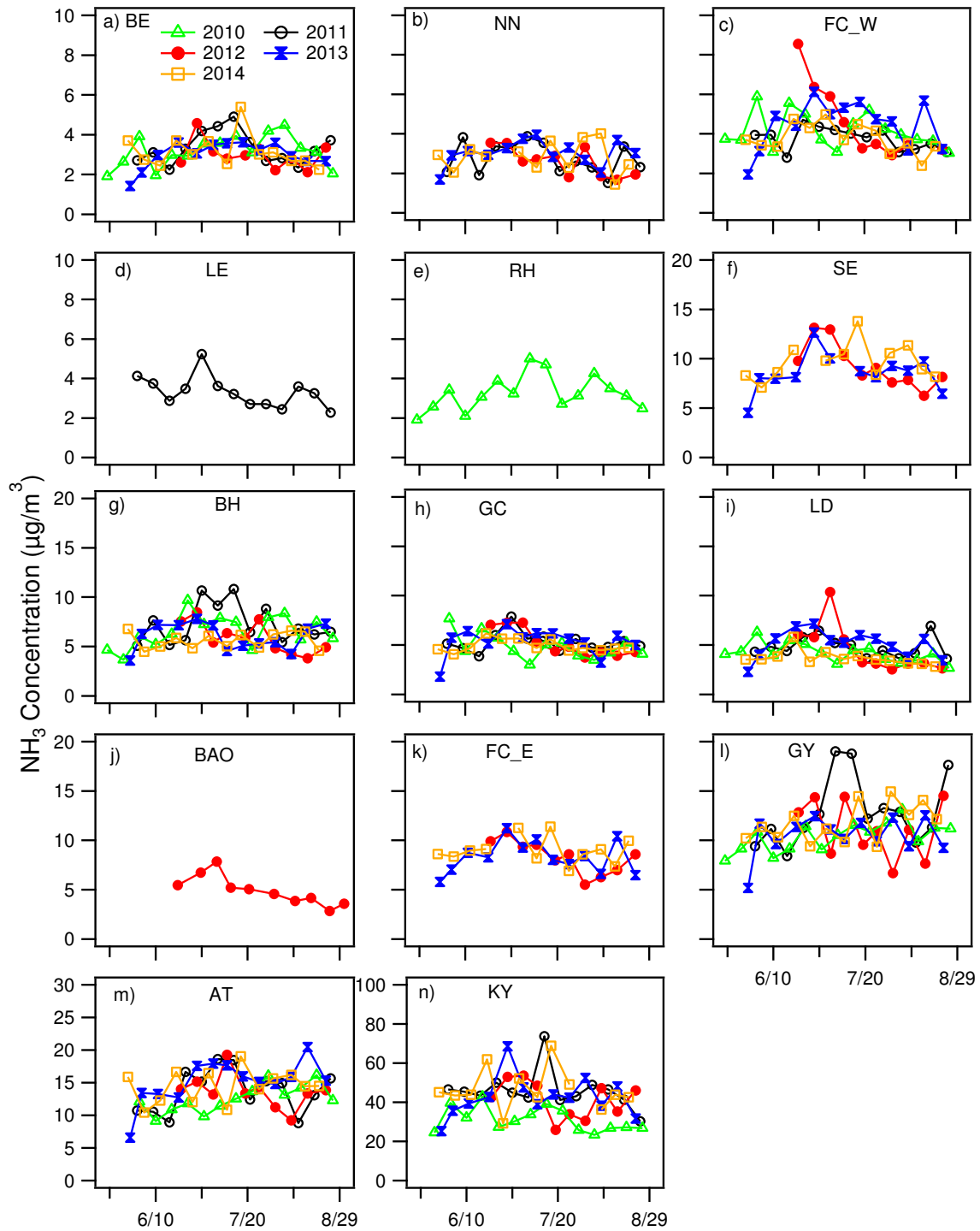
Figure 4.3 Temporal variations of NH₃ concentrations (unit: µg/m³) at each site from 2010 through 2014. Note the differences in the y-axis values.

4.2 Vertical distribution of NH_3

While surface measurements of NH_3 concentrations remain uncommon, measurements of vertical profiles of NH_3 concentrations above the surface are extremely rare. Time series of vertical profiles of ambient NH_3 concentrations measured at the BAO tower across the full year of 2012 are shown in Figure 4.4. During most sampling periods, the NH_3 concentration exhibited a maximum at 10 m decreasing both toward the lowest (1 m) measurement point and with height above 10 m. The minimum concentration was observed at the highest measurement point at the top (300 m) of the BAO tower. While the major sources of NH_3 are surface emissions, it is not surprising to see a gradient of decreasing concentration near the surface at this location where local emissions are expected to be small and the net local flux represents surface deposition (van Pul et al., 2009). The long time average (1-2 weeks) measured in this study precludes a determination of surface removal rates based on the observed concentration gradient.
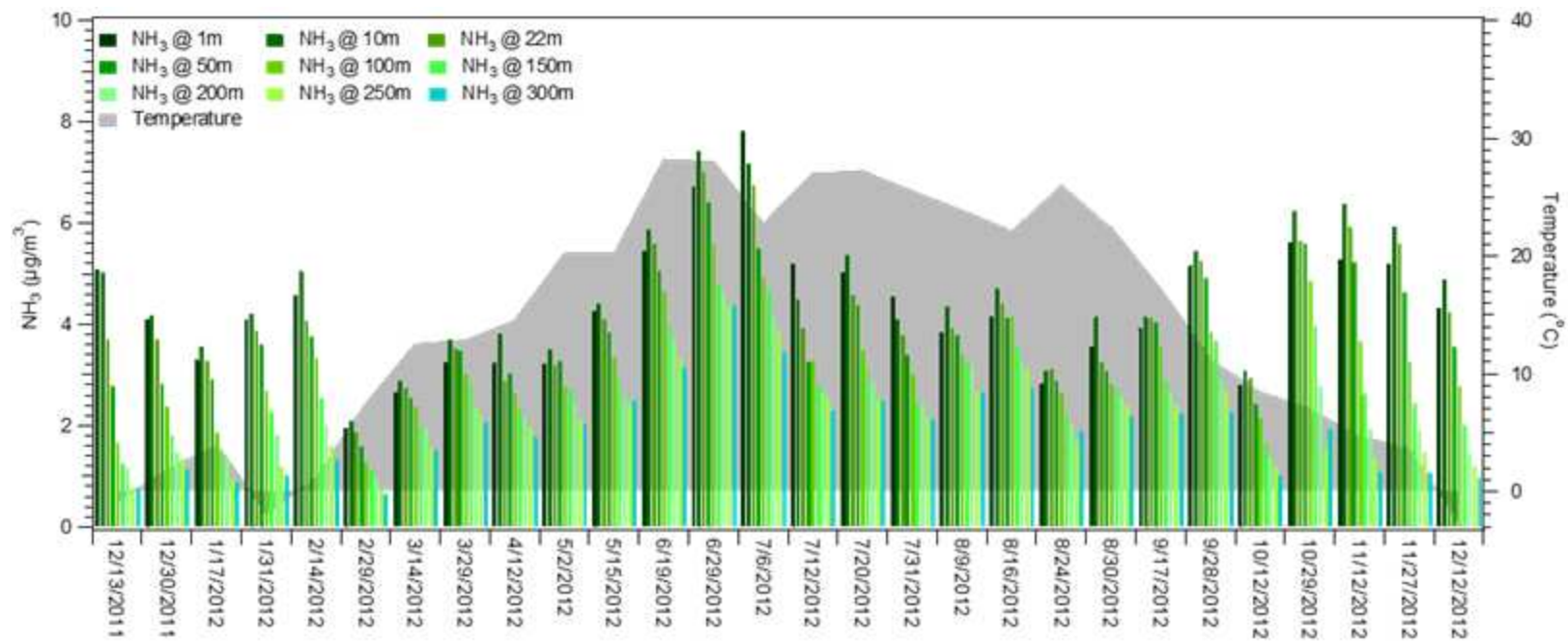
Figure 4.4 Time series of vertical distribution of NH_3 concentrations and surface temperature measured at the BAO tower from 12/13/2011 to 01/09/2013.

Seasonal variations in the vertical profile of NH_3 are depicted in Figure 4.5 with March, April and May defined as spring; June, July and August as summer; September, October and November as fall; and December, January and February as winter. Vertical concentration differences were greatest in winter (from an average concentration greater than 4 µg/m^3 near the surface to approximately 1 µg/m^3 at 300 m) followed by fall. Low level temperature inversions which trap emissions closer to the surface are common in both seasons (fall and winter). The highest concentrations across the profile were observed in summer, when emissions increase due to higher temperatures and vertical mixing is enhanced. Increased NH_3 concentrations in summer also may reflect a shift in thermodynamic equilibrium of particulate NH_4NO_3 toward its gas phase precursors NH_3 and HNO_3. Previous studies have reported increased concentrations in summer and/or reduced concentrations in winter due to the seasonal changes of NH_3 emissions and gas-particle partitioning (Li et al., 2014; Meng et al., 2011; Plessow et al., 2005; Walker et al., 2004; Zbieranowski and Aherne, 2012). Day et al. (2012) previously suggested that trapping of regional NH_3 emissions in a shallow winter boundary layer can produce elevated surface concentrations. The BAO tower observations in Figure 4.5a provide further evidence in support of this hypothesis, as concentrations are elevated near the surface but fall off quickly at heights greater than 10-20 m. Evidence of winter temperature inversions is present even in the average winter temperature profile shown in Figure 4.5b.
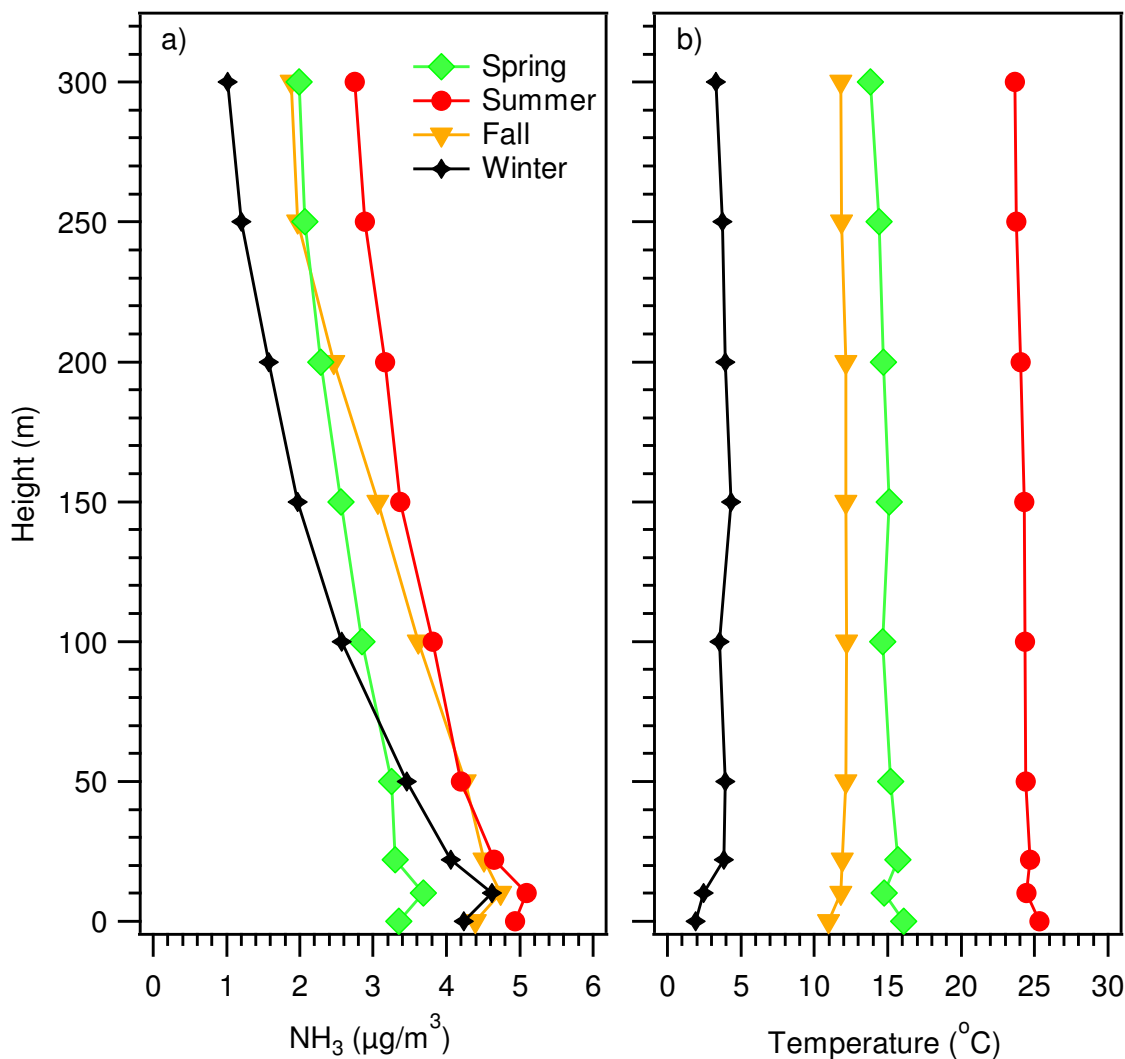
Figure 4.5 Comparison of seasonal average vertical profiles of (a) NH_3 and (b) temperature measured at the BAO tower from 12/13/2011 to 01/09/2013.

In order to explore the influence of inversion layers on the vertical distribution of NH_3 concentrations, the temperature and NH_3 vertical profiles from 10 to 150 m were analyzed in greater detail. The frequency (%) of inversion layer (T_{100} - T_{10} > 0) occurrence between 100 (T_{100}) and 10 (T_{10}) m was calculated based on the continuous temperature recording on the tower during each sampling period. A linear regression was applied between the altitude and NH_3 concentration and the resulting gradient of the NH_3 vertical profile was expressed as the slope (k). A negative slope corresponds to a decrease in concentration with height; the lower the absolute magnitude of

the slope, the bigger the concentration change with height from 10 m to 150 m. Clear positive correlation was found between the frequency of inversion layer occcurrence and the concentration slope (k) during the fall (R^2=0.39) and especially during winter (R^2=0.66), with only low correlation in the spring (R^2=0.01) and summer (R^2=0.15) (Figure 4.6). This suggests that the steep decline in concentration between 10 and 150 m observed in fall and winter is likely associated with prevalent thermal inversions in those seasons that trap NH_3 emissions near the surface.
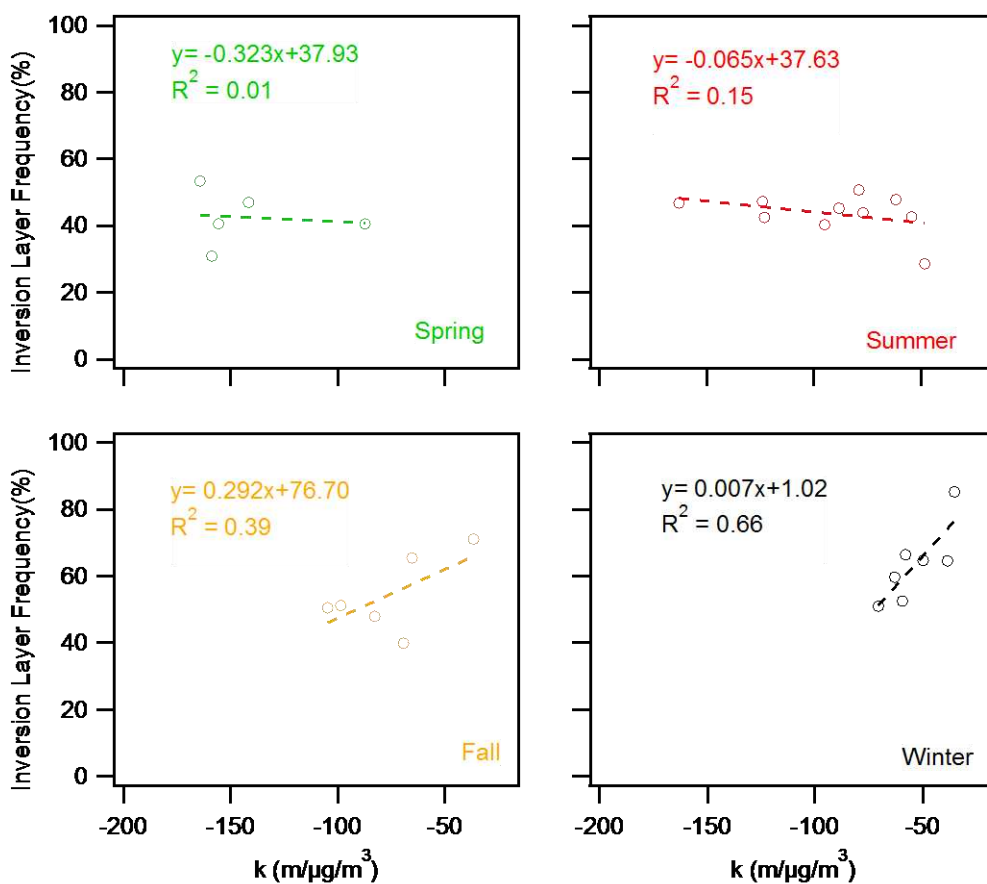
Figure 4.6 Seasonal relationships of the inversion layer frequency versus the vertical concentration gradient (slope k), measured on the BAO tower. See text for description.

Several long-term measurements have shown a strong correlation between NH_3 concentrations and ambient temperature, due to enhanced NH_3 emissions from soil and volatilization from NH_4NO_3

particulate matter (Bari et al., 2003; Ianniello et al., 2010; Lin et al., 2006; Meng et al., 2011). Almost no correlation ($R^2 = 0.02$) between NH_3 and temperature was observed at 1 m height in the current study; higher correlation ($R^2 = 0.65$) was found at the top of the tower (Figure 4.7a). The correlation coefficients increase substantially with height (Figure 4.7b), particularly above 50 m, suggesting that temperature might strongly influence ambient NH_3 concentrations at this location at higher altitude but is not a dominant factor at the surface (Figure 4.7b). This pattern might reflect the prevalence of typically greater vertical mixing during warmer periods, as discussed above.

In order to investigate the possible influence of changes in NH_4NO_3 aerosol-gas partitioning on vertical NH_3 concentration profiles, thermodynamic simulations were performed using the ISORROPIA II model (Fountoukis and Nenes, 2007) (Figure 4.8). Model inputs included BAO site URG denuder/filter-pack surface measurements of key species (gaseous NH_3 and HNO_3 and $PM_{2.5}$ NH_4^+, NO_3^-, and SO_4^{2-}) and measurements of temperature and relative humidity at each tower measurement height. Because vertical differences in temperature and relative humidity were generally small, little change was predicted with height in the thermodynamic partitioning of the NH_3-HNO_3-NH_4NO_3 system. Consequently, a shift in partitioning toward the particle phase as temperatures cool at higher altitudes appears not to account for much of the observed decrease in NH_3 concentration with height. For this location and for the lowest 300 m of the atmosphere, the vertical thermal structure of the atmosphere and associated mixing, ambient dilution, and NH_3 surface deposition appear to be the major factors determining vertical distributions of atmospheric NH_3.
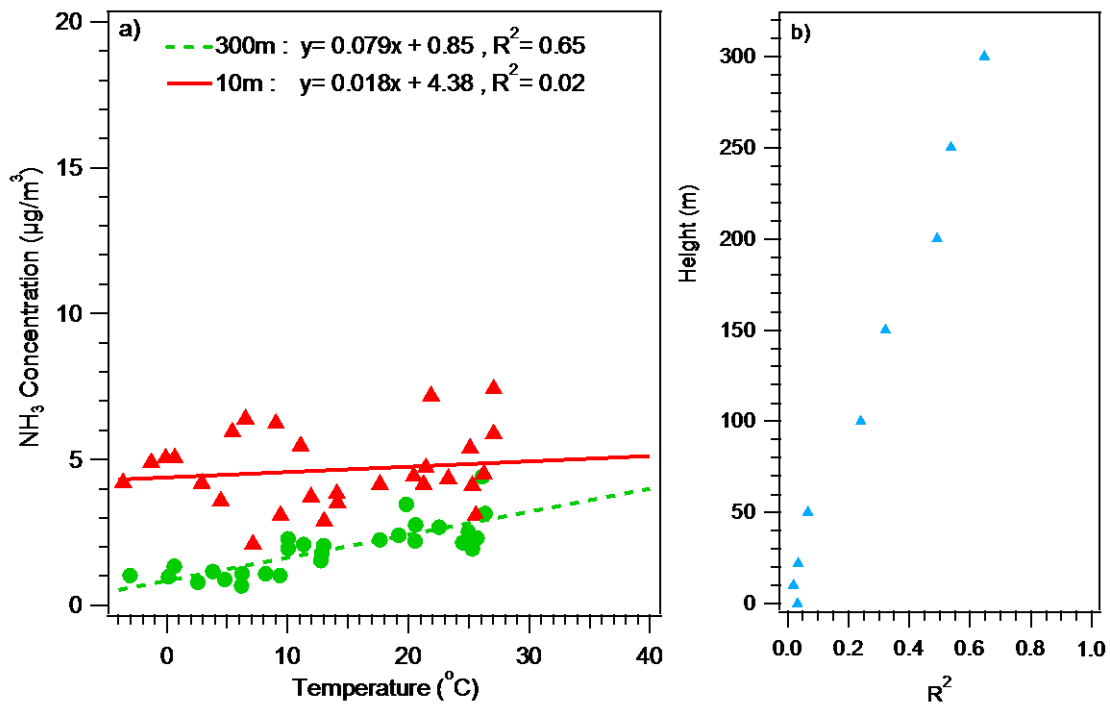
Figure 4.7 (a) NH_3 concentration versus temperature at 10 m and 300 m and (b) correlation coefficients between NH_3 concentration and temperatures at different heights of the BAO tower.
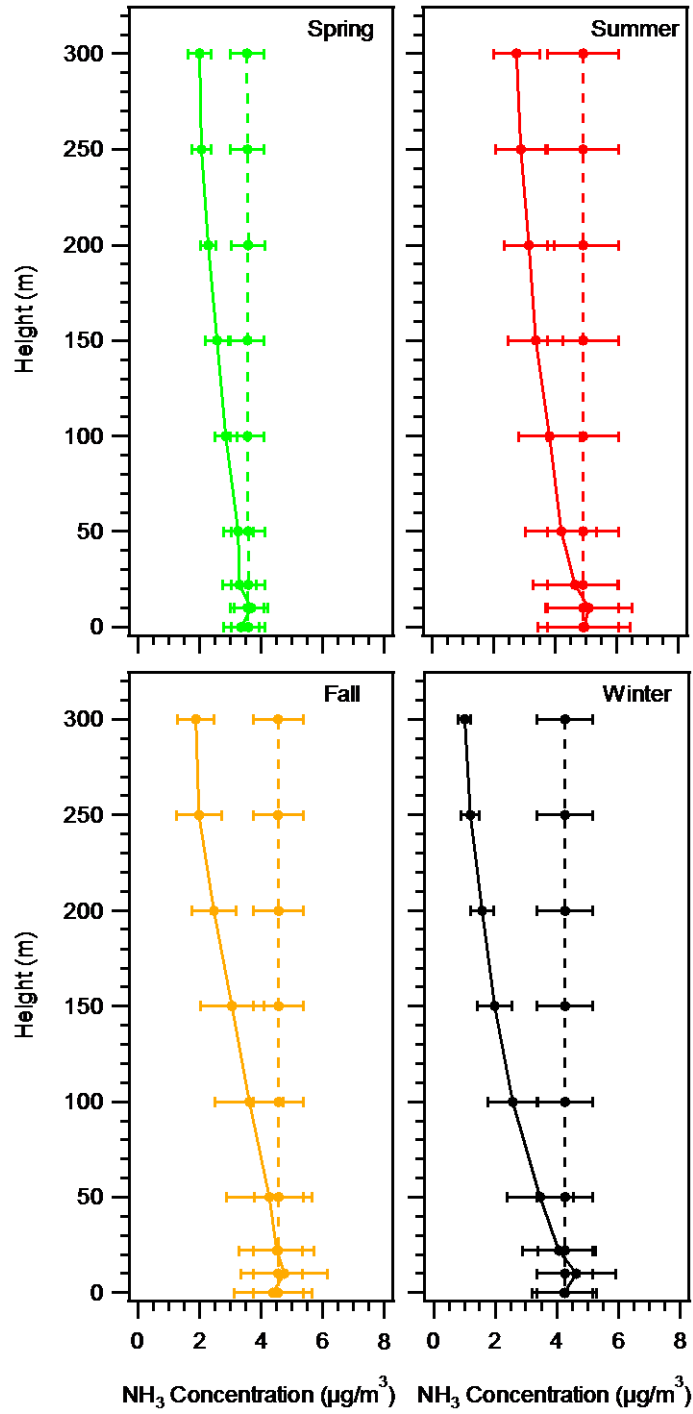
Figure 4.8 Seasonal average vertical profiles of NH_3 measured at the BAO tower (solid line) and ISORROPIA II model results (dashed line) in 2012. The x-error bars represent the relative standard deviation of NH_3 concentrations.

4.3 Comparison with Satellite Observations

Several recent studies have used surface NH_3 measurements to evaluate or improve remote sensing techniques for retrieving NH_3 concentrations and determining distributions (Heald et al., 2012; Pinder et al., 2011; Van Damme et al., 2015; Zhu et al., 2013). The Infrared Atmospheric Sounding Interferometer (IASI) is a passive infrared Fourier transform spectrometer onboard the MetOp platforms, operating in nadir (Clerbaux et al., 2009). IASI provides a quasi-global coverage twice a day with overpass times at around 9:30 am and 9:30 pm (when crossing the equator) at a relatively small pixel size (circle with 12 km diameter at nadir, distorted to ellipse-shaped pixels off-nadir). The combination of low instrumental noise (~0.2K at 950 cm^{-1} and 280K), a medium spectral resolution (0.5 cm^{-1} apodized) and a continuous spectral coverage between 645 and 2760 cm^{-1} make IASI a suitable tool to measure various constituents of the atmosphere (Clarisse et al., 2011).

The IASI-NH_3 data set is based on a recently developed retrieval scheme presented in detail in Van Damme et al. (2014a). The first step of the retrieval scheme is to calculate a so-called Hyperspectral Range Index (HRI) for each IASI spectrum, which is representative of the amount of NH_3. This HRI is subsequently converted into NH_3 total columns using look-up tables built on numerous simulations performed at various atmospheric conditions. The main advantages of the retrieval scheme are that it is very fast and it provides an associated error estimate for each observation. The main drawbacks are the fixed profile shape used for the simulations over land and the fact that only clear-sky scenes (cloud cover below 25%) are processed. It is worth noting

that the distribution and time-series presented in the following are weighted by the relative error associated with each IASI observation.

The IASI-NH$_3$ data set has been evaluated against model simulations over Europe and has shown its consistency (Van Damme et al., 2014b). The first steps of the validation work have been performed and highlighted the need to expand the NH$_3$ monitoring network to achieve a more complete validation of the NH$_3$ satellite observations (Van Damme et al., 2015). The comparison here is a contribution to that effort and benefits from a relatively high spatial density of monitoring sites in a region with substantial ammonia emission and concentration gradients.

In Figure 4.9, IASI-retrieved column distributions are compared with the Radiello passive NH$_3$ surface concentration measurements in northeastern Colorado. Three years of data were selected for comparison in the latitude range from 39.8°N to 41.0°N and longitude range from 103.4°W to 105.3°W. Overall, the IASI observations and Radiello passive measurements show similar spatial patterns. The IASI columns exceed 3×10^{16} molec/cm^2 around the KY site and decrease moving away from concentrated agricultural areas.
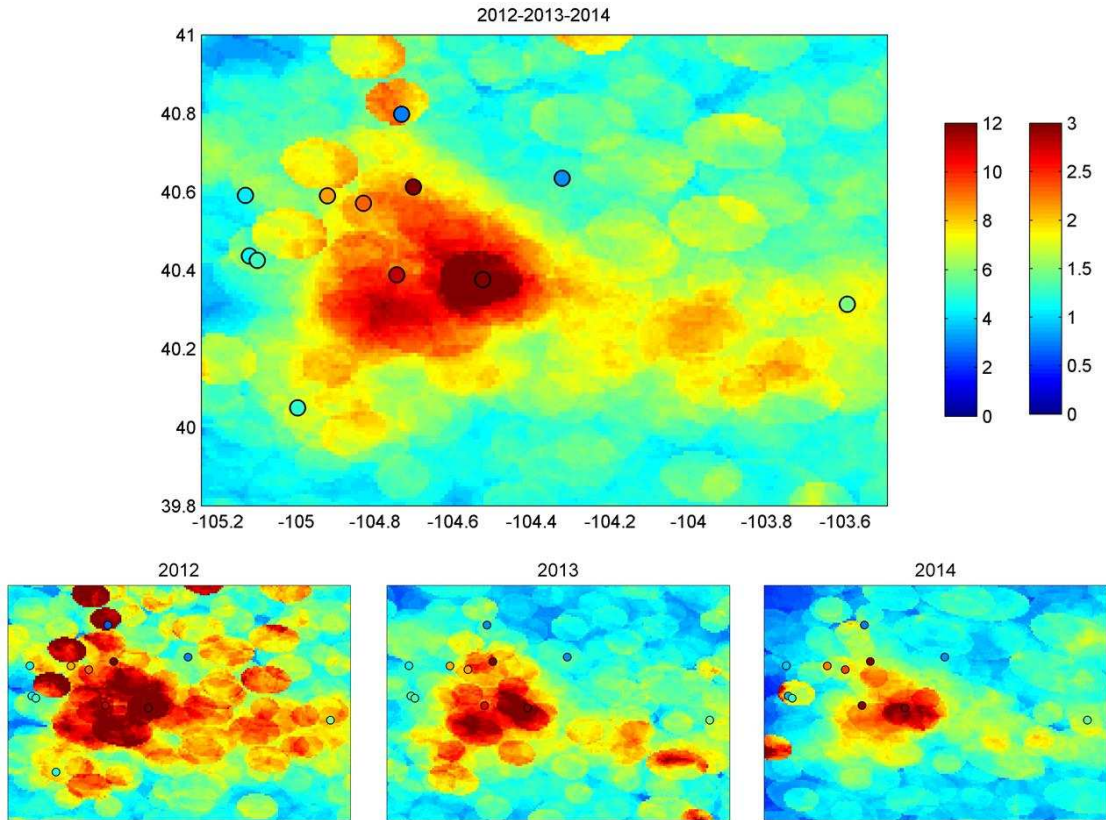
Figure 4.9 Radiello passive sampler surface measured averaged NH$_3$ concentrations (µg/m³, left color bar) plotted on top of IASI-NH$_3$ satellite column distributions ($\times 10^{16}$ molec /cm², right color bar). The average for 2012, 2013 and 2014 shown on the bottom and the cumulative 3 years average shown on the top. The BAO site was only sampled in the summer of 2012.
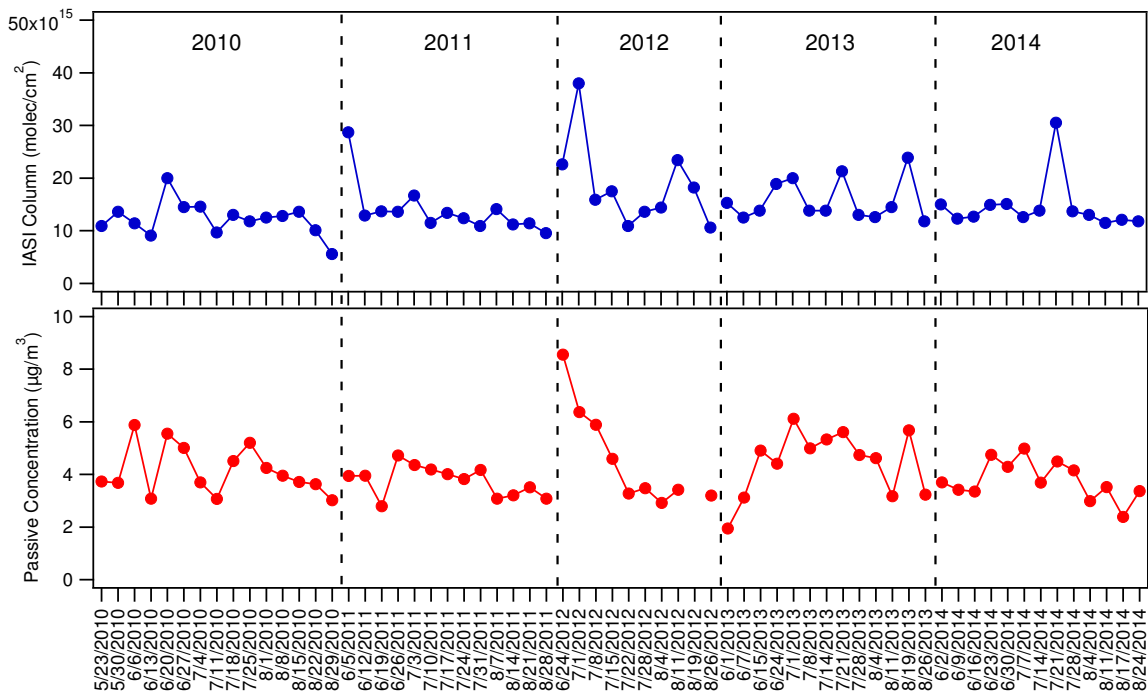
Figure 4.10 Time series of weekly averaged IASI-NH$_3$ satellite column (top, blue) and surface concentrations measured by Radiello passive sampler (below, red) at the FC_W site.

In order to further explore the temporal concentration variability, including the postulated contributions from wildfire to local ambient NH$_3$ concentrations, weekly averages of IASI measurements (based on Radiello passive sampling periods) above the FC_W site are shown in Figure 4.10. In general, similar temporal trends are found between the Radiello passive measurements and IASI observations. Elevated NH$_3$ concentrations during the High Park Fire period in June 2012 are seen in both the satellite and surface measurements. It is also interesting to note that the high satellite total column NH$_3$ measured at the beginning of June 2011 (2.87×10^{16} molec /cm²) might be linked with wildfire plumes at higher altitude (Figure 4.11a) transported from other areas and not captured by the surface measurements. A peak in the satellite observations July 25th to 31st, 2014 occurred due to the combined impacts of low IASI observations (high cloud coverage) and a fire plume crossing the satellite footprint (Figure 4.11b).
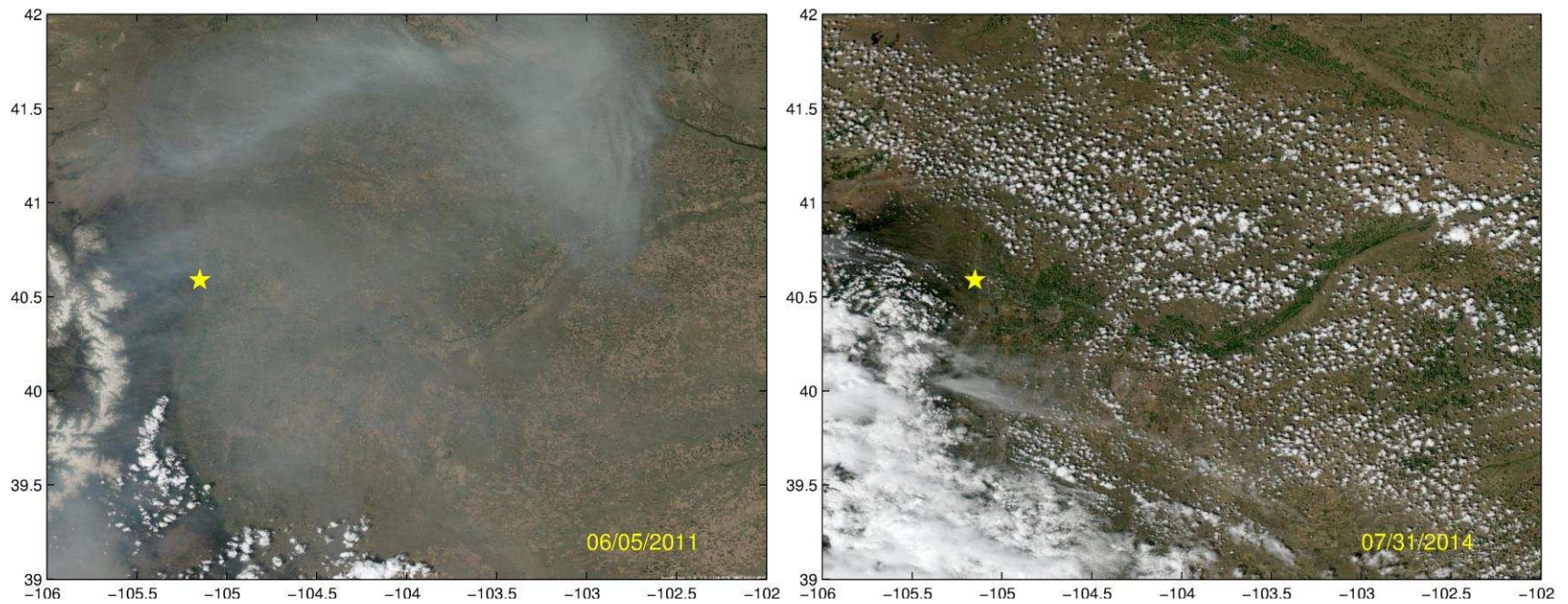
Figure 4.11 Satellite image of the wildfire plume (a) and high cloud coverage with wildfire plume (b) over northeastern Colorado caught by the Moderate Resolution Imaging Spectroradiometer (MODIS) (Image downloaded at http://loatec.univ-lille1.fr/TerreEtCiel/module.php?lang=us). The FC_W site is indicated by a yellow star.

4.4 Comparison with CAMx Model Simulations

Models frequently have a difficult time accurately simulating spatial concentrations of NH_3 concentrations. In addition to the typical model difficulties in accurately simulating transport, NH_3 emissions are not well constrained and the parameterization of NH_3 deposition is challenging. Measurements are compared here to modeled concentrations of ammonia estimated using the Comprehensive Air quality Model with extensions (CAMx, http://www.camx.com/files/camxusersguide_v6-20.pdf). CAMx is a photochemical model that simulates the emissions, transport, chemistry and removal of chemical species in the atmosphere. CAMx is one of US EPA's recommended regional chemical transport models and is often used by the US EPA for air quality analysis (EPA, 2007, 2011). The 2011 modeling episode presented here (version base_2011a), including inputs representing emissions and meteorology, was developed for the Western Air Quality Data Warehouse (WAQDW), and details on modeling protocol and model performance are available on the WAQDW website (http://www.wrapair2.org/).

Simulations with CAMx version 6.1 were performed with two-way nested domains with horizontal grid size resolutions of 36 km, 12 km, and 4 km as shown in Figure 4.12. The outermost domain includes the continental United States, southern Canada, and northern Mexico, the 4-km domain extends over Colorado, Wyoming and Utah, while the 12-km domain extends over the western states. The Weather Research & Forecasting Model (WRF), Advanced Research WRF (ARW) v3.5.1, was used to develop meteorological inputs to the air quality model (Skamarock et al., 2005). The input meteorological data represent conditions as they occurred in 2011. A performance evaluation of the WRF data was conducted by The University of North Carolina at Chapel Hill

(Three-State Air Quality Modeling Study (3SAQS) – Weather Research Forecast 2011 Meteorological Model Application/Evaluation available at: http://vibe.cira.colostate.edu/wiki/Attachments/Modeling/3SAQS_2011_WRF_MPE_v05Mar2015.pdf).

The Sparse Matrix Operator Kernel Emissions (SMOKE) processing system (https://www.cmascenter.org/smoke/documentation/3.1/html/) (Houyoux et al., 2000) was used to prepare the emissions inventory data in a format that reflects the spatial, temporal, and chemical speciation parameters required by CAMx. The emissions inventory is based on the 2011 National Emissions Inventory (NEI) v1 (http://www.epa.gov/ttn/chief/net/2011nei/2011_nei_tsdv1_draft2_june2014.pdf). Important updates to the 2011 NEI included a detailed oil and gas inventory, and the spatial allocation of livestock emissions using latitude/longitude location data of livestock facilities (WAQDW). Boundary conditions were developed using the Model for Ozone and Related chemical Tracers (MOZART) and represent the 2011 modeling period (Emmons et al., 2010).
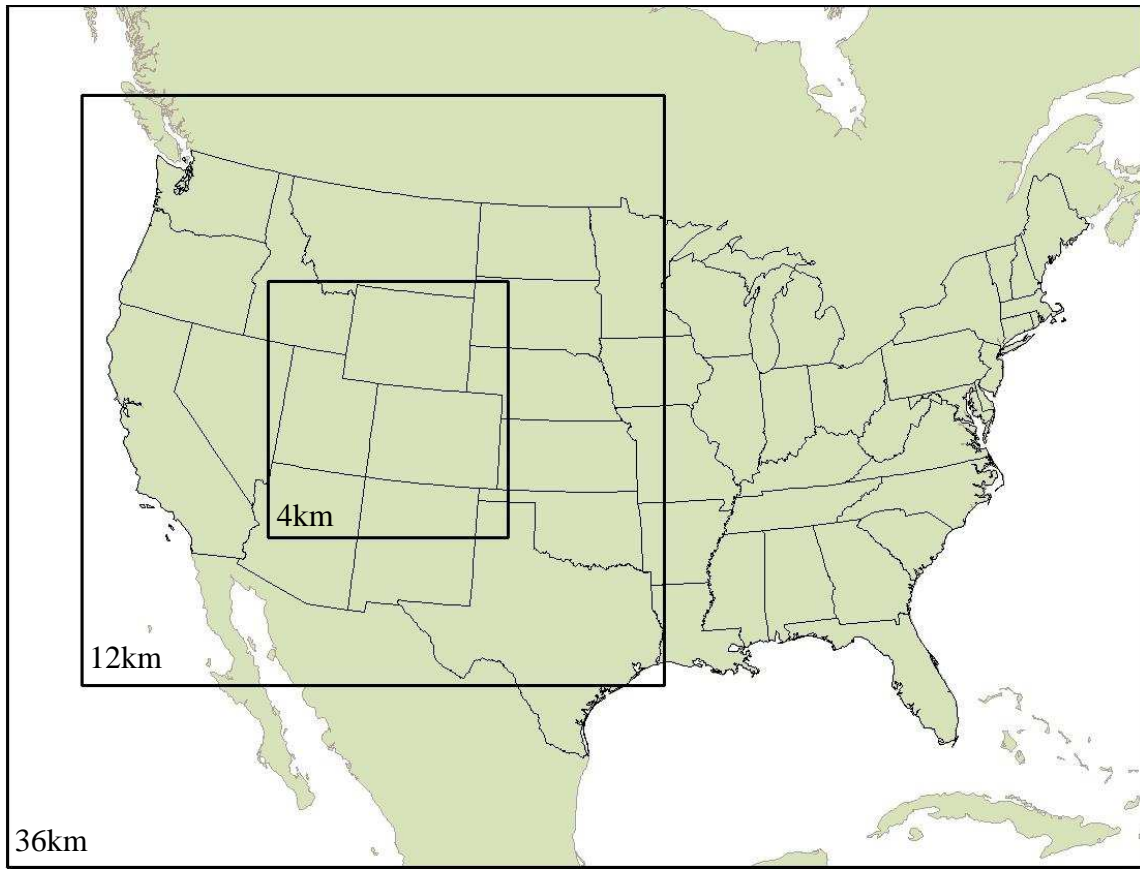
Figure 4.12 The 36-km horizontal grid resolution outer domain, represented by the extent of the larger box, covers the contiguous United States, northern Mexico, and southern Canada. The 12-km domain includes states surrounding Colorado. The inner 4-km domain extends over Colorado, Utah, Wyoming and portions of surrounding states.

Figure 4.13 illustrates an evaluation of stimulated NH_3 concentrations by the CAMx model both spatially and across time. Generally speaking, CAMx reasonably reproduces observed NH_3 in the northeastern plains of Colorado. However, CAMx generally performs better near the major NH_3 sources (e.g., Kersey and Greeley), but underestimates NH_3 concentrations at sites further away from feedlot locations (Figure 4.14). The modest overestimation of NH_3 concentration at the KY site is likely an artifact of model resolution and the assumption that emissions are immediately and homogeneously dispersed throughout the grid cell in which they are emitted. A model-measurement mismatch moving away from ammonia source locations could result from a number

95

of factors, including smaller and/or non-agricultural sources (e.g., suburban N-fertilization or transportation) underrepresented in the emissions inventory, possible overestimation of NH_3 deposition in the model, which does not account for the bidirectional nature of ammonia exchange with the surface, or a tendency for the model to more actively move surface ammonia emissions aloft during downwind transport than occurs in the real atmosphere.
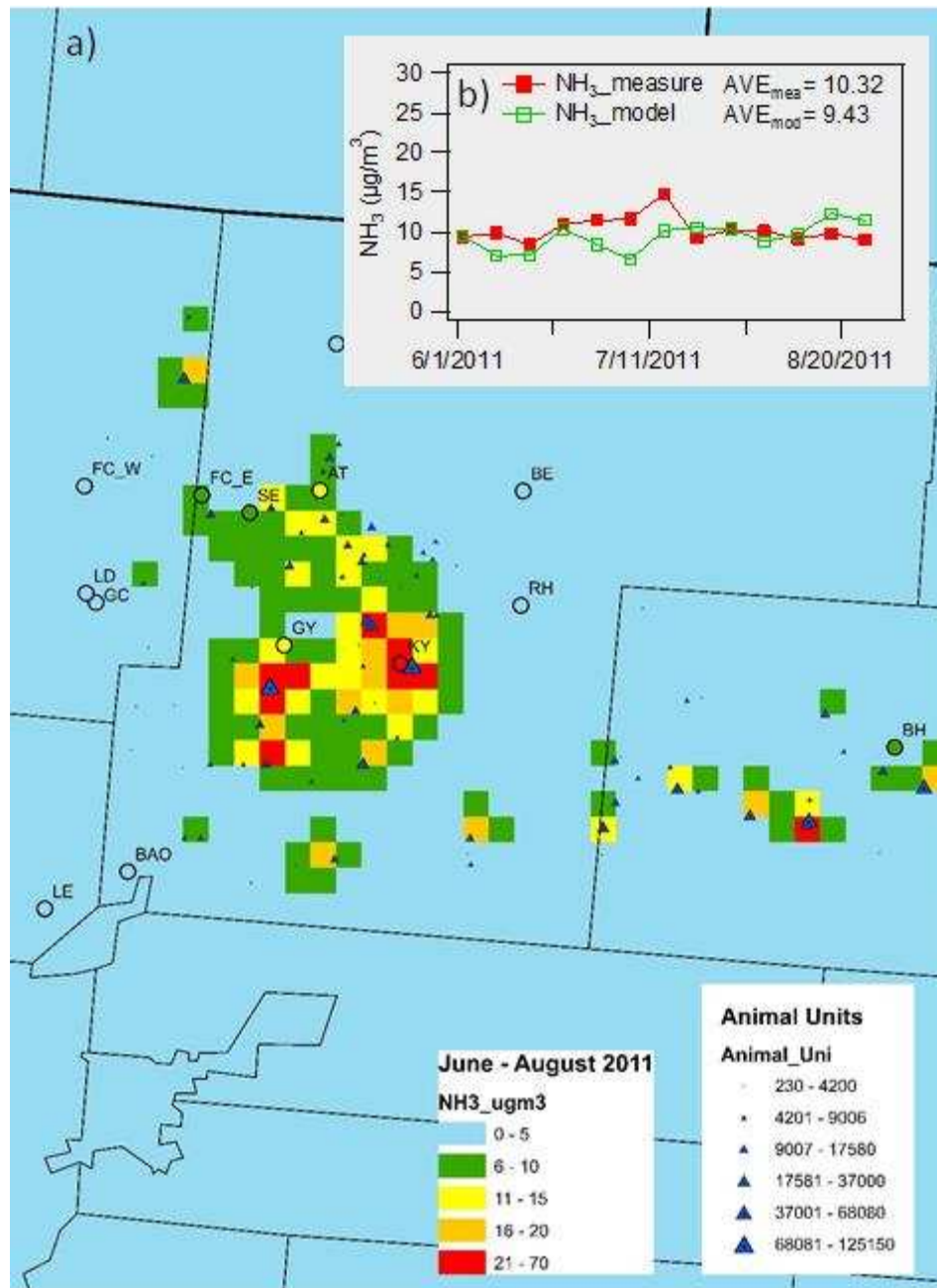
Figure 4.13 Comparison of spatial patterns (a) and time series (b) of average NH₃ concentrations measured by passive sampler and modeled by CAMx in the summer of 2011(06/02/2011-08/31/2011). The time series represent the average NH₃ concentrations modeled and measured at the surface monitoring locations.
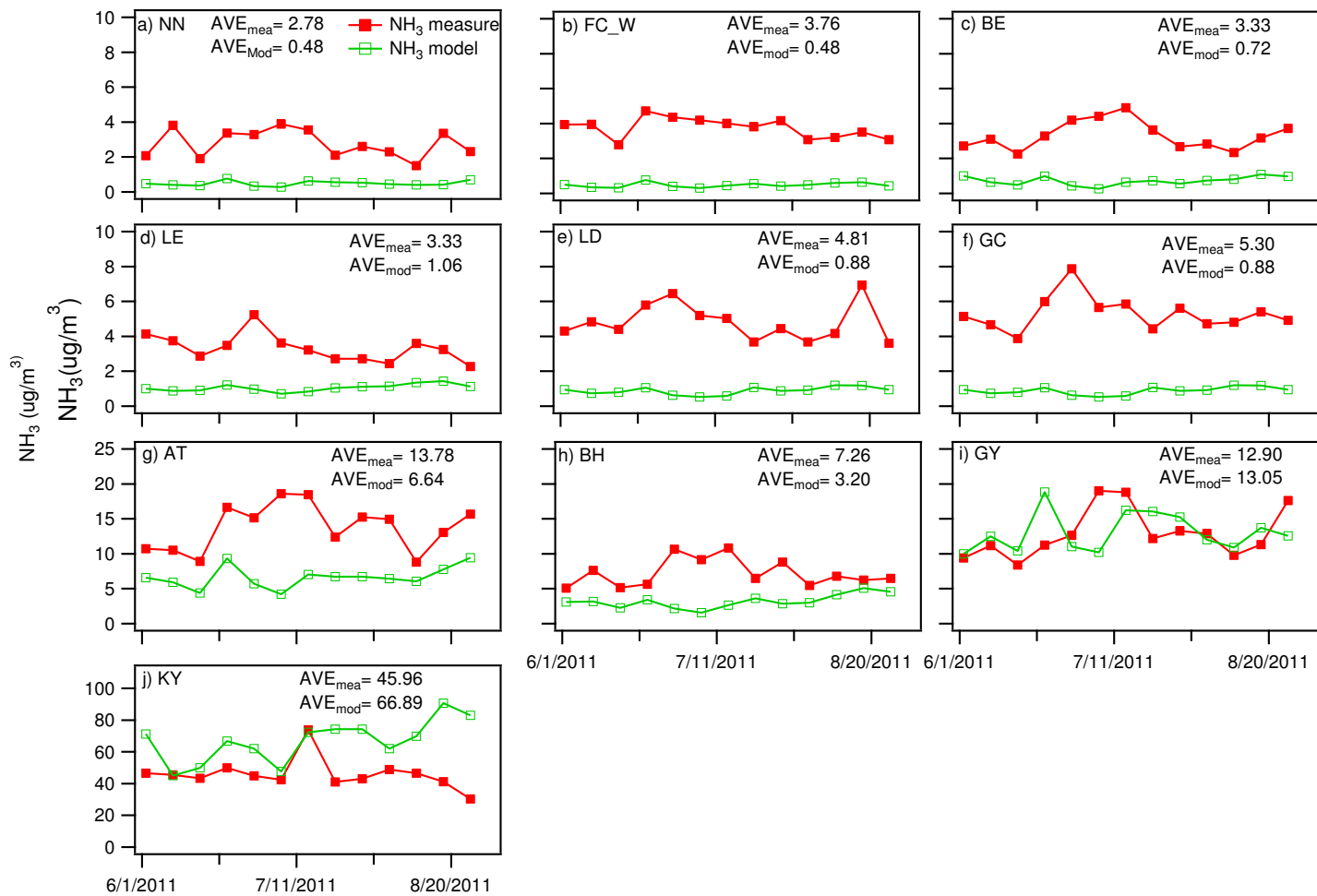
Figure 4.14 Time series of weekly NH$_3$ concentrations measured (red) and modeled (green) in the summer of 2011(06/02/2011-08/31/2011) at all the sites.

Figure 4.15 shows both measured (measurements taken in 2012) and modeled (2011) vertical concentrations of NH_3 at the BAO Tower location. Although these comparisons are for two adjacent years, the results presented above demonstrate that seasonal average concentrations across the region are typically similar from year to year. Modeled vertical NH_3 concentrations are reported from the lowest 6 levels of the model, up to approximately 325 m above the surface. The model height represented by the value plotted on the y-axis in Figure 4.16 represents the top of the layer from which the corresponding concentration is reported (ie: the surface or lowest model layer is reported at 24 meters – the approximate height of the surface layer). Model layer height is based on the meteorological model and modeled pressure and is not fixed (http://vibe.cira.colostate.edu/wiki/Attachments/Modeling/3SAQS_2011_WRF_MPE_v05Mar2015.pdf). The vertical concentrations are homogeneous within each model layer. Therefore, the model is not able to capture the detailed vertical pattern shown from 0 to 10 to 20 meters by the observations.

The model-measurement comparisons of vertical profiles demonstrate a significant underprediction by the model at all elevations in all four seasons. The underprediction at the surface is consistent with the observation above that the model tends to underestimate ammonia concentrations farther from the major regional feedlot sources. The fact that the model also underpredicts ammonia aloft suggests that the surface mismatch is not simply a result of excess vertical transport of ammonia in the model. Normalized model vertical NH_3 concentration profiles are shown in Figure 4.16. These profiles suggest that the model does a fairly reasonable job of capturing the shape of the observed vertical concentration gradient, although the relative concentration decrease with height in the model is a bit stronger than observed in each season.

99
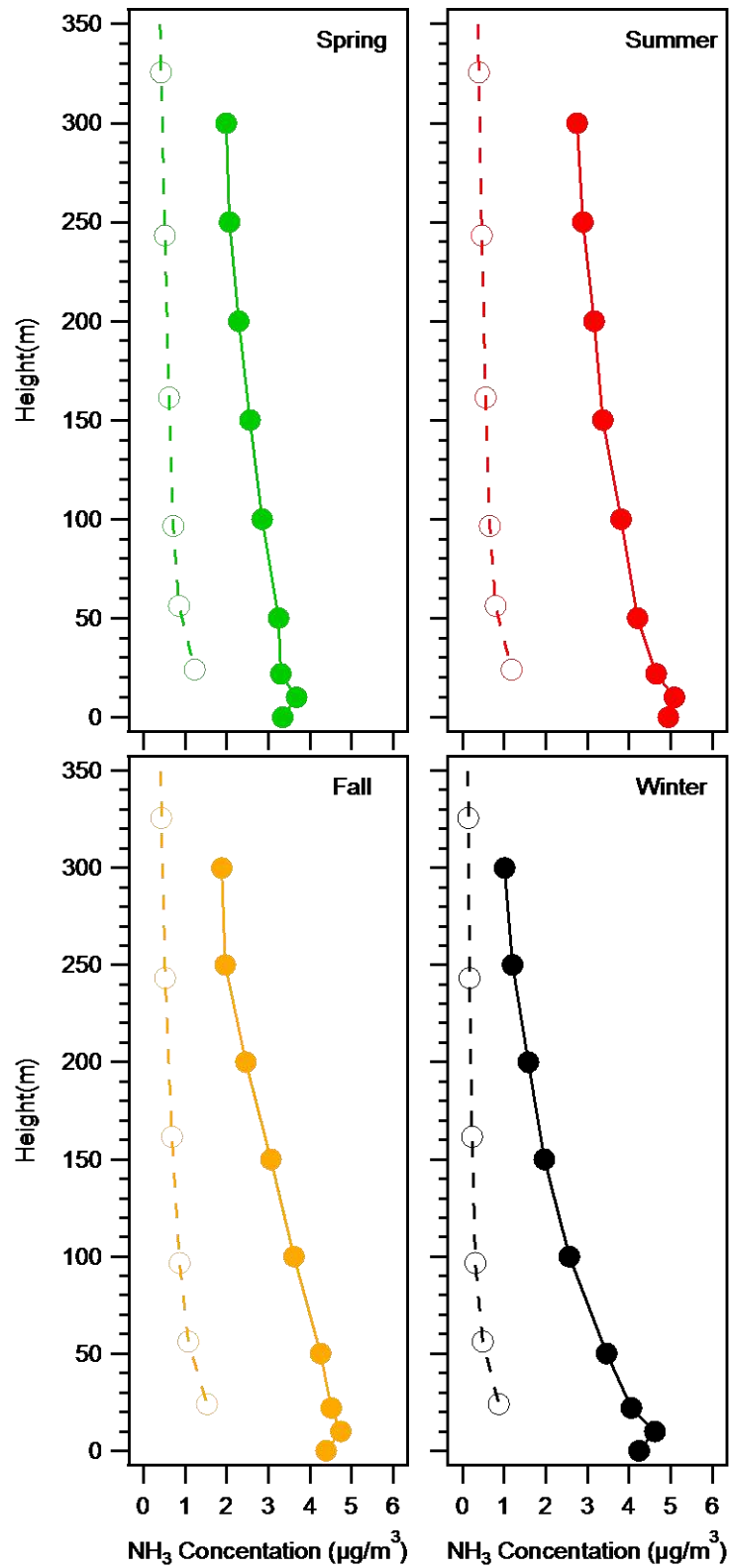
Figure 4.15 Comparison of seasonal 2012 NH₃ passive measurements (solid lines) and 2011 CAMx modeling results (dashed lines).
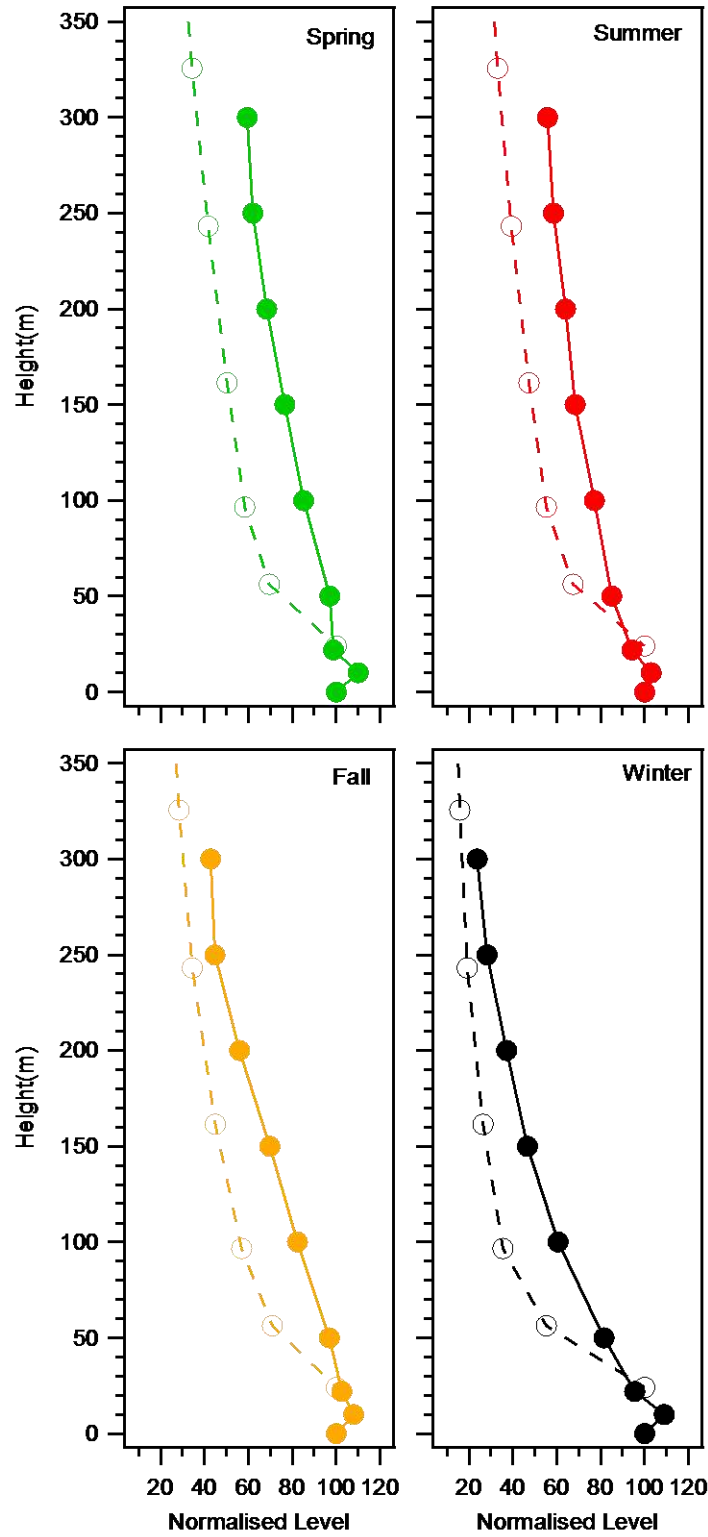
Figure 4.16 Comparison of seasonal normalized NH$_3$ passive measurements (solid lines) and CAMx modeling results (dashed lines). Each profile is normalized such that the concentration at the lowest level is set to 100.

4.5 Summary

Five years of observed NH_3 concentrations revealed strong spatial gradients in NH_3 concentrations in northeastern Colorado. Summer average weekly NH_3 concentrations ranged from 2.8 $\mu g/m^3$ to 41.3 $\mu g/m^3$. The lowest average NH_3 concentration always occurred at a remote prairie site, while NH_3 concentrations nearly a factor of 13 greater were observed at a site near a large animal feeding operation. No clear regional trends are present in NH_3 concentrations in NE Colorado across the study period, consistent with relative stability in regional livestock headcounts and similarity in meteorological conditions. The NH_3 concentration levels observed in this study, however, are expected to provide an important reference point for evaluating the success of future efforts to mitigate regional NH_3 emissions through voluntary implementation of BMPs as part of a strategy to reduce nitrogen deposition levels and impacts in Rocky Mountain National Park.

Measurement of NH_3 at the BAO meteorological tower near Erie, Colorado provide the first long-term insights into vertical gradients of NH_3 in the region and some of the first long-term measurements of this type anywhere in the world. A general pattern of decreased NH_3 concentrations with height above 10 m was observed in all seasons as was a decrease in concentration below 10 m height. Surface deposition, vertical dilution, and the formation of thermal inversions that limit the vertical mixing of regional, surface-based NH_3 emissions appear to have greater influence than temperature and humidity-driven changes in NH_4NO_3 gas-particle partitioning on the observed vertical concentration profiles.

Comparison of measured NH_3 spatial and vertical distributions with IASI satellite retrieved NH_3 columns reveals that IASI is able to accurately capture some of the spatial variability observed in

the lower atmosphere, even in the presence of strong spatial gradients. Spatial gradients throughout NE Colorado were represented reasonably well by the satellite measurements. Some periods of poorer agreement were associated with the detection of NH_3 rich elevated smoke plumes observed by the satellite but not by the surface measurement stations.

A comparison of measured NH_3 concentrations with concentrations simulated by the CAMx model reveal both strengths and weaknesses of the model simulation. Extra effort spent accurately locating large NH_3 emission sources resulted in relatively close agreement between model and measurement in source-rich regions. The model, however, underestimated concentrations substantially at locations further from large CAFO sources. This underestimation, observed throughout the lower atmosphere, may come from underestimation of non-agricultural ammonia emissions and/or from a tendency to overpredict ammonia surface deposition in the model. Future efforts to include bidirectional treatment of ammonia surface exchange in chemical transport models are expected to reduce net deposition rates and, therefore, should improve model-observation agreement at greater distance from major source.

5. THE INCREASING IMPORTANCE OF DEPOSITION OF REDUCED NITROGEN IN THE UNITED STATES[3]

Analyses of wet deposition records provide important insight into the shift from oxidized to reduced nitrogen deposition across the contiguous U.S. Recently expanded measurements of gas and particle phase reactive nitrogen species permit an assessment of current contributions of oxidized and reduced nitrogen to the U.S. N_r dry deposition budget. By combining these analyses, we gain a clear picture of the importance of both oxidized and reduced nitrogen to the total (wet + dry) N_r deposition budget across much of the U.S.

5.1 Oxidized vs. Reduced N in Wet N Deposition

Figure 5.1 compares percentage contributions of NH_4^+ to wet inorganic N ($NH_4^+ + NO_3^-$) deposition across the U.S. in the 3-yr periods centered on 1991 and 2011. To help visualize spatial patterns, isopleths in Figure 5.1 were produced by interpolating NH_4^+ mole percentages at individual monitoring sites using a cubic inverse-distance weighting of all sites within 500 km of each observation station in ESRI ArcMap 10.3. While wet N deposition was dominated by oxidized N (NO_3^-) across much of the country in the early 1990s, most locations now receive a

---

[3] *This chapter is a draft of material for the results and discussion and conclusion sections of a planned journal manuscript. Yi Li will be the lead author. Contributing co-authors include Bret A. Schichtel, John Walker, Donna B. Schwede, Xi Chen, Christopher Lehmann, Melissa Puchalski, David Gay, and Jeffrey L. Collett, Jr.*

majority of their wet N deposition as reduced N (NH_4^+), a trend also recently reported by Du et al. (2014). During the period 1990-1992, 69% of the observation sites saw oxidized N contributions in excess of 50%; twenty years later 69% of the sites instead saw wet deposition of reduced N in excess of 50%.
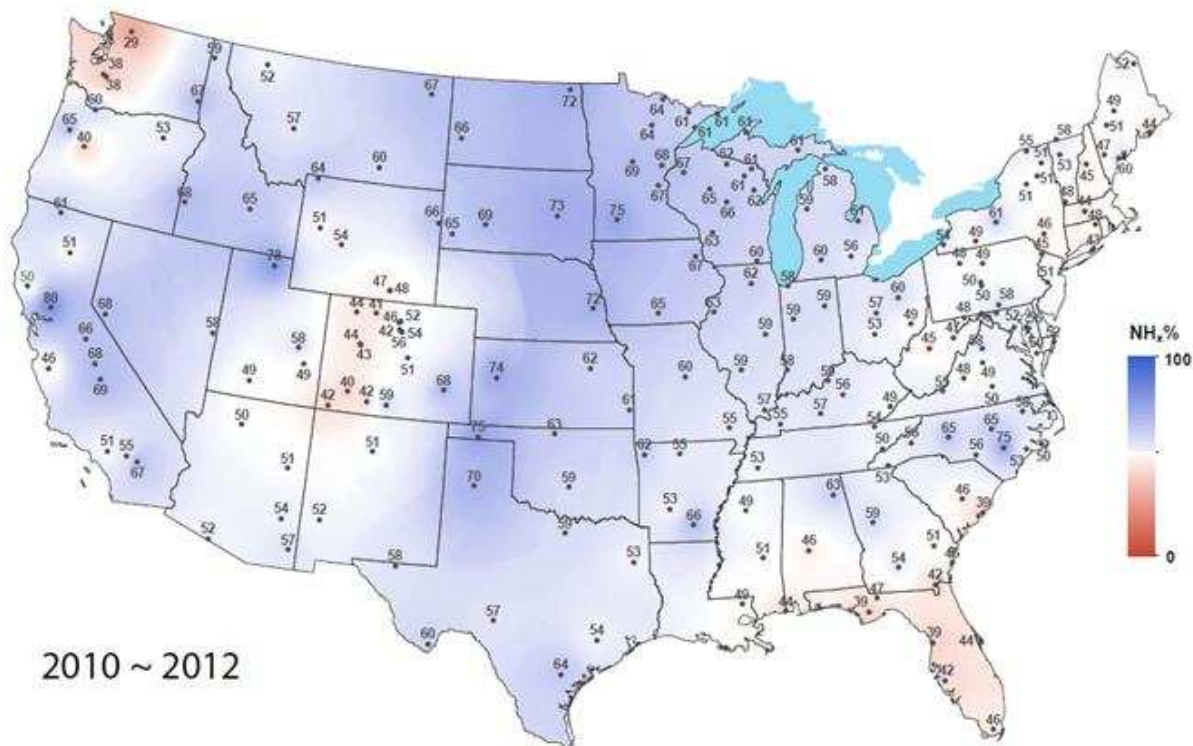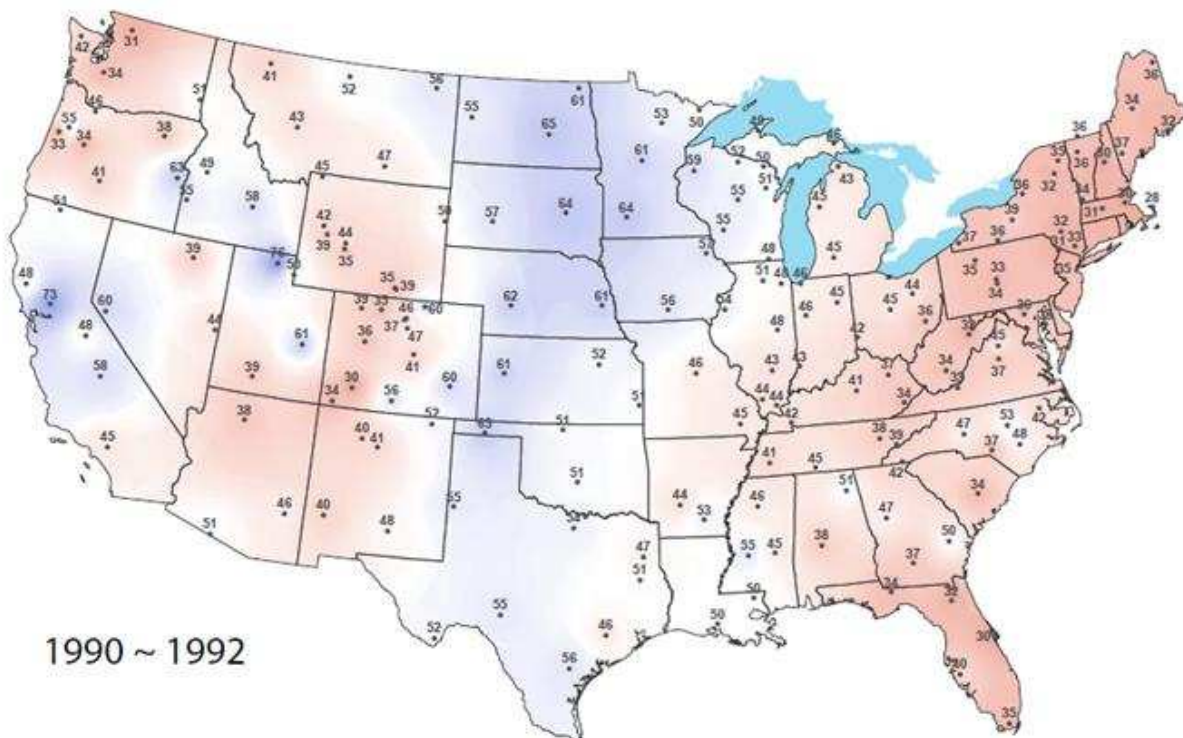
Figure 5.1 Comparisons of the 3-year average NH_4^+ mole ratio (as a percentage of wet inorganic nitrogen) across the U.S. in 1990-1992 (above) and 2010-2012 (below). NH_4^+ percentage (NH_4^+ %) = (NH_4^+-N)/(NO_3^--N+NH_4^+-N)×100%. The circles on the map represent locations

Changes in fractional contributions of oxidized and reduced N depend on the combined changes in wet deposition fluxes of NH_4^+ and NO_3^-. Figure 5.2 examines these changes for 45 of the 48 contiguous United States with available data. In every state but North Dakota, nitrate wet deposition fluxes decreased, with an average decrease of 29%. The nationwide decrease of oxidized N in wet deposition is consistent with the downward trend of U.S. NO_x emissions. With the successful implementation of the Clean Air Act (CAA) and the 1990 Amendments, NO_x emissions have been estimated to decline by 36% between 1990 and 2008 (Davidson et al., 2012). Nitrate wet deposition decreases were largest in the northeastern U.S., an area where large NO_x emissions reductions were implemented. Lehmann and Gay (2011) examined trends in nitrate concentrations in U.S. wet deposition in detail for a slightly earlier period, ending in 2009, and also highlight large reductions in the northeastern U.S. In contrast to decreasing nitrate, many sites experienced an increase in ammonium wet deposition. Thirty seven of the 45 states shown in Figure 5.2 saw an increase in ammonium wet deposition over the past two decades; for these states the average increase was 22%. Increases in ammonium wet deposition were especially common in the northern plains states, including Nebraska, Wyoming, Montana, the Dakotas, and Minnesota; relatively large increases were also seen in North Carolina, Kentucky, Maryland, and New Jersey. Substantial increases in ammonium ion concentrations in precipitation in the central and western U.S. were previously reported through 2004 by Lehmann et al. (2007). Increases in both ammonium ion concentrations in precipitation and ammonium wet deposition are not surprising given the increases in U.S. ammonia emissions.

a)

NH

MA

NJ

MD

NH$_4$$^+$% NO$_3$$^-$%

100
50
0
-50
-100

$$\text{Change\%} = \frac{(C_{10\sim12} - C_{90\sim92})*100}{C_{90\sim92}}$$
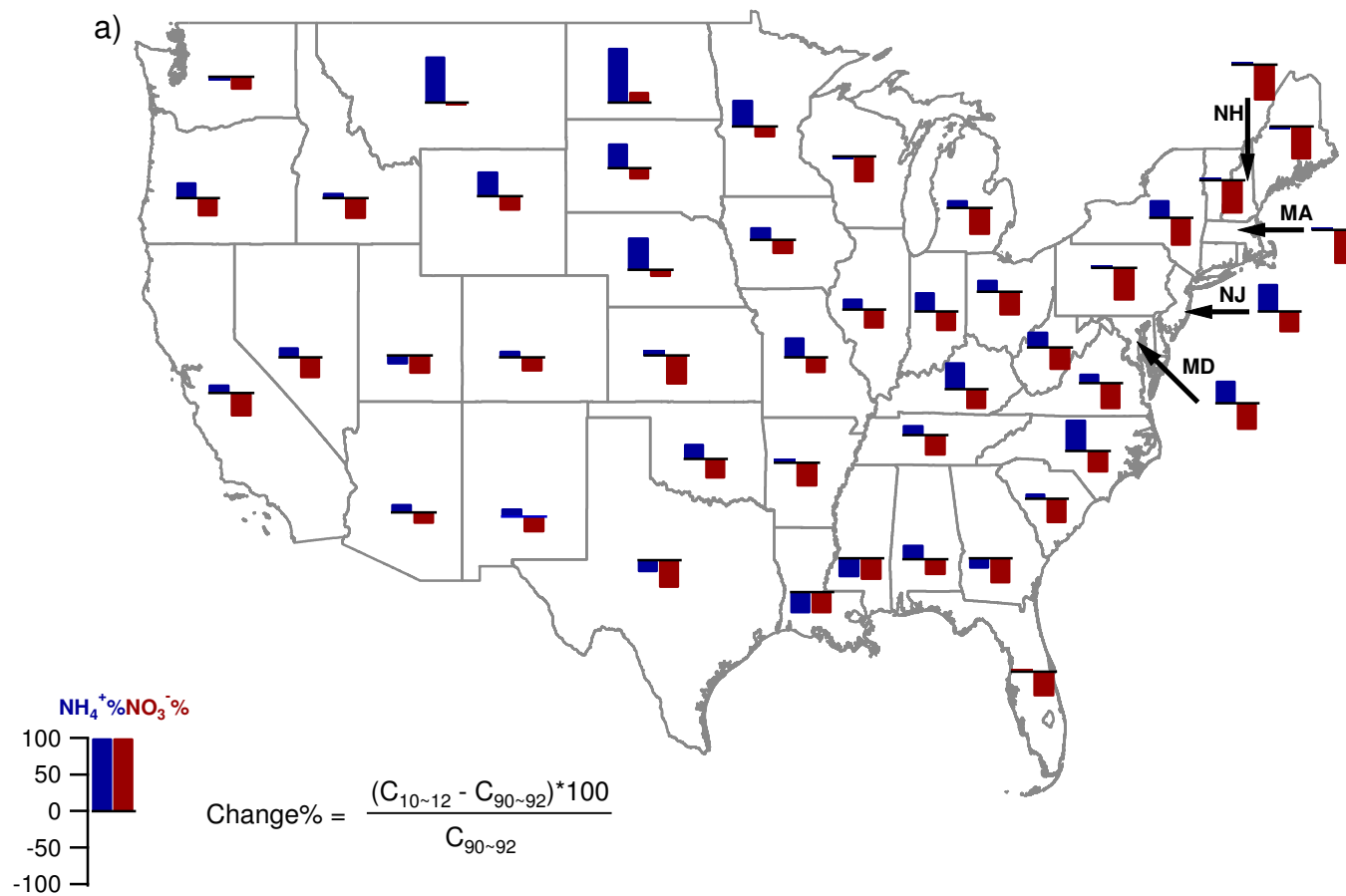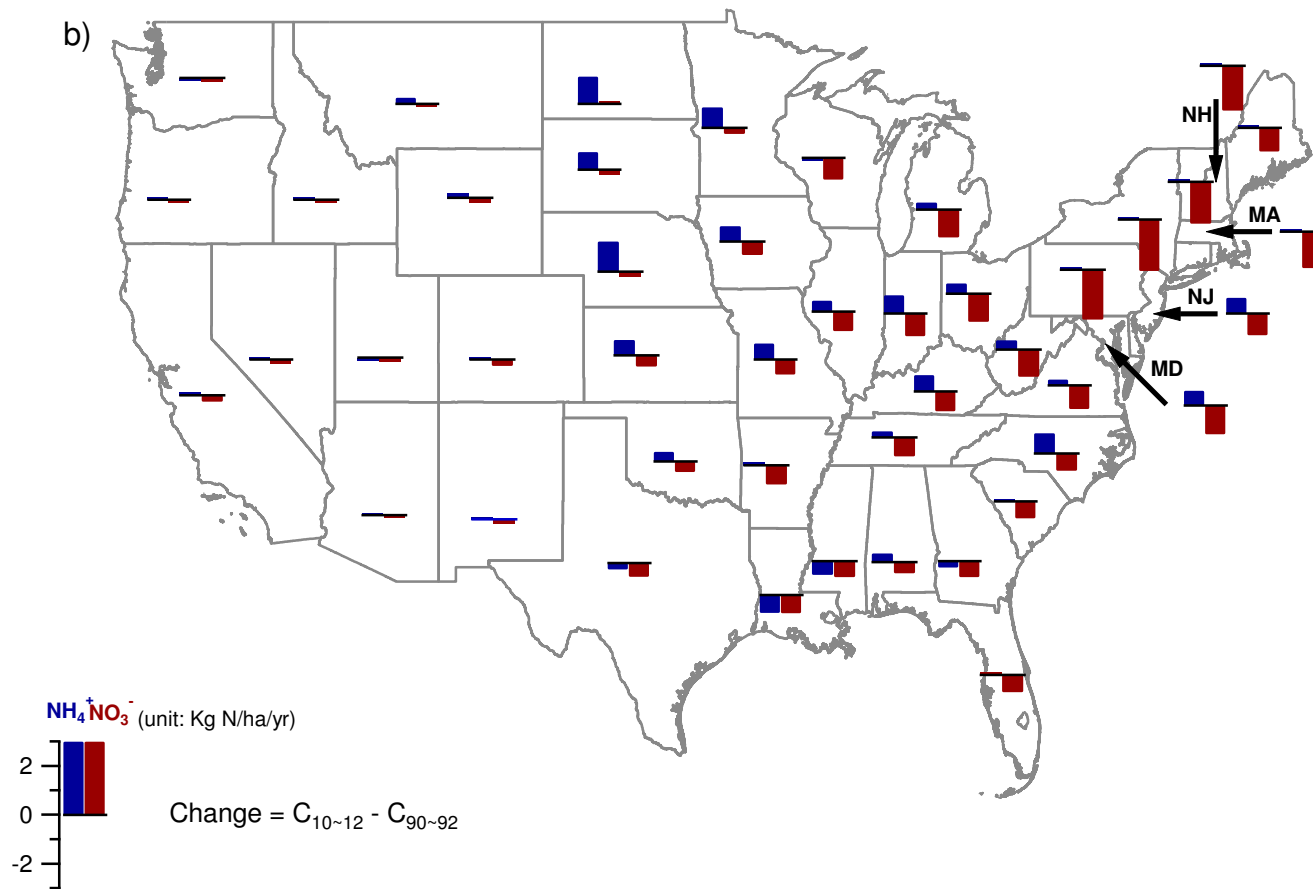
Figure 5.2 (a) Percentage change and (b) absolute wet deposition flux change of NH_4^+ and NO_3^- in wet N deposition across the country. C10~12 is the average NH_4^+ or NO_3^- flux (Kg N/ha/yr) in each state between 2010 and 2012 and C90~92 is the average NH_4^+ or NO_3^- flux (Kg N/ha/yr) between 1990 and 1992. Only sites in Figure 5.1 with both 1990-1992 and 2010-2012 data available are used to calculate the average flux for each state

5.3 Oxidized vs. Reduced Dry Inorganic N Deposition

Gas phase nitric acid and ammonia and particulate ammonium and nitrate are potentially important contributors to dry inorganic N deposition, especially in dry climates. Limited historical measurements, especially for ammonia, prevent an analysis of long-term trends of oxidized vs. reduced dry inorganic nitrogen deposition like those presented above for wet deposition. Recent efforts to more routinely measure gas phase ammonia concentrations by AMoN and the IMPROVE NHx pilot network, however, allow a comparison of the current balance between oxidized and reduced inorganic N dry deposition. We focus here on characterizing spatial patterns for the period 2011-2013. Figure 5.3 illustrates (by circle size) the current status of dry inorganic N deposition across the U.S. Significant spatial variability is seen from site to site, reflecting differences in species concentrations. Estimated annual sums of dry deposition by gaseous ammonia and nitric acid and particulate ammonium and nitrate range from 0.49 kgN ha^{-1} a^{-1} (WY08) to 13.4 kgN ha^{-1} a^{-1} (NE98). Reduced N contributes more than 50% of the total calculated dry inorganic N deposition at all sites except Mesa Verde National Park (CO99) (44%) in southwest Colorado. This remote, arid site is expected to have relatively small agricultural impacts (Chen et al., 2014) but greater influence of NO$_x$ emitted from nearby oil and gas development (Rodriguez et al., 2009) and the Four Corners and San Juan power plants, two of the largest coal-fired power plants in the western U.S. The highest fractional and absolute reduced N contributions are seen, not surprisingly, in areas with substantial agricultural activity, including sites in Illinois (site IL37 exhibits the highest reduced N fraction at 90%), Nebraska, and the Central Valley of California.
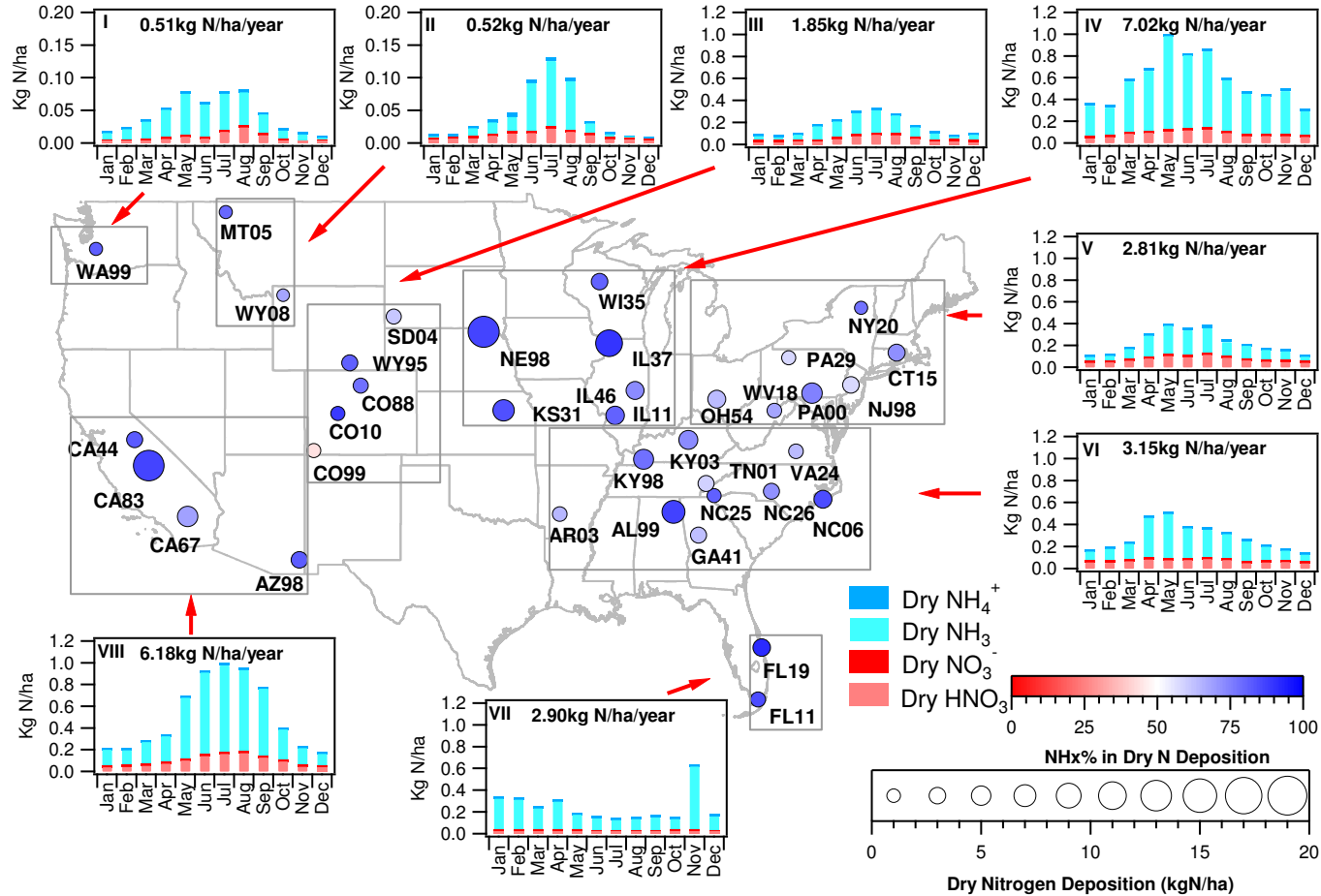
Figure 5.3 Spatial and temporal trends in dry inorganic N deposition at 37 locations across the U.S. Included are deposition of gaseous nitric acid and ammonia and PM$_{2.5}$ ammonium and nitrate. Fractional reduced N contributions are represented by circle color. The total deposition from these four species is indicated by circle size. The bar charts depict monthly average contributions of individual dry reduced and oxidized N deposition pathways for 8 selected regions. The total dry inorganic N deposition flux in different regions are shown by the number in each figure.

To examine overall dry deposition patterns, sites were grouped into eight regions (by proximity and similar trends) as follows (see Table 5.1): Region I (Washington), Region II (Montana and northern Wyoming), Region III (Western South Dakota, Southern Wyoming , Colorado), Region IV (Wisconsin, Illinois, eastern Kansas, eastern Nebraska), Region V (New York, Connecticut, New Jersey, Pennsylvania, Ohio, West Virginia), Region VI (Kentucky, Virginia, Tennessee, North Carolina, Georgia, Alabama, Arkansas), Region VII (Florida), and Region VIII (California and southern Arizona). Regional site assignments are grouped as indicated by the boxes in Figure 5.3. The lowest regional average value of dry N deposition was found in Region I (0.51 kg N/ha/year) and the highest value was found in Region IV (7.0 kg N/ha/year), one of the nation's primary food production areas with large NH_3 emissions from livestock and fertilizer use. In most regions, dry ammonia and nitric acid deposition display strong seasonal patterns, with higher values in summer and lower values in winter. These seasonal patterns are driven mostly by seasonal concentration patterns rather than seasonal changes in deposition velocity. Ammonia emissions increase with warmer summertime temperatures due to enhanced volatilization (Brunke et al., 1988; Sommer et al., 1991). Active summertime photochemistry speeds conversion of emitted NO_x to nitric acid while warmer summertime temperatures reduce the formation of fine particle ammonium nitrate, leaving more nitric acid and ammonia in the gas phase (Li et al., 2014). Interestingly, there is still considerable dry NH_3 deposition estimated during the winter in the central U.S. (Region IV). Higher winter ammonia concentrations in this region might reflect trapping of cold season ammonia emissions (from livestock and/or winter fertilizer application) near the surface by a shallow boundary layer (Chen et al., 2014). Dry N deposition exhibits a winter seasonal maximum in Florida. Increased summertime precipitation here suppresses summertime atmospheric concentrations, and therefore dry deposition, of reduced and oxidized N

113

species. Ammonia and nitric acid are both quite soluble at typical precipitation pH values while fine particle nitrate and ammonium can be efficiently scavenged by heterogeneous nucleation in clouds and incorporated into precipitation. Wet N deposition contributed over 75% of total (wet + dry) inorganic N deposition during the summer when there was more precipitation (Figure 5.4); dry deposition of reduced N was the dominant input during the drier winter season. The highest input occurs in November when precipitation reached an annual minimum.

Table 5.1 Locations of network sites and period of record plotted in Figure 5.3 and Figure 5.5

Group	Site_ID	Site Name	State	Latitude(ºN)	Longitude(ºW)	Period of record	AMoN site	CASTNET site	NTN site	IMPROVE NHx site
Region I	WA99	Mount Rainier National Park	WA	46.7582	-122.124	07/11~06/13	WA99	MOR409	WA99	
Region II	MT05	Glacier National Park	MT	48.5105	-113.997	07/11~06/12*		GLR468	MT05	GLACS
	WY08	Yellowstone National Park	WY	44.5653	-110.4	07/11~06/12*		YELL408	WY08	YELLS
Region III	CO10	Gothic	CO	38.9561	-106.986	09/12~06/13**	CO10	GTH161	CO10	
	CO88	Rocky Mountain National Park	CO	40.2778	-105.545	07/11~06/13	CO88	ROM406	CO19	
	CO99	Mesa Verde National Park	CO	37.1984	-108.491	07/11~06/12*		MEV405	CO99	MEVES
	SD04	Wind Cave	SD	43.5576	-103.484	07/11~06/12*		WNC429	SD04	WICAS
	WY95	Brooklyn Lake	WY	41.3647	-106.241	07/12~06/13*	WY95	CNT169	WY95	
Region IV	IL11	Bondville	IL	40.0528	-88.3719	07/11~06/13	IL11	BVL130	IL11	
	IL37	Stockton	IL	42.2869	-89.9997	07/11~06/13	IL37	STK138	IL18	
	IL46	Alhambra	IL	38.8689	-89.6219	07/11~06/13	IL46	ALH157	IL46	
	KS31	Konza Prairie	KS	39.1022	-96.6092	07/11~06/13	KS31	KNZ184	KS31	
	NE98	Santee	NE	42.8292	-97.8541	07/11~06/13	NE98	SAN189	SD99	
	WI35	Perkinstown	WI	45.2064	-90.5978	07/11~06/13	WI35	PRK134	WI35	
Region V	CT15	Abington	CT	41.84	-72.0101	07/11~06/13	CT15	ABT147	CT15	
	NJ98	Washington Crossing	NJ	40.3125	-74.8729	07/11~06/13	NJ98	WSP144	NJ99	
	NY20	Huntington Wildlife	NY	43.9731	-74.2231	07/12~06/13*	NY20	HWF187	NY20	
	OH54	Deer Creek State Park	OH	39.6359	-83.2606	07/11~06/13	OH54	DCP114	OH54	
	PA00	Arendtsville	PA	39.9231	-77.3078	07/11~06/13	PA00	ARE128	PA00	
	PA29	Kane Experimental Forest	PA	41.5978	-78.7675	07/11~06/13	PA29	KEF112	PA29	
	WV18	Parsons	WV	39.0897	-79.6622	07/11~06/13	WV18	PAR107	WV18	
Region VI	AL99	Sand Mountain Research & Extension Center	AL	34.2886	-85.9699	07/11~06/13	AL99	SND152	AL99	
	AR03	Caddo Valley	AR	34.1795	-93.0992	07/11~06/13	AR03	CAD150	AR03	
	GA41	Georgia Station	GA	33.1805	-84.4103	07/11~06/13	GA41	GAS153	GA41	
	KY03	Mackville	KY	37.7047	-85.0489	07/11~06/13	KY03	MCK131	KY03	
	KY98	Cadiz	KY	36.7841	-87.8499	07/11~06/13	KY98	CDZ171	KY99	
	NC06	Beaufort	NC	34.8846	-76.6207	07/11~06/13	NC06	BFT142	NC06	
	NC25	Coweeta	NC	35.0605	-83.4305	07/11~06/13	NC25	COW137	NC25	
	NC26	Candor	NC	35.2632	-79.8365	07/11~06/13	NC26	CND125	NC36	
	TN01	Great Smoky Mountains National Park	TN	35.6331	-83.9422	07/11~06/13	TN01	GRS420	TN01	
	VA24	Prince Edward	VA	37.1652	-78.3073	07/11~06/13	VA24	PED108	VA24	

Region VII	FL11	Everglades National Park	FL	25.39	-80.68	07/11~06/13	FL11	EVE419	FL11
	FL19	Indian River	FL	27.8492	-80.4554	07/11~06/13	FL19	IRL141	FL99
Region VIII	AZ98	Chiricahua National Monument	AZ	32.0097	-109.389	07/11~06/13	AZ98	CHA467	AZ98
	CA44	Yosemite National Park	CA	37.7133	-119.706	07/11~06/13	CA44	YOS404	CA99
	CA67	Joshua Tree National Park	CA	34.0695	-116.389	07/11~06/13	CA67	JOT403	CA67
	CA83	Sequoia National Park	CA	36.4894	-118.823	07/11~06/13	CA83	SEK430	CA75

*   The record period of data was one year

** The record period of data was one year
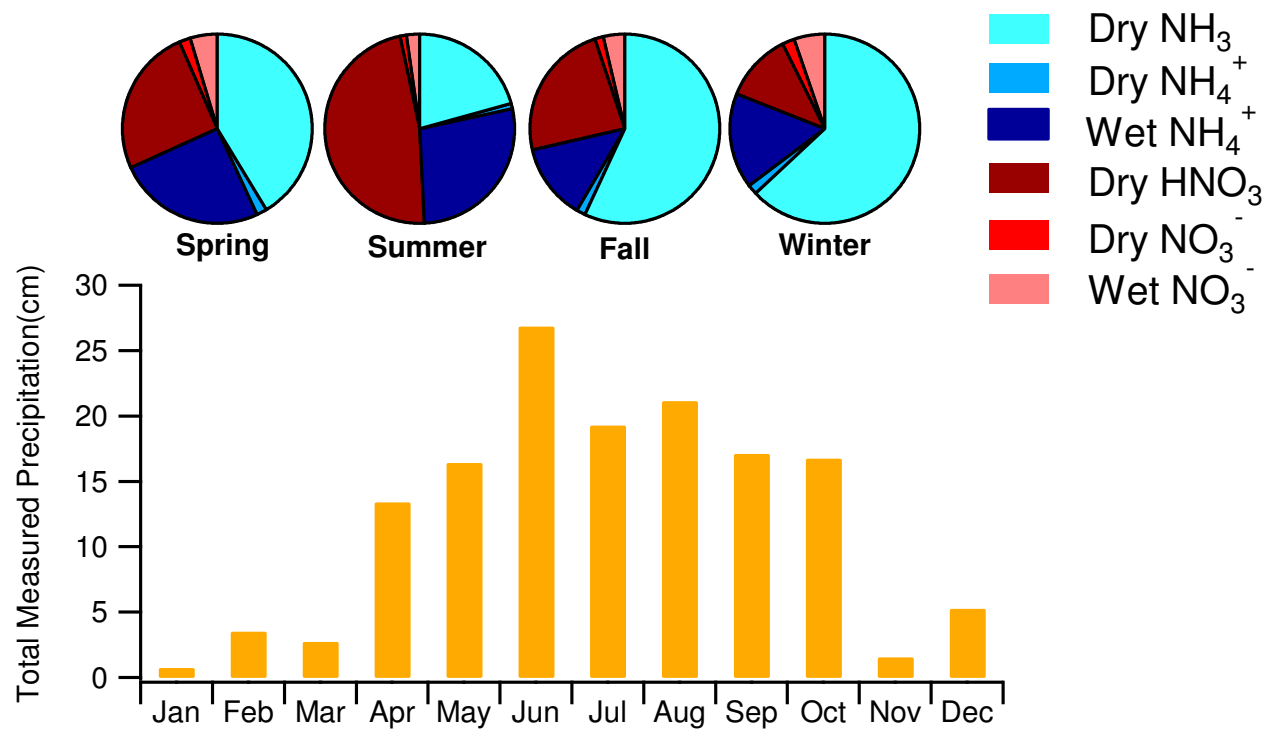
Figure 5.4 Pie charts of seasonal N deposition species pathways (top) and total monthly measured precipitation (bottom) in Florida (FL 11 and FL19)

To assess the potential uncertainty in the MLM deposition velocity approach used for the NH_3 dry deposition assessment (the NH_3 dry deposition velocity is set equal to 0.7 times the MLM modeled HNO_3 deposition velocity), this method was compared to the more mechanistically representative bi-directional flux model (Figure 5.5). At the annual scale, deposition rates estimated using the MLM approach are larger than those derived from the bi-directional model by a factor of 1.68 (median of 35 sites listed in Figure 5.5). Model differences result from stomatal and ground compensation points, as well as the effects of surface acidity, represented in the bi-directional framework. The net result of these processes is to reduce the gradient in NH_3 concentration, and therefore the flux, between the atmosphere and land surface relative to the unidirectional (deposition velocity) MLM approach, which assumes a zero surface concentration. This reduction in NH_3 dry deposition rates, relative to the unidirectional flux framework, was also observed upon implementation of NH_3 bi-directionality in the Community Multiscale Air Quality Model.
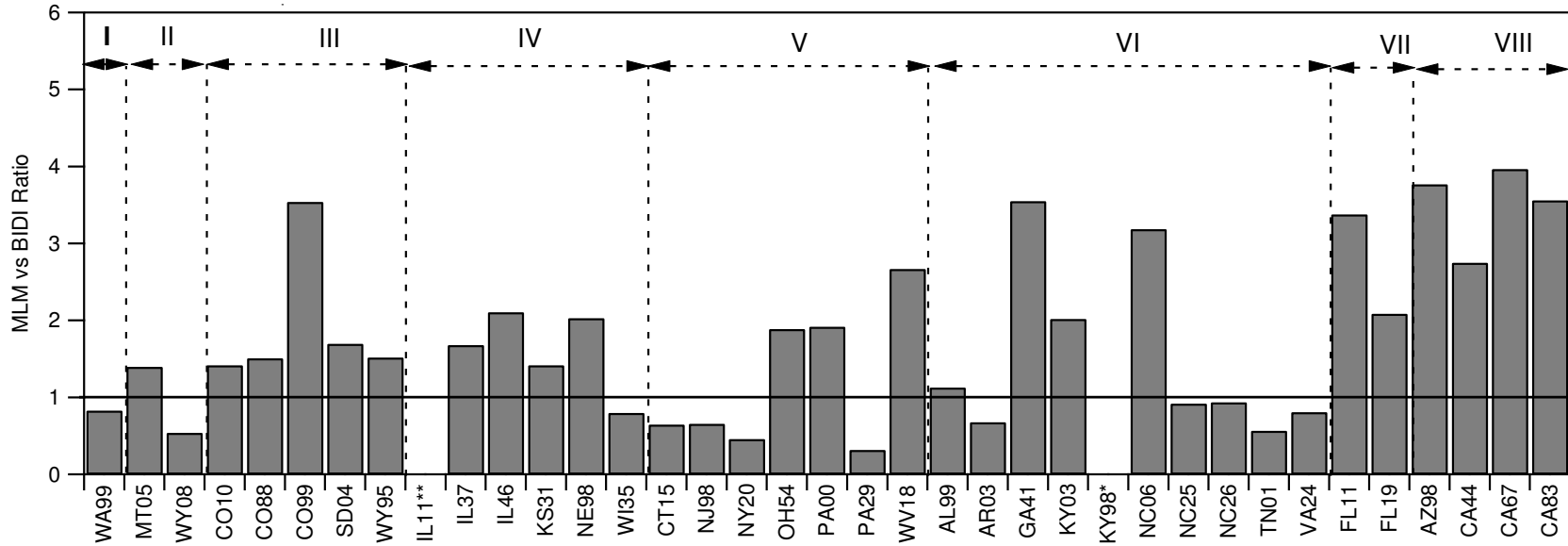
Figure 5.5 Ratio of annual NH$_3$ dry deposition rates estimated using the MLM versus bi-directional approaches. Regions are indicated at top of graph

* Due to lack of meteorological data, bi-directional flux model is not parametrized appropriately for the KY98 site.

** Due to feature of surface plants, bi-directional flux model is not parametrized appropriately for the IL11 site

Across regions (Figure 5.5), there is considerable variability in the difference between MLM and bi-directional estimates among sites. In some cases, bi-directional flux estimates exceed MLM estimates. However, MLM estimates consistently exceed bi-directional flux estimates in regions III, VII, and VIII. In regions VII and VIII, this is largely due to relatively low atmospheric concentrations of SO_2 and HNO_3 (see acid ratio, Appendix A), which in turn yields less acidic vegetation surfaces under the bi-directional framework and corresponding lower rates of NH_3 deposition to leaf cuticles than would occur on more acidic surfaces. In region III, model differences arise from a combination of processes. Site CO99 experiences very low NH_3 air concentrations. During warm conditions, the stomatal compensation point exceeds the atmospheric NH_3 concentration, resulting in a net stomatal emission that offsets deposition to the leaf cuticle and ground, thereby producing a low net annual deposition flux. Similar competing flux processes are observed at sites SD04 and WY95, particularly during warm months.

5.4 Fractional Reduced N contributions to the Total Inorganic N Deposition Budget

With wet and dry deposition estimates available for 37 locations, the total wet plus dry nitrogen deposition fractions can be estimated across the U.S. by regions (Figure 5.6). Fractional deposition contributions by each wet and dry deposition pathway for each of the 8 defined deposition regions are illustrated in the inset pie charts in Figure 5.6. Fractional wet plus dry inorganic N deposition contributions by reduced species are indicated by the color of the circle for each measurement site. With most U.S. sites exhibiting a majority of both wet and dry inorganic N deposition attributable to reduced N species, as discussed above, the combined deposition budget is again dominated by reduced N inputs. Reduced N deposition fractions in the eight regions range from 58% (Region I) to 78% (Region VIII), with dry NH_3 deposition alone contributing between 19% (Region II) and 63% (Region VIII). Fractional reduced N contributions at individual sites range from 42% at CO99 (Mesa Verde National Park) to 84% at CA83 in California's Central Valley. The largest ammonia dry deposition fraction was also observed at CA83 (74%) while the smallest was at PA27 (11%). The spatial patterns of reduced N deposition fraction generally reflect spatial variations in agricultural activity including animal husbandry. Assuming that the biases between the MLM deposition velocity and bi-directional flux approaches shown in Figure 5.5 are generally representative, a full assessment using the bi-directional approach would, at many sites, reduce overall deposition rates and the relative fraction of NH_3 dry deposition. However, the general pattern observed in Figure 5.6 remains consistent; NH_x continues to dominate inorganic N deposition budgets at the national scale.
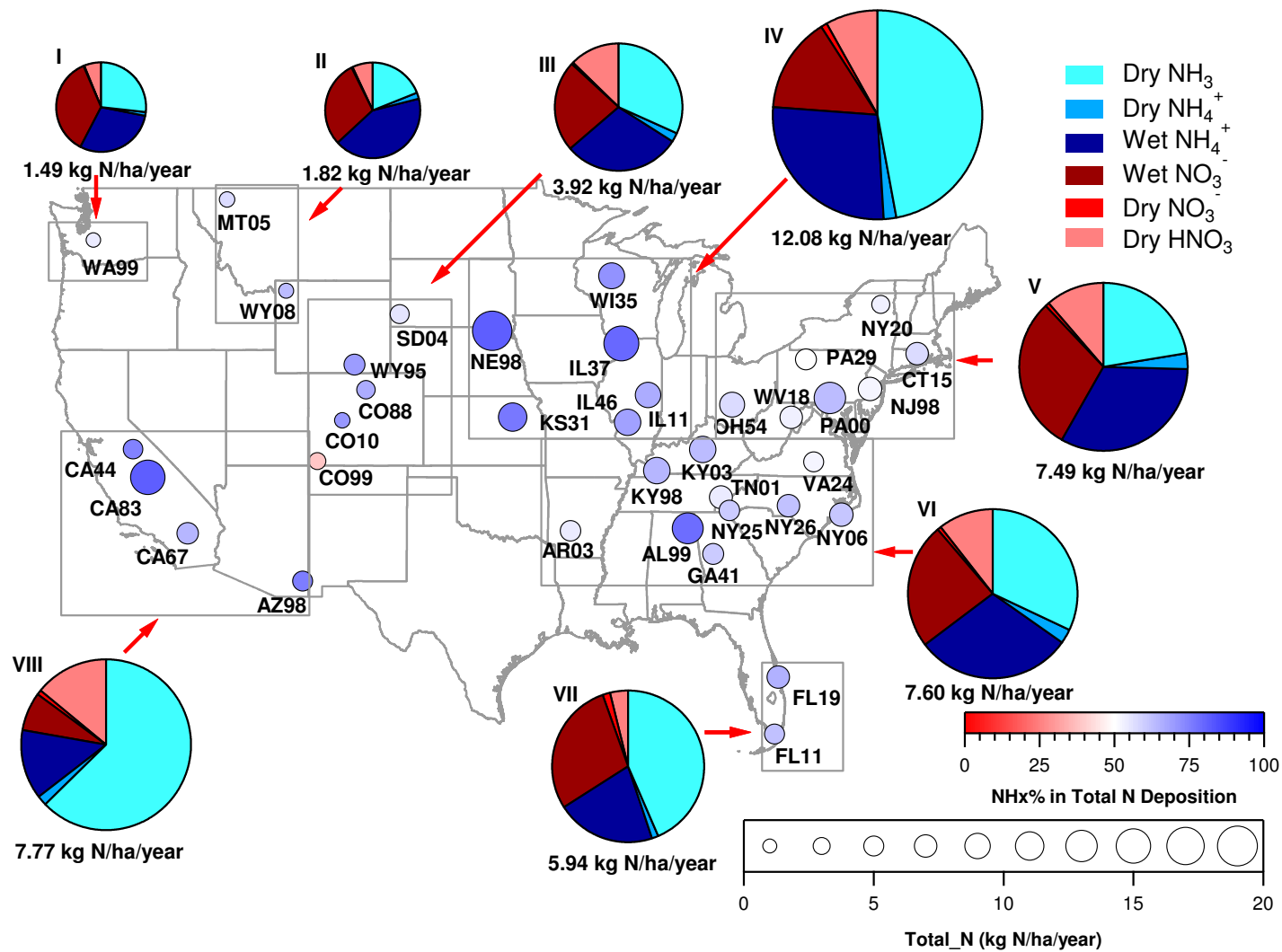
Figure 5.6 Spatial trends in total reactive inorganic N deposition across the U.S. from July 2011 to June 2013. Fractional reduced N contributions to total N deposition (dry + wet) at the 37 sites are represented by circle color. The total inorganic nitrogen deposition is

indicated by circle size. The pie charts show average fractional contributions of individual reduced and oxidized N deposition pathways for the same 8 regions identified in Table 5.1, with each pie area proportional to the average total inorganic nitrogen deposition listed under each pie chart.

The site-specific circle sizes in Figure 5.6 indicate the combined wet plus dry inorganic N deposition fluxes. Some regions exhibit majority dry deposition (e.g., dry deposition contributions of 58% and 79% in Regions IV and VIII, respectively) while others are more strongly influenced by wet deposition (e.g., wet deposition contributions of 66% and 72% in Regions I and VI). Note that the largest deposition fluxes at individual sites tend to be observed at locations where fractional reduced N contributions are large. The maximum regional average inorganic N deposition flux (12.1 kg N/ha/year) was observed in the Midwest region (Region IV); relatively large deposition fluxes were also observed for California and the eastern U.S. These spatial patterns are similar to those identified in recent model simulations (Bash et al., 2013; Schwede and Lear, 2014).

5.5 Summary

Rapid development of agricultural activities and fossil fuel combustion in the United States has led to a great increase in reactive nitrogen (N_r) emissions in the second half of the twentieth century. These emissions have been linked to excess nitrogen (N) deposition (i.e. deposition exceeding critical loads) in natural ecosystems through dry and wet deposition pathways. U.S. efforts to reduce nitrogen oxides (NO_x) emissions since the 1970s have substantially reduced nitrate deposition, as evidenced by decreasing trends in long-term wet deposition data. These decreases in nitrate deposition along with increases in wet ammonium deposition have altered the balance between oxidized (nitrate) and reduced (ammonium) nitrogen deposition. Across most of the U.S., wet deposition has transitioned from being nitrate-dominated in the 1980s to ammonium dominated in recent years. Because ammonia has not been a regulated air pollutant in the U.S., it

has historically not commonly been measured. Recent measurement efforts, however, provide a more comprehensive look at ammonia concentrations across several regions of the U.S. These data, along with more routine measurements of gas phase nitric acid and fine particle ammonium and nitrate, permit new insight into the balance of oxidized and reduced nitrogen in the total (wet + dry) U.S. inorganic reactive nitrogen deposition budget. Utilizing two years of N-containing gas and fine particle observations from 37 U.S. monitoring sites, we estimate that reduced nitrogen contributes, on average, approximately 65 percent of the total inorganic N deposition budget. Dry deposition of ammonia plays an especially key role in N deposition compared with other N deposition pathways, contributing from 19% to 65% in different regions. With reduced N species now dominating the wet and dry reactive N deposition budgets in much of the country, the U.S. will need to consider ways to reduce ammonia emissions if it is to continue progress toward reducing N deposition to sustainable levels defined by ecosystem critical loads.

CONCLUSIONS AND RECOMMENDATIONS FOR FUTURE WORK

A five-year study of concentrations of gaseous NH_3 and HNO_3 and of fine particle inorganic ions was conducted in an active gas production region in Boulder, Wyoming. The five-year annual mean concentrations of NH_3, HNO_3, NH_4^+, NO_3^- and SO_4^{2-} were 0.17, 0.19, 0.26, 0.32, and 0.48 $\mu g/m^3$, respectively. NH_3 exhibited a strong seasonal variation, with higher concentrations during the summer and lower concentrations during the winter. The low annual average NH_3 mixing ratio of 0.30 ppb suggests that the default value of 1 ppb often used in regional assessments of visibility impacts from NO_x source emissions is higher than necessary.

Observed NH_3 concentrations correlated well with ambient temperature indicating the important influence of temperature on emissions and, likely, the greater long distance transport of those emissions during warmer times of year when mixing layers deepen. By contrast, higher concentrations of particulate NO_3^- were observed in the winter when lower temperatures favor formation of NH_4NO_3. HNO_3 concentrations showed an unusual bimodal seasonal variation with higher levels both in summer (an expected result of active photochemical oxidation and a tendency for NH_4NO_3 to decompose at higher temperatures) and in winter. The unusual winter HNO_3 peak appears to be the result of active photochemical processing of local NO_x emissions in a shallow boundary layer during periods of snow cover and a lack of NH_3 to fully tie up HNO_3 through fine particle NH_4NO_3 formation. Examination of the equilibrium thermodynamics of NH_4NO_3 formation, seasonal local temperatures, and available concentrations of gaseous NH_3 and HNO_3, indicates that NH_4NO_3 should be expected primarily in winter, as observed.

Five years of observed NH_3 concentrations revealed strong spatial differences in NH_3 concentrations in northeastern Colorado. Summer average weekly NH_3 concentrations ranged from 2.8 $\mu g/m^3$ to 41.3 $\mu g/m^3$. The lowest average NH_3 concentration always occurred at a remote prairie site, while average NH_3 concentrations nearly a factor of 13 greater were observed at a site near a large animal feeding operation. Based on several years of available data, no significant inter-annual trends can be detected in NH_3 concentrations in the region except BH site, consistent with similar seasonal meteorological conditions and relative stability in regional livestock headcounts over the period. The NH_3 concentration levels observed in this study provide an important reference point for evaluating the success of future efforts to mitigate regional NH_3 emissions through voluntary implementation of BMPs as part of a strategy to reduce nitrogen deposition levels and impacts in Rocky Mountain National Park.

Measurement of NH_3 at the BAO meteorological tower near Erie, Colorado provide the first long-term insights into vertical gradients of NH_3 concentrations in the region and some of the first long-term measurements of this type anywhere in the world. A general pattern of decreased NH_3 concentrations with height above 10 m was observed in all seasons as was a decrease in concentration below 10 m height. Moderate average concentrations were observed in winter at the surface along with a steeper vertical concentration gradient. Higher average concentrations were observed in summer at all altitudes along with a shallower vertical concentration gradient. Surface deposition, vertical dilution, and the formation of thermal inversions that limit the vertical mixing of regional, surface-based NH_3 emissions appear to have greater influence than temperature and humidity-driven changes in NH_4NO_3 gas-particle partitioning on the observed vertical concentration profiles.

Comparison of measured NH$_3$ spatial distributions with IASI satellite retrieved NH$_3$ columns reveals both monitoring techniques capture similar spatial and temporal variability in northeastern Colorado. Some temporal differences at the FC_ W site appear to reflect NH$_3$ in elevated wildfire plumes that are observed from the satellite but are not sampled at the surface. This highlights the value of satellite measurements and the need for more comprehensive NH$_3$ datasets such as NH$_3$ vertical profile measurements.

Measured spatial distributions of NH$_3$ concentrations also provide a good basis for comparison to regional air quality model simulations. A comparison with CAMx simulations finds that the model does a fairly good job capturing ammonia concentrations in source regions, but underpredicts concentrations at locations further from major regional feedlot sources. A comparison of measured and modeled vertical profiles in a non-source region reveals an undeprediction of modeled ammonia from the surface up to 300 m in all seasons. The mismatch aloft provides evidence that the model difficulty reproducing surface observations away from sources is not a simple result of excess vertical mixing of ammonia emissions in the model. Rather, the model emission inventory may be missing or underpredicting smaller or non-agricultural ammonia sources or, perhaps more likely, the model may be overpredicting surface ammonia deposition due to the absence of bidirectional treatment of ammonia atmosphere-surface exchange. Although additional research is definitely needed, we expect the NH$_3$ concentrations and spatial/vertical differences presented here to be useful in constraining future simulated concentrations of atmospheric NH$_3$ in chemical transport models.

Increases in agricultural emissions of ammonia and the success of regulatory policies to reduce NO_x emissions over the past two decades are changing the face of U.S. reactive nitrogen deposition. While U.S. wet inorganic N deposition was once dominated by nitrate, wet inorganic N deposition now comes mostly from ammonium at nearly 70% of U.S. monitoring sites. Although estimates of dry deposition fluxes of inorganic N inherently contain more uncertainty, dry and total (wet plus dry) inorganic N deposition fluxes also appear to be dominated by reduced N in most parts of the country. Reductions in wet and dry deposition fluxes of oxidized inorganic N species are expected to continue into the future as the U.S. continues to reduce NO_x emissions. Current projections of ammonia emissions growth, meanwhile, suggest that reduced N deposition levels will grow in the future. While ammonia emissions have been regulated since 2001 in Europe, U.S. air quality regulators have thus far chosen not to regulate ammonia air emissions. In addition to the adverse impacts of reduced N deposition on ecosystem health, ammonia is an important precursor to fine particle formation. Fine particles decrease visibility (Malm, 1999) and negatively impact human health and increase health care costs (Paulot and Jacob, 2014; Stokstad, 2014). Reductions in U.S. ammonia emissions from agricultural and non-agricultural sources, whether by regulation or voluntary actions (e.g., agricultural producer adoption of best management practices), would yield a variety of positive benefits for ecosystems and society. Increased study of atmospheric ammonia concentrations and improved measures of ammonia dry deposition fluxes are needed to design optimal strategies for achieving such benefits.

Even though the results from field studies, model simulations, and national network observations reported here provide many new insights into the characteristics of NH_3 concentrations and

deposition in the United States, there are still many aspects we can work on to expand our knowledge of NH_3 and its impacts. Here are several suggestions for future research efforts:

- Continued measurements of ammonia are needed in northeastern Colorado for trend analysis. The measurements reported to date provide an important baseline against which effects of ongoing regional efforts to reduce emissions can be evaluated. Exploring correlations between emissions from nearby sources and observed NH_3 concentrations, such as studying how weekly NH_3 concentrations vary at the Kersey site in conjunction with changing numbers of cattle in the nearby feedlot, will aid in identifying factors controlling NH_3 concentrations at local scales. Online measurements and mobile sampling are also highly recommended in this area to better depict spatial variability across this important source region and determine how emitted NH_3 is carried by upslope winds to contribute to reactive nitrogen deposition in Rocky Mountain National Park. Recent implementation of continuous ammonia measurements at Greeley and Loveland are a good step in this direction. By combining these with mobile sampling, we could better determine the spatial structure of ammonia plumes being carried westward toward the mountain. Use of all of this information to better determine what sources (agriculture, transportation and industry) contribute to NH_3 in northeastern Colorado and how emitted ammonia evolves during downwind transport would aid in the design of better strategies to reduce reactive nitrogen deposition to sensitive alpine ecosystems.

- While the BAO vertical profile measurements of NH_3 are novel and helpful for evaluating model simulations and satellite measurements, the low time resolution associated with the passive sampler measurements precludes a clear determination of surface deposition rates via gradient

methods. It would be very helpful to make high time resolution measurements near the surface to gain knowledge about NH_3 deposition or emission. For example, two online NH_3 samplers (such as the Picarro G2103 Analyzer) could be installed at 1m and 10m heights on the BAO tower, respectively. With high time-resolution NH_3 concentration measurements at different heights, we could use gradient flux determination techniques to estimate surface deposition/emission of NH_3.

- Model simulations did not fully represent NE Colorado NH_3 distributions measured here by passive samplers. In prior work, it has also been seen that models do not adequately account for ammonia transported from this region to Rocky Mountain National Park. One known limitation to current model treatments is a lack of capacity to treat bidirectional exchange with the surface; this should be added to future model simulations. Preliminary results from Community Multiscale Air Quality (CMAQ) modeling work incorporating bidirectional exchange show that its addition helps reduce the gap between model results and measurements at most sites in northeastern Colorado (Figure 6.1).
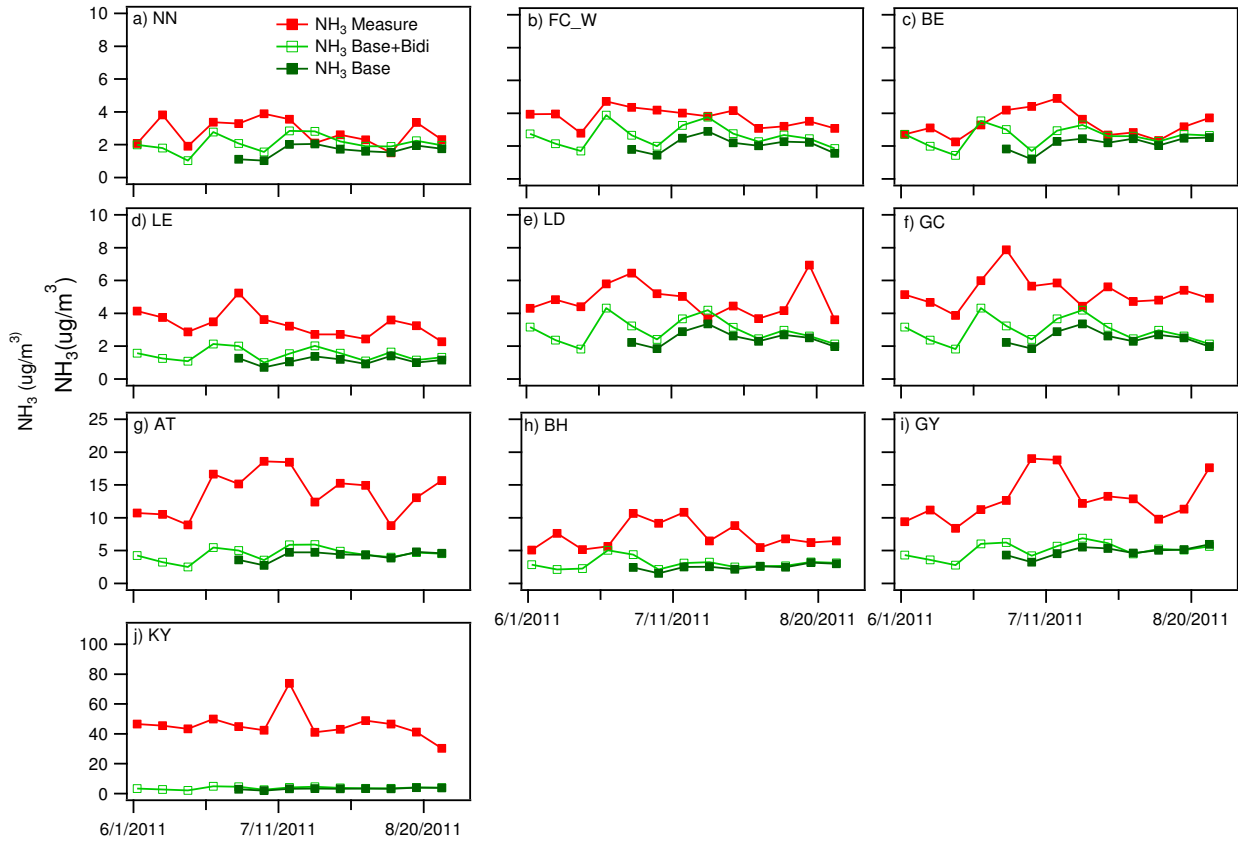
Figure 6. 1 Time series of weekly NH₃ concentrations measured and preliminary modeled (CMAQ) including the bidirectional processes in the summer of 2011(06/02/2011-08/31/2011) at all the sites. Simulation results provided by Tammy Thompson, CIRA.

- There are only 37 sites in 23 states within the US that currently have enough measured information to fully represent dry and wet deposition budgets of oxidized and reduced inorganic nitrogen. The biggest shortcoming is the availability of gas phase ammonia measurements to determine ammonia dry deposition budgets. The expansion of routine ammonia monitoring efforts, such as those within AMON, would greatly help nationwide nitrogen deposition budget estimates. More sites in areas such as Texas, Utah, North Dakota and Minnesota, would be especially helpful in improving spatial coverage. Furthermore, organic nitrogen wet deposition and dry deposition of organic nitrogen species, such as peroxyacetyl nitrate and amines, were not included in the deposition budget calculations in this thesis due to a lack of measurements. However, deposition

of organic nitrogen is an important constituent of reactive nitrogen deposition, as reported in several previous studies such as RoMANS and GrandTReNDS (Benedict et al., 2013a; Benedict et al., 2013b). To better understand dry and wet deposition of reactive nitrogen, more routine measurements are needed at several sites across the United States.

- Expansion of ammonia monitoring efforts is also needed to better represent background ammonia concentrations regionally and their contributions to fine particle formation and visibility degradation. The Wyoming dataset reported here has already drawn significant interest from industry and from air quality regulators because it provides previously unavailable information concerning ammonia concentrations in the rural western U.S. More measurements like this would help to better predict impacts of NO_x emissions from anthropogenic sources on visibility. By including measurements of both gas and particle phase species, such datasets would also be very useful for evaluating model simulations of the total concentration and phase partitioning of NH_x and help assess the likely effectiveness of future regional efforts to reduce fine particle concentrations.

- One major limitation in computing deposition budgets is the lack of understanding of appropriate deposition velocities for ammonia. While models are being developed to treat bidirectional exchange of ammonia with surfaces, detailed observations of NH_3 deposition at high time resolution in a variety of ecosystem types and at a variety of ambient ammonia concentration levels are needed to improve our understanding of NH_3 bidirectional exchange in the real world and to support better parameterizations and estimation of NH_3 deposition in models.

- Evidence presented in this dissertation concerning contributions of biomass burning to ammonia emissions, joins a small but growing body of literature on discussing this issue. A more thorough investigation of this phenomenon is needed both to elucidate the magnitude of emissions and to examine whether increases in ammonium deposition observed, for example, in the western U.S. may be a result of an increase in wild and prescribed fires in the region.

REFERENCES

Adon, M., Galy-Lacaux, C., Yoboué, V., Delon, C., Lacaux, J., Castera, P., Gardrat, E., Pienaar, J., Ourabi, H.A., Laouali, D., 2010. Long term measurements of sulfur dioxide, nitrogen dioxide, ammonia, nitric acid and ozone in Africa using passive samplers. Atmospheric Chemistry and Physics 10, 7467-7487.

Anatolaki, C., Tsitouridou, R., 2007. Atmospheric deposition of nitrogen, sulfur and chloride in Thessaloniki, Greece. Atmospheric Research 85, 413-428.

Anderson, N., Strader, R., Davidson, C., 2003. Airborne reduced nitrogen: ammonia emissions from agriculture and other sources. Environment International 29, 277-286.

ANDREAE, M.O., 1983. Soot Carbon and Excess Fine Potassium: Long-Range Transport of Combustion-Derived Aerosols. Science 220, 1148-1151.

Aneja, V.P., Nelson, D.R., Roelle, P.A., Walker, J.T., Battye, W., 2003. Agricultural ammonia emissions and ammonium concentrations associated with aerosols and precipitation in the southeast United States. Journal of Geophysical Research: Atmospheres 108, 4152.

Aneja, V.P., Roelle, P.A., Murray, G.C., Southerland, J., Erisman, J.W., Fowler, D., Asman, W.A.H., Patni, N., 2001. Atmospheric nitrogen compounds II: emissions, transport, transformation, deposition and assessment. Atmospheric Environment 35, 1903-1911.

Arya, P.S., 2001. Introduction to micrometeorology. Academic press.

Asman, W.A.H., 1995. Parameterization of below-cloud scavenging of highly soluble gases under convective conditions. Atmospheric Environment 29, 1359-1368.

Asman, W.A.H., Sutton, M.A., SchjØRring, J.K., 1998. Ammonia: emission, atmospheric transport and deposition. New Phytologist 139, 27-48.

Bari, A., Ferraro, V., Wilson, L.R., Luttinger, D., Husain, L., 2003. Measurements of gaseous HONO, HNO_3, SO_2, HCl, NH_3, particulate sulfate and $PM_{2.5}$ in New York, NY. Atmospheric Environment 37, 2825-2835.

Barsanti, K., McMurry, P.H., Smith, J., 2009. The potential contribution of organic salts to new particle growth. Atmospheric Chemistry and Physics 9, 2949-2957.

Bash, J.O., Cooter, E.J., Dennis, R.L., Walker, J.T., Pleim, J.E., 2013. Evaluation of a regional air-quality model with bidirectional NH_3 exchange coupled to an agroecosystem model. Biogeosciences 10, 1635-1645.

Bash, J.O., Walker, J.T., Katul, G.G., Jones, M.R., Nemitz, E., Robarge, W.P., 2010. Estimation of in-canopy ammonia sources and sinks in a fertilized Zea mays field. Environmental Science & Technology 44, 1683-1689.

Beem, K.B., Raja, S., Schwandner, F.M., Taylor, C., Lee, T., Sullivan, A.P., Carrico, C.M., McMeeking, G.R., Day, D., Levin, E., Hand, J., Kreidenweis, S.M., Schichtel, B., Malm, W.C., Collett Jr, J.L., 2010. Deposition of reactive nitrogen during the Rocky Mountain Airborne Nitrogen and Sulfur (RoMANS) study. Environmental Pollution 158, 862-872.

Behera, S.N., Sharma, M., 2010. Investigating the potential role of ammonia in ion chemistry of fine particulate matter formation for an urban environment. Science of The Total Environment 408, 3569-3575.

Benedict, K.B., Carrico, C.M., Kreidenweis, S.M., Schichtel, B., Malm, W.C., Collett, J.L., 2013a. A seasonal nitrogen deposition budget for Rocky Mountain National Park. Ecological Applications 23, 1156-1169.

Benedict, K.B., Chen, X., Sullivan, A.P., Li, Y., Day, D., Prenni, A.J., Levin, E., Kreidenweis, S.M., Malm, W.C., Schichtel, B.A., 2013b. Atmospheric concentrations and deposition of reactive nitrogen in Grand Teton National Park. Journal of Geophysical Research: Atmospheres 118, 11,875-811,887.

Benedict, K.B., Day, D., Schwandner, F.M., Kreidenweis, S.M., Schichtel, B., Malm, W.C., Collett Jr, J.L., 2013c. Observations of atmospheric reactive nitrogen species in Rocky Mountain National Park and across northern Colorado. Atmospheric Environment 64, 66-76.

Biswas, K.F., Ghauri, B.M., Husain, L., 2008. Gaseous and aerosol pollutants during fog and clear episodes in South Asian urban atmosphere. Atmospheric Environment 42, 7775-7785.

Bowker, G.E., Schwede, D.B., Lear, G.G., Warren-Hicks, W.J., Finkelstein, P.L., 2011. Quality assurance decisions with air models: a case study of imputation of missing input data using EPA's multi-layer model. Water Air Soil Pollut 222, 391-402.

Brook, J.R., Wiebe, A.H., Woodhouse, S.A., Audette, C.V., Dann, T.F., Callaghan, S., Piechowski, M., Dabek-Zlotorzynska, E., Dloughy, J.F., 1997. Temporal and spatial relationships in fine particle strong acidity, sulphate, PM_{10}, and $PM_{2.5}$ across multiple canadian locations. Atmospheric Environment 31, 4223-4236.

Brunke, R., Alvo, P., Schuepp, P., Gordon, R., 1988. Effect of Meteorological Parameters on Ammonia Loss from Manure in the Field. Journal of Environmental Quality 17, 431-436.

Bytnerowicz, A., Tausz, M., Alonso, R., Jones, D., Johnson, R., Grulke, N., 2002. Summer-time distribution of air pollutants in Sequoia National Park, California. Environmental Pollution 118, 187-203.

Carslaw, D.C., Rhys-Tyler, G., 2013. New insights from comprehensive on-road measurements of NO_x, NO_2 and NH_3 from vehicle emission remote sensing in London, UK. Atmospheric Environment 81, 339-347.

Chen, X., Day, D., Schichtel, B., Malm, W., Matzoll, A.K., Mojica, J., McDade, C.E., Hardison, E.D., Hardison, D.L., Walters, S., Van De Water, M., Collett Jr, J.L., 2014. Seasonal ambient ammonia and ammonium concentrations in a pilot IMPROVE NHx monitoring network in the western United States. Atmospheric Environment 91, 118-126.

Chiwa, M., 2010. Characteristics of atmospheric nitrogen and sulfur containing compounds in an inland suburban-forested site in northern Kyushu, western Japan. Atmospheric Research 96, 531-543.

Cisneros, R., Bytnerowicz, A., Schweizer, D., Zhong, S., Traina, S., Bennett, D.H., 2010. Ozone, nitric acid, and ammonia air pollution is unhealthy for people and ecosystems in southern Sierra Nevada, California. Environmental Pollution 158, 3261-3271.

Clarisse, L., Clerbaux, C., Dentener, F., Hurtmans, D., Coheur, P.-F., 2009. Global ammonia distribution derived from infrared satellite observations. Nature Geoscience 2, 479-483.

Clarisse, L., R'Honi, Y., Coheur, P.-F., Hurtmans, D., Clerbaux, C., 2011. Thermal infrared nadir observations of 24 atmospheric gases. Geophysical Research Letters 38, L10802.

Clark, C.M., Tilman, D., 2008. Loss of plant species after chronic low-level nitrogen deposition to prairie grasslands. Nature 451, 712-715.

Clerbaux, C., Boynard, A., Clarisse, L., George, M., Hadji-Lazaro, J., Herbin, H., Hurtmans, D., Pommier, M., Razavi, A., Turquety, S., 2009. Monitoring of atmospheric composition using the thermal infrared IASI/MetOp sounder. Atmospheric Chemistry and Physics 9, 6041-6054.

Coheur, P.-F., Clarisse, L., Turquety, S., Hurtmans, D., Clerbaux, C., 2009. IASI measurements of reactive trace species in biomass burning plumes. Atmospheric Chemistry and Physics 9, 5655-5667.

Davidson, C.I., Phalen, R.F., Solomon, P.A., 2005. Airborne Particulate Matter and Human Health: A Review. Aerosol Science and Technology 39, 737-749.

Davidson, E., David, M.B., Galloway, J.N., Goodale, C.L., Haeuber, R., Harrison, J.A., Howarth, R.W., Jaynes, D.B., Lowrance, R.R., Nolan, B.T., 2012. Excess Nitrogen in the U. S. Environment: Trends, Risks, and Solutions. Issues in Ecology, 1-16.

Day, D.E., Chen, X., Gebhart, K.A., Carrico, C.M., Schwandner, F.M., Benedict, K.B., Schichtel, B.A., Collett, J.L., 2012. Spatial and temporal variability of ammonia and other inorganic aerosol species. Atmospheric Environment 61, 490-498.

Dentener, F.J., Crutzen, P.J., 1993. Reaction of N_2O_5 on tropospheric aerosols: Impact on the global distributions of NOx , O_3, and OH. Journal of Geophysical Research: Atmospheres 98, 7149-7163.

Draaijers, G.P.J., Ivens, W.P.M.F., Bos, M.M., Bleuten, W., 1989. The contribution of ammonia emissions from agriculture to the deposition of acidifying and eutrophying compounds onto forests. Environmental Pollution 60, 55-66.

Du, E., de Vries, W., Galloway, J.N., Hu, X., Fang, J., 2014. Changes in wet nitrogen deposition in the United States between 1985 and 2012. Environmental Research Letters 9, 095004.

Du, H., Kong, L., Cheng, T., Chen, J., Yang, X., Zhang, R., Han, Z., Yan, Z., Ma, Y., 2010. Insights into ammonium particle-to-gas conversion: non-sulfate ammonium coupling with nitrate and chloride. Aerosol and Air Quality Research 10, 589-595.

Duan, F., Liu, X., Yu, T., Cachier, H., 2004. Identification and estimate of biomass burning contribution to the urban aerosol organic carbon concentrations in Beijing. Atmospheric Environment 38, 1275-1282.

Edgerton, E.S., Saylor, R.D., Hartsell, B.E., Jansen, J.J., Alan Hansen, D., 2007. Ammonia and ammonium measurements from the southeastern United States. Atmospheric Environment 41, 3339-3351.

Ellis, R.A., Murphy, J.G., Markovic, M.Z., VandenBoer, T.C., Makar, P.A., Brook, J., Mihele, C., 2011. The influence of gas-particle partitioning and surface-atmosphere exchange on ammonia during BAQS-Met. Atmospheric Chemistry and Physics 11, 133-145.

Emmons, L., Walters, S., Hess, P., Lamarque, J.-F., Pfister, G., Fillmore, D., Granier, C., Guenther, A., Kinnison, D., Laepple, T., 2010. Description and evaluation of the Model for Ozone and Related chemical Tracers, version 4 (MOZART-4). Geoscientific Model Development 3, 43-67.

EPA, U., 2007. Guidance on the use of models and other analyses for demonstrating attainment of air quality goals for ozone, $PM_{2.5}$, and regional haze. EPA-454/B07-002.

EPA, U., 2011. Air Quality Modeling Final Rule Technical Support Document. EPA Office of Air Quality Planning and Standards

Erisman, J.W., Galloway, J., Seitzinger, S., Bleeker, A., Butterbach-Bahl, K., 2011. Reactive nitrogen in the environment and its effect on climate change. Current Opinion in Environmental Sustainability 3, 281-290.

Farquhar, G.D., Firth, P.M., Wetselaar, R., Weir, B., 1980. On the gaseous exchange of ammonia between leaves and the environment: determination of the ammonia compensation point. Plant Physiology 66, 710-714.

Fenn, M.E., Haeuber, R., Tonnesen, G.S., Baron, J.S., Grossman-Clarke, S., Hope, D., Jaffe, D.A., Copeland, S., Geiser, L., Rueth, H.M., Sickman, J.O., 2003. Nitrogen Emissions, Deposition, and Monitoring in the Western United States. BioScience 53, 391-403.

Fountoukis, C., Nenes, A., 2007. ISORROPIA II: a computationally efficient thermodynamic equilibrium model for K^+–Ca^{2+}–Mg^{2+}–NH_4^+–Na^+–SO_4^{2-}–NO_3^-–Cl^-–H_2O aerosols. Atmospheric Chemistry and Physics 7, 4639-4659.

Fowler, D., Sutton, M.A., Smith, R.I., Pitcairn, C.E.R., Coyle, M., Campbell, G., Stedman, J., 1998. Regional mass budgets of oxidized and reduced nitrogen and their relative contribution to the nitrogen inputs of sensitive ecosystems. Environmental Pollution 102, 337-342.

Galloway, J.N., Cowling, E.B., 2002. Reactive Nitrogen and The World: 200 Years of Change. AMBIO: A Journal of the Human Environment 31, 64-71.

Galloway, J.N., Cowling, E.B., Seitzinger, S.P., Socolow, R.H., 2002. Reactive nitrogen: too much of a good thing? AMBIO: A Journal of the Human Environment 31, 60-63.

Galloway, J.N., Dentener, F.J., Capone, D.G., Boyer, E.W., Howarth, R.W., Seitzinger, S.P., Asner, G.P., Cleveland, C.C., Green, P.A., Holland, E.A., Karl, D.M., Michaels, A.F., Porter, J.H., Townsend, A.R., Vöosmarty, C.J., 2004. Nitrogen Cycles: Past, Present, and Future. Biogeochemistry 70, 153-226.

Galloway, J.N., Townsend, A.R., Erisman, J.W., Bekunda, M., Cai, Z.C., Freney, J.R., Martinelli, L.A., Seitzinger, S.P., Sutton, M.A., 2008. Transformation of the nitrogen cycle: Recent trends, questions, and potential solutions. Science 320, 889-892.

Gilbert, R.O., 1987. Statistical methods for environmental pollution monitoring. John Wiley & Sons.

Gong, L., Lewicki, R., Griffin, R.J., Flynn, J.H., Lefer, B.L., Tittel, F.K., 2011. Atmospheric ammonia measurements in Houston, TX using an external-cavity quantum cascade laser-based sensor. Atmospheric Chemistry and Physics 11, 9721-9733.

Gruber, N., Galloway, J.N., 2008. An Earth-system perspective of the global nitrogen cycle. Nature 451, 293-296.

Gupta, A., Kumar, R., Kumari, K.M., Srivastava, S.S., 2003. Measurement of NO_2, HNO_3, NH_3 and SO_2 and related particulate matter at a rural site in Rampur, India. Atmospheric Environment 37, 4837-4846.

Hand, J., Schichtel, B., Malm, W., Pitchford, M., 2012. Particulate sulfate ion concentration and SO_2 emission trends in the United States from the early 1990s through 2010. Atmospheric Chemistry and Physics 12, 10353-10365.

Heald, C.L., Collett Jr, J., Lee, T., Benedict, K., Schwandner, F., Li, Y., Clarisse, L., Hurtmans, D., Van Damme, M., Clerbaux, C., 2012. Atmospheric ammonia and particulate inorganic nitrogen over the United States. Atmospheric Chemistry and Physics 12, 10295-10312.

Hegg, D.A., Radke, L.F., Hobbs, P.V., Riggan, P.J., 1988. Ammonia emissions from biomass burning. Geophysical Research Letters 15, 335-337.

Hicks, B., Baldocchi, D., Meyers, T., Hosker Jr, R., Matt, D., 1987. A preliminary multiple resistance routine for deriving dry deposition velocities from measured quantities. Water, Air, and Soil Pollution 36, 311-330.

Hicks, B.B., 1985. On the use of monitored air concentrations to infer dry deposition (1985). United States Department of Commerce, National Oceanic and Atmospheric Administration, Environmental Research Laboratories, Air Resources Laboratory.

Hoek, G., Mennen, M.G., Allen, G.A., Hofschreuder, P., Van Der Meulen, T., 1996. Concentrations of acidic air pollutants in The Netherlands. Atmospheric Environment 30, 3141-3150.

Holtgrieve, G.W., Schindler, D.E., Hobbs, W.O., Leavitt, P.R., Ward, E.J., Bunting, L., Chen, G., Finney, B.P., Gregory-Eaves, I., Holmgren, S., 2011. A coherent signature of anthropogenic nitrogen deposition to remote watersheds of the northern hemisphere. Science 334, 1545-1548.

Hong, Y.-M., Lee, B.-K., Park, K.-J., Kang, M.-H., Jung, Y.-R., Lee, D.-S., Kim, M.-G., 2002. Atmospheric nitrogen and sulfur containing compounds for three sites of South Korea. Atmospheric Environment 36, 3485-3494.

Houyoux, M., Vukovich, J., Brandmeyer, J., Seppanen, C., Holland, A., 2000. Sparse Matrix Operator Kernel Emissions Modeling System-SMOKE User Manual. Prepared by MCNC-North Carolina Supercomputing Center, Environmental Programs, Research Triangle Park, NC.

Hu, M., Wu, Z., Slanina, J., Lin, P., Liu, S., Zeng, L., 2008. Acidic gases, ammonia and water-soluble ions in $PM_{2.5}$ at a coastal site in the Pearl River Delta, China. Atmospheric Environment 42, 6310-6320.

Huai, T., Durbin, T.D., Miller, J.W., Pisano, J.T., Sauer, C.G., Rhee, S.H., Norbeck, J.M., 2003. Investigation of NH_3 Emissions from New Technology Vehicles as a Function of Vehicle Operating Conditions. Environmental Science & Technology 37, 4841-4847.

Ianniello, A., Spataro, F., Esposito, G., Allegrini, I., Rantica, E., Ancora, M., Hu, M., Zhu, T., 2010. Occurrence of gas phase ammonia in the area of Beijing (China). Atmospheric Chemistry and Physics 10, 9487-9503.

Igawa, M., Tsutsumi, Y., Mori, T., Okochi, H., 1998. Fogwater chemistry at a mountainside forest and the estimation of the air pollutant deposition via fog droplets based on the atmospheric quality at the mountain base. Environmental Science & Technology 32, 1566-1572.

Jaffe, D., Hafner, W., Chand, D., Westerling, A., Spracklen, D., 2008. Interannual variations in $PM_{2.5}$ due to wildfires in the western United States. Environmental Science & Technology 42, 2812-2818.

Janssens, I., Dieleman, W., Luyssaert, S., Subke, J.-A., Reichstein, M., Ceulemans, R., Ciais, P., Dolman, A.J., Grace, J., Matteucci, G., 2010. Reduction of forest soil respiration in response to nitrogen deposition. Nature Geoscience 3, 315-322.

Kean, A.J., Harley, R.A., Littlejohn, D., Kendall, G.R., 2000. On-Road Measurement of Ammonia and Other Motor Vehicle Exhaust Emissions. Environmental Science & Technology 34, 3535-3539.

Langford, A., Fehsenfeld, F., Zachariassen, J., Schimel, D., 1992. Gaseous ammonia fluxes and background concentrations in terrestrial ecosystems of the United States. Global Biogeochemical Cycles 6, 459-483.

Langridge, J.M., Lack, D., Brock, C.A., Bahreini, R., Middlebrook, A.M., Neuman, J.A., Nowak, J.B., Perring, A.E., Schwarz, J.P., Spackman, J.R., 2012. Evolution of aerosol properties impacting visibility and direct climate forcing in an ammonia‐rich urban environment. Journal of Geophysical Research: Atmospheres 117.

Lee, H.S., Kang, C.-M., Kang, B.-W., Kim, H.-K., 1999. Seasonal variations of acidic air pollutants in Seoul, South Korea. Atmospheric Environment 33, 3143-3152.

Lee, H.S., Wadden, R.A., Scheff, P.A., 1993. Measurement and evaluation of acid air pollutants in Chicago using an annular denuder system. Atmospheric Environment. Part A. General Topics 27, 543-553.

Lee, T., Kreidenweis, S.M., Collett, J.L., 2004. Aerosol Ion Characteristics During the Big Bend Regional Aerosol and Visibility Observational Study. Journal of the Air & Waste Management Association 54, 585-592.

Lee, T., Yu, X.-Y., Ayres, B., Kreidenweis, S.M., Malm, W.C., Collett Jr, J.L., 2008a. Observations of fine and coarse particle nitrate at several rural locations in the United States. Atmospheric Environment 42, 2720-2732.

Lee, T., Yu, X.-Y., Kreidenweis, S.M., Malm, W.C., Collett, J.L., 2008b. Semi-continuous measurement of $PM_{2.5}$ ionic composition at several rural locations in the United States. Atmospheric Environment 42, 6655-6669.

Lehmann, C.M., Bowersox, V.C., Larson, R.S., Larson, S.M., 2007. Monitoring long-term trends in sulfate and ammonium in US precipitation: Results from the National Atmospheric Deposition Program/National Trends Network, Acid Rain-Deposition to Recovery. Springer, pp. 59-66.

Lehmann, C.M., Gay, D.A., 2011. Monitoring long-term trends of acidic wet deposition in US precipitation: Results from the National Atmospheric Deposition Program. Power Plant Chemistry 13, 378.

Lehmann, C.M.B., Bowersox, V.C., Larson, S.M., 2005. Spatial and temporal trends of precipitation chemistry in the United States, 1985–2002. Environmental Pollution 135, 347-361.

Li, Y., Schwandner, F.M., Sewell, H.J., Zivkovich, A., Tigges, M., Raja, S., Holcomb, S., Molenar, J.V., Sherman, L., Archuleta, C., Lee, T., Collett Jr., J.L., 2014. Observations of ammonia, nitric acid, and fine particles in a rural gas production region. Atmospheric Environment 83, 80-89.

Lin, Y.-C., Cheng, M.-T., Ting, W.-Y., Yeh, C.-R., 2006. Characteristics of gaseous HNO_2, HNO_3, NH_3 and particulate ammonium nitrate in an urban city of Central Taiwan. Atmospheric Environment 40, 4725-4733.

Liu, T., Wang, X., Wang, B., Ding, X., Deng, W., Lü, S., Zhang, Y., 2014. Emission factor of ammonia (NH_3) from on-road vehicles in China: tunnel tests in urban Guangzhou. Environmental Research Letters 9, 064027.

Liu, X., Zhang, Y., Han, W., Tang, A., Shen, J., Cui, Z., Vitousek, P., Erisman, J.W., Goulding, K., Christie, P., 2013. Enhanced nitrogen deposition over China. Nature 494, 459-462.

Loflund, M., Kasper-Giebl, A., Stopper, S., Urban, H., Biebl, P., Kirchner, M., Braeutigam, S., Puxbaum, H., 2002. Monitoring ammonia in urban, inner alpine and pre-alpine ambient air. Journal of Environmental Monitoring 4, 205-209.

Malm, W.C., 1999. Introduction to visibility. Cooperative Institute for Research in the Atmosphere, NPS Visibility Program, Colorado State University.

Malm, W.C., Schichtel, B.A., Pitchford, M.L., Ashbaugh, L.L., Eldred, R.A., 2004. Spatial and monthly trends in speciated fine particle concentration in the United States. Journal of Geophysical Research: Atmospheres 109, D03306.

Marchetto, A., Rogora, M., Arisci, S., 2013. Trend analysis of atmospheric deposition data: A comparison of statistical approaches. Atmospheric Environment 64, 95-102.

Massad, R.-S., Nemitz, E., Sutton, M., 2010. Review and parameterisation of bi-directional ammonia exchange between vegetation and the atmosphere. Atmospheric Chemistry and Physics 10, 10359-10386.

Matsumoto, M., Okita, T., 1998. Long term measurements of atmospheric gaseous and aerosol species using an annular denuder system in Nara, Japan. Atmospheric Environment 32, 1419-1425.

McCulloch, R.B., Stephen Few, G., Murray Jr, G.C., Aneja, V.P., 1998. Analysis of ammonia, ammonium aerosols and acid gases in the atmosphere at a commercial hog farm in eastern North Carolina, USA. Environmental Pollution 102, 263-268.

McElroy, M.B., 2002. The Atmospheric Environment: Effects of Human Activity. Princeton University Press.

McMeeking, G.R., Kreidenweis, S.M., Baker, S., Carrico, C.M., Chow, J.C., Collett, J.L., Hao, W.M., Holden, A.S., Kirchstetter, T.W., Malm, W.C., Moosmüller, H., Sullivan, A.P., Wold, C.E., 2009. Emissions of trace gases and aerosols during the open combustion of biomass in the laboratory. Journal of Geophysical Research: Atmospheres 114, D19210.

McMurray, J., Roberts, D., Fenn, M., Geiser, L., Jovan, S., 2013. Using Epiphytic Lichens to Monitor Nitrogen Deposition Near Natural Gas Drilling Operations in the Wind River Range, WY, USA. Water Air Soil Pollut 224, 1-14.

Meng, Z., Lin, W., Jiang, X., Yan, P., Wang, Y., Zhang, Y., Jia, X., Yu, X., 2011. Characteristics of atmospheric ammonia over Beijing, China. Atmospheric Chemistry and Physics 11, 6139-6151.

Meyers, T.P., Finkelstein, P., Clarke, J., Ellestad, T.G., Sims, P.F., 1998. A multilayer model for inferring dry deposition using standard meteorological measurements. Journal of Geophysical Research: Atmospheres 103, 22645-22661.

Nemitz, E., Milford, C., Sutton, M.A., 2001. A two-layer canopy compensation point model for describing bi-directional biosphere-atmosphere exchange of ammonia. Quarterly Journal of the Royal Meteorological Society 127, 815-833.

Nicholson, K.W., 1988. The dry deposition of small particles: A review of experimental measurements. Atmospheric Environment (1967) 22, 2653-2666.

Nowak, J.B., Neuman, J.A., Bahreini, R., Brock, C.A., Middlebrook, A.M., Wollny, A.G., Holloway, J.S., Peischl, J., Ryerson, T.B., Fehsenfeld, F.C., 2010. Airborne observations of ammonia and ammonium nitrate formation over Houston, Texas. Journal of Geophysical Research: Atmospheres 115, D22304.

Pakkanen, T.A., 1996. Study of formation of coarse particle nitrate aerosol. Atmospheric Environment 30, 2475-2482.

Park, R.J., Jacob, D.J., Kumar, N., Yantosca, R.M., 2006. Regional visibility statistics in the United States: Natural and transboundary pollution influences, and implications for the Regional Haze Rule. Atmospheric Environment 40, 5405-5423.

Parry, M.L., 2007. Climate Change 2007: impacts, adaptation and vulnerability: contribution of Working Group II to the fourth assessment report of the Intergovernmental Panel on Climate Change. Cambridge University Press.

Paulot, F., Jacob, D.J., 2014. Hidden cost of US agricultural exports: particulate matter from ammonia emissions. Environmental science & technology 48, 903-908.

Perrino, C., Catrambone, M., 2004. Development of a variable-path-length diffusive sampler for ammonia and evaluation of ammonia pollution in the urban area of Rome, Italy. Atmospheric Environment 38, 6667-6672.

Perrino, C., Catrambone, M., Di Menno Di Bucchianico, A., Allegrini, I., 2002. Gaseous ammonia in the urban area of Rome, Italy and its relationship with traffic emissions. Atmospheric Environment 36, 5385-5394.

Phoenix, G.K., Emmett, B.A., Britton, A.J., Caporn, S.J.M., Dise, N.B., Helliwell, R., Jones, L., Leake, J.R., Leith, I.D., Sheppard, L.J., Sowerby, A., Pilkington, M.G., Rowe, E.C., Ashmore, M.R., Power, S.A., 2012. Impacts of atmospheric nitrogen deposition: responses of multiple plant and soil parameters across contrasting ecosystems in long-term field experiments. Global Change Biology 18, 1197-1215.

Pinder, R.W., Walker, J.T., Bash, J.O., Cady-Pereira, K.E., Henze, D.K., Luo, M., Osterman, G.B., Shephard, M.W., 2011. Quantifying spatial and seasonal variability in atmospheric ammonia with in situ and space-based observations. Geophysical Research Letters 38, L04802.

Pio, C.A., Santos, I.M., Anacleto, T.D., Nunes, T.V., Leal, R.M., 1991. Particulate and gaseous air pollutant levels at the portuguese West Coast. Atmospheric Environment. Part A. General Topics 25, 669-680.

Plessow, K., Spindler, G., Zimmermann, F., Matschullat, J., 2005. Seasonal variations and interactions of N-containing gases and particles over a coniferous forest, Saxony, Germany. Atmospheric Environment 39, 6995-7007.

Prenni, A., Chen, X., Hecobian, A., Kreidenweis, S., Collett, J., Schichtel, B., 2012. Measurements of gas phase reactive nitrogen during two wildfires in Colorado, AGU Fall Meeting Abstracts, p. 0618.

Prenni, A., Levin, E., Benedict, K., Sullivan, A., Schurman, M., Gebhart, K., Day, D., Carrico, C., Malm, W., Schichtel, B., 2014. Gas-phase reactive nitrogen near Grand Teton National Park: Impacts of transport, anthropogenic emissions, and biomass burning. Atmospheric Environment 89, 749-756.

Pryor, S.C., Barthelmie, R.J., Jensen, B., Jensen, N.O., Sørensen, L.L., 2002. HNO_3 fluxes to a deciduous forest derived using gradient and REA methods. Atmospheric Environment 36, 5993-5999.

Puchalski, M.A., Sather, M.E., Walker, J.T., Lehmann, C.M., Gay, D.A., Mathew, J., Robarge, W.P., 2011. Passive ammonia monitoring in the United States: Comparing three different sampling devices. Journal of Environmental Monitoring 13, 3156-3167.

Puxbaum, H., Haumer, G., Moser, K., Ellinger, R., 1993. Seasonal variation of HNO_3, HCl, SO_2, NH_3 and particulate matter at a rural site in northeastern Austria (wolkersdorf, 240 m a.s.l.). Atmospheric Environment. Part A. General Topics 27, 2445-2447.

Reche, C., Viana, M., Karanasiou, A., Cusack, M., Alastuey, A., Artiñano, B., Revuelta, M.A., López-Mahía, P., Blanco-Heras, G., Rodríguez, S., Sánchez de la Campa, A.M., Fernández-Camacho, R., González-Castanedo, Y., Mantilla, E., Tang, Y.S., Querol, X., 2015. Urban NH_3 levels and sources in six major Spanish cities. Chemosphere 119, 769-777.

Reis, S., Pinder, R., Zhang, M., Lijie, G., Sutton, M., 2009. Reactive nitrogen in atmospheric emission inventories. Atmospheric Chemistry and Physics 9, 7657-7677.

Rodriguez, M.A., Barna, M.G., Moore, T., 2009. Regional impacts of oil and gas development on ozone formation in the western United States. Journal of the Air & Waste Management Association 59, 1111-1118.

Ruijgrok, W., Tieben, H., Eisinga, P., 1997. The dry deposition of particles to a forest canopy: A comparison of model and experimental results. Atmospheric Environment 31, 399-415.

Schnell, R.C., Oltmans, S.J., Neely, R.R., Endres, M.S., Molenar, J.V., White, A.B., 2009. Rapid photochemical production of ozone at high concentrations in a rural site during winter. Nature Geoscience 2, 120-122.

Schuepp, P.H., 1977. Turbulent transfer at the ground: on verification of a simple predictive model. Boundary-Layer Meteorology 12, 171-186.

Schwartz, J., Neas, L.M., 2000. Fine Particles Are More Strongly Associated than Coarse Particles with Acute Respiratory Health Effects in Schoolchildren. Epidemiology 11, 6-10.

154

Schwede, D.B., Lear, G.G., 2014. A novel hybrid approach for estimating total deposition in the United States. Atmospheric Environment 92, 207-220.

Seinfeld, J.H., Pandis, S.N., 2012. Atmospheric chemistry and physics: from air pollution to climate change. John Wiley & Sons.

Sharma, M., Kishore, S., Tripathi, S., Behera, S., 2007. Role of atmospheric ammonia in the formation of inorganic secondary particulate matter: a study at Kanpur, India. J Atmos Chem 58, 1-17.

Shen, X., Lee, T., Guo, J., Wang, X., Li, P., Xu, P., Wang, Y., Ren, Y., Wang, W., Wang, T., Li, Y., Carn, S.A., Collett Jr, J.L., 2012. Aqueous phase sulfate production in clouds in eastern China. Atmospheric Environment 62, 502-511.

Skamarock, W.C., Klemp, J.B., Dudhia, J., Gill, D.O., Barker, D.M., Wang, W., Powers, J.G., 2005. A description of the advanced research WRF version 2. DTIC Document.

Sommer, S.G., Olesen, J.E., Christensen, B.T., 1991. Effects of temperature, wind speed and air humidity on ammonia volatilization from surface applied cattle slurry. The Journal of Agricultural Science 117, 91-100.

Soner Erduran, M., Tuncel, S.G., 2001. Gaseous and particulate air pollutants in the Northeastern Mediterranean Coast. Science of The Total Environment 281, 205-215.

Stelson, A.W., Seinfeld, J.H., 1982. Relative humidity and temperature dependence of the ammonium nitrate dissociation constant. Atmospheric Environment (1967) 16, 983-992.

Stocker, D.W., Stedman, D.H., Zeller, K.F., Massman, W.J., Fox, D.G., 1993. Fluxes of nitrogen oxides and ozone measured by eddy correlation over a shortgrass prairie. Journal of Geophysical Research: Atmospheres 98, 12619-12630.

Stokstad, E., 2014. Ammonia Pollution From Farming May Exact Hefty Health Costs. Science 343, 238.

Sutton, M.A., Dragosits, U., Tang, Y.S., Fowler, D., 2000. Ammonia emissions from non-agricultural sources in the UK. Atmospheric Environment 34, 855-869.

Sutton, M.A., Place, C.J., Eager, M., Fowler, D., Smith, R.I., 1995. Assessment of the magnitude of ammonia emissions in the United Kingdom. Atmospheric Environment 29, 1393-1411.

Theil, H., 1992. A Rank-Invariant Method of Linear and Polynomial Regression Analysis, in: Raj, B., Koerts, J. (Eds.), Henri Theil's Contributions to Economics and Econometrics. Springer Netherlands, pp. 345-381.

Todd, R.W., Cole, N.A., Waldrip, H.M., Aiken, R.M., 2013. Arrhenius Equation for Modeling Feedyard Ammonia Emissions Using Temperature and Diet Crude Protein. Journal of Environmental Quality 42, 666-671.

Trebs, I., Metzger, S., Meixner, F.X., Helas, G., Hoffer, A., Rudich, Y., Falkovich, A.H., Moura, M.A., da Silva, R.S., Artaxo, P., 2005. The NH_4^+ - NO_3^- - Cl^- - SO_4^{2-} - H_2O aerosol system and its gas phase precursors at a pasture site in the Amazon Basin: How relevant are mineral cations and soluble organic acids? Journal of Geophysical Research: Atmospheres 110.

Tsai, C.-J., Perng, S.-N., 1998. Artifacts of ionic species for hi-vol PM_{10} and PM_{10} dichotomous samplers. Atmospheric Environment 32, 1605-1613.

Twomey, S., 1977. Atmospheric aerosols. Elsevier Scientific Pub. Co.

USEPA, 2004. National Emission Inventory – Ammonia Emissions from Animal Husbandry – Draft Report. US Environmental Protection Agency, Washington, D.C. Jan. 30, 2004.

Van Damme, M., Clarisse, L., Dammers, E., Liu, X., Nowak, J.B., Clerbaux, C., Flechard, C.R., Galy-Lacaux, C., Xu, W., Neuman, J.A., Tang, Y.S., Sutton, M.A., Erisman, J.W., Coheur, P.F., 2015. Towards validation of ammonia (NH_3) measurements from the IASI satellite. Atmospheric Measurement Techniques 8, 1575-1591.

Van Damme, M., Clarisse, L., Heald, C., Hurtmans, D., Ngadi, Y., Clerbaux, C., Dolman, A., Erisman, J.W., Coheur, P.-F., 2014a. Global distributions, time series and error characterization of atmospheric ammonia (NH_3) from IASI satellite observations. Atmospheric Chemistry and Physics 14, 2905-2922.

Van Damme, M., Wichink Kruit, R., Schaap, M., Clarisse, L., Clerbaux, C., Coheur, P.F., Dammers, E., Dolman, A., Erisman, J., 2014b. Evaluating 4 years of atmospheric ammonia (NH_3) over Europe using IASI satellite observations and LOTOS‐EUROS model results. Journal of Geophysical Research: Atmospheres 119, 9549-9566.

van Pul, A., Hertel, O., Geels, C., Dore, A., Vieno, M., van Jaarsveld, H., Bergström, R., Schaap, M., Fagerli, H., 2009. Modelling of the Atmospheric Transport and Deposition of Ammonia at a National and Regional Scale, in: Sutton, M., Reis, S., Baker, S.H. (Eds.), Atmospheric Ammonia. Springer Netherlands, pp. 301-358.

Vitousek, P.M., Aber, J.D., Howarth, R.W., Likens, G.E., Matson, P.A., Schindler, D.W., Schlesinger, W.H., Tilman, D.G., 1997. Human alteration of the global nitrogen cycle: sources and consequences. Ecological applications 7, 737-750.

Vogt, E., Held, A., Klemm, O., 2005. Sources and concentrations of gaseous and particulate reduced nitrogen in the city of Münster (Germany). Atmospheric Environment 39, 7393-7402.

Walker, J.T., Whitall, D.R., Robarge, W., Paerl, H.W., 2004. Ambient ammonia and ammonium aerosol across a region of variable ammonia emission density. Atmospheric Environment 38, 1235-1246.

Wen, L., Chen, J., Yang, L., Wang, X., Caihong, X., Sui, X., Yao, L., Zhu, Y., Zhang, J., Zhu, T., Wang, W., 2015. Enhanced formation of fine particulate nitrate at a rural site on the North China

Plain in summer: The important roles of ammonia and ozone. Atmospheric Environment 101, 294-302.

Wesely, M., 1989. Parameterization of surface resistances to gaseous dry deposition in regional-scale numerical models. Atmospheric Environment (1967) 23, 1293-1304.

Wesely, M.L., Hicks, B.B., 2000. A review of the current status of knowledge on dry deposition. Atmospheric Environment 34, 2261-2282.

Whitehead, J.D., Longley, I.D., Gallagher, M.W., 2007. Seasonal and Diurnal Variation in Atmospheric Ammonia in an Urban Environment Measured Using a Quantum Cascade Laser Absorption Spectrometer. Water, Air, and Soil Pollution 183, 317-329.

Wolfe, A.H., Patz, J.A., 2002. Reactive Nitrogen and Human Health:Acute and Long-term Implications. AMBIO: A Journal of the Human Environment 31, 120-125.

Wu, Z., Hu, M., Shao, K., Slanina, J., 2009. Acidic gases, NH_3 and secondary inorganic ions in PM_{10} during summertime in Beijing, China and their relation to air mass history. Chemosphere 76, 1028-1035.

Yao, X., Hu, Q., Zhang, L., Evans, G.J., Godri, K.J., Ng, A.C., 2013. Is vehicular emission a significant contributor to ammonia in the urban atmosphere? Atmospheric Environment 80, 499-506.

Yao, X., Yan Ling, T., Fang, M., Chan, C.K., 2006. Comparison of thermodynamic predictions for in situ pH in $PM_{2.5}$. Atmospheric Environment 40, 2835-2844.

Yeatman, S.G., Spokes, L.J., Jickells, T.D., 2001. Comparisons of coarse-mode aerosol nitrate and ammonium at two polluted coastal sites. Atmospheric Environment 35, 1321-1335.

Yu, X.-Y., Lee, T., Ayres, B., Kreidenweis, S.M., Malm, W., Collett Jr, J.L., 2006. Loss of fine particle ammonium from denuded nylon filters. Atmospheric Environment 40, 4797-4807.

Zbieranowski, A.L., Aherne, J., 2012. Spatial and temporal concentration of ambient atmospheric ammonia in southern Ontario, Canada. Atmospheric Environment 62, 441-450.

Zhang, L., Jacob, D.J., Knipping, E.M., Kumar, N., Munger, J.W., Carouge, C., Van Donkelaar, A., Wang, Y., Chen, D., 2012. Nitrogen deposition to the United States: distribution, sources, and processes.

Zhu, L., Henze, D., Cady‐Pereira, K., Shephard, M., Luo, M., Pinder, R., Bash, J., Jeong, G.R., 2013. Constraining US ammonia emissions using TES remote sensing observations and the GEOS‐Chem adjoint model. Journal of Geophysical Research: Atmospheres 118, 3355-3368.

APPENDIX A INFORMATION ABOUT BI-DIRECTIONAL AMMONIA FLUX MODEL

Dry deposition velocities used in this dissertation were obtained from CASTNET application of the MLM model. NH_3 deposition velocities were scaled to HNO_3 deposition velocities, as described below. In order to evaluate the accuracy of the NH_3 deposition velocity scaling assumption, Dr. John Walker and Dr. Donna Schwede of USEPA helped construct and run a bi-directional NH_3 flux model. The following model description was provided by Dr. John Walker.

A1. Bi-directional ammonia flux model

The net air-surface flux of NH_3 above natural terrestrial ecosystems is governed by the competing processes of emission and deposition within the underlying vegetation and soil. Vegetation (i.e., apoplast) and soil pore water contain dissolved NH_4^+ and a corresponding NH_3 gas phase equilibrium, therefore exhibiting a "compensation point" relative to the surrounding atmosphere (Farquhar et al., 1980; Langford et al., 1992). The NH_3 compensation point is the atmospheric concentration at which the net surface exchange is zero, i.e., the NH_3 concentration at which the atmosphere is at equilibrium with the underlying surface. The surface is a sink for atmospheric NH_3 when the atmospheric concentration exceeds the compensation point and emits NH_3 to the atmosphere under the opposite condition. Though there are many instances where NH_3 only deposits to or emits from the surface (i.e., unidirectional flux), from a mechanistic standpoint NH_3 air-surface exchange is considered "bi-directional".

Bi-directional NH$_3$ flux is calculated using the two-layer canopy compensation point model developed by Nemitz et al. (2001), which relates the net canopy-scale NH$_3$ flux (F_t) to the net emission potential of the canopy (i.e., foliage and soil), or surface concentration ($\chi_{(z_o)}$), which is in turn related to the canopy compensation point (χ_c). The system of equations describing the net canopy flux (F_t), as well as component vegetation [i.e., stomatal (F_s), cuticular (F_w)] and ground (F_g) fluxes, is given by Nemitz et al. (2001). The model requires inputs of atmospheric NH$_3$ concentration along with parameterizations for atmospheric [aerodynamic resistance (R$_a$) and boundary layer (R$_b$)], in-canopy [aerodynamic (R_{ac}), boundary-layer resistances (R_{bg}) and ground ($R_g = R_{ac} + R_{bg}$)], and leaf-level [stomatal (R$_s$) and cuticular (R$_w$)] resistances as well as stomatal (Γs) and ground (Γg) emission potentials. Here the ground emission potential does not distinguish between soil and litter layers but is rather a bulk property of the surface.

The aerodynamic resistance is calculated as a function of the standard deviation of the measured wind direction (σ_θ), and wind speed (u) according to Hicks et al. (1987), assuming that the atmosphere is considered unstable when global radiation (G) exceeds 100 W m^{-2} (Meyers et al., 1998). The boundary-layer resistance is calculated according to Hicks et al. (1987) where friction velocity (u_*) is calculated from the near-neutral approximation as a function of R_a and u. The in-canopy aerodynamic (turbulent) resistance (R_{ac}) is calculated according to Massad et al. (2010) as a function of u_* and canopy height. The additional boundary layer resistance (R_{bg}) at the ground is calculated according to Schuepp (1977) where the ground friction velocity assumes the form of Bash et al. (2010). For calculating R_{bg}, the upper limit of the logarithmic profile of wind speed just above the ground surface is taken as 0.01m for grassland and 0.1 for other surfaces. The sum of R_{ac} and R$_{bg}$ establishes the total ground resistance (R_g).

The bulk stomatal resistance to NH_3 transfer (R_s) is assumed equal to that of water vapor (H_2O) corrected for differences in molecular diffusivity. Stomatal resistance to H_2O is calculated as a function of G, air temperature (T), and the vegetation specific minimum resistance (R_{smin}) according to the rather simple parameterization of Wesely (1989). Minimum stomatal resistances assume the same values specified for the Multi-Layer Model (MLM) (Meyers et al., 1998). Parameterization of the cuticular resistance (R_w) is calculated according to Massad et al. (2010) as a function of relative humidity, surface type (forest, semi-natural, grassland), and the atmospheric acid ratio (AR). Site-specific values of AR were calculated seasonally using CASTNET measured concentrations of SO_2 and HNO_3, AMoN measured NH_3 concentrations, and assuming an atmospheric HCl concentration of 0.005 µmol/m^3.

The stomatal (i.e. vegetation) emission potential Γ_s was parameterized according to Massad et al. (2010) as a function of total nitrogen deposition assuming the "un-managed" case and a value of $\Gamma_g = 20$ was assigned for the ground emission potential. Emission potentials are calculated for each AMoN site using collocated NADP/NTN wet deposition and CASTNET dry deposition data averaged over a five year period between 2006 and 2010. Vegetation and soil emission potentials are then used to calculate vegetation (χ_s) and ground (χ_g) compensation points (in units of µg m^{-3} to represent air concentration) as a function of temperature following (Nemitz et al., 2001). Note that N deposition derived from NADP/NTN wet deposition and CASTNET dry deposition does not include dry deposition of NH_3 or deposition of organic N compounds and therefore represents a lower limit for total N deposition and thus the vegetation emission potential. Canopy height and leaf area index assume the same values used for the MLM. Roughness length is specified as

0.15×canopy height. Zero plane displacement is estimated using the Stanhill approximation (Arya, 2001).

A2. Implementation of bi-directional NH_3 model

Similar to the MLM, the bi-directional NH_3 model was run at an hourly time step using hourly CASTNET meteorology and assuming an hourly NH_3 air concentration equivalent to the corresponding two-week integrated AMoN concentration. Note that for this analysis, AMoN and CASTNET are collocated. Hourly fluxes are summed over time to produce seasonal and annual total (net, F_t) and component (F_s, F_w, and F_g) fluxes.

A3. Comparison of bi-directional and unidirectional NH_3 dry deposition models

The net flux estimated from the bi-directional NH_3 model was directly compared to the unidirectional (deposition) flux estimated by multiplying the AMoN NH_3 concentration by $0.7 \times$ the MLM (CASTNET) derived deposition velocity for HNO_3. Common inputs of hourly CASTNET meteorology, AMoN NH_3 concentrations, and canopy physical characteristics were used to compare seasonal and annual fluxes for the dominant vegetation type at each collocated CASTNET/AMoN site. The objective of this exercise was to examine the relative differences in fluxes to inform the potential uncertainty of the scaled MLM HNO_3 approach. The comparison is only valid for the natural surfaces for which the bi-directional NH_3 model has been parameterized, which excludes fertilized and nitrogen fixing crops and other surfaces specified by CASTNET including, water, sand, and rock.

Meteorological data were discontinued at CASTNET sites in 2010 at all but 5 sites. For this reason, the meteorological dataset for each site was chosen based on 90% completeness for the required variables starting at 2009 and working backward until the 90% annual completeness criteria was met. This meteorological dataset was then matched with AMoN NH_3 concentration data for the year of 2012 (NH_3 Data in 2013 was used for GTH161 and CNT169 site). Because the objective was to compare the models using common inputs, it was not necessary to match the year chosen for meteorology with that of the chemical inputs (AMoN, NADP). At each site, the models assume the dominant vegetation type as specified by the CASTNET site characteristics for MLM.

A4. Seasonal differences in MLM versus bi-directional NH_3 dry deposition estimates

Differences in MLM versus bi-directional model estimates are generally greatest in summer (Figure 2.9). Though highest atmospheric NH_3 concentrations typically occur during the hottest months, the temperature driven stomatal and soil compensation points are also at a maximum, yielding lower deposition rates via these pathways than is predicted under the assumption of a zero compensation (i.e., unidirectional MLM approach) point. In some cases (e.g., WV18 and GA41), the exponential relationship between temperature and compensation point produces net emissions during summer. Furthermore, atmospheric acidity generally reaches a minimum during summer owing to seasonally lower concentrations of SO_2 and higher concentrations of NH_3. Leaf surfaces are therefore less acidic, resulting in lower cuticular deposition rates relative to what would be observed for that same atmospheric NH_3 concentration in other seasons. The bi-directional model yields larger fluxes relative to the MLM approach during winter when compensation points are lowest and surfaces are more acidic (i.e., larger acid ratios).
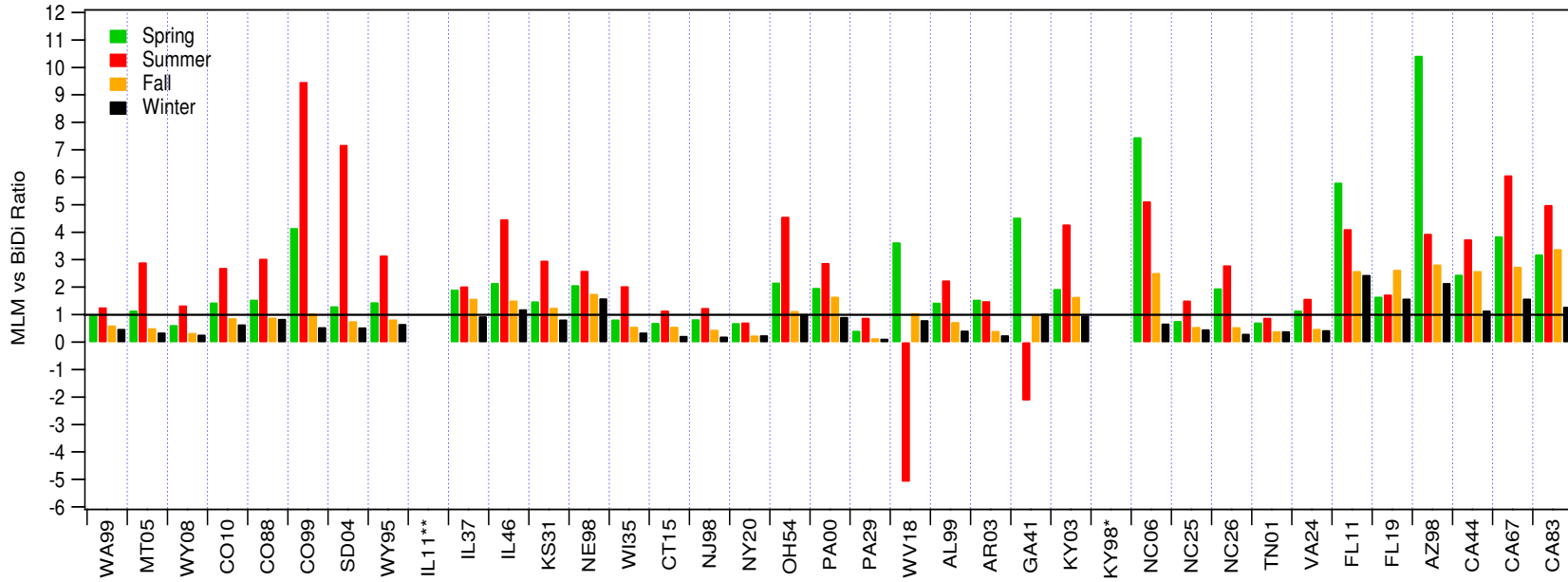
Figure A1 Seasonal ratios of MLM ($0.7\times$ Vd,HNO$_3$) versus bi-directional NH$_3$ dry deposition estimates
* Due to lack of meteorological data, bi-directional flux model is not parametrized appropriately for the KY98 site.
**Due to feature of surface plants, bi-directional flux model is not parametrized appropriately for the IL11 site

APPENDIX B COMPARISON OF NE COLORADO AMMONIA OBSERVATIONS WITH

TROPOSPHERIC EMISSIONS SPECTROMETER (TES) SATELLITE RETRIEVALS

Several recent studies have used surface NH_3 measurements to evaluate or improve remote sensing techniques for retrieving NH_3 concentrations and determining distributions (Heald et al., 2012; Pinder et al., 2011; Zhu et al., 2013). The Tropospheric Emissions Spectrometer (TES) is a high-resolution infrared Fourier transform spectrometer carried by NASA's Aura satellite that has been shown to be capable of detecting the spatial and vertical distribution of NH_3 from space (Beer et al., 2008). The TES products and retrieved NH_3 used in this study are available from NASA(http://avdc.gsfc.nasa.gov/index.php?site=635564035&id=10&go=list&path=/NH3). TES has a footprint of 5.3 x 8.3 km and an ascending overpass at 13:30 mean solar time. The vertical sensitivity of the NH_3 retrieval peaks between 900 and 700 hPa, although this varies based on thermal contrast, NH_3 concentration, and cloud cover. Because the degrees of freedom (DOF) are generally less than 1; in this study, the Representative Volume Mixing Ratio (RVMR) is used for spatial distributions. The RVMR is a boundary layer averaged value weighted by TES sensitivity and reduced reliance on the a priori choice (Shephard et al., 2011) and provides a helpful indicator for comparing with surface measurements. Since DOFs decrease with increasing cloud optical depths, observations are only used when cloud optical depths are < 1.0. Pinder et al. (2011) show that TES NH_3 RVMRs strongly correspond to spatial and seasonal variations in surface measurements in North Carolina and even find significant correlations with number of livestock facilities. Here TES NH_3 RVMRs are compared with the results from the NH_3 spatial measurements in northeastern Colorado. We are also able to provide a novel look at the TES-retrieved vertical NH_3 concentration profile using the vertical measurements on the BAO tower.

TES observations for the period of May through August from 2010 to 2012 were selected for the spatial comparison within the latitude range from 39.9°N to 41.2°N and the longitude range from 103.4°W to 105.3°W (Figure B1). Due to cloud depth filtering and geographic and time sampling limitations, there are only a few valid TES NH_3 observations in northeastern Colorado. Pinder et al. (2011) note that due to several limitations and sampling differences, for example daily variations of NH_3, perfect agreement will not be found by direct comparison between weekly surface measurement and the satellite retrieval. However, both spatial NH_3 measurements from this study and TES data showed a generally similar spatial distribution of NH_3 in NE Colorado. When the retrieval locations were away from concentrated agricultural areas, TES NH_3 concentrations were below 10 ppb, similar to NH_3 concentrations measured at ground observation sites.
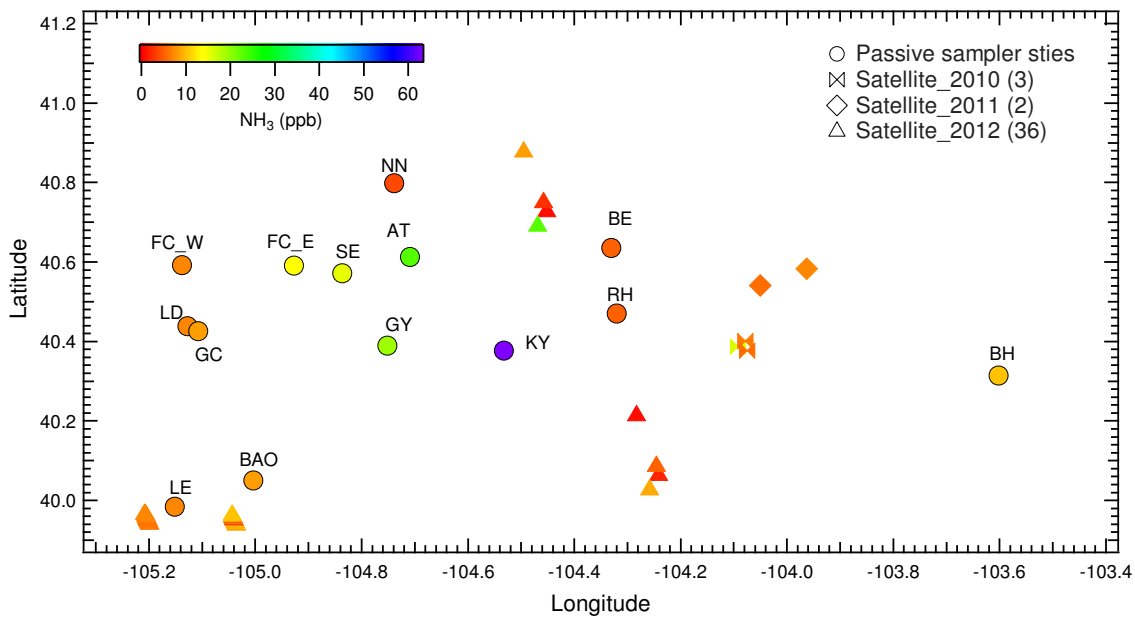
Figure B1 TES NH_3 data from 2010 to 2012 (bowties, diamonds, and triangles) and passive sampler three-year (2010 - 2012) surface measured NH_3 average concentrations (circles). The passive NH_3 concentrations were converted from $\mu g/m^3$ to a mixing ratio (ppb) using ambient pressure calculated by the elevation of each site and mean temperature measured at FC_W.

There were only 3 (bowtie), 2 (diamond) and 36 (triangle) valid TES data points in the region between May and August in 2010, 2011 and 2012, respectively.

The locations of TES data points for the vertical comparisons were selected within the $1° × 1°$ latitudinal and longitudinal grid of the BAO tower (40.05±0.5°N, 105.00±0.5°W). Fifteen profiles are available in this area, all from August 2012. Ambient pressure (P) for the BAO tower is calculated as following based on the altitude above sea level (h):

$$P = 101325 \times (1 - 2.25577 \times 10^{-5} \times h)^{5.25588}$$

TES profiles provide concentration estimates at only two vertical layers (825.45 and 834.79 mb) within the BAO tower measurement from 806.27 to 836.67 mb. Figure B1 shows that the vertical passive sampler and satellite measurements of NH_3 concentrations were similar near the ground level. However, as height increased, the NH_3 concentrations measured on the tower decreased somewhat more rapidly than those in the TES retrievals.
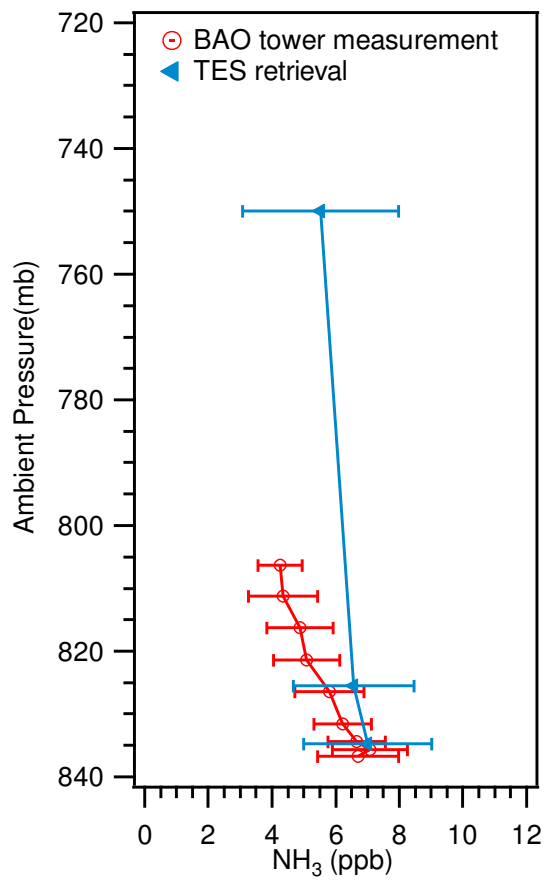
Figure B2 Comparison of TES NH$_3$ data and BAO tower vertical NH$_3$ measurements in August 2012. The x-error bars represent the relative standard deviation of measured and retrieved NH$_3$ concentrations.

APPENDIX C BOULDER WYOMING MEASUREMENT DATA FROM URG SAMPLING (2007-2011)

Sample_ID	Start_datetime	End_datetime	Elapsed_time	Air Volume	NH_3 (g) $\mu g/m^3$	HNO_3 (g) $\mu g/m^3$	NO_3^- (p) $\mu g/m^3$	SO_4^{2-} (p) $\mu g/m^3$	NH_4^+ (p) $\mu g/m^3$	K^+ (p) $\mu g/m^3$
WY010107	1/1/07 8:00 AM	1/5/07 8:00 AM	96.00	55.50	0.0076	0.2358	0.4880	0.5103	0.2579	b.d
WY010507	1/5/07 8:00 AM	1/8/07 8:00 AM	72.00	42.57	0.0171	0.0597	0.2230	0.1581	0.0704	b.d
WY010807	1/8/07 8:00 AM	1/12/07 8:00 AM	96.00	56.49	0.0124	0.1988	0.4379	0.2229	0.2037	b.d
WY011207	1/12/07 8:00 AM	1/15/07 8:00 AM	72.00	32.11	0.0073	0.2916	0.7578	0.4521	0.3170	0.0242
WY011507	1/15/07 8:00 AM	1/19/07 8:00 AM	96.00	53.45	0.0040	1.0561	1.3839	0.4416	0.7651	b.d
WY011907	1/19/07 8:00 AM	1/22/07 8:00 AM	72.00	43.37	0.0038	0.3959	1.1827	0.3652	0.4854	b.d
WY012207	1/22/07 8:00 AM	1/26/07 8:00 AM	96.00	56.93	0.0000	0.6637	0.9205	0.2915	0.3928	0.0159
WY012607	1/26/07 8:00 AM	1/29/07 8:00 AM	72.00	43.86	0.0048	0.4791	0.9612	0.5156	0.6065	0.0203
WY012907	1/29/07 8:00 AM	2/2/07 8:00 AM	96.00	54.41	0.0029	0.5219	0.5383	0.4107	0.3287	b.d
WY020207	2/2/07 8:00 AM	2/5/07 8:00 AM	72.00	42.99	0.0087	0.2557	0.4828	0.2280	0.2846	b.d
WY020507	2/5/07 8:00 AM	2/9/07 8:00 AM	96.00	56.70	0.0000	0.3958	0.8250	0.1602	0.4777	b.d
WY020907	2/9/07 8:00 AM	2/12/07 8:00 AM	72.00	44.39	0.0119	0.1717	0.6336	0.3148	0.2973	b.d
WY021207	2/12/07 8:00 AM	2/16/07 8:00 AM	96.00	55.70	0.0010	0.1061	0.2423	0.1742	0.1695	b.d
WY021607	2/16/07 8:00 AM	2/19/07 8:00 AM	72.00	43.47	0.0062	0.1478	0.2278	0.2363	0.1649	b.d
WY021907	2/19/07 8:00 AM	2/23/07 8:00 AM	96.00	57.71	0.0025	0.1982	0.2401	0.2540	0.2070	b.d
WY022307	2/23/07 8:00 AM	2/26/07 8:00 AM	72.00	42.92	0.0162	0.1103	0.9635	0.2644	0.1896	b.d
WY022607	2/26/07 8:00 AM	3/2/07 8:00 AM	96.00	56.30	0.0096	0.7043	0.4163	0.2155	0.2031	0.0241
WY030207	3/2/07 8:00 AM	3/5/07 8:00 AM	72.00	43.28	0.0107	0.1447	0.2948	0.2264	0.2007	b.d
WY030507	3/5/07 8:00 AM	3/9/07 8:00 AM	96.00	56.43	0.1119	0.2774	0.7366	0.3002	0.3658	0.0239
WY030907	3/9/07 8:00 AM	3/12/07 8:00 AM	72.00	44.19	0.0052	0.0978	0.1917	0.3472	0.1657	b.d
WY031207	3/12/07 8:00 AM	3/16/07 8:00 AM	96.00	56.04	0.3582	0.2241	0.1755	0.3162	0.1687	0.0270
WY031607	3/16/07 8:00 AM	3/19/07 8:00 AM	72.00	44.18	0.1089	0.1175	0.1825	0.2808	0.1568	0.0334
WY031907	3/19/07 8:00 AM	3/23/07 8:00 AM	96.00	57.76	0.0183	0.1469	0.2076	0.3943	0.2026	0.0251
WY032307	3/23/07 8:00 AM	3/26/07 8:00 AM	72.00	44.58	0.0082	0.0906	0.1923	0.2930	0.1634	0.0191
WY032607	3/26/07 8:00 AM	3/30/07 8:00 AM	96.00	55.34	0.1619	0.1424	0.1362	0.3873	0.2149	b.d
WY033007	3/30/07 8:00 AM	4/2/07 8:00 AM	72.00	43.61	0.0247	0.1194	0.3662	0.7548	0.4555	b.d
WY040207	4/2/07 8:00 AM	4/6/07 8:00 AM	96.00	58.91	0.0047	0.0949	0.2586	0.9968	0.6374	b.d
WY040607	4/6/07 8:00 AM	4/9/07 8:00 AM	72.00	43.79	0.0042	0.1327	0.3526	0.8273	0.5618	b.d
WY040907	4/9/07 8:00 AM	4/13/07 8:00 AM	96.00	57.08	0.0245	0.1063	0.1345	0.2447	0.1929	b.d
WY041307	4/13/07 8:00 AM	4/16/07 8:00 AM	72.00	44.76	0.0805	0.2367	0.1974	0.4629	0.2921	0.0182
WY041607	4/16/07 8:00 AM	4/20/07 8:00 AM	96.00	59.31	0.0493	0.3711	0.2459	0.7392	0.4748	
WY042007	4/20/07 8:00 AM	4/23/07 8:00 AM	72.00	48.86	0.0198	0.1434	0.2016	0.7168	0.3400	0.0245

WY042307	4/23/07 8:00 AM	4/27/07 8:00 AM	96.00	57.60	0.1400	0.1183	0.1698	0.5190	0.2540	0.0203
WY042707	4/27/07 8:00 AM	4/30/07 8:00 AM	72.00	45.27	0.2385	0.1963	0.2396	0.6576	0.2226	0.0292
WY043007	4/30/07 8:00 AM	5/4/07 8:00 AM	96.00	57.02	0.1836	0.2245	0.2149	0.9029	0.3212	0.0259
WY050407	5/4/07 8:00 AM	5/7/07 8:00 AM	72.00	45.08	0.0072	0.0371	0.2033	0.5890	0.2553	b.d
WY050707	5/7/07 8:00 AM	5/11/07 8:00 AM	96.00	40.66	0.1112	0.5395	0.1957	1.2826	0.4650	0.0358
WY051107	5/11/07 8:00 AM	5/14/07 8:00 AM	75.10	50.96	0.1842	0.4867	0.1611	0.7285	0.3069	0.0293
WY051407	5/14/07 8:00 AM	5/18/07 8:00 AM	96.00	60.29	0.0779	0.3884	0.2073	2.0802	0.2900	0.0379
WY051807	5/18/07 8:00 AM	5/21/07 8:00 AM	68.60	41.21	0.2539	0.3631	0.3452	1.5507	0.4988	0.0413
WY052107	5/21/07 8:00 AM	5/25/07 8:00 AM	96.00	114.64	0.1782	0.1004	0.0644	0.6072	0.1957	0.0142
WY052507	5/25/07 8:00 AM	5/28/07 8:00 AM	72.60	47.34	0.3183	0.5166	0.1242	0.7745	0.3797	0.0294
WY052807	5/28/07 8:00 AM	6/1/07 8:00 AM								
WY060107	6/1/07 8:00 AM	6/4/07 8:00 AM	71.30	45.20	0.0881	0.1540	0.1147	0.5712	0.2176	0.0257
WY060407	6/4/07 8:00 AM	6/8/07 8:00 AM	96.00	57.66	0.0991	0.1494	0.1303	0.5473	0.1835	0.0208
WY060807	6/8/07 8:00 AM	6/11/07 8:00 AM	71.00	46.69	0.0491	0.2151	0.0907	0.5491	0.2223	0.0214
WY061107	6/11/07 8:00 AM	6/15/07 8:00 AM	96.00	56.75	0.1032	0.1496	0.1245	0.5695	0.2175	0.0213
WY061507	6/15/07 8:00 AM	6/18/07 8:00 AM	72.00	46.80	0.1196	0.2157	0.1122	0.5509	0.2188	0.0379
WY061807	6/18/07 8:00 AM	6/22/07 8:00 AM	96.00	63.92	0.1522	0.1561	0.1007	0.4350	0.1826	0.0314
WY062207	6/22/07 8:00 AM	6/25/07 8:00 AM	72.00	44.50	0.2604	0.4316	0.1997	0.7620	0.3371	0.0498
WY062507	6/25/07 8:00 AM	6/29/07 8:00 AM	96.00	66.51	0.2277	0.2886	0.1733	0.6488	0.2551	0.0617
WY062907	6/29/07 8:00 AM	7/2/07 2:00 PM	78.00	52.97	0.2707	0.4822	0.2087	0.7124	0.3052	0.0423
WY070207	7/2/07 8:00 AM	7/6/07 8:00 AM	96.00	61.74	0.2277	0.3008	0.0708	0.6930	0.2562	0.0209
WY070607	7/6/07 2:00 PM	7/9/07 8:00 AM	65.80	48.12	0.3284	0.3077	0.1882	0.7846	0.3285	0.1688
WY070907	7/9/07 8:00 AM	7/13/07 8:00 AM	92.60	59.90	0.2492	0.2955	0.1628	0.6961	0.2987	0.0700
WY071307	7/13/07 8:00 AM	7/16/07 8:00 AM	71.90	42.31	0.8111	0.2638	0.1857	0.6105	0.3888	0.0619
WY071607	7/16/07 8:00 AM	7/20/07 8:00 AM	96.00	64.43	0.5899	0.3905	0.1087	0.7831	0.3994	0.0393
WY072007	7/20/07 8:00 AM	7/23/07 8:00 AM	61.90	37.86	0.5661	0.4927	0.3885	0.7711	0.4218	0.2188
WY072307	7/23/07 8:00 AM	7/27/07 8:00 AM	95.00	61.51	0.4043	0.3929	0.1141	0.4911	0.2979	0.0275
WY072707	7/27/07 8:00 AM	7/30/07 8:00 AM	72.00	44.41	0.4575	0.2475	0.0799	0.4138	0.2202	0.0304
WY073007	7/30/07 8:00 AM	8/3/07 8:00 AM	96.00	63.96	0.5052	0.2501	0.1083	0.6115	0.3387	0.0237
WY080307	8/3/07 8:00 AM	8/6/07 11:20 AM	75.20	46.50	0.8412	0.2388	0.2130	0.6084	0.3895	0.0556
WY080607	8/6/07 8:00 AM	8/10/07 8:00 AM	96.00	65.03	0.4587	0.2871	0.1722	0.5719	0.3011	0.0452
WY081007	8/10/07 11:20 AM	8/13/07 8:00 AM	68.10	45.86	0.3046	0.2191	0.1859	0.6677	0.2942	0.0404
WY081307	8/13/07 8:00 AM	8/17/07 8:00 AM	96.00	57.54	0.5064	0.3255	0.0979	0.7737	0.4152	0.0262
WY081707	8/17/07 8:00 AM	8/20/07 8:00 AM	64.90	45.75	0.4263	0.1152	0.0439	0.5865	0.3001	0.0614

WY082007	8/20/07 8:00 AM	8/24/07 8:00 AM	96.00	61.50	0.1706	0.1151	0.0972	0.2292	0.0806	0.0122
WY082407	8/24/07 8:00 AM	8/27/07 8:00 AM	96.00	49.32	0.3713	0.2592	0.1200	0.4030	0.2389	0.0269
WY082707	8/27/07 8:00 AM	8/31/07 9:00 AM	97.10	64.86	0.2899	0.3887	0.0970	0.5498	0.2561	0.0181
WY083107	8/31/07 8:00 AM	9/3/07 8:00 AM	72.00	47.58	0.3421	b.d	0.0955	0.6323	0.2889	0.0154
WY090307	9/3/07 9:00 AM	9/7/07 8:00 AM	94.60	59.99	0.2792	0.2219	0.1487	0.4192	0.2637	0.0236
WY090707	9/7/07 8:00 AM	9/10/07 8:00 AM	72.00	43.79	0.2348	0.2061	0.2032	0.5955	0.3966	0.0295
WY091007	9/10/07 8:00 AM	9/19/07 12:39 PM	148.50	92.71	0.0897	0.1883	0.0294	0.5464	0.1520	0.0328
WY091407	9/14/07 8:00 AM	9/17/07 8:00 AM	72.00	46.29	0.2175	0.2766	0.2703	0.5970	0.2918	0.0331
WY091707	9/19/07 12:39 PM	9/21/07 8:00 AM	43.10	24.26	0.1041	0.5950	0.2910	0.8308	0.4015	0.0367
WY092107	9/21/07 8:00 AM	9/24/07 8:00 AM	72.00	39.21	0.1582	0.1849	0.1323	0.5237	0.2389	0.0166
WY092407	9/24/07 8:00 AM	10/1/07 11:35 AM	99.70	57.45	0.0609	0.0486	0.1453	0.3109	0.2014	0.0147
WY092807	9/28/07 8:00 AM	10/1/07 8:00 AM	72.00	40.58	0.0607	0.1212	0.1666	0.5576	0.1852	0.0144
WY100107	10/1/07 11:35 AM	10/5/07 8:00 AM	92.10	52.21	0.0962	0.1650	0.0843	0.6492	0.2762	0.0151
WY100507	10/5/07 8:00 AM	10/8/07 8:00 AM	71.70	39.09	0.0806	0.0120	0.1253	0.4539	0.1810	0.0062
WY100807	10/8/07 8:00 AM	10/12/07 8:00 AM	96.00	53.45	0.0494	0.0813	0.0043	0.3167	0.1054	0.0092
WY101207	10/12/07 8:00 AM	10/15/07 8:00 AM	72.00	41.29	0.1161	0.1499	0.2421	0.8875	0.3549	0.0081
WY101507	10/15/07 8:00 AM	10/19/07 7:50 AM	96.00	52.72	0.1048	0.0728	0.1912	0.4837	0.2087	0.0080
WY101907	10/19/07 8:00 AM	10/22/07 8:00 AM	72.00	33.04	0.0703	0.0219	0.0436	0.0242	b.d	0.0021
WY102207	10/22/07 8:00 AM	10/26/07 8:00 AM	96.00	52.66	0.0494	0.1359	0.1246	0.3001	0.1360	0.0032
WY102607	10/26/07 8:00 AM	10/29/07 8:00 AM	72.00	41.33	0.0437	0.1320	0.4172	0.8403	0.4231	0.0265
WY102907	10/29/07 8:00 AM	11/2/07 8:01 AM	96.00	53.85	0.1123	0.1157	0.1962	0.5474	0.2637	0.0262
WY110207	11/2/07 8:00 AM	11/5/07 8:00 AM	72.90	40.23	0.0210	0.0619	0.1981	1.3811	0.4236	0.0189
WY110507	11/5/07 8:00 AM	11/9/07 7:55 AM	96.00	53.83	0.0180	0.1808	0.1851	0.9104	0.3366	0.0132
WY110907	11/9/07 8:00 AM	11/12/07 8:00 AM	72.00	42.02	0.1227	0.1683	0.2696	1.0471	0.4086	0.0107
WY111207	11/12/07 8:00 AM	11/16/07 7:50 AM	96.00	54.53	0.0421	0.0584	0.1753	0.3822	0.1609	0.0077
WY111607	11/16/07 8:00 AM	11/19/07 8:00 AM	74.30	42.33	0.0954	0.0909	0.2434	0.3032	0.1346	0.0045
WY111907	11/19/07 8:00 AM	11/23/07 7:45 AM	96.00	55.45	0.0193	0.0305	0.0913	1.4739	0.3723	0.0177
WY112307	11/23/07 8:00 AM	11/26/07 8:00 AM	72.00	38.72	0.0025	0.0452	0.0977	0.4331	0.1833	0.0032
WY112607	11/26/07 8:00 AM	11/30/07 7:50 AM	96.00	55.02	0.0156	0.0716	0.2595	0.2110	0.1828	0.0037
WY113007	11/30/07 8:00 AM	12/3/07 8:00 AM	72.00	39.86	0.0211	0.0331	0.7006	0.4782	0.3036	0.0056
WY120307	12/3/07 8:00 AM	12/7/07 8:00 AM	96.00	55.63	0.0159	0.0120	0.2813	0.2237	0.1334	0.0032
WY120707	12/7/07 8:00 AM	12/10/07 11:20 AM	76.70	42.60	0.0064	0.0400	0.4464	0.5348	0.2843	0.0014
WY121007	12/10/07 8:00 AM	12/14/07 8:00 AM	96.00	53.85	0.0019	0.0898	0.5980	0.5146	0.4318	0.0016
WY121407	12/14/07 11:20 AM	12/17/07 8:00 AM	67.20	36.22	0.0113	0.0532	1.0498	0.3534	0.3968	0.0014

WY121707	12/17/07 8:00 AM	12/21/07 8:00 AM	96.00	53.00	0.0008	0.0543	1.1158	0.5401	0.3852	0.0012
WY122107	12/21/07 8:00 AM	12/24/07 8:00 AM	72.00	40.32	0.0004	0.0182	0.1527	0.1485	0.4435	0.0015
WY122407	12/24/07 8:00 AM	12/28/07 6:50 AM	96.00	50.35	0.0176	0.0180	0.1571	0.1026	0.0670	0.0003
WY122807	12/28/07 8:00 AM	12/31/07 8:00 AM	72.00	37.99	b.d	0.0540	0.5200	0.1729	0.2235	0.0010
WY123107	12/31/07 8:00 AM	1/4/07 8:00 AM	96.00	50.62	0.0002	0.4034	1.1177	0.1350	0.3214	0.0594
WY010408	1/4/08 8:00 AM	1/7/08 2:30 PM	79.60	42.34	0.0015	0.1201	0.3923	0.2206	0.1699	0.0029
WY010708	1/7/08 8:00 AM	1/11/07 8:00 AM	96.00	50.95	b.d	0.3575	1.2891	0.1779	0.3510	0.0029
WY011108	1/11/08 8:00 AM	1/14/07 8:00 AM	64.30	33.43	b.d	0.1106	0.5316	0.1158	0.1368	0.0008
WY011408	1/14/08 8:00 AM	1/18/07 8:00 AM	94.90	48.95	0.0010	0.1278	0.4506	0.1864	0.1908	0.0013
WY011808	1/18/08 8:00 AM	1/21/07 8:00 AM	72.00	39.49	0.0012	0.0786	0.6389	0.3696	0.3699	0.0026
WY012108	1/21/08 8:00 AM	1/25/07 6:55 AM	96.00	47.68	0.0001	0.5038	1.3948	0.4482	0.3066	0.0023
WY012508	1/25/08 8:00 AM	1/28/08 8:00 AM	72.00	40.04	b.d	0.5400	1.8204	0.5633	0.4152	0.0022
WY012808	1/28/08 8:00 AM	2/1/08 6:50 AM	96.00	50.22	0.0190	0.1178	0.3386	0.1949	0.1647	b.d
WY020108	2/1/08 8:00 AM	2/4/08 8:00 AM	72.00	39.22	b.d	0.2315	0.4326	0.4313	0.1931	0.0019
WY020408	2/4/08 8:00 AM	2/8/08 6:50 AM	96.00	53.43	0.0019	0.0624	0.3172	0.2774	0.1806	0.0006
WY020808	2/8/08 8:00 AM	2/13/08 5:00 AM	130.00	72.22	b.d	0.6113	1.3717	0.1812	0.2899	0.0015
WY021108	2/11/08 8:00 AM	2/15/08 8:00 AM	83.80	45.91	0.0029	0.0633	0.3371	0.1977	0.1223	b.d
WY021508	2/17/08 5:00 PM	2/18/08 6:45 AM	13.40	7.26	0.0262	0.1505	0.1539	0.2023	0.0302	b.d
WY021808	2/18/08 8:00 AM	2/22/08 6:45 AM	96.00	54.58	0.0007	0.5653	2.0915	0.3936	0.4822	0.0047
WY022208	2/22/08 8:00 AM	2/25/08 8:00 AM	70.20	38.89	0.0090	1.4041	2.1145	0.8504	0.6270	0.0025
WY022508	2/25/08 6:45 AM	2/29/08 7:00 AM	88.50	51.12	0.0009	0.1998	0.8109	0.1641	0.3154	b.d
WY022908	2/29/08 8:00 AM	3/3/08 8:00 AM	72.00	33.63	0.0333	0.3616	0.3205	0.1327	0.2094	b.d
WY030308	3/3/08 7:00 AM	3/7/08 7:05 AM	96.00	48.85	0.0377	0.0744	0.3965	0.4419	0.2752	0.0065
WY030708	3/7/08 8:00 AM	3/10/08 8:00 AM	71.90	38.96	b.d	0.2763	2.6917	0.3974	0.8275	0.0012
WY031008	3/10/08 7:00 AM	3/14/08 8:00 AM	96.00	59.78	0.0216	0.1101	1.8079	0.3973	0.5699	0.0016
WY031408	3/14/08 8:00 AM	3/17/08 8:00 AM	72.00	32.13	0.0240	0.0748	0.1127	0.0362	0.1278	b.d
WY031708	3/17/08 8:00 AM	3/21/08 8:00 AM	96.00	57.07	0.0610	0.0675	0.5996	0.6785	0.4458	0.0073
WY032108	3/21/08 8:00 AM	3/24/08 8:00 AM	72.00	40.05	0.0288	0.1087	0.3616	1.0066	0.3868	0.0150
WY032408	3/24/08 8:00 AM	3/28/08 8:00 AM	92.30	51.69	0.0914	0.0564	0.3676	0.6459	0.3799	0.0060
WY032808	3/28/08 8:00 AM	3/31/08 8:00 AM	72.00	39.54	0.0634	0.0069	0.3838	0.5905	0.1885	0.0053
WY033108	3/31/08 8:00 AM	4/4/08 8:00 AM	91.80	49.15	0.0472	b.d	0.4844	0.4531	0.2327	0.0046
WY040408	4/4/08 8:00 AM	4/7/08 8:00 AM	72.00	40.56	0.0650	b.d	0.5432	0.4105	0.1975	0.0042
WY040708	4/7/08 8:00 AM	4/11/08 8:00 AM	85.50	47.24	0.0499	b.d	0.3825	0.9963	0.3242	0.0091
WY041108	4/11/08 8:00 AM	4/14/08 8:00 AM	72.00	39.83	0.0526	b.d	0.1501	0.4831	b.d	b.d

WY041408	4/14/08 8:00 AM	4/18/08 8:00 AM	96.00	52.21	0.0542	0.0058	0.1926	0.4225	0.1409	0.0082
WY041808	4/18/08 8:00 AM	4/21/08 8:00 AM	70.40	40.52	0.0608	0.0003	0.3292	0.5018	0.1478	0.0155
WY042108	4/21/08 8:00 AM	4/25/08 8:00 AM	96.00	54.37	0.0427	b.d	0.2310	0.4622	0.1439	0.0098
WY042508	4/25/08 8:00 AM	4/28/08 8:00 AM	71.60	38.62	0.0897	b.d	0.1817	0.5205	0.1551	0.0084
WY042808	4/28/08 8:00 AM	5/2/08 8:00 AM	87.70	50.17	0.1254	b.d	0.2564	0.4958	0.1436	0.0083
WY050208	5/2/08 8:00 AM	5/5/08 8:00 AM	71.90	41.77	0.0917	b.d	0.2858	0.5044	0.1672	0.0054
WY050508	5/5/08 8:00 AM	5/9/08 8:00 AM	95.00	56.61	0.1312	0.0037	0.2742	0.9412	0.2530	0.0082
WY050908	5/9/08 8:00 AM	5/12/08 8:00 AM	72.00	40.50	0.0593	b.d	0.1733	0.6583	0.1680	0.0052
WY051208	5/12/08 8:00 AM	5/16/08 8:00 AM	96.00	53.46	0.0389	b.d	0.0564	0.4054	0.0968	0.0023
WY051608	5/16/08 8:00 AM	5/19/08 8:00 AM	72.00	42.66	0.1175	0.0353	0.1021	0.4487	0.1088	0.0051
WY051908	5/19/08 8:00 AM	5/23/08 8:00 AM	96.00	51.87	0.0896	b.d	0.0852	0.2505	0.0692	0.0029
WY052308	5/23/08 8:00 AM	5/26/08 8:00 AM	72.00	40.89	0.0468	b.d	0.1536	0.2766	0.0981	0.0023
WY052608	5/26/08 8:00 AM	5/30/08 8:00 AM	96.00	54.57	0.0418	b.d	0.1544	0.4929	0.1570	0.0027
WY053008	5/30/08 8:00 AM	6/2/08 8:00 AM	72.00	41.71	0.0860	0.0204	0.1361	0.5222	0.1587	b.d
WY060208	6/2/08 8:00 AM	6/6/08 8:00 AM	96.00	54.42	0.0418	0.0111	0.0833	0.3878	0.0973	b.d
WY060608	6/6/08 8:00 AM	6/9/08 8:00 AM	72.00	37.91	0.1422	0.0423	0.1462	0.3850	0.1973	0.0030
WY060908	6/9/08 8:00 AM	6/13/08 8:00 AM	96.00	55.22	0.1453	0.0246	0.0978	0.2261	0.0947	0.0013
WY061308	6/13/08 8:00 AM	6/16/08 8:00 AM	72.00	41.41	0.2654	0.1040	0.1691	0.6255	0.2142	0.0218
WY061608	6/16/08 8:00 AM	6/20/08 8:00 AM	96.00	57.07	0.2675	0.1433	0.1480	0.5228	0.2033	0.0179
WY062008	6/20/08 8:00 AM	6/23/08 8:00 AM	72.00	42.22	0.2796	0.1957	0.1381	0.6324	0.1996	0.0060
WY062308	6/23/08 8:00 AM	6/27/08 8:00 AM	96.00	56.52	0.3776	0.1665	0.2583	1.0465	0.3929	0.0410
WY062708	6/27/08 8:00 AM	6/30/08 8:00 AM	72.00	42.33	0.3518	0.1620	0.1298	0.3915	0.1275	0.0044
WY063008	6/30/08 8:00 AM	7/4/08 7:55 AM	96.00	56.83	0.4511	0.2808	0.1838	0.7611	0.2921	0.0189
WY070408	7/4/08 8:00 AM	7/7/08 8:00 AM	71.60	43.06	0.4470	0.2363	0.1947	0.7231	0.2780	0.0362
WY070708	7/7/08 8:00 AM	7/11/08 8:00 AM	96.00	50.25	0.2216	0.2476	0.2001	0.5543	0.2413	0.0264
WY071108	7/11/08 8:00 AM	7/14/08 8:00 AM	72.00	45.00	0.1788	0.2467	0.0487	0.2309	0.0971	0.0118
WY071408	7/14/08 8:00 AM	7/18/08 8:00 AM	96.00	49.74	0.7470	0.3868	0.2252	1.0715	0.5789	0.0724
WY071808	7/18/08 8:00 AM	7/21/08 8:00 AM	69.70	54.47	0.4835	0.3367	0.1866	0.8092	0.3701	0.0393
WY072108	7/21/08 8:00 AM	7/25/08 8:00 AM	94.20	42.44	1.2242	0.5686	0.2679	1.5674	0.6115	0.0369
WY072508	7/25/08 8:00 AM	7/28/08 8:00 AM	72.00	46.31	0.6634	0.0752	0.0762	1.1130	0.3869	0.0319
WY072808	7/28/08 8:00 AM	8/1/08 8:00 AM	96.00	59.86	0.8146	0.0694	0.2485	0.6755	0.4068	0.0871
WY080108	8/1/08 8:00 AM	8/4/08 8:00 AM	72.00	42.85	0.0432	0.3966	0.3766	0.8466	1.5876	0.0678
WY080408	8/4/08 8:00 AM	8/8/08 8:00 AM	96.00	58.36	1.5572	0.3999	0.5115	0.9635	0.4626	0.0442
WY080808	8/8/08 8:00 AM	8/11/08 8:00 AM	67.40	39.82	0.9165	0.2447	0.1910	0.7588	0.2328	0.0187

WY081108	8/11/08 8:00 AM	8/15/08 8:00 AM	95.70	54.93	0.5215	0.0117	0.0181	0.8240	0.3148	0.0172
WY081508	8/15/08 8:00 AM	8/18/08 8:00 AM	72.00	45.06	0.2821	0.1932	0.1108	1.0983	0.3982	0.0035
WY081808	8/18/08 8:00 AM	8/22/08 8:00 AM	96.00	58.47	0.4756	0.3318	0.1509	1.1567	0.4742	0.0448
WY082208	8/22/08 8:00 AM	8/25/08 8:00 AM	72.00	46.24	0.3369	0.3006	0.1447	0.9066	0.3941	0.0237
WY082508	8/25/08 8:00 AM	8/29/08 8:00 AM	96.00	59.20	0.4710	0.2315	0.2078	0.8410	0.3854	0.0537
WY082908	8/29/08 8:00 AM	9/1/08 8:00 AM	72.00	44.22	0.4932	0.1640	0.1740	0.8065	0.3942	0.0111
WY090108	9/1/08 8:00 AM	9/5/08 8:00 AM	96.00	55.15	0.5212	0.2563	0.0847	0.2646	0.1398	0.0239
WY090508	9/5/08 8:00 AM	9/8/08 7:52 AM	71.70	42.63	0.3734	0.1660	0.0609	0.4095	0.1704	0.0055
WY090808	9/8/08 8:00 AM	9/12/08 7:50 AM	96.00	56.31	0.5582	0.1854	0.1462	0.7922	0.3365	0.0100
WY091208	9/12/08 8:00 AM	9/15/08 8:00 AM	72.00	44.13	0.2935	0.1646	0.1303	0.6086	0.2316	0.0115
WY091508	9/15/08 8:00 AM	9/19/08 8:00 AM	96.00	60.74	0.2820	0.3418	0.1517	0.9000	0.3574	0.0222
WY091908	9/19/08 8:00 AM	9/22/08 8:00 AM	71.90	43.62	0.3430	0.2066	0.1499	1.1913	0.3898	0.0133
WY092208	9/22/08 8:00 AM	9/26/08 8:00 AM	96.00	56.23	0.1918	0.1675	0.1451	0.8603	0.3337	0.0101
WY092608	9/26/08 8:00 AM	9/29/08 8:00 AM	71.90	43.90	0.2654	0.2453	0.1361	0.6683	0.3259	0.0211
WY092908	9/29/08 8:00 AM	10/3/08 8:00 AM	96.00	58.49	0.2532	0.4161	0.1663	0.8692	0.3731	0.0363
WY100308	10/3/08 8:00 AM	10/6/08 7:50 AM	72.00	40.52	0.2822	0.0811	0.1726	0.6900	0.2919	0.0269
WY100608	10/6/08 8:00 AM	10/10/08 7:59 AM	95.90	53.72	0.2602	0.1842	0.1370	0.5127	0.2403	0.0093
WY101008	10/10/08 8:00 AM	10/13/08 8:00 AM	71.80	40.46	0.0184	0.0423	0.1080	0.4267	0.1121	0.0026
WY101308	10/13/08 8:00 AM	10/17/08 8:00 AM	96.00	52.66	0.0837	0.0892	0.2432	0.6630	0.3289	0.0068
WY101708	10/17/08 8:00 AM	10/20/08 8:00 AM	72.00	39.55	0.3039	0.3595	0.3612	1.0757	0.5246	0.0309
WY102008	10/20/08 8:00 AM	10/24/08 8:00 AM	96.00	53.99	0.0540	0.0770	0.1022	0.3963	0.1675	0.0080
WY102408	10/24/08 8:00 AM	10/27/08 8:00 AM	72.00	40.93	0.0075	b.d	b.d	b.d	b.d	b.d
WY102708	10/27/08 8:00 AM	10/31/08 8:00 AM	95.90	54.90	0.1154	0.3833	0.1901	0.5337	0.2610	0.0213
WY103108	10/31/08 8:00 AM	11/3/08 8:00 AM	72.00	42.19	0.1554	0.2294	0.1951	0.6186	0.2500	0.0103
WY110308	11/3/08 8:00 AM	11/7/08 8:00 AM	96.00	51.76	0.1053	0.0292	0.1090	0.3879	0.1439	0.0039
WY110708	11/7/08 8:00 AM	11/10/08 8:00 AM	71.90	40.29	0.0510	0.0489	0.1857	0.2582	0.1614	0.0018
WY111008	11/10/08 8:00 AM	11/14/08 8:00 AM	96.00	53.84	0.0563	0.0357	0.0800	0.2199	0.0758	0.0013
WY111408	11/14/08 8:00 AM	11/17/08 8:00 AM	72.00	39.61	0.0144	0.0666	0.0731	0.2307	0.0993	0.0061
WY111708	11/17/08 8:00 AM	11/21/08 8:00 AM	96.00	55.23	0.0616	0.1754	0.1943	0.2867	0.1782	0.0083
WY112108	11/21/08 8:00 AM	11/24/08 8:00 AM	72.00	39.68	b.d	0.2037	0.2355	0.5320	0.2505	0.0126
WY112408	11/24/08 8:00 AM	11/28/08 8:00 AM	96.00	48.09	0.0476	0.1877	0.3354	0.4626	0.1998	0.0136
WY112808	11/28/08 8:00 AM	12/1/08 8:00 AM	144.00	39.17	0.0556	b.d	b.d	b.d	0.0085	b.d
WY120108	12/1/08 8:00 AM	12/5/08 8:00 AM	96.00	53.64	0.0116	0.0629	0.1100	0.2600	0.1515	0.0026
WY120508	12/5/08 8:00 AM	12/8/08 8:00 AM	72.00	38.73	0.0102	0.1391	0.1395	0.2238	0.1340	0.0045

WY120808	12/8/08 8:00 AM	12/12/08 8:00 AM	96.00	53.21	0.0011	0.0577	0.1522	0.1860	0.0875	0.0075
WY121208	12/12/08 8:00 AM	12/15/08 8:00 AM	70.70	38.84	0.0053	0.0888	0.2508	0.2354	0.1676	0.0057
WY121508	12/15/08 8:00 AM	12/19/08 8:00 AM	96.00	51.96	b.d	0.1014	0.6426	0.3236	0.2942	0.0069
WY121908	12/19/08 8:00 AM	12/22/08 8:00 AM	72.00	37.46	0.0552	0.1818	0.6073	0.7801	0.4032	0.0087
WY122208	12/22/08 8:00 AM	12/26/08 8:00 AM	96.00	48.20	b.d	0.1607	b.d	b.d	b.d	b.d
WY122608	12/26/08 8:00 AM	12/29/08 8:00 AM	72.00	37.46	0.0552	0.1818	0.6073	0.7801	0.4032	0.0087
WY122908	12/29/08 8:00 AM	1/2/09 8:00 AM	96.00	48.20	b.d	0.1607	b.d	b.d	b.d	b.d
WY010209	1/2/09 7:00 AM	1/5/09 7:00 AM	70.30	37.02	0.0171	0.1212	0.2721	0.1750	0.0879	0.0194
WY010509	1/5/09 7:00 AM	1/9/09 7:00 AM	96.00	52.28	0.0142	0.1139	0.3346	0.1690	0.0987	0.0318
WY010909	1/9/09 7:00 AM	1/12/09 7:00 AM	71.90	38.50	0.0169	0.0864	0.2430	0.2037	0.0945	0.0322
WY011209	1/12/09 7:05 AM	1/16/09 6:50 AM	94.70	52.72	0.0182	0.0890	0.1222	0.1680	0.0634	0.0229
WY011609	1/16/09 7:00 AM	1/19/09 7:00 AM	72.00	40.42	0.0120	0.2943	3.1109	0.2362	0.8268	0.0425
WY011909	1/19/09 7:00 AM	1/23/09 7:00 AM	96.00	55.05	0.0777	0.4646	0.7157	0.0971	0.2094	0.0258
WY012309	1/23/09 7:00 AM	1/26/09 7:00 AM	71.90	39.54	0.0448	0.1935	0.7250	0.5892	0.3032	0.0326
WY012609	1/26/09 7:00 AM	1/30/09 6:50 AM	96.00	50.69	0.0131	0.1183	0.5908	0.8333	0.3119	0.0282
WY013009	1/30/09 6:50 AM	2/2/09 7:00 AM	72.00	39.65	0.0130	0.1833	0.7678	0.3430	0.2041	0.0321
WY020209	2/2/09 7:00 AM	2/6/09 6:50 AM	96.00	52.28	0.0318	0.1837	1.2462	0.3547	0.4318	0.0333
WY020609	2/6/09 7:00 AM	2/9/09 6:55 AM	72.00	40.31	0.0108	0.1935	0.9771	0.4109	0.3896	0.0284
WY020909	2/9/09 7:00 AM	2/13/09 6:50 AM	96.00	53.24	0.0116	0.1586	0.5204	0.3121	0.2260	0.0187
WY021309	2/13/09 7:00 AM	2/16/09 7:00 AM	72.00	41.74	0.0474	0.2646	0.9013	0.3760	0.3053	0.0235
WY021609	2/16/09 7:00 AM	2/20/09 6:50 AM	96.00	55.15	0.0467	0.2041	0.7610	0.3280	0.2657	0.0183
WY022009	2/20/09 7:00 AM	2/23/09 7:00 AM	72.00	42.77	0.0108	0.4506	1.4745	0.3984	0.5032	0.0243
WY022309	2/23/09 7:00 AM	2/27/09 6:55 AM	96.00	57.84	0.0759	0.1717	0.7414	0.4116	0.2703	0.0154
WY022709	2/27/09 6:55 AM	3/2/09 7:00 AM	69.40	42.41	0.0083	0.3020	0.4667	0.2099	0.1809	0.0175
WY030209	3/2/09 7:00 AM	3/6/09 6:55 AM	96.00	62.24	0.1544	0.2298	0.5101	0.6522	0.2169	0.0235
WY030609	3/6/09 7:05 AM	3/9/09 7:00 AM	71.90	42.22	0.0118	0.0843	0.0989	0.2661	0.1403	0.0135
WY030909	3/9/09 7:00 AM	3/13/09 7:00 AM	96.00	58.34	0.0588	0.0971	0.3699	0.2861	0.1625	0.0121
WY031309	3/13/09 8:00 AM	3/16/09 8:00 AM	72.00	45.48	0.0761	0.1802	0.4352	0.3922	0.2002	0.0082
WY031609	3/16/09 8:00 AM	3/20/09 7:59 AM	96.00	60.85	0.3559	0.0406	0.1614	0.6302	0.1318	0.0120
WY032009	3/20/09 8:00 AM	3/23/09 8:00 AM	144.00	91.77	0.4079	0.0924	0.2967	0.6639	0.2094	0.0103
WY032309	3/23/09 8:00 AM	3/27/09 8:00 AM	96.00	57.51	0.1244	0.0035	0.1063	0.5687	0.1482	0.0047
WY032709	3/27/09 8:00 AM	3/30/09 7:50 AM	71.83	0.00	0.4079	0.0924	0.2967	0.6639	0.2094	0.0103
WY033009	3/30/09 8:00 AM	4/3/09 7:50 AM	95.90	59.42	0.1604	0.0054	0.2118	0.7818	0.2381	0.0059
WY040309	4/3/09 8:00 AM	4/6/09 8:00 AM	72.00	46.47	0.1842	0.0217	0.1818	0.8201	0.2226	0.0044

WY040609	4/6/09 8:00 AM	4/10/09 7:45 AM	96.00	66.70	0.2765	0.1189	0.1837	0.4316	0.1286	0.0053
WY041009	4/10/09 8:00 AM	4/13/09 8:00 AM	134.90	93.12	0.3218	0.0876	0.1918	0.7134	0.2280	0.0069
WY041309	4/13/09 8:00 AM	4/17/09 8:00 AM	56.50	39.37	0.3055	0.3004	0.1411	0.7841	0.1940	0.0087
WY041709	4/17/09 8:00 AM	4/20/09 8:00 AM	72.00	0.00	0.3218	0.0876	0.1918	0.7134	0.2280	0.0069
WY042009	4/20/09 8:00 AM	4/24/09 7:55 AM	96.00	72.35	0.4129	0.3401	0.1034	0.5496	0.1547	0.0092
WY042409	4/24/09 8:00 AM	4/27/09 8:00 AM	72.00	48.69	0.0544	0.1687	0.1290	0.9197	0.2826	0.0097
WY042709	4/27/09 8:00 AM	5/1/09 7:55 AM	96.00	66.76	0.2638	0.0358	0.2225	1.1154	0.3279	0.0082
WY050109	5/1/09 8:00 AM	5/4/09 8:00 AM	60.10	45.57	0.1072	0.0681	0.1185	0.4891	0.1312	0.0150
WY050409	5/4/09 8:00 AM	5/8/09 7:50 AM	96.00	69.64	0.2076	0.0551	0.0818	0.3888	0.0897	0.0111
WY050809	5/8/09 8:00 AM	5/11/09 8:00 AM	71.90	51.40	0.0607	0.1134	0.1603	0.5281	0.1856	0.0144
WY051109	5/11/09 8:00 AM	5/15/09 8:00 AM	96.00	76.76	0.1302	0.0700	0.1271	0.6791	0.1875	0.0135
WY051509	5/15/09 8:00 AM	5/18/09 8:00 AM	72.00	51.76	0.1772	0.1619	0.1850	1.3463	0.3730	0.0252
WY051809	5/18/09 8:00 AM	5/22/09 8:00 AM	96.00	74.93	0.2777	0.1901	0.1740	0.7930	0.2423	0.0189
WY052209	5/22/09 8:00 AM	5/25/09 8:00 AM	72.00	57.12	0.2896	0.1290	0.1176	0.7890	0.2069	0.0154
WY052509	5/25/09 8:00 AM	5/29/09 7:57 AM	95.90	73.06	0.4723	0.1726	0.1106	0.5478	0.1458	0.0115
WY052909	5/29/09 8:25 AM	6/1/09 7:55 AM	71.30	55.89	0.6021	0.1943	0.1055	0.4100	0.0566	b.d
WY060109	6/1/09 8:00 AM	6/5/09 7:55 AM	95.90	72.28	0.2507	0.1288	0.1104	0.4900	0.0807	b.d
WY060509	6/5/09 8:00 AM	6/8/09 7:55 AM	69.90	51.41	0.2829	0.0836	0.0522	0.2912	0.1459	b.d
WY060809	6/8/09 8:00 AM	6/12/09 7:55 AM	96.00	70.96	0.1826	0.0676	0.0682	0.2753	0.1583	b.d
WY061209	6/12/09 8:00 AM	6/15/09 7:55 AM	80.60	51.80	0.1338	0.0864	0.0660	0.3568	0.1645	b.d
WY061509	6/15/09 8:00 AM	6/19/09 6:40 AM	94.40	89.48	0.2040	0.0435	0.0457	0.2186	0.1097	b.d
WY061909	6/19/09 8:00 AM	6/22/09 8:00 AM	72.00	55.24	0.2968	0.1097	0.0995	0.7061	0.3393	0.0209
WY062209	6/22/09 8:00 AM	6/26/09 8:00 AM	65.20	70.69	0.6491	0.2133	0.1071	0.7370	0.3174	0.0213
WY062609	6/26/09 8:00 AM	6/29/09 7:38 AM	70.20	55.48	0.2976	0.1346	0.0543	0.7217	0.2993	0.0195
WY062909	6/29/09 8:00 AM	7/3/09 7:55 AM	96.20	69.11	0.5967	0.2807	0.0701	0.6795	0.3178	0.0168
WY070309	7/3/09 8:10 AM	7/6/09 8:00 AM	71.70	54.03	0.4729	0.1693	0.0623	0.4726	0.2425	0.0229
WY070609	7/6/09 8:00 AM	7/10/09 8:00 AM	96.00	75.57	0.5589	0.2036	0.0759	0.6322	0.3050	0.0196
WY071009	7/10/09 8:00 AM	7/13/09 7:43 AM	71.60	53.49	0.4680	0.3328	0.1425	0.4881	0.2317	0.0219
WY071309	7/13/09 8:00 AM	7/17/09 7:48 AM	34.60	71.63	0.3444	0.1697	0.0475	0.4918	0.2384	0.0158
WY071709	7/17/09 8:00 AM	7/20/09 7:51 AM	71.90	58.33	0.3995	0.3668	0.0517	0.4489	0.2385	0.0216
WY072009	7/20/09 8:00 AM	7/24/09 7:32 AM	95.60	72.86	0.5367	0.2875	0.0404	0.3662	0.2062	0.0167
WY072409	7/24/09 8:00 AM	7/27/09 8:00 AM	73.00	55.84	0.5873	0.2901	0.0529	0.3429	0.1839	0.0196
WY072709	7/27/09 8:50 AM	7/31/09 8:00 AM	92.90	73.23	0.4647	0.1680	0.0649	0.4600	0.2578	0.0156
WY073109	7/31/09 8:25 AM	8/3/09 7:43 AM	69.90	50.22	1.1946	0.4203	0.0935	0.7244	0.3755	0.0262

WY080309	8/3/09 8:00 AM	8/7/09 8:00 AM	96.20	72.31	0.3651	0.1537	0.0317	0.2373	0.1442	0.0173
WY080709	8/7/09 8:11 AM	8/10/09 7:55 AM	71.80	49.12	0.4005	0.1667	0.0733	0.2940	0.1942	0.0262
WY081009	8/10/09 8:00 AM	8/14/09 7:21 AM	95.30	72.36	0.6381	0.3594	0.0739	0.5123	0.2591	0.0239
WY081409	8/14/09 7:43 AM	8/17/09 8:14 AM	72.50	48.38	0.3553	0.1065	0.0448	0.3053	0.1275	0.0244
WY081709	8/17/09 8:17 AM	8/21/09 8:57 AM	96.60	69.64	0.2704	0.1791	0.0440	0.3454	0.1864	0.0184
WY082109	8/21/09 9:07 AM	8/24/09 6:33 AM	69.40	53.59	0.4575	0.2990	0.0615	0.4035	0.2027	0.0259
WY082409	8/24/09 6:47 AM	8/28/09 8:36 AM	97.80	72.34	0.3370	0.2208	0.0601	0.3728	0.2063	0.0167
WY082809	8/28/09 8:52 AM	8/31/09 8:07 AM	71.20	55.29	0.2920	0.1658	0.0663	0.6390	0.2963	0.0290
WY083109	8/31/09 8:13 AM	9/4/09 8:12 AM	95.90	71.99	0.4109	0.2528	0.0607	0.3882	0.2035	0.0343
WY090409	9/4/09 8:21 AM	9/7/09 9:33 AM	73.20	53.27	0.6158	0.2808	0.1517	0.8483	0.3976	0.0513
WY090709	9/7/09 9:34 AM	9/11/09 8:42 AM	95.00	67.74	0.3851	0.2005	0.0569	0.3865	0.1742	0.0183
WY091109	9/11/09 8:50 AM	9/14/09 8:27 AM	71.60	50.60	0.3185	0.2399	0.0628	0.4879	0.1894	0.0226
WY091409	9/14/09 8:31 AM	9/18/09 8:34 AM	95.80	69.82	0.5144	0.1785	0.0685	0.7486	0.3461	0.0177
WY091809	9/18/09 8:41 AM	9/21/09 8:38 AM	71.90	53.14	0.2913	0.2312	0.0644	0.5479	0.1963	0.0106
WY092109	9/21/09 8:42 AM	9/28/09 11:07 AM	170.40	113.53	0.2128	0.1532	0.0825	0.4022	0.1685	0.0240
WY092509										
WY092809	9/28/09 11:16 AM	10/2/09 9:00 AM	93.70	61.19	0.2689	0.1907	0.1857	0.4740	0.2234	0.0277
WY100209	10/2/09 9:07 AM	10/5/09 8:06 AM	70.90	44.80	0.1413	0.0674	0.1116	0.3339	0.1392	0.0107
WY100509	10/5/09 8:11 AM	10/9/09 7:44 AM	95.50	60.65	0.0463	0.0675	0.1850	0.3308	0.1891	0.0094
WY100909	10/9/09 7:58 AM	10/12/09 7:51 AM	71.20	43.93	b.d	0.0738	0.1757	0.7715	0.2958	0.0136
WY101209	10/12/09 8:02 AM	10/16/09 7:43 AM	95.60	65.96	0.1637	0.0702	0.1115	0.3367	0.1547	0.0116
WY101609	10/16/09 7:52 AM	10/19/09 7:50 AM	71.90	49.07	0.2013	0.1205	0.0949	0.2099	0.1103	0.0158
WY101909	10/19/09 7:55 AM	10/23/09 7:39 AM	95.70	58.36	0.2105	0.0523	0.0796	0.2694	0.1441	0.0104
WY102309	10/23/09 7:55 AM	10/26/09 7:55 AM	72.00	42.72	0.0965	0.0891	0.1077	0.4088	0.1791	0.0152
WY102609	10/26/09 7:55 AM	10/30/09 7:24 AM	95.30	53.16	0.0178	0.0649	0.0757	0.2743	0.0893	0.0107
WY103009	10/30/09 7:30 AM	11/2/09 8:39 AM	73.10	45.72	0.0430	0.0780	0.0716	0.1998	0.0540	0.0116
WY110209	11/2/09 7:45 AM	11/6/09 7:53 AM	96.13	61.07	0.0858	0.2229	0.1349	0.7134	0.2663	0.0194
WY110609	11/6/09 8:02 AM	11/9/09 8:31 AM	72.40	43.80	0.0187	0.0969	0.0846	0.2598	0.0932	0.0158
WY110909	11/9/09 8:33 AM	11/13/09 8:03 AM	68.30	58.63	0.0678	0.1505	0.1704	0.5991	0.2484	0.0166
WY111309	11/13/09 8:15 AM	11/16/09 8:27 AM	72.20	35.66	0.0624	0.0581	0.1404	0.4237	0.1996	0.0046
WY111609	11/16/09 8:29 AM	11/20/09 8:01 AM	95.50	54.74	0.1120	0.2358	0.1929	0.3596	0.1897	0.0058
WY112009	11/20/09 8:09 AM	11/23/09 7:30 AM	71.30	39.31	0.0441	0.2361	0.0982	0.2001	0.0581	0.0016
WY112309	11/23/09 7:31 AM	11/30/09 8:08 AM	168.50	93.33	0.0521	0.1142	0.0867	0.1778	0.0980	0.0023
WY112709										

WY113009	11/30/09 8:17 AM	12/4/09 7:46 AM	95.40	48.50	b.d	0.1519	0.1402	0.3282	0.1581	0.0043
WY120409	12/4/09 7:50 AM	12/7/09 7:42 AM	71.80	35.04	0.0219	0.1496	0.1476	0.4506	0.1364	0.0061
WY120709	12/7/09 8:48 AM	12/11/09 9:31 AM	97.70	43.64	0.0183	0.1461	0.5690	0.7529	0.3954	0.0098
WY121109	12/11/09 9:53 AM	12/14/09 8:08 AM	70.20	36.31	0.1150	0.1888	1.0045	0.4803	0.3789	0.0054
WY121409	12/14/09 8:10 AM	12/18/09 7:47 AM	95.00	48.72	0.0159	0.3719	1.6536	0.1337	0.6170	0.0069
WY121809	12/18/09 8:02 AM	12/21/09 7:58 AM	71.90	38.42	0.0503	0.1311	0.3633	0.1561	0.1211	0.0015
WY122109	12/21/09 8:04 AM	12/28/09 11:56 AM	171.80	83.34	0.0227	0.1498	0.9955	0.3223	0.4336	0.0035
WY122509										
WY122809	12/28/09 12:01 PM	1/2/10 7:32 AM	114.50	56.29	0.0100	0.2240	1.1919	0.2903	0.5157	0.0080
WY010110	1/2/10 7:00 AM	1/5/10 7:52 AM	72.87	36.57	0.0117	0.1654	0.5528	0.0963	0.2621	0.0030
WY010410	1/5/10 8:02 AM	1/8/10 8:47 AM	72.80	34.90	b.d	0.1371	0.4777	0.3905	0.2921	0.0033
WY010810	1/8/10 9:25 AM	1/11/10 7:47 AM	70.40	36.45	0.0095	0.6060	1.1565	0.1868	0.4244	0.0049
WY011110	1/11/10 7:50 AM	1/15/10 8:08 AM	96.20	50.11	0.0086	0.2879	2.0591	0.2606	0.6685	0.0053
WY011510	1/15/10 8:19 AM	1/18/10 8:21 AM	71.90	38.80	0.0047	0.3159	0.8927	0.1902	0.3650	0.0043
WY011810	1/18/10 8:27 AM	1/22/10 8:00 AM	95.50	50.37	0.0084	0.1128	0.3777	0.4794	0.2375	0.0016
WY012210	1/22/10 8:05 AM	1/25/10 7:36 AM	71.50	36.74	0.0669	0.0532	0.1175	0.0939	0.1254	0.0020
WY012510	1/25/10 7:40 AM	1/30/10 10:58 AM	75.00	39.65	0.0178	0.3303	1.1944	0.2099	0.5637	0.0102
WY012910	1/30/10 11:07 AM	2/2/10 7:58 AM	68.80	35.25	0.0060	0.2518	0.8677	0.5966	0.4699	0.0100
WY020110	2/2/10 8:03 AM	2/5/10 7:26 AM	71.30	37.15	0.0106	0.2039	0.5527	0.1824	0.2940	0.0103
WY020510	2/5/10 7:37 AM	2/8/10 7:45 AM	72.20	39.42	0.0045	0.1527	0.4349	0.1809	0.2540	0.0052
WY020810	2/8/10 7:50 AM	2/12/10 7:17 AM	95.40	47.37	0.0032	0.0970	0.4863	0.6575	0.3810	0.0194
WY021210	2/12/10 8:50 AM	2/15/10 7:34 AM	70.70	36.93	0.0178	0.0585	0.1443	0.1437	0.1172	0.0037
WY021510	2/15/10 7:43 AM	2/19/10 8:00 AM	96.30	51.74	0.0616	0.0768	0.4557	0.2185	0.3893	0.0065
WY021910	2/19/10 8:03 AM	2/22/10 8:27 AM	72.22	35.37	0.0089	0.0732	0.2397	0.8589	0.3677	0.0092
WY022210	2/22/10 8:30 AM	2/26/10 8:18 AM	95.70	49.35	0.0230	0.0909	0.3570	0.3300	0.2339	0.0077
WY022610	2/26/10 8:33 AM	3/1/10 7:41 AM	71.10	41.13	0.0508	0.2175	0.4915	0.1953	0.2762	0.0067
WY030110	3/1/10 7:46 AM	3/5/10 8:59 AM	71.10	55.27	0.1387	0.1696	0.5459	0.5935	0.4424	0.0111
WY030510	3/5/10 9:02 AM	3/8/10 7:49 AM	70.60	41.27	0.0945	0.0692	0.3518	0.9506	0.5401	0.0162
WY030810	3/8/10 7:50 AM	3/12/10 8:08 AM	96.20	52.46	0.0744	0.0473	0.2220	0.5132	0.3012	0.0102
WY031210	3/12/10 8:18 AM	3/16/10 8:43 AM	96.30	57.10	0.1537	0.0586	0.1577	0.5439	0.2224	0.0134
WY031510	3/16/10 8:44 AM	3/19/10 10:06 AM	73.20	43.40	0.0639	0.1153	0.1208	0.2841	0.1303	0.0050
WY031910	3/19/10 10:11 AM	3/22/10 9:44 AM	71.50	40.20	0.0539	0.0642	0.1741	0.3846	0.2059	0.0078
WY032210	3/22/10 9:48 AM	3/26/10 8:06 AM	93.30	52.85	0.0945	0.0544	0.2509	0.7053	0.3523	0.0116
WY032610	3/26/10 8:47 AM	3/29/10 8:11 AM	71.40	62.19	0.0143	0.0260	0.0385	0.1068	0.0490	0.0035

WY032910	3/29/10 7:20 AM	4/2/10 7:15 AM	95.90	53.62	0.1362	0.0501	0.1572	0.3350	0.1486	0.0130
WY040210	4/2/10 7:26 AM	4/6/10 8:06 AM	95.60	53.57	0.0854	0.0270	0.2710	0.7681	0.2837	0.0172
WY040510	4/6/10 8:07 AM	4/9/10 8:06 AM	71.90	39.24	0.0252	0.0484	0.1739	0.2271	0.1389	0.0050
WY040910 WY041210	4/9/10 8:16 AM	4/12/10 8:09 AM	71.80	42.92	0.0757	0.0845	0.2130	0.8780	0.3492	0.0307
WY041610	4/16/10 8:12 AM	4/19/10 7:55 AM	70.70	45.34	0.3021	0.1830	0.2417	0.7548	0.2757	0.0141
WY041910	4/19/10 8:00 AM	4/23/10 8:05 AM	95.20	54.54	0.1944	0.1574	0.1978	0.5928	0.2244	0.0110
WY042310	4/23/10 8:12 AM	4/26/10 7:38 AM	71.40	41.73	0.0209	0.0645	0.1063	0.3515	0.1952	0.0083
WY042610	4/26/10 7:40 AM	4/30/10 8:09 AM	95.00	57.62	0.1258	0.0002	0.1603	0.3092	0.1122	0.0095
WY043010	4/30/10 8:19 AM	5/3/10 8:13 AM	71.90	47.43	0.0649	0.0405	0.1275	0.2005	0.1278	0.0029
WY050310	5/3/10 8:18 AM	5/8/10 8:28 AM	121.10	78.00	0.0563	0.0642	0.1735	0.4988	0.2342	0.0105
WY050710 WY051010	5/8/10 8:00 AM	5/13/10 2:11 PM	123.50	84.76	0.0830	0.0769	0.0768	0.6089	0.2438	0.0087
WY051410	5/14/10 8:57 AM	5/17/10 7:55 AM	76.10	56.39	0.2230	0.1505	0.1061	0.6493	0.2684	0.0084
WY051710	5/17/10 8:00 AM	5/21/10 2:25 PM	96.00	66.17	0.1974	0.1805	0.0725	0.5229	0.2281	0.0145
WY052110	5/21/10 2:16 PM	5/24/10 8:00 AM	69.30	47.24	0.1321	0.0409	0.1240	0.4592	0.1567	0.0092
WY052410	5/24/10 8:00 AM	5/28/10 10:37 AM	96.00	67.05	0.1932	0.2073	0.0931	0.5351	0.2024	0.0090
WY052810 WY053110	5/28/10 10:48 AM	5/31/10 8:00 AM	69.10	46.66	0.2341	0.0661	0.0515	0.1172	0.0925	0.0035
WY060410	6/4/10 7:22 AM	6/7/10 6:45 AM	71.30	49.05	0.1265	0.1068	0.0223	0.1181	0.0791	0.0018
WY060710	6/7/10 6:50 AM	6/11/10 7:31 AM	96.30	64.87	0.2251	0.1018	0.0467	0.3039	0.1546	0.0054
WY061110	6/11/10 7:45 AM	6/14/10 6:42 AM	70.90	46.54	0.1408	0.0337	0.0279	0.0813	0.0684	0.0012
WY061410	6/14/10 6:46 AM	6/18/10 7:01 AM	96.20	58.01	0.3238	0.1411	0.0468	0.2912	0.2093	0.0054
WY061810	6/18/10 7:12 AM	6/21/10 7:11 AM	71.90	51.87	0.1798	0.2057	0.1185	0.3296	0.1810	0.0120
WY062110	6/21/10 7:16 AM	6/25/10 6:35 AM	95.30	65.42	0.2825	0.3895	0.1014	0.4729	0.2213	0.0140
WY062510	6/25/10 6:43 AM	6/28/10 7:09 AM	72.40	51.28	0.3623	0.2847	0.0559	0.3820	0.2615	0.0108
WY062810	6/28/10 7:15 AM	7/2/10 7:25 AM	96.10	68.67	0.4768	0.3538	0.0501	0.4597	0.2184	0.0145
WY070210	7/2/10 7:37 AM	7/6/10 8:04 AM	96.40	64.98	0.2669	0.1772	0.0213	0.2002	0.1682	0.0118
WY070510	7/6/10 8:09 AM	7/9/10 7:26 AM	71.30	46.53	0.2499	0.1710	0.0695	0.4048	0.1719	0.0063
WY070910	7/9/10 7:33 AM	7/12/10 7:05 AM	71.50	48.22	0.4649	0.2200	0.0392	0.2279	0.1900	0.0130
WY071210	7/12/10 7:07 AM	7/16/10 10:14 AM	99.00	65.40	0.3468	0.3025	0.0332	0.2846	0.1310	0.0189
WY071610	7/16/10 10:22 AM	7/19/10 6:45 AM	68.40	49.97	0.5213	0.3107	0.0399	0.4016	0.2233	0.0111
WY071910 WY072310	7/19/10 6:49 AM	7/22/10 6:41 PM	83.10	57.34	0.5388	0.2678	0.0611	0.3343	0.1909	0.0088

WY072610	7/26/10 7:08 AM	7/30/10 7:28 AM	96.30	72.84	0.6556	0.3481	0.0459	0.5092	0.2259	0.0304
WY073010	7/30/10 7:42 AM	8/2/10 7:14 AM	66.10	48.21	0.5540	0.2336	0.0876	0.5407	0.2989	0.0535
WY080210										
WY080610	8/5/10 3:09 PM	8/9/10 8:13 AM	89.00	62.10	0.3849	0.2448	0.0671	0.3925	0.2266	0.0154
WY080910	8/9/10 8:23 AM	8/13/10 7:06 AM	94.80	64.80	0.1577	0.2672	0.0550	0.4550	0.1966	0.0121
WY081310	8/13/10 7:19 AM	8/17/10 10:55 AM	96.60	63.69	0.2802	0.2812	0.0454	0.2534	0.1108	0.0056
WY081610	8/17/10 10:59 AM	8/20/10 7:37 AM	68.60	46.02	0.1858	0.2522	0.0644	0.4123	0.1600	0.0120
WY082010	8/20/10 7:43 AM	8/23/10 7:29 AM	71.70	52.84	0.2969	0.3570	0.0962	0.4653	0.1968	0.0188
WY082310	8/23/10 7:29 AM	8/27/10 7:22 AM	95.80	66.50	0.2356	0.2701	0.0709	0.3534	0.1450	0.0403
WY082710	8/27/10 7:30 AM	8/30/10 7:26 AM	70.80	46.96	0.3637	0.1849	0.1539	0.5071	0.1742	0.0177
WY083010	8/30/10 7:32 AM	9/3/10 10:03 AM	98.50	58.41	0.2113	0.1054	0.0542	0.2405	0.1174	0.0060
WY090310	9/3/10 10:15 AM	9/6/10 8:00 AM	69.70	45.92	0.1961	0.2913	0.0592	0.4013	0.1478	0.0105
WY090610	9/6/10 8:00 AM	9/10/10 4:19 PM	92.30	57.89	0.2306	0.1391	0.0584	0.5037	0.1764	0.0084
WY091010	9/10/10 4:30 AM	9/13/10 11:01 AM	78.40	45.59	0.1458	0.1563	0.0463	0.1858	0.0959	0.0025
WY091310	9/13/10 11:05 AM	9/17/10 7:20 AM	92.20	59.66	0.0906	0.3446	0.0996	0.5355	0.2046	0.0709
WY091710	9/17/10 7:32 AM	9/20/10 10:04 AM	74.50	51.53	0.1342	0.4325	0.0745	0.4421	0.1557	0.0258
WY092010	9/20/10 10:08 AM	9/24/10 8:31 AM	94.40	53.07	0.2483	0.2107	0.0972	0.3969	0.1467	0.0102
WY092410	9/24/10 8:39 AM	9/27/10 8:00 AM	71.30	40.74	0.3948	0.2919	0.0698	0.3295	0.1310	0.0221
WY092710	9/27/10 8:05 AM	9/30/10 7:03 PM	83.00	47.99	0.3741	0.4563	0.1083	0.3539	0.1521	0.0431
WY100110	9/30/10 7:10 PM	10/6/10 12:23 PM	137.10	78.69	0.3843	0.3830	0.1025	0.5154	0.2078	0.0223
WY100410	10/6/10 12:23 PM	10/9/10 1:38 PM	73.20	34.36	0.1550	0.0859	0.1516	0.7744	0.2879	0.0066
WY100810	10/9/10 2:35 PM	10/12/10 4:09 PM	73.60	36.06	0.0866	0.0611	0.0603	0.5516	0.2276	0.0063
WY101110	10/12/10 4:17 PM	10/15/10 11:24 AM	67.10	32.24	0.1093	0.2002	0.0955	0.5924	0.2005	0.0327
WY101510	10/15/10 11:44 AM	10/25/10 9:28 AM	140.20	69.23	0.1768	0.1356	0.0937	0.4389	0.1750	0.0140
WY101810	10/18/10 8:05 AM	10/25/10 9:27 AM	97.40	50.28	0.1006	0.2152	0.0865	0.3591	0.1404	0.0099
WY102210										
WY102510	10/25/10 9:48 AM	10/29/10 6:20 AM	92.70	35.77	0.0074	0.0677	0.0495	0.0891	0.0246	0.0014
WY102910	10/29/10 6:28 AM	11/2/10 8:27 AM	98.00	46.87	0.0524	0.1082	0.1475	0.3088	0.1525	0.0048
WY110110	11/2/10 8:31 AM	11/5/10 10:20 AM	73.80	37.31	0.0131	0.1277	0.0853	0.1368	0.0775	0.0039
WY110510	11/5/10 10:27 AM	11/8/10 6:54 AM	68.40	34.57	0.0824	0.1641	0.1000	0.2564	0.1267	0.0095
WY110810	11/8/10 7:00 AM	11/12/10 2:33 PM	103.50	38.63	0.0019	0.0331	0.1087	0.2401	0.1397	0.0064
WY111210	11/12/10 2:40 PM	11/16/10 10:19 AM	91.60	34.24	0.0027	0.0140	0.0916	0.1509	0.0962	0.0023
WY111510	11/16/10 10:22 AM	11/19/10 9:12 AM	66.50	34.12	0.0147	0.0715	0.0895	0.1878	0.1112	0.0047
WY111910	11/19/10 9:23 AM	11/22/10 3:38 PM	78.20	48.13	0.0124	0.0856	0.0843	0.3294	0.0926	0.0035

WY112210	11/22/10 3:40 PM	11/30/10 9:22 AM	178.20	105.40	0.0024	0.0721	0.3022	0.3840	0.1835	0.0099
WY112610										
WY112910	11/30/10 9:32 AM	12/3/10 9:07 AM	71.60	42.81	b.d	0.1396	0.4462	0.3099	0.2492	0.0068
WY120310	12/3/10 9:16 AM	12/6/10 8:00 AM	46.90	28.11	0.0076	0.0443	0.1648	0.0542	0.0814	0.0025
WY120610	12/6/10 8:00 AM	12/10/10 8:05 AM	48.00	29.52	0.0034	0.1661	0.6828	0.2560	0.2779	0.0071
WY121010	12/10/10 8:10 AM	12/13/10 8:32 AM	70.40	42.89	0.0117	0.0551	0.1634	0.1524	0.1102	0.0010
WY121310	12/13/10 8:35 AM	12/17/10 5:11 PM	104.50	61.76	0.0189	0.0411	0.3081	0.2003	0.1785	0.0049
WY121710	12/17/10 5:19 PM	12/20/10 8:00 AM	30.60	18.43	0.0269	0.2310	0.8847	0.0925	0.1849	0.0050
WY122010	12/20/10 8:05 AM	12/23/10 4:17 PM	48.00	29.10	0.0125	0.1388	0.8089	0.6286	0.3106	0.0045
WY122410	12/23/10 4:25 PM	12/27/10 7:43 AM	87.20	51.56	0.0041	0.4572	2.8163	0.2027	0.6892	0.0176
WY122710	12/27/10 7:50 AM	1/3/11 11:01 AM	171.20	93.33	0.0016	0.2381	1.0556	0.5337	0.3768	0.0135
WY123110										
WY010311	1/3/11 11:14 AM	1/7/11 8:39 AM	93.40	55.69	0.0012	0.0994	0.5917	0.2786	0.2384	0.0064
WY010711	1/7/11 8:42 AM	1/10/11 7:17 AM	72.60	44.13	0.0180	0.0885	0.9556	0.2683	0.3154	0.0081
WY011011	1/10/11 9:20 AM	1/14/11 1:01 PM	99.40	56.52	0.0138	0.4906	3.0765	0.2878	0.8467	0.0198
WY011411	1/14/11 1:08 PM	1/18/11 11:30 AM	94.37	54.84	0.0122	0.1122	0.3930	0.1001	0.1569	0.0023
WY011711	1/18/11 11:33 AM	1/22/11 3:21 PM	194.10	57.32	0.0019	0.0433	0.1195	0.1234	0.1073	0.0023
WY012111	1/22/11 3:43 PM	1/25/11 10:30 AM	194.10	38.83	0.0235	0.0693	0.5643	0.1945	0.2334	0.0049
WY012411	1/25/11 10:32 AM	1/29/11 9:14 AM	161.50	55.07	b.d	0.1491	0.7880	0.1320	0.2857	0.0078
WY012811	1/29/11 9:27 AM	1/31/11 7:27 AM	46.00	27.88	0.0149	0.3960	2.1910	0.2190	0.6611	0.0188
WY013111	1/31/11 7:35 AM	2/4/11 9:27 AM	97.80	54.94	0.0422	0.1983	0.8043	0.7014	0.3894	0.0152
WY020411	2/4/11 9:37 AM	2/7/11 8:47 AM	71.10	40.68	0.0146	0.0718	0.2513	0.1782	0.1203	0.0042
WY020711	2/7/11 8:50 AM	2/11/11 5:05 PM	104.20	59.62	0.0006	0.1217	0.4432	0.5215	0.2644	0.0092
WY021111	2/11/11 5:10 PM	2/15/11 9:44 AM	88.50	51.79	0.0045	0.3300	1.4722	0.3105	0.4278	0.0628
WY021411	2/15/11 9:48 AM	2/18/11 9:23 AM	71.50	41.33	0.0039	0.1706	0.3909	0.3053	0.2031	0.0104
WY021811	2/18/11 9:29 AM	2/21/11 12:36 PM	75.10	43.24	b.d	0.1931	1.0403	0.3992	0.4213	0.0154
WY022111	2/21/11 12:39 PM	2/24/11 5:09 PM	76.40	44.30	b.d	0.2842	1.0382	0.3666	0.3677	0.0121
WY022511	2/24/11 5:18 PM	2/28/11 8:15 AM	86.70	50.32	0.0007	0.1370	0.3700	0.3970	0.1983	0.0129
WY022811	2/28/11 8:20 AM	3/4/11 8:46 AM	96.40	57.60	0.0021	0.9135	2.9804	0.8353	0.7789	0.0315
WY030411	3/4/11 8:53 AM	3/7/11 8:16 AM	71.30	41.35	0.0091	0.5486	1.2691	0.6171	0.4962	0.0190
WY030711	3/7/11 8:19 AM	3/11/11 10:21 AM	98.00	57.21	0.0175	0.3377	0.6608	0.5564	0.3441	0.0117
WY031111	3/11/11 10:37 AM	3/14/11 12:08 PM	73.50	42.14	0.0226	0.4599	1.8434	0.3526	0.5171	0.0192
WY031411	3/14/11 12:12 PM	3/18/11 9:00 AM	92.70	54.06	0.0457	0.1799	0.5383	0.3412	0.2473	0.0091
WY031811	3/18/11 9:19 AM	3/21/11 12:56 PM	75.60	44.67	b.d	0.1529	0.7764	1.2191	0.5081	0.0352

WY032111										
WY032511	3/25/11 8:50 AM	3/28/11 8:36 AM	71.70	42.70	0.0181	0.0815	0.3203	0.3589	0.2058	0.0062
WY032811	3/28/11 8:38 AM	4/1/11 7:14 AM	94.60	54.97	0.0744	0.0949	0.3088	0.1853	0.1856	0.0048
WY040111										
WY040411	4/1/11 7:29 AM	4/8/11 9:22 AM	169.80	99.39	0.1412	0.0563	0.2066	0.5692	0.2011	0.0111
WY040811	4/8/11 9:36 AM	4/11/11 8:08 AM	70.50	41.51	0.0468	0.0342	0.2256	0.8873	0.2775	0.0108
WY041111	4/11/11 8:12 AM	4/15/11 12:06 PM	99.90	57.94	0.2462	0.0403	0.3140	1.0008	0.4003	0.0248
WY041511	4/15/11 12:16 PM	4/18/11 9:30 AM	69.20	41.54	0.0544	0.0416	0.2523	1.3779	0.4328	0.0347
WY041811	4/18/11 9:34 AM	4/22/11 10:17 AM	96.70	56.25	0.0243	0.0465	0.2707	0.9431	0.3629	0.0185
WY042211	4/22/11 11:00 AM	4/25/11 10:02 AM	71.00	42.56	0.0003	0.0724	0.3721	1.1045	0.4436	0.0275
WY042511	4/25/11 10:06 AM	4/30/11 11:37 AM	121.50	70.46	0.0817	0.0442	0.0840	0.3134	0.1381	0.0051
WY042911	4/30/11 11:43 AM	5/2/11 7:27 AM	43.50	25.80	0.0157	0.0249	0.0597	0.3870	0.1321	0.0042
WY050211	5/2/11 7:20 AM	5/7/11 9:23 AM	122.00	69.56	0.1415	0.1055	0.1706	0.5396	0.2280	0.0120
WY050611	5/7/11 9:27 AM	5/10/11 11:06 AM	73.60	30.69	0.1859	0.0534	0.1811	0.7282	0.2433	0.0079
WY050911	5/10/11 11:15 AM	5/14/11 6:26 PM	103.20	53.98	0.0853	0.0973	0.1098	0.3530	0.1815	0.0048
WY051311	5/14/11 6:26 PM	5/16/11 10:11 AM	39.60	19.23	0.0187	0.0997	0.3474	1.1866	0.1608	0.0040
WY051611	5/16/11 10:16 AM	5/23/11 12:06 PM	169.80	83.50	0.1601	0.0476	0.0201	0.1018	0.1105	0.0038
WY052011										
WY052311	5/23/11 12:18 PM	5/27/11 9:54 AM	90.50	47.33	0.0944	0.0636	0.1041	0.4722	0.2038	0.0066
WY052711										
WY053011	5/30/11 2:00 PM	6/3/11 5:39 AM	87.60	52.30	0.0311	0.1591	0.0819	0.6445	0.2636	0.0177
WY060311	6/3/11 5:45 AM	6/6/11 8:00 AM	95.00	55.86	0.1756	0.0943	0.0474	0.3041	0.1848	0.0073
WY060511	6/6/11 8:00 AM	6/10/11 9:14 AM	73.20	42.94	0.0986	0.1987	0.0838	0.4831	0.1713	0.0120
WY061011	6/10/11 9:23 AM	6/13/11 3:49 PM	78.40	45.73	0.1859	0.1030	0.0683	0.6223	0.2771	0.0122
WY061311	6/13/11 3:55 PM	6/17/11 4:06 PM	96.20	55.92	0.2742	0.0954	0.1011	0.6513	0.2741	0.0111
WY061711	6/17/11 4:14 PM	6/20/11 6:53 AM	62.60	36.87	0.0862	0.0529	0.0371	0.2572	0.1495	0.0077
WY062011	6/20/11 6:56 AM	6/27/11 5:20 AM	166.40	98.41	0.3474	0.1603	0.0430	0.4565	0.1866	0.0097
WY062411										
WY062711	6/27/11 5:26 AM	7/1/11 9:49 AM	100.30	59.82	0.3066	0.2417	0.0860	0.7068	0.2900	0.0214
WY070111	7/1/11 10:00 AM	7/4/11 8:17 AM	70.30	43.07	0.2400	0.2749	0.0378	0.4762	0.2761	0.0120
WY070411	7/4/11 8:22 AM	7/8/11 6:16 AM	93.90	56.45	0.4624	0.2852	0.0843	0.6247	0.2569	0.0226
WY070811	7/8/11 6:33 AM	7/15/11 8:00 AM	97.40	58.58	0.5347	0.2511	0.1082	0.6754	0.3658	0.0138
WY071111	7/11/11 8:05 AM	7/18/11 6:49 AM	142.80	81.87	0.3838	0.3696	0.0876	0.6481	0.2501	0.0107
WY071511										

WY071811	7/18/11 7:11 AM	7/22/11 6:13 AM	95.00	30.30	0.4157	0.3165	0.0885	0.4707	0.2254	0.0096
WY072211	7/22/11 6:20 AM	7/25/11 6:59 AM	72.60	43.48	0.4328	0.3104	0.0402	0.2860	0.3372	0.0074
WY072511	7/25/11 7:02 AM	7/28/11 9:48 AM	74.50	41.16	0.4224	0.3502	0.0830	0.5311	0.2624	0.0188
WY072911	7/28/11 9:56 AM	8/1/11 10:09 AM	94.50	55.71	0.5210	0.1561	0.1150	0.4880	0.2541	0.0193
WY080111	8/1/11 10:09 AM	8/5/11 9:12 AM	94.70	54.75	0.3162	0.2361	0.0757	0.4200	0.1821	0.0092
WY080511	8/5/11 9:27 AM	8/8/11 6:07 AM	68.60	39.67	0.2013	0.1650	0.0870	0.4475	0.2758	0.0225
WY080811	8/8/11 6:12 AM	8/12/11 9:13 AM	99.00	56.17	0.2918	0.1815	0.0584	0.3536	0.1787	0.0214
WY081211	8/12/11 9:22 AM	8/16/11 7:47 AM	94.00	55.12	0.2376	0.1927	0.1133	0.3714	0.1832	0.0507
WY081511	8/16/11 7:51 AM	8/19/11 9:55 AM	74.00	42.13	0.2440	0.2253	0.1119	0.3694	0.1774	0.0900
WY081911	8/19/11 10:05 AM	8/22/11 7:49 AM	69.50	40.26	0.3699	0.2560	0.1173	0.4441	0.2098	0.0184
WY082211	8/22/11 7:53 AM	8/26/11 10:40 AM	96.00	54.78	0.2928	0.3786	0.0971	0.6033	0.2311	0.0122
WY082611	8/26/11 10:50 AM	8/29/11 10:15 AM	71.40	40.67	b.d	0.3376	0.0982	0.7030	0.3702	0.0145
WY082911	8/29/11 10:18 AM	9/2/11 9:11 AM	94.80	53.73	b.d	0.1758	0.1088	0.5366	0.2284	0.0244
WY090211	9/2/11 9:18 AM	9/5/11 2:00 PM	76.70	43.39	0.4504	0.1527	0.0679	0.3195	0.1394	0.0173
WY090511	9/5/11 2:03 PM	9/9/11 8:33 AM	90.40	50.94	0.1996	0.1970	0.1239	0.5724	0.3454	0.0254
WY090911	9/9/11 8:39 AM	9/12/11 9:00 AM	72.30	41.47	0.5352	0.2134	0.1347	0.5563	0.2602	0.0158
WY091211	9/12/11 9:05 AM	9/17/11 10:17 AM	121.10	68.00	0.0903	0.1366	0.1067	0.4964	0.2198	0.0183
WY091611	9/17/11 10:28 AM	9/19/11 2:02 PM	46.90	25.98	0.1777	0.0743	0.0798	0.4267	0.1981	0.0228
WY091911	9/19/11 2:09 PM	9/23/11 8:51 PM	90.60	49.79	0.1263	0.1250	0.0812	0.4746	0.1672	0.0221
WY092311	9/23/11 9:02 AM	9/26/11 8:12 AM	71.10	41.22	0.1556	0.2907	0.0803	0.4745	0.2072	0.0323
WY092611	9/26/11 8:17 AM	9/30/11 5:51 PM	105.50	59.10	0.2145	0.2747	0.0784	0.3570	0.1632	0.0186
WY093011	9/30/11 5:59 PM	10/4/11 1:05 PM	91.10	50.80	0.1718	0.3463	0.1134	0.6551	0.2630	0.0168
WY100311	10/4/11 1:08 PM	10/8/11 10:04 AM	92.90	50.40	0.1551	0.1487	0.0259	0.1529	0.0866	0.0002
WY100711	10/8/11 10:08 AM	10/10/11 10:54 AM	48.70	26.88	0.1135	0.1869	0.1068	0.5413	0.1938	0.0009
WY101011	10/10/11 10:58 AM	10/14/11 10:40 AM	93.80	51.10	0.1643	0.0933	0.1086	0.4551	0.1946	0.0110
WY101411	10/14/11 10:50 AM	10/19/11 11:38 AM	120.80	67.34	0.0477	0.1111	0.0455	0.3044	0.1267	0.0075
WY101711	10/19/11 11:41 AM	10/21/11 12:01 PM	48.30	26.85	0.0128	0.2997	0.0851	0.4143	0.2422	0.0087
WY102111	10/21/11 12:10 PM	10/24/11 8:24 PM	68.20	37.92	0.0378	0.2270	0.0906	0.3085	0.1649	0.0094
WY102411	10/24/11 8:32 AM	10/28/11 8:01 AM	95.40	52.13	0.0029	0.1250	0.0675	0.6207	0.2357	0.0151
WY102811	10/28/11 8:10 AM	10/31/11 9:15 AM	73.00	40.28	0.0551	0.1624	0.1110	1.2178	0.4163	0.0436
WY103111	10/31/11 9:19 AM	11/4/11 9:00 AM	95.60	52.34	0.0399	0.1592	0.1438	0.4730	0.2073	0.0103
WY110411	11/4/11 9:11 AM	11/7/11 8:00 AM	71.10	39.08	0.0045	0.1981	0.3001	0.4403	0.2494	0.0114
WY110711	11/7/11 8:00 AM	11/11/11 11:23 AM	44.00	23.82	0.0046	0.2148	0.1916	0.5573	0.2484	0.0103
WY111111	11/11/11 11:30 AM	11/14/11 7:47 AM	68.20	37.36	0.0075	0.1357	0.1215	0.3630	0.1836	0.0053

WY111411	11/14/11 7:48 AM	11/18/11 11:34 AM	99.70	52.91	0.0018	0.0834	0.0945	0.3788	0.1850	0.0084
WY118111	11/18/11 12:00 AM	11/21/11 8:51 AM	68.80	38.05	0.0259	0.2683	0.4203	0.1207	0.1462	0.0051
WY112111	11/21/11 9:55 AM	11/25/11 8:51 AM	95.90	51.99	0.0109	0.2145	1.0842	0.6246	0.5311	0.0108
WY112511										
WY112811	11/28/11 8:50 AM	12/2/11 9:04 AM	96.20	51.94	0.0146	0.2046	0.1340	0.3372	0.2071	0.0054
WY120211	12/2/11 9:13 AM	12/5/11 7:41 AM	70.40	38.90	0.0084	0.0729	0.0825	0.2396	0.0897	0.0037
WY120511	12/5/11 7:45 AM	12/9/11 9:39 AM	97.90	51.31	b.d	0.0827	0.3532	0.3108	0.2451	0.0089
WY120911	12/9/11 9:49 AM	12/12/11 9:14 AM	71.40	38.79	0.0105	0.1832	0.8090	0.2011	0.3285	0.0110
WY121211	12/12/11 9:19 AM	12/16/11 9:43 AM	96.40	51.14	0.0054	0.1202	0.8862	0.5998	0.5305	0.0135
WY121611	12/16/11 9:50 AM	12/19/11 11:21 AM	73.50	40.49	0.0372	0.0891	0.9377	0.3249	0.4097	0.0074
WY121911	12/19/11 11:24 AM	12/23/11 9:23 AM	93.90	49.18	0.0024	0.0999	0.5119	0.2571	0.2772	0.0057
WY122311	12/23/11 9:31 AM	12/27/11 7:51 AM	94.30	51.75	0.1110	0.0853	0.1325	0.1230	0.1093	0.0027
WY122611	12/27/11 7:51 AM	12/30/11 9:07 AM	73.20	39.65	0.0055	0.1942	0.3014	0.2984	0.1963	0.0098
WY123011	12/30/11 9:09 AM	1/3/12 3:03 PM	101.90	55.72	0.0219	0.0929	0.1641	0.1592	0.0863	0.0066
WY010212	1/3/12 3:05 PM	1/6/12 8:30 AM	65.40	35.74	0.0129	0.1916	0.1663	0.1510	0.1120	0.0091
WY010612	1/6/12 8:44 AM	1/9/12 8:00 AM	71.20	39.04	0.0204	0.0931	0.1749	0.1799	0.0897	0.0051
WY010912	1/9/12 8:05 AM	1/13/12 7:49 AM	95.70	50.57	0.0579	0.1011	0.1949	0.1725	0.1249	0.0082
WY011312	1/13/12 7:56 AM	1/16/12 7:44 AM	71.8	41.48	0.0070	0.2065	0.1202	0.2069	0.0731	0.0076
WY011612	1/16/12 7:48 AM	1/20/12 7:44 AM	95.9	53.16	0.0302	0.1014	0.1109	0.1055	0.0729	0.0039
WY012012	1/20/12 7:48 AM	1/23/12 7:56 AM	72.1	40.96	0.0006	0.1002	0.1216	0.1388	0.1346	0.0097
WY012312	1/23/12 8:00 AM	1/27/12 8:37 AM	96.6	53.95	0.0009	0.1272	0.3913	0.2008	0.1884	0.0071
WY012712	1/27/12 4:07 PM	1/30/12 8:08 AM	64	35.61	0.0131	0.3452	0.6374	0.3468	0.2783	0.0168
WY013012	1/30/12 8:17 AM	2/3/12 7:34 AM	95.3	55.02	0.0005	0.2998	1.0260	0.2098	0.3638	0.0100
WY020312	2/3/12 7:37 AM	2/6/12 7:16 AM	71.6	39.52	0.0133	0.3876	1.0867	0.2840	0.3803	0.0114
WY020612	2/6/12 7:19 AM	2/10/12 7:50 AM	96.5	54.02	0.0000	0.4154	0.8616	0.5535	0.4270	0.0110
WY021012	2/10/12 7:54 AM	2/13/12 8:03 AM	72.1	43.03	0.0056	0.1905	0.4991	0.4954	0.2738	0.0090
WY021312	2/13/12 8:06 AM	2/17/12 7:50 AM	95.7	53.30	0.0038	0.2478	0.7457	0.2516	0.3375	0.0100
WY021712	2/17/12 7:54 AM	2/20/12 7:56 AM	72	41.09	0.0070	0.1507	0.2935	0.2557	0.2167	0.0042
WY022012	2/20/12 8:00 AM	2/24/12 7:59 AM	95.9	53.09	0.0233	0.1187	0.3155	0.0839	0.1387	0.0036
WY022412	2/24/12 8:02 AM	2/27/12 7:11 AM	71.1	41.24	0.0171	0.1723	0.3927	0.1524	0.1662	0.0047
WY022712	2/27/12 7:15 AM	3/2/12 7:36 AM	96.3	52.22	0.0061	0.1388	0.2839	0.2878	0.2137	0.0059
WY030212	3/2/12 7:39 AM	3/6/12 7:02 AM	71.3	41.57	0.0402	0.1499	0.3152	0.2184	0.2037	0.0024
WY030512	3/5/12 7:05 AM	3/9/12 7:03 AM	95.9	53.62	0.0573	0.1783	0.4735	0.4731	0.2926	0.0056
WY030912	3/9/12 7:06 AM	3/13/12 6:44 AM	71.6	41.55	0.0803	0.2152	0.6077	0.5541	0.3749	0.0134

WY031312	3/13/12 6:44 AM	3/16/12 7:18 AM	96.5	54.62	0.2181	0.1580	0.3278	0.4940	0.2261	0.0092
WY031612	3/16/12 7:20 AM	3/19/12 8:10 AM	72.8	42.00	0.1081	0.1268	0.2420	0.3954	0.1415	0.0128
WY031912	3/19/12 8:12 AM	3/23/12 7:52 AM	95.6	54.06	0.0970	0.0851	0.1100	0.1913	0.1064	0.0009
WY032312	3/23/12 7:55 AM	3/26/12 7:50 AM	71.9	42.75	0.1606	0.1802	0.1299	0.3081	0.1124	0.0033
WY032612	3/26/12 7:52 AM	3/30/12 7:34 AM	95.7	54.03	0.2212	0.1076	0.1618	0.3824	0.1262	0.0031
WY033012	3/30/12 7:50 AM	4/2/12 10:02 AM	74.2	43.55	0.4767	0.1260	0.2326	0.3370	0.0865	0.0063
WY040212	4/2/12 10:06 AM	4/6/12 10:20 AM	96.2	55.23	0.0740	0.1358	0.2055	0.4544	0.2421	0.0048
WY040612	4/6/12 10:28 AM	4/9/12 6:58 AM	68.4	40.47	0.0237	0.1387	0.3134	1.2485	0.4056	0.0156
WY040912	4/9/12 7:00 AM	4/13/12 7:08 AM	96.1	55.10	0.1335	0.1692	0.1655	0.6751	0.2424	0.0088
WY041312	4/13/12 7:17 AM	4/16/12 6:25 AM	71.1	41.21	0.0730	0.0613	0.1603	0.5204	0.2049	0.0056
WY041612	4/16/12 6:27 AM	4/20/12 7:36 AM	97	55.56	0.1725	0.1100	0.0962	0.4001	0.1734	0.0058
WY042012	4/20/12 7:36 AM	4/23/12 6:32 AM	70.9	42.75	0.1927	0.1331	0.1745	0.6743	0.2805	0.0115
WY042312										
WY042712	4/27/12 8:48 AM	4/30/12 8:11 AM	71.3	41.39	0.1640	0.1022	0.1995	0.4820	0.2374	0.0108
WY043012	4/30/12 8:16 AM	5/4/12 8:55 AM	97.5	55.73	0.0968	0.0821	0.1536	0.8293	0.3043	0.0163
WY050412	5/4/12 9:05 AM	5/7/12 8:02 AM	71	40.93	0.2557	0.0688	0.2168	0.8015	0.2779	0.0152
WY050712	5/7/12 8:02 AM	5/11/12 9:25 AM	97.3	56.09	0.1675	0.1379	0.1548	0.8434	0.3078	0.0168
WY051112	5/11/12 9:32 AM	5/14/12 8:48 AM	70.2	41.89	0.0834	0.1272	0.1452	0.7987	0.2934	0.0105
WY051412	5/14/12 8:52 AM	5/18/12 6:53 AM	95	55.47	0.3090	0.1912	0.1370	1.0124	0.3278	0.0169
WY051812	5/18/12 7:00 AM	5/25/12 7:02 AM	168	99.16	0.2482	0.0747	0.1054	0.4955	0.1852	0.0085
WY052512	5/25/12 7:02 AM	6/1/12 4:34 PM	177.6	102.33	0.2589	0.0764	0.1291	0.6279	0.2628	0.0157
WY060812	6/8/12 7:42 AM	6/18/12 10:38 AM	242.9	144.66	0.3522	0.1246	0.0542	0.3786	0.1610	0.0088
WY061512	6/18/12 10:41 AM	6/22/12 9:09 AM	94.4	55.39	0.2445	0.0483	0.3804	0.1654	0.0103
WY062912	6/29/12 2:53 PM	7/6/12 12:26 PM	165.5	100.84	1.3550	0.2876	0.2859	0.6938	0.2942	0.1076
WY070612	7/6/12 12:29 PM	7/13/12 9:01 AM	164.5	97.16	0.7044	0.2581	0.0803	0.6120	0.2208	0.0425
WY071312	7/13/12 9:15 AM	7/20/12 9:40 AM	168.4	101.48	0.8375	0.2847	0.1336	0.7517	0.2644	0.0199
WY072012	7/20/12 9:43 AM	7/27/12 9:32 AM	167.8	100.09	0.5672	0.2981	0.0860	0.5814	0.2131	0.0120
WY072712	7/27/12 9:43 AM	8/5/12 4:54 PM	223.1	134.62	0.4343	0.3146	0.0800	0.6060	0.2087	0.0307
WY080312	8/5/12 4:57 PM	8/10/12 9:31 AM	112.5	67.54	0.6669	0.3865	0.2532	0.8568	0.3678	0.1856
WY081012	8/10/12 9:38 AM	8/17/12 8:50 AM	167.2	98.81	0.8445	0.2894	0.3329	0.5837	0.3406	0.1588
WY081712	8/17/12 8:56 AM	8/24/12 9:19 AM	168.0	98.03	0.7437	0.2266	0.2088	0.5249	0.3386	0.0981
WY082412	8/24/12 9:36 AM	8/31/12 8:55 AM	167.3	98.98	0.5375	0.2697	0.0816	0.4906	0.2043	0.0236
WY083112	8/31/12 8:58 AM	9/11/12 10:36 AM	265.6	154.17	0.5419	0.1739	0.1306	0.5489	0.2359	0.0279
WY090712	9/11/12 10:47 AM	9/14/12 8:31 AM	69.7	40.30	0.3151	0.1627	0.1876	0.3107	0.2141	0.0915

WY091412	9/14/12 8:35 AM	9/21/12 9:00 AM	168.4	98.66	0.5170	0.1879	0.2908	0.5209	0.3878	0.1008
WY092112	9/21/12 9:08 AM	9/28/12 8:02 AM	166.9	99.22	0.4879	0.2630	0.1834	0.7434	0.3394	0.0431
WY092812	9/28/12 8:02 AM	10/5/12 9:49 AM	169.7	99.66	0.2400	0.1543	0.0806	0.4185	0.1947	0.0186
WY100512	10/5/12 9:58 AM	10/12/12 8:08 AM	166.1	96.41	0.1373	0.1472	0.1359	0.3843	0.1899	0.0207
WY101212	10/12/12 8:12 AM	10/19/12 6:22 AM	166.0	94.60	0.2127	0.1368	0.1175	0.4367	0.1817	0.0113
WY101912	10/19/12 6:28 AM	10/26/12 7:25 AM	168.9	98.21	0.1945	0.0930	0.1193	0.3130	0.1484	0.0089
WY102612	10/26/12 7:27 AM	11/2/12 8:38 AM	169.2	98.63	0.1631	0.1392	0.1405	0.2195	0.1324	0.0072
WY110212	11/2/12 8:45 AM	11/9/12 9:18 AM	168.5	98.73	0.1000	0.0901	0.0474	0.1397	0.0918	0.0067
WY110912	11/9/12 9:20 AM	11/16/12 9:30 AM	168.1	95.75	0.0519	0.0766	0.2720	0.5135	0.2637	0.0164
WY111612	11/16/12 9:35 AM	11/26/12 9:03 AM	239.4	139.77	0.0846	0.0986	0.2329	0.2316	0.1537	0.0063
WY112312	11/26/12 9:05 AM	11/30/12 9:32 AM	96.4	55.96	0.0238	0.1480	0.1615	0.1940	0.1387	0.0084
WY113012	11/30/12 9:37 AM	12/7/12 10:23 AM	168.7	98.62	b.d	0.0640	0.0445	0.1155	0.1112	0.0037
WY120712	12/7/12 10:25 AM	12/14/12 9:37 AM	167.2	94.14	0.0168	0.1223	0.1533	0.2692	0.1438	0.0062
WY121412	12/14/12 9:43 AM	12/22/12 12:03 PM	194.3	107.87	0.0037	0.1629	0.4075	0.2415	0.1990	0.0082
WY122112	12/22/12 12:10 PM	12/28/12 1:00 PM	144.8	83.82	0.0074	0.1691	0.3847	0.3282	0.2373	0.0077
WY122812	12/28/12 1:13 PM	1/4/13 9:05 AM	161.8	81.87	0.0099	0.2963	1.4202	0.3627	0.3947	0.0173

* b.d means the concentration was below the detection limits
** The gap between the rows means there was no data available during that sampling period

188

APPENDIX D NH$_3$ DATA IN NORTHEASTERN COLORADO FROM RADIELLO PASSIVE SAMPLING

D1. Spatial NH$_3$ Data

Start Date	Stop Date	FC_W µg/m³	NN µg/m³	AT µg/m³	BE µg/m³	BH µg/m³	KY µg/m³	GY µg/m³	LD µg/m³	GC µg/m³	LE µg/m³	FC_W µg/m³	SE µg/m³	RH µg/m³
5/20/2010	5/27/2010	3.73			1.9	4.66		7.94	4.07					1.9
5/27/2010	6/3/2010	3.68			2.63	3.67	24.5	9.16	4.33					2.57
6/3/2010	6/10/2010	5.88		12.09	3.91	6.04	39.56	10.86	6.29	7.68				3.42
6/10/2010	6/17/2010	3.08		9.13	1.95	5.22	32.04	8.2	3.96	4.38				2.1
6/17/2010	6/24/2010	5.55		10.9	2.97	6.24	42.82	9.14	5.47	6.66				3.06
6/24/2010	7/1/2010	5.01		11.81	2.94	9.67	27.28	11.42	5.07	5.73				3.88
7/1/2010	7/8/2010	3.7		9.79	3.54	7.23	30.28	9.06	4.21	4.37				3.23
7/8/2010	7/15/2010	3.07		11.43	3.58	7.89	33.71	10.52	3.08	3.01				5.01
7/15/2010	7/22/2010	4.51		12.52	3.94	7.47	39.08	11.53	4.45	5.03				4.7
7/22/2010	7/29/2010	5.2		13.67	3.1	4.63	35.62	10.84	4.66	5.2				2.71
7/29/2010	8/5/2010	4.25		16.04	4.19	7.95	25.8	11.77	3.57	3.92				3.12
8/5/2010	8/12/2010	3.95		13.11	4.48	8.36	23.3	13.11	3.18	3.47				4.26
8/12/2010	8/19/2010	3.71		14.2	3.33	5.68	26.77	9.89	3.48	4.23				3.49
8/19/2010	8/26/2010	3.63		16.16	3.14	7.5	27.19	11.26	4.11	5.24				3.11
8/26/2010	9/2/2010	3.02		12.27	2.04	5.83	26.79	11.18	2.67	4.09				2.48
6/2/2011	6/9/2011	3.94	2.07	10.73	2.71	5.09	46.55	9.41	4.31	5.14	4.13			
6/9/2011	6/16/2011	3.95	3.82	10.53	3.11	7.64	45.43	11.16	4.83	4.67	3.75			
6/16/2011	6/23/2011	2.79	1.91	8.91	2.25	5.15	43.36	8.4	4.4	3.87	2.87			
6/23/2011	6/30/2011	4.72	3.37	16.66	3.29	5.63	49.99	11.25	5.8	5.99	3.48			
6/30/2011	7/7/2011	4.36	3.28	15.15	4.19	10.67	44.84	12.65	6.45	7.87	5.23			
7/7/2011	7/14/2011	4.19	3.88	18.61	4.42	9.14	42.38	19.02	5.2	5.65	3.62			
7/14/2011	7/21/2011	4.01	3.55	18.47	4.9	10.83	73.78	18.79	5.03	5.85	3.22			
7/21/2011	7/28/2011	3.82	2.11	12.41	3.63	6.46	41.09	12.19	3.67	4.43	2.71			
7/28/2011	8/4/2011	4.17	2.61	15.24	2.68	8.81	43.02	13.26	4.44	5.61	2.71			
8/4/2011	8/11/2011	3.08	2.3	14.94	2.83	5.45	48.9	12.88	3.67	4.72	2.44			
8/11/2011	8/18/2011	3.21	1.51	8.82	2.34	6.8	46.6	9.78	4.16	4.81	3.6			
8/18/2011	8/25/2011	3.51	3.36	13.06	3.18	6.22	41.24	11.31	6.94	5.4	3.25			
8/25/2011	8/31/2011	3.08	2.31	15.67	3.72	6.49	30.32	17.63	3.61	4.91	2.27			
6/21/2012	6/28/2012	8.55	3.54	14.01	2.61	7.56	42.72	12.84	6.09	7.03		9.92	9.79	
6/28/2012	7/5/2012	6.37	3.53	15.16	4.58	8.45	52.9	14.37	5.8	7.24		10.84	13.14	
7/5/2012	7/11/2012	5.89	2.6	13.2	3.16	5.41	53.55	8.66	10.37	7.27		9.36	12.97	
7/11/2012	7/19/2012	4.59	2.71	19.27	2.8	6.36	48.48	14.42	5.56	5.26		9.56	10.28	
7/19/2012	7/25/2012	3.27	2.88	13.36	2.96	5.89	25.93	9.55	3.25	4.37		7.97	8.3	

7/25/2012	8/1/2012	3.48	1.81	14.35	3.29	7.75	33.88	10.94	3.13	4.82	8.6	9.07
8/1/2012	8/8/2012	2.92	3.33	11.24	2.22	4.84	30.46	6.68	2.55	3.74	5.52	7.59
8/8/2012	8/15/2012	3.42	1.85	9.25	2.83	4.21	47.22	11.09	3.13	4.24	6.27	7.84
8/15/2012	8/23/2012		1.68	13.33	2.12	3.8	35.31	7.65	3.14	3.91	7	6.24
8/23/2012	8/29/2012	3.2	1.95	13.83	3.35	4.93	46.08	14.51	2.65	4.29	8.59	8.17
5/30/2013	6/4/2013	1.95	1.69	6.56	1.42	3.59	25.2	5.19	2.29	1.81	5.79	4.52
6/4/2013	6/11/2013	3.12	2.91	13.41	2.11	6.27	35.66	11.69	4.02	5.74	7.04	8.04
6/11/2013	6/20/2013	4.91	3.12	13.28	2.98	7.18	39.4	9.63	5.66	6.4	8.73	7.97
6/20/2013	6/28/2013	4.41	2.93	12.75	3.61	7.17	42.7	11.36	6.89	5.16	8.29	8.14
6/28/2013	7/5/2013	6.12	3.28	17.59	3.07	7.8	68.61	12.44	7.16	7.11	11.24	12.66
7/5/2013	7/11/2013	4.99	3.75	17.93	3.49	7.15	47.52	11.11	5.5	5.76	9.28	10.05
7/11/2013	7/18/2013	5.33	3.95	17.65	3.57	4.54	38.95	10.13	5.23	6.19	10.09	
7/18/2013	7/25/2013	5.61	2.83	15.98	3.62	5.08	43.97	11.77	6.01	6.18	8.04	8.74
7/25/2013	8/1/2013	4.74	3.3	15.1	3.23	5.3	42.33	9.9	5.64	5.63	7.6	8.12
8/1/2013	8/8/2013	4.62	2.68	14.82	3.59	5.43	52.39	12.3	4.83	5.25	8.42	9.28
8/8/2013	8/15/2013	3.17	2.04	15.89	2.91	4.25	38.23	9.41	3.8	3.24	6.61	8.79
8/15/2013	8/23/2013	5.68	3.68	20.47	2.69	6.8	48.06	12.54	5.61	5.94	10.41	9.73
8/23/2013	8/29/2013	3.23	3.03	15.32	2.67	7.32	31.73	9.25	3.46	5	6.49	6.45
5/29/2014	6/5/2014	3.7	2.94	15.88	3.71	6.79	45.11	10.21	3.53	4.58	8.61	8.3
6/5/2014	6/12/2014	3.42	2.05	10.44	2.75	4.47	43.46	11.35	3.55	4.07	8.37	7.1
6/12/2014	6/19/2014	3.35	3.22	12.26	2.45	5.01	43.8	10.32	3.85	4.68	8.96	8.64
6/19/2014	6/26/2014	4.75	2.84	16.64	3.71	5.87	61.94	12.49	5.82	6.18	9.12	10.89
6/26/2014	7/3/2014	4.29		12.03	3.01	4.82	29.22	9.41	3.31	5.63		
7/3/2014	7/11/2014	4.98	3.1	16.45	3.67	6.07	52.12	11.19	4.28	5.66	11.27	9.82
7/11/2014	7/17/2014	3.69	2.3	10.86	2.53	5.04	42.53	9.84	3.59	4.69	8.19	10.47
7/17/2014	7/25/2014	4.49	3.65	19.03	5.4	6.17	68.82	14.46	3.88	5.56	11.38	13.79
7/25/2014	7/31/2014	4.15	2.29	13.99	3.01	4.91	49.13	9.35	3.53	4.44	6.92	8.39
7/31/2014	8/8/2014	2.99	3.83	15.67	3.12	6.23		14.95	3.41	4.7	8.59	10.57
8/8/2014	8/14/2014	3.52	4.01	16.2	2.68	6.62	36.29	12.58	3.15	4.48	9.11	11.35
8/14/2014	8/20/2014	2.39	1.43	14.46	2.7	6.51	43.88	14.08	3.09	4.63	7.38	8.95
8/20/2014	8/28/2014	3.37	2.45	14.5	2.24	4.57	42.56	12.16	2.83	4.72	9.96	8.18

D2. Vertical NH$_3$ Data

Sample_ID	Start Time	End Time	Time Elapse Min	Temp. °C	300m µg/m^3	250m µg/m^3	200m µg/m^3	150m µg/m^3	100m µg/m^3	50m µg/m^3	22m µg/m^3	10m µg/m^3	1m µg/m^3
BAO121311	12/13/2011 13:00	12/30/2011 10:42	24342	-0.89	0.79	0.79	1.17	1.27	1.69	2.8	3.71	5.05	5.1
BAO123011	12/30/2011 10:42	1/17/2012 11:09	25947	1.91	1.16	1.34	1.48	1.82	2.39	2.85	3.72	4.19	4.12
BAO011712	1/17/2012 11:09	1/31/2012 11:20	20171	3.98	0.89	0.97	1.32	1.5	1.87	2.94	3.31	3.58	3.32
BAO013112	1/31/2012 11:20	2/14/2012 10:28	20108	-1.97	1.02	1.21	1.82	2.29	2.71	3.62	3.89	4.22	4.11
BAO021412	2/14/2012 10:28	2/29/2012 10:20	21592	1.2	1.34	1.61	2.03	2.57	3.34	3.78	4.08	5.06	4.6
BAO022912	2/29/2012 10:25	3/14/2012 10:58	20193	7.43	0.66	0.77	0.97	1.16	1.3	1.6	1.88	2.11	1.96
BAO031412	3/14/2012 10:58	3/29/2012 14:10	21792	12.54	1.53	1.59	1.94	2	2.4	2.56	2.76	2.9	2.68
BAO032912	3/29/2012 14:10	4/12/2012 14:14	20164	12.85	2.09	2.25	2.37	2.86	3.04	3.5	3.54	3.73	3.28
BAO041212	4/12/2012 14:14	5/2/2012 9:20	28506	14.52	1.79	1.96	2.16	2.32	2.65	3.04	2.89	3.83	3.26
BAO050112	5/2/2012 9:20	5/15/2012 14:33	19033	20.19	2.05	2.13	2.42	2.74	2.79	3.29	3.21	3.53	3.24
BAO051512	5/15/2012 14:33	6/19/2012 14:28	50395	20.19	2.5	2.44	2.56	2.89	3.37	3.85	4.12	4.42	4.27
BAO061912	6/19/2012 14:28	6/29/2012 14:28	14400	28.2	3.14	3.34	3.69	4.03	4.66	5.08	5.62	5.89	5.47
BAO062912	6/29/2012 14:28	7/6/2012 14:35	10087	28	4.4	4.38	4.65	4.8	5.6	6.42	7.01	7.43	6.74
BAO070612	7/6/2012 14:35	7/12/2012 14:40	8645	22.7	3.46	3.89	4.14	4.67	4.93	5.51	6.77	7.18	7.84
BAO071212	7/12/2012 14:40	7/20/2012 14:28	11508	26.98	2.31	2.56	2.68	2.83	3.3	3.28	3.95	4.5	5.21
BAO072012	7/20/2012 14:28	7/31/2012 11:30	15662	27.26	2.52	2.55	2.87	3.14	3.5	4.39	4.6	5.4	5.05
BAO072712	7/31/2012 11:30	8/9/2012 14:30	13140	25.54	2.14	2.17	2.43	2.46	3.03	3.41	3.8	4.12	4.57
BAO080912	8/9/2012 14:30	8/16/2012 14:44	10094	23.91	2.68	2.71	3.21	3.23	3.4	3.8	3.93	4.36	3.86
BAO081612	8/16/2012 14:44	8/24/2012 15:10	11546	22.14	2.76	3.14	3.29	3.54	4.17	4.14	4.43	4.72	4.18
BAO082412	8/24/2012 15:10	8/30/2012 20:40	8970	26.02	1.92	1.7	2.06	2.27	2.66	2.89	3.12	3.1	2.85
BAO083012	8/30/2012 20:40	9/17/2012 15:05	25585	22.37	2.2	2.42	2.59	2.77	2.84	3.08	3.28	4.16	3.59
BAO091712	9/17/2012 15:05	9/28/2012 11:10	15605	17.12	2.25	2.43	2.68	2.9	3.57	4.06	4.14	4.16	3.94
BAO092812	9/28/2012 11:10	10/12/2012 14:30	20360	11.23	2.29	2.71	2.97	3.7	3.86	4.93	5.26	5.47	5.17
BAO101212	10/12/2012 14:30	10/29/2012 14:20	24470	8.44	1.02	1.19	1.38	1.67	2.17	2.44	2.95	3.09	2.81
BAO102912	10/29/2012 14:20	11/12/2012 14:50	20190	7.03	1.95	1.54	2.79	3.98	4.87	5.6	5.67	6.25	5.64
BAO111212	11/12/2012 14:50	11/27/2012 16:00	21670	4.66	1.09	1.37	1.95	2.63	3.68	5.25	5.93	6.4	5.3
BAO112712	11/27/2012 16:00	12/12/2012 16:10	21610	3.68	1.08	1.49	1.91	2.46	3.28	4.65	5.62	5.94	5.22
BAO121212	12/12/2012 16:10	1/9/2013 15:00	40250	-2.7	0.98	1.2	1.47	2.02	2.8	3.57	4.26	4.91	4.33